

**Research project SPR-06-37 (C-06-37)**

**Tool for Analysis of Early Age Transverse Cracking of Composite Bridge Decks**

**Final Report**

**August 29, 2011**

Consortium: Transportation Infrastructure Research Consortium – Contract #C010331

Investigators:

Principal Investigator:

Levon Minnetyan, Professor  
Department of Civil and Environmental Engineering  
W. J. Rowley Research Laboratories  
Clarkson University  
8 Clarkson Avenue  
Potsdam, New York 13699-5710  
Tel: (315)-268-7741  
Cell: (315)-265-6851  
Fax: (315)-268-7985  
<http://www.clarkson.edu/cee>  
E-mail: [levon@clarkson.edu](mailto:levon@clarkson.edu)

Co-Principal Investigator:

Kerop D. Janoyan, Associate Professor  
Same address as Principal Investigator  
Tel: (315)-268-6506  
E-mail: [kerop@clarkson.edu](mailto:kerop@clarkson.edu)

# TABLE OF CONTENTS

TABLE OF CONTENTS.....	1
Executive Summary:.....	4
Part 1 Significance of Deck Cracking Problem .....	5
1.1. Safety and Durability Effects.....	5
1.2. Influential Factors of Bridge Deck Cracking .....	5
1.3. Shrinkage and Creep .....	6
1.4. Thermal Effects .....	8
1.5. Load Effects.....	8
1.6. Analysis of Cracking .....	9
1.7. Summary of Part 1 .....	11
Part 2. Composite Bridge Analysis (CBRAN) Computational Framework .....	12
2.1 Model Development .....	13
2.2 Creation of Finite Element Model Geometry.....	13
2.3 Definition of Material Properties.....	18
2.4 Definition of Ply Properties for Composite Material Analysis .....	18
2.5 Use of Tying Equations Instead of Duplicate Nodes for Improved Accuracy .....	21
2.6 Improvement of the Tying Equations Model.....	22
2.7 Integrated girder plus deck finite element model .....	24
2.8 Conclusions of Part 2.....	28
Part 3. Development of mathematical models for temperature and moisture gradients and shrinkage in the deck slab .....	29
3.1 Effect of temperature rise during curing of concrete deck: .....	29
3.2 Determining time history of the convective heat transfer coefficient, h: .....	30
3.3 Determining heat generation, $Q_i$ : .....	33

3.4 Thermal Conductivity and Specific Heat Capacity of Concrete: .....	38
3.5 Incorporation of Temperature Models into Thermal Finite Element Analysis Program: .....	40
3.6 Input Data for Thermal Finite Element Analysis across the Concrete Deck Thickness:.....	41
3.7 Results of Thermal Time-History Finite Element Analysis across the Concrete Deck Thickness:.....	42
3.8 Development of Moisture Model for Curing Concrete Bridge Deck: .....	42
3.9 Development of Shrinkage Models for Concrete Bridge Deck: .....	45
3.6 Summary and Conclusions of Part 3 .....	49
Part 4. Implementation of the formulated theoretical framework in finite element progressive cracking simulation software .....	50
Corrections to Task 4 Report: .....	50
Work Done in Task 4: .....	52
Discussion.....	59
Part 5. Model calibration and software validation .....	60
1. Thermal finite element model: .....	60
2. Strains and residual stresses developed due to thermal expansion and shrinkage .....	62
3. Load levels to produce cracking:.....	64
4. Crack opening and spacing: .....	65
Part 6. Integration with Structural Health Monitoring (SHM): Experimental Testing of Early Age Transverse Cracking of Composite Bridge Decks .....	66
Part 7. Implementation and technology transfer with recommendations for bridge deck cracking mitigation.....	70
Results of Part 7: .....	71
Alternate Model of Deck with Thin Steel Rebar Layers .....	72
Conclusions .....	73
References .....	74
APPENDIX 1: Making Software Operational on PC:.....	78

Appendix 2: Manual computation of bending stress using beam diagram from AISC manual and strength of materials (for reference) .....	94
Appendix 3A: Thermal Finite Element Analysis Program Listing .....	97
Appendix 3B: Format for Input File for Thermal Finite Element Analysis Program.....	108
Appendix 3C: Input File for Thermal Finite Element Analysis Case 3(b) of Bridge Deck Curing .....	112
Appendix 4-1 Subroutine UPDBK is used to update DATABANK properties .....	115
Appendix 4-2 Listing of subroutine TEMPRD .....	117
Appendix 4-3 CBRAN MAIN program:.....	118
Appendix 4-4 Computation of shrinkage strains .....	120
Appendix 4-5 Incremental time history residual stress analysis with creep .....	123
Appendix 4-6 WPSMHM preprocessor to write OMHOST plane strain local analysis input file to compute crack width and spacing .....	126
Appendix 5-1 TEMPRTRS.LYR file (Time is in hours and temperatures are in °F):.....	128
Appendix 7-1a preprocessor to generate CBRAN input file for laboratory test specimen .....	134
Appendix 7-1b Residual stresses from FOR091.DAT file after 28 days for lab specimen.....	141
Appendix 7-2a Layer structure from FOR085.ORG input file for composite bridge deck with 36" girder .....	143
Appendix 7-2b preprocessor to generate CBRAN input file for two-span composite bridge model ...	145
Appendix 7-2c Residual stresses from FOR091.DAT file after 28 days for composite bridge deck with 36" girder followed by HS25 loading .....	151
Appendix 7-3a Layer structure from FOR085.ORG input file for composite bridge deck with 55" girder .....	153
Appendix 7-3b Residual stresses from FOR091.DAT file after 28 days for composite bridge deck with 55" girder .....	155
Appendix 7-4a Layer structure for thin steel layer model of bridge deck with 36" girder.....	157
Appendix 7-4b preprocessor to generate CBRAN input file for two-span composite bridge model with thin rebar steel layers .....	159
Appendix 7-4c Residual stresses from FOR091.DAT file after 28 days for composite bridge deck with 36" girder and thin rebar steel layers .....	165

**Executive Summary:** Computational methods and associated software were developed to compute stresses in HP concrete composite bridge decks due to temperature, shrinkage, and vehicle loading. The structural analysis program uses a layered finite element model. Before running the structural analysis code, layer-by-layer time history temperatures due to hydration heat are computed using a thermal finite element analysis program. Nodal coordinates for the thermal finite element analysis are generated from the layer thicknesses of the structural analysis finite element model. Autogeneous shrinkage, drying shrinkage, and stress relaxation due to creep are taken into account using models based on HP concrete test data. The software computes time-history residual stresses for 28 days. After 28 days an HS25 vehicle load is additionally applied. Longitudinal stress levels are printed layer by layer for comparison with the modulus of rupture and assessment of cracking. A composite bridge specimen was built in the structures testing lab in Clarkson University with thermocouple and strain gage instrumentation. After monitoring temperatures and strains for 28 days, the test specimen was loaded by a concentrated load applied by universal testing machine. Cracking under loading was observed and monitored. Software predictions were compared with test data. A one-day training course was conducted in Albany for NYSDOT engineers on August 3, 2011 to communicate the research findings and recommendations as well as provide training for the use of the developed software.

This report is organized into seven parts. Each part number is associated with the corresponding task number.

## **Part 1 Significance of Deck Cracking Problem**

Early age cracking of concrete bridge decks is a frequent problem throughout the United States, including New York State (NYS). More than 100,000 of the country's bridges developed early cracking of their decks (Krauss and Rogalla 1995). A NYSDOT survey of 63 existing bridges in northern New York found that only fifteen of the bridges had not experienced deck cracking. 38% of the single-span bridges and 67% of those with multiple spans had significant cracking on the concrete deck (Curtis and White 2007). The problem of bridge deck cracking in NYS is still significant, even after the adoption of high performance concrete (HPC) for bridge decks in 1996. A separate NYSDOT survey observed that 48% of an 84 bridge decks built between 1995 and 1998 using HP concrete have developed transverse cracks (Alampalli and Owens 2000). Early age cracks usually develop in the transverse direction of the traffic. The cracking could initiate almost immediately after construction and sometimes appear within a few months after the deck is constructed.

### ***1.1. Safety and Durability Effects***

Deck cracking has no immediate effect on the bridge safety, but it has detrimental effects on the long-term performance. Cracks interconnect the voids and the isolated microcracks in the concrete deck to form preferential pathways for the ingress of chlorides from deicing chemicals thus accelerating reinforcement corrosion. Fanous et al. (2000) observed severe corrosion of black and epoxy coated rebar extracted from cracked locations in different bridge decks. Also, leakage of water through cracks increases the degree of water saturation in the bridge substructure, therefore increasing the risk of freeze-thaw damage. As a result, the bridge service life is reduced and maintenance and rehabilitation costs rise.

### ***1.2. Influential Factors of Bridge Deck Cracking***

Curtis and White (2007) identified the most influential factors on whether or not a bridge deck will crack as: (a) the strength of the concrete, (b) the thickness of the concrete cover above the reinforcing steel, and (c) the temperature at which the concrete was poured. It was also noted that the main causes of tensile stresses in concrete bridge decks are thermal effects from heat of hydration during curing and daily temperature cycling, live load stresses, such as those from the flow of traffic along the bridge, and shrinkage of concrete. In a finite element study, Saadeghvaziri and Hadidi (2005) performed linear and non-linear analyses to show the importance of design factors on transverse cracking in concrete bridge decks. Through an investigation of crack patterns and stress histories, it was shown that design factors, such as structural stiffness, can have a significant impact on transverse cracking. Based on the results from this study, a variety of recommendations were made that suggest several ways to reduce transverse cracking in bridge decks during the design phase. For example, steel reinforcement should be placed in uniform meshes on the top and bottom of the deck. The importance of accounting for shrinkage during the design process is stressed. An accurate crack prediction model would have to include a shrinkage model that takes into account a variety of concrete and structural design properties.

### **1.3. Shrinkage and Creep**

Bridge deck cracking occurs when restrained volumetric changes associated with moisture and temperature changes take place. The Division of Research at the Indiana Department of Transportation showed that restrained shrinkage of concrete bridge decks is the main cause of transverse deck cracking (Frosch 2003). Volumetric changes mainly result from autogenous shrinkage, drying shrinkage, thermal shrinkage, and creep. These major causes of concrete volume change with time depend primarily on the material properties and mix design, design details, construction practices, and environmental conditions. Concrete properties are the most important factors affecting transverse deck cracking since they control the shrinkage and thermal strains that cause stresses and control the relationship between strains and stresses. Understanding the concrete properties is central to reliably modeling the mechanisms contributing to the cracking of concrete decks. The user interface of the implemented computer program will enable the user to input the properties of the concrete being monitored.

The composite action between the deck and the girders provides restraining to the deck. When concrete shrinks, the external restraint from the girder, as well as the internal restraints from the reinforcement and aggregates, produces tensile stresses in the longitudinal direction of the deck. When these stresses reach the tensile strength of concrete (low at early ages), transverse cracks are developed in the deck starting from the bottom and extending to the top surface. In continuous beams or in beams with fixed-end restraint, the negative moments resulting from mechanical loads produce tensile stress in the deck, which, when combined with the shrinkage stresses, aggravate the problem of deck cracking. Although individually the tensile stresses resulting from each of these factors may not exceed the tensile strength of the bridge deck, the combination of stresses can be damaging.

Shrinkage and creep stresses have been cited as one of the leading causes of transverse deck cracking in concrete bridges. D'Ambrosia et al. (2004) studied early age creep and shrinkage of a concrete bridge under restrained conditions and experiencing a constant applied load for the first week after it was cast. A uniaxial test procedure was employed to measure the shrinkage stress and strain, while the tensile creep and resultant stress relaxation were determined using superposition analysis. Modifications were made to an existing prediction model to account for the early age of the concrete at the time the measurements were taken in this study. The validity of the early age model was assessed by comparison against current creep and shrinkage models. The early age model was shown by these comparisons to be accurate. Goel et al. (2006) found the GL2000 model to exhibit the greatest accuracy in predicting creep and shrinkage strains in prestressed concrete. This model, as well as several others, including the ACI-209R-82 model, B3 model, and CEB-FIP model code 90, was compared to experimental results to determine the relative accuracy of each.

Transverse cracks on high performance (HP) concrete decks are characteristically more distinct and wider than those in conventional concrete bridge decks. Pozzolanic materials such as silica fume and water reducing admixtures/superplasticizers are used to produce HP concrete with higher strength, greater resistance to free-thaw cycles, and significantly lower creep properties. HP concrete has a compressive strength,  $f_c'$ , that is greater than 6,000 psi. It has been shown that the higher compressive strength  $f_c'$  of concrete cannot be the main reason affecting the crack size (Minnetyan and Assamany 2004). This is reasonable since compressive strength increases stiffness as well as bond strength and tensile strength by the same proportions. The

effect of higher stiffness will be to increase crack width and higher bond/tensile strengths will decrease crack width by approximately the same amount. Therefore, the net effects of higher  $f_c'$  cannot account for the wider cracks on HP concrete decks. A detailed finite element progressive cracking analysis code will be able to account for the effects of all properties of the deck and composite girders on crack widths. Examination of other factors affecting the maximum crack width and their inclusion in the FEA model is required. Concrete shrinks when exposed to a drying environment. If concrete is restrained from shrinkage, tensile stresses develop and concrete may crack. Maximum crack widths develop where load-induced stresses are superimposed on the residual stresses from shrinkage. Crack sizes and shrinkage strain measurements indicate significantly higher shrinkage occurs in HP concrete unless moisture content is very carefully controlled during the first 24 hours of curing (Streeter 1999, Wiegink et al. 1996). Furthermore, construction can affect transverse deck cracking. Careful construction practices are often required to reduce such a risk where the first large stresses in a concrete deck develop in the first 12 to 24 hours, when temperatures change rapidly from early hydration. The exposure to environmental conditions, e.g. ambient humidity and temperature, has a major effect on transverse cracks.

For structures exposed to harsh environments, such as bridge decks exposed to deicing salts, ACI 350 recommends limiting crack width in the range of 0.0085 inch to 0.010 inch. If the HP concrete mix and current construction practices are maintained, then longitudinal temperature and shrinkage (T&S) steel needs to be increased sufficiently to limit bridge deck crack size to 0.010 inch. Minimum T&S steel (#5 at 18 inches) required by AASHTO 17<sup>th</sup> Edition Bridge Design Manual has been sufficient to limit crack sizes for conventional concrete but is not sufficient to limit crack widths for HP concrete. It has been shown that for HP concrete, with current construction practices, if the maximum crack size at the negative moment regions is to be limited to 0.010 inch, then for a typical bridge deck #5 epoxy coated bars at 4.14 inch maximum spacing are required for the top layer of T&S reinforcement at the negative moment regions (Minnetyan and Assamany 2004). The alternative is to modify the HP concrete mix and/or improve construction practices to eliminate excessive shrinkage and perhaps encourage a reasonable amount of creep necessary for relaxation of shrinkage stresses.

Compressive strength and elastic modulus increase with increasing amounts of silica fume included in the concrete mix. Presence of silica fume increases shrinkage by approximately 20 to 25 percent, especially if HP concrete is allowed to experience early age drying shrinkage. Creep is reduced by more than 60 percent due to the presence of 10 percent silica fume (Wiegink et al. 1996). Shrinkage of concrete produces tensile stresses that produce cracks. Conventional concrete is able to creep, therefore the tensile stresses caused by shrinkage are relaxed and crack size is limited. HP concrete with greatly reduced creep is unable to dissipate tensile stresses, therefore, it cracks. The combination of increase in shrinkage due to early age mishandling and reduced creep properties of HP concretes containing silica fume and superplasticizers is detrimental and produces large cracks. From the shrinkage and creep data, one can deduce that HP concretes containing silica fumes are likely to develop crack widths that are at least twice those developed in conventional concrete decks without significant amounts of silica fume (Minnetyan and Assamany 2004). Yazdani et al. (2007) investigated a means by which HP concrete can be cured more rapidly without an increase in shrinkage cracks. Silica fume, a common additive in HP concrete mixes, causes accelerated curing of the concrete. This causes an elevation in heat of hydration and increased water demand. Steam curing has been

tested in an effort to offset the increased shrinkage caused by accelerated curing. A bridge steam cured for 12 hours was found to have no cracking at one year.

A case study was performed on a bridge in Tennessee built on one half with high strength concrete and on the other with normal strength concrete. Its construction included instruments for monitoring the strains and temperature variations in its beams, deck, and diaphragms. The study found that the high strength concrete experienced differential shrinkage with respect to the concrete in the bridge deck. Rapidly developed creep and shrinkage strains were observed, as well as rapidly developed time-dependent cambers. Recommendations were made for using a fogging system during placement of high strength concrete in order to reduce moisture loss due to evaporation, leading to a decrease in shrinkage (Huo et al. 2006). Inclusion of such construction practices would need to be integrated into the prediction model for greater accuracy.

#### **1.4. Thermal Effects**

As concrete cures, it experiences temperature variations resulting from multiple sources. Primarily, the temperature of concrete is affected by the heat of hydration from the curing process and from changes in environmental conditions due to daily and seasonal cycling of temperatures. Kapila et al. (1997) developed a model that can simulate the temperature variations that take place during the curing process of concrete. The model is accurate within 2°C. It was created based on fundamental heat and mass transfer principles and also has the capability to track the water mole fraction and unreacted cement fraction for the first 72 hours of curing. Considered in this model are various environmental factors, such as wind speeds and the changes in solar radiation during different hours of the day and different seasons in the year. Wojcik and Fitzjarrald (2001) developed an empirical model for concrete curing that considers thermal and moisture behaviors during the first several days after concrete placement. The investigation performed looks at the curing process from the standpoint of energy balances and heat transfer between the atmosphere and the concrete surface. No previous work had been done to understand these energy balances.

#### **1.5. Load Effects**

Dead load and live load stresses have a significant impact on transverse cracking of bridge decks. Previous work has been done to understand the effects of loading on transverse deck cracking, particularly the effects of repeated loading. Soehardjono et al. (2006) used a fracture mechanics approach to develop a design equation capable of predicting maximum crack width and crack spacing in precast reinforced concrete slabs. It was found that steel stress ratio, reinforcement ratio, and repeated loading do affect the maximum crack width in concrete. Chung and Sotelino (2005) developed a finite element model capable of predicting, with good accuracy, the load level at which cracking will initiate in a composite steel girder bridge, the ultimate load capacity that will be experienced, and the overall crack pattern. Oh and Kim adjusted a previous crack width prediction model to account for the stress-slip behavior between concrete and its reinforcing steel. This model focuses on repeated loading of reinforced concrete beams. The software developed in this research quantifies all temperature, shrinkage, and load effects that produce cracking.

## **1.6. Analysis of Cracking**

A finite element based structural analysis code that is able to take into account the effects of particulate and chopped fiber additives to concrete as well as shrinkage, creep, and composite action of the deck and girders is needed. Additionally, the developed software needs to track and evaluate crack growth processes. Chung and Sotelino (2005) developed a finite element model that uses a multi-layer approach to construct the bridge deck and steel girders. Multipoint constraints ensure accurate composite action. The shell elements are created as shear flexible elements, while Timoshenko beam elements are used to idealize the structural steel girder. In addition, a material model is created for reinforced concrete using the strain decomposition approach, which enables inclusion of the effects of the concrete surface based on physical behavior such as aggregate interlock. The material model is integrated with the various structural elements in ABAQUS software.

Experimental and analytical models have been developed to enable bridge designers to calculate shrinkage and thermal stresses in bridge decks (French et al. 1999; Krauss and Rogalla 1996), so that they can evaluate and modify designs to reduce these stresses and the risk of transverse deck cracking. Previous studies have focused primarily on unveiling the extent and significance of cracking and trying to pinpoint possible causes. While there is agreement among researchers on the major causes, the relative contribution of each factor has not been completely determined and the problem of premature deck cracking still exists. The predominant reason for this is because most of the factors have simply been discussed qualitatively and there has been little quantitative analysis of these mechanisms. In the last few years, researchers have developed numerical models using finite element or finite difference methods to simulate real structures under different environmental conditions. Saadeghvaziri and Hadidi (2002) studied the developed tensile stresses in bridge decks under the effect of many design factors, e.g. girder stiffness, deck thickness, girder spacing, relative stiffness of deck to girder, and amount of reinforcements; in their simulation, they assumed that the shrinkage strain is constant in value and over the deck depth. Kwak et al. (2000) used a previously developed algorithm to theoretically investigate transverse cracking of bridge decks based on the effects of the concrete slab placing sequence. These effects were found to be negligible relative to the ultimate shrinkage strain results from drying shrinkage, which is expressed as a function of concrete slump and relative humidity. In the calculations for ultimate shrinkage strain, physical properties, such as unit weight of the cement and air content of the concrete, were assumed based on typical values for concrete batches. Sheban et al. (2006) studied the drying shrinkage-induced damage in concrete structures and they developed a finite element simulation program capable of estimating the stress and strain variations with time in bridge decks. This program can be used to study the effects of many parameters, e.g. concrete mixing ingredients, types and proportions, ambient dry environment, and support restraints. With some modifications, e.g. the effect of thermal stresses and stress relaxation, the computer program can be used for analysis of early age transverse cracks in composite bridge decks.

Several models have been developed capable of predicting various behaviors in concrete bridge decks. HIPERPAV, a software package, has the capability to predict early-age behavior of jointed plain concrete pavement (JPCP). A second version of the program has been established which possesses enhanced prediction capabilities. In addition to early-age behavior of JPCP, it can also model long-term performance of JPCP, as well as early-age behavior of

continuously reinforced concrete pavement (CRCP) (Ruiz et al. 2005). Gilbert (2008) developed a crack width calculation procedure that incorporates the development of concrete bridge deck cracking with time as well as the time-dependent increase in shrinkage and how it affects crack width. A variety of slabs and beams were tested in a lab under sustained service loads, and this calculation procedure was shown to provide good agreement with lab results for crack spacing and width. Okui and Nagai (2007) developed a finite element model for performing a time-dependent creep and shrinkage analysis of I-girders. Unique to this model is its incorporation of the shear-lag effect in the concrete deck. The Euler method was used for creep analysis. In a comparison against beam theory analysis, the finite element model was found to be more accurate because it includes the shear-lag effect and can account for sudden changes in concrete stiffness, which occur due to creep and shrinkage. Xia and Brownjohn (2004) used a finite element model to assess the structural condition of bridges. Based on investigations of bridge deck damage, residual stiffness and load-carrying capacity were determined. Performing a quantitative condition assessment of the damage enables more objective inspection, moving away from simple visual investigations.

In the development of finite element based structural analysis software, every possible failure mode must be accounted for in the damage tracking process to enable accurate representation of progressive damage and fracture (Zhang and Minnetyan 2007). Particulate, fibrous, and fiber-composite reinforcement for structures must take into account problems of chemical compatibility, bond strength, ductility, and environmental hazards. It is proposed to include in the finite element model the following factors: (1) Chemical and physical compatibility of materials that constitute the concrete. (2) Physical stiffness, strength, and ductility of concrete. (3) Chemical and physical compatibility of the concrete with the particulate and fibrous materials included in the concrete mix. (4) Chemical and physical compatibility of the concrete mix with bar and mesh reinforcement materials. (5) Effects of external physical and chemical environments such as temperature, moisture, freezing and thawing, and deicing salts. (6) Structural durability under expected service loads and possible overloads. (7) Environmental contamination and safety in case of structural damage. (8) Effects of all constituents of the concrete mix on creep and shrinkage properties of the concrete. Concrete deck structural degradations due to hygrothermal exposure duration and cycles will be taken into account in the evaluation of long-term durability (Minnetyan et al. 1992; Shah and Chamis 1996). Proposed software will rely on the existing computational infrastructure developed by the PI over the past nineteen years (Minnetyan et al. 1990, 1998; Huang and Minnetyan 1998, 2001; Minnetyan and Abdi 2004).

The implemented computer program will be based on an award winning software methodology (NASA software of the year 1999 and R&D Magazine's 100 Best for the year 2000) that will utilize proven algorithms for integration of FEA (Nakazawa et al. 1987) with composite mechanics (Murthy and Chamis 1986) and damage/crack propagation analysis (Huang and Minnetyan 1998). This foundation focuses on hierarchical progressive failure analyses and verification at each step of the simulation process. Verification of basic material constituents, built up to sub components, such as concrete constituents, deck geometry, reinforcement bar distribution/locations/coating, shear studs, and structural steel design details (i.e. girder depth, width, spacing, stiffeners, diaphragms) to the final composite deck structure. The elements of PFA simulation of composite bridge decks involve: 1) structural layering methodology utilizing FEA plate elements with through-the-thickness representation, 2) simulation of effects on global

static, cyclic fatigue strength and environmental tolerance, including material effects and conditions which include rebar coating and the resulting interphase properties with the surrounding concrete, residual stresses, and creep, 3) inclusion of material nonlinearities through periodic updating of material property parameters, 4) simulation of the initiation and growth of cracking under static, impact, fatigue as well as temperature and shrinkage loads, and 5) determining sensitivities of failure modes to such design parameters as concrete mix, slab thickness, reinforcement distribution, and girder properties.

Our analytical approach uses 4 key elements to minimize program cost and risk and maximize product performance: (1) Minimize Code development by integrating, in modular form, available and proven software, (2) Invoke the best available algorithms for simulating all physical and material behavior, (3) Use bridge deck test results and actual material test data to calibrate the simulation process, and (4) Construct analytical models and execute the codes in an Integrated Structural Analysis Process.

### ***1.7. Summary of Part 1***

Bridge deck cracking is a significant problem. Sensitivity studies have identified the main causes. Recommendations have been made and new design practices are expected to reduce cracking by adding more longitudinal reinforcement. Finite element analyses have identified the locations of crack initiation. Semi-empirical models are used to compute the crack widths. The next task is the formulation of the computational framework including the (a) Finite Element Analysis software module, (b) composite mechanics module, and (c) damage tracking module. A two-span composite bridge deck model shall be included.

## Part 2. Composite Bridge Analysis (CBRAN) Computational Framework

The computational framework of the computer program designed to evaluate the effects of design and construction parameters on concrete deck cracking is described. The computer program uses finite element analysis of deck and girders. Mindlin type thick plate/shell quadrilateral elements are used to represent the reinforced concrete deck as well as the girder elements. The concrete deck is subdivided into layers using composite mechanics to evaluate stresses and strains through the thickness that will be used to assess cracking. The layered representation can also account for the effects of cure temperature and differences in the cure temperature layer by layer across the deck thickness. Residual stresses due to cooling down to the use temperature can be computed by the composite mechanics module and added to the load induced stresses. Crack initiation, growth, fracture progression, and crack size will be simulated under the developed computational framework. An example deck-girder structure is used to demonstrate the computation of deck stresses under point loading. Computational capabilities to quantify the internal stresses through the thickness of the deck are demonstrated. The software accounts for the presence of the deck main reinforcement and the temperature and shrinkage (T&S) reinforcement and can analyze the composite deck behavior under any loading, geometry, material combinations, reinforcement, and boundary conditions. The computer code is developed for the analysis of composite structures (Minnetyan et al 1990). It is composed of an executive module, an analysis package for micromechanics and macromechanics (ICAN), and a finite element analysis module (MHOST). The ICAN (Murthy and Chamis 1986) (Integrated Composites ANalyzer) and MHOST (Nakazawa et al 1987) computer codes are originally independent codes that have been integrated into the software as computational modules. The ICAN computer code is used to assemble the through-the-thickness finite element properties that define the relationships between the generalized through-the-thickness stresses and strains (Definitions of MHOST thick shell element generalized stress and strain components are given in the MHOST Users Manual). ICAN computes the anisotropic elastic constants from the physical information on the layered composite structure. After a finite element analysis ICAN is used to compute the layer-by-layer stresses and strains. Localized damage and cracking is assessed by applying failure criteria to the state of stress in each layer. Effects of loading and residual stresses due to temperature and shrinkage are taken into account in computing the stress and strain state in each layer. The failure criteria include the positive and negative limits of the six stress components and a modified distortion energy failure criterion. Additional user defined failure criteria may be added. ICAN utilizes a databank file that contains the properties of typical constituent materials that may be defined as “fiber” and/or “matrix” properties. The integration of ICAN with a general purpose structural analysis code results in an incremental loading composites analyzer with equilibrium checks at each local iteration for each load increment. The piecewise linear constitutive relationships determined by ICAN are supplied to the MHOST finite element analysis module for the definition of nodal finite element properties at each load increment. The executive module of the software determines the appropriate step size for each

load increment and directs the computational simulation of structural analysis under loading. The use of MHOST as the structural analysis module is facilitated by the ability of the MHOST quadrilateral shell element (MHOST Users Manual defines the quadrilateral shell element properties) to accept the generalized through-the-thickness force-deformation relations computed by ICAN. The software has the capability of predicting the locations of surface and interior cracking and damage initiation as well as fracture progression and coalescence.

For the purpose of a demonstration example a composite bridge deck-girder segment is selected. The deck reinforcement and girder elements were selected similar to those of the Route 56 Bridge on Raquette River in Colton, NY. However the model attempted is to represent a two-span rather than a three-span composite deck/girder system. Also the #7 top longitudinal bars alternating with the #5 bars at 1'-6", extending 40 ft from the center of each pier are not included in the model. Only one span is modeled applying symmetry conditions at the continuous support. The finite element model consists of 360 or 1,440 rectangular elements for the coarse and refined models, respectively. The pattern of node numbering for each cross-section is shown in Figure 2-1. Cross-section locations are shown in Figures 2-2 and 2-3, for the 450 node and 1,830 node models, respectively. The model is subjected to a 1,000 lb concentrated loading at a 60 ft (720 in) distance from the continuous support. The concentrated load is transversely distributed on the concrete deck immediately above the girder.

## ***2.1 Model Development***

In order to test the program being created as the computational framework for this project, the initial input file was developed in three segments. One file segment contains a collection of matrices defining the location of the nodes, element connectivity, and duplicate nodes in a Finite Element model of the bridge section. Another file segment contains the necessary material properties for all of the different materials in the bridge. The third file segment is a compilation of the data from the first file and information defining the materials of the bridge in terms of layered representation (plies) for a composite material analysis. The first file segment is created using a Matlab program that creates a text file containing all the information produced. The other file segments require assembly in a simple text editor (Microsoft Notepad was used in this instance). These two file segments are constructed based on templates created previously to work with the computational framework.

## ***2.2 Creation of Finite Element Model Geometry***

As stated, the creation of the first file was performed by a Matlab program. The program creates three different matrices, which together describe the geometry of a finite element model of the bridge section being considered. The model is fixed at one end representing symmetry condition (corresponding to the location of the continuous support) and simply supported at the other. The dimensions and node and element numbering schemes for the bridge section tested are shown in 2-1. All units are in inches.



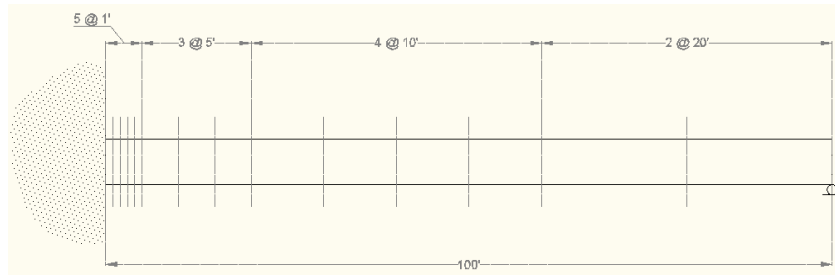


Figure 2-2 – Cross-section locations along the length of the bridge for 450 node model

To evaluate convergence of the finite element solution a more refined model with 1830 nodes was created. The cross-section spacing scheme of the 1830 node model for the bridge can be seen in Figure 2-3.

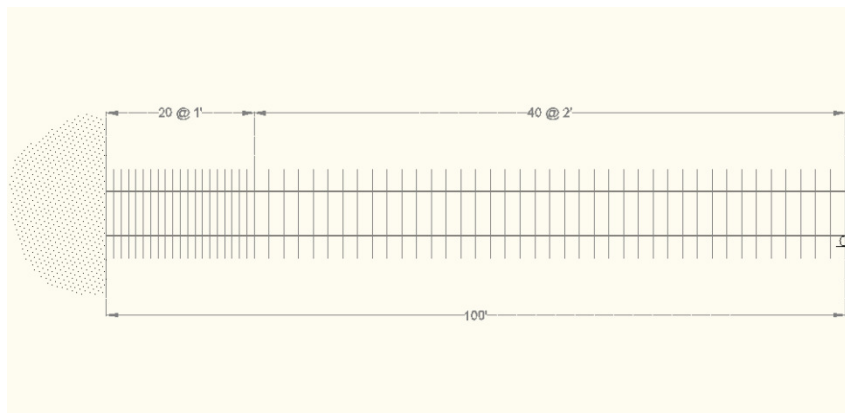


Figure 2-3– Cross-section locations along the length of the bridge for 1830 node model

Using all of this predetermined information, a Matlab program was written to generate the finite element model data. The first matrix produced by the program contains the x-, y-, and z-coordinates for all 450 nodes in the finite element model, as well as the thickness of the cross-section at the node, and the node type. Currently, this is created from a single hand-calculated matrix containing the information for one cross-section, using a loop to project the information along the length of the bridge segment considered. The last column in this first matrix contains the node type information. The bridge investigated contains five different material layer types (LTYP), as listed below

- 1 : Reinforced concrete deck slab
- 2 : Reinforced concrete deck slab with haunch
- 3 : Top flange of steel girder
- 4 : Web of steel girder
- 5 : Bottom flange of steel girder

Depending on the location of the node in the cross-section, it is applied an appropriate value of 1 to 5. For now, these are superficial quantities. The actual properties of each of these materials are defined in the other two input files, to be explained shortly.

The second matrix produced by the Matlab program contains the element connectivity information for the model. Since plate elements are used in this analysis, four nodes must be defined for each element. The matrix contains five columns, the first of which being the element number and the remaining four containing the node numbers that act as the four corners of the element. The nodes are connected in a counter-clockwise fashion as observed from the positive z axis. The coordinate system used for the finite element model must be a right handed coordinate system. A single matrix, which contains the connectivity information for the elements spanning the first and second cross-sections, is assembled by hand. Then, again using a loop, this information is projected along the x-axis through the length of the model, creating a matrix with the connectivity information for the whole one-hundred foot long model. There are a total of 336 elements in the coarse model. The refined model has 1440 elements. The maximum deck tensile stress computed by the coarse model in layer 1 of node 8 is 13.54 psi. The stress computed by the refined model is 13.65 psi. Since the difference is less than one percent the finite element solution is considered to be converged.

Lastly, the Matlab program creates a two-column matrix containing the duplicate node information for the model, applying master/slave relations to specific nodes on each cross-section. In each relation, the slave node is constrained to translate and rotate with the master node. In terms of deciding which nodes to make masters and which to make slaves, there are a few considerations to observe. First of all, a node cannot be both a slave and a master, even in different relationships. However, a master may have multiple slaves, but a slave may have only one master. For this bridge, nodes 6-10 are assigned as the masters of nodes 16-20 in order to assure connected behavior between the girder and the bridge deck. Also, 6 is the master of 5 and 10 the master of 11 to make sure the portions of the bridge deck with changing dimensions still responded as one connected unit. Similarly, node 8 is made the master of node 21 and 25 the master of 28 to ensure that the girder acts as one solid unit during the analysis as well. The matrix containing the master/slave relation information, like the other two, is created by projecting a single, hand-produced matrix along the x-direction to produce a matrix with information for all fifteen cross-sections. The two columns contain the node numbers of the master node and slave node for each relation, in that order. An alternative to the master/slave relationships is to use tying equations or rigid beam elements between the corresponding nodes in the haunch and flange.

The information contained in the three matrices described above defines a finite element model which is the basis of the analysis. For visual verification of the model, the Matlab program also creates a three-dimensional plot of the nodes and the elements connecting them. This image is shown in Figure 2-4.

For convenience, in Task 7 of this research project the Matlab program approach was replaced by preprocessor programs for the rapid generation of structural analysis input files in one step.

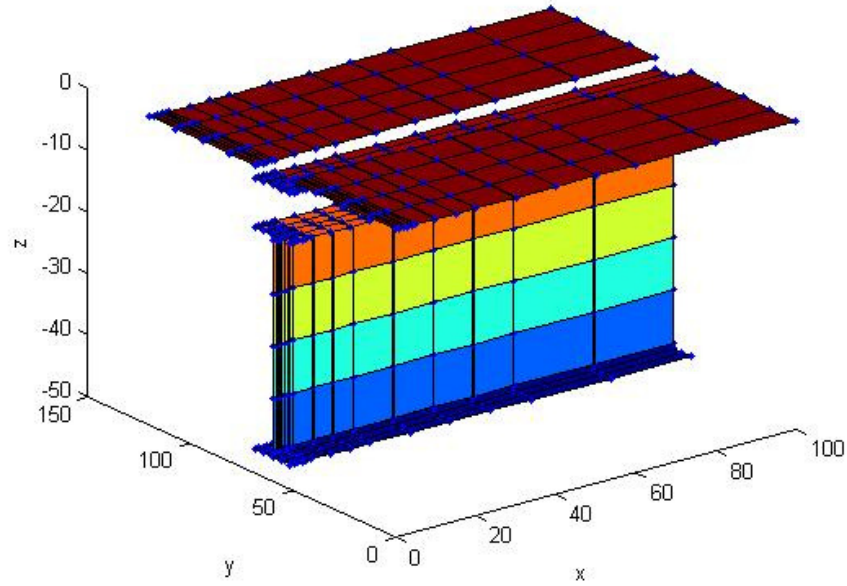


Figure 2-4 - Three-dimensional image (not to scale) of the 450 Node Finite Element Model

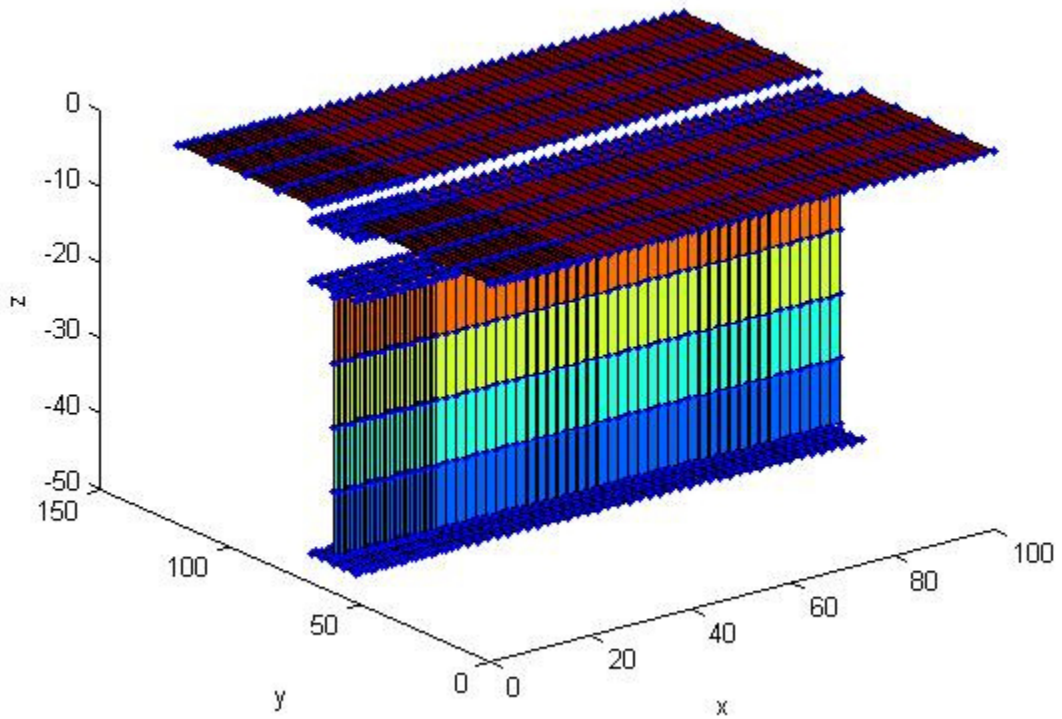


Figure 2-5 - Three-dimensional image (not to scale) of the 1830 Node Finite Element Model

Finally, the Matlab program saves a text file containing the three matrices to the working directory, which can then be read by the computational framework to assemble the required input file for the bridge model.

## **2.3 Definition of Material Properties**

The second input file, referred to as the databank, contains the necessary material properties for the analysis. There are several materials defined here, each of which is designated as a matrix or fiber material. Matrices are the primary materials that compose the different portions of the bridge. Fibers are secondary materials located within a matrix, such as reinforcing steel bars within a concrete bridge deck. Appendix 1 contains databank properties of constituent materials used in the analysis of bridge deck models. The constituent materials databank file is organized as described in the ICAN users and programmers manual (Murthy and Chamis 1986), a scanned copy of which is included in the final CD.

Depending on whether a material is a fiber or a matrix, there are different properties used for its definition. For matrices, the required information is weight density ( $\rho_m$ ), normal modulus ( $E_m$ ), Poisson's ratio ( $\nu_m$ ), coefficient of thermal expansion ( $\alpha_m$ ), thermal conductivity ( $K_m$ ), heat capacity ( $C_m$ ), tensile strength ( $S_{mT}$ ), compressive strength ( $S_{mC}$ ), shear strength ( $S_{mS}$ ), allowable tensile strain ( $\varepsilon_{mT}$ ), allowable compressive strain ( $\varepsilon_{mC}$ ), allowable shear strain ( $\varepsilon_{mS}$ ), allowable torsional strain ( $\varepsilon_{mTOR}$ ), void conductivity ( $K_v$ ), and melting temperature ( $T_{gdr}$ ). For materials that are fibers, the number of fibers per end ( $N_f$ ), fiber diameter ( $d_f$ ), weight density ( $\rho_f$ ), melting temperature ( $Temp_{mf}$ ), normal modulus (11) ( $E_{f11}$ ), normal modulus (22) ( $E_{f22}$ ), Poisson's ratio (12) ( $\nu_{f12}$ ), Poisson's ratio (23) ( $\nu_{f23}$ ), shear modulus (12) ( $G_{f12}$ ), shear modulus (23) ( $G_{f23}$ ), coefficient of thermal expansion (11) ( $\alpha_{f11}$ ), coefficient of thermal expansion (22) ( $\alpha_{f22}$ ), thermal conductivity (11) ( $K_{f11}$ ), thermal conductivity (22) ( $K_{f22}$ ), heat capacity ( $C_f$ ), tensile strength (11) ( $S_{f11T}$ ), compressive strength (11) ( $S_{f11C}$ ), tensile strength (22) ( $S_{f22T}$ ), compressive strength (22) ( $S_{f22C}$ ), torsion strength (12) ( $S_{f12S}$ ), and torsion strength (23) ( $S_{f23S}$ ) are listed. All of these properties must be supplied in the databank file. The units are inches, pounds, hours, and degrees Fahrenheit. For both types of materials, there may also be initial (reference) normal and shear stresses and stress rates, as well as a table of exponents to define nonlinear stress-strain behavior which is not pertinent in this analysis and is not expected to be needed in this research, but may be added to the databank to ensure compatibility of the files with certain commercial software.

## **2.4 Definition of Ply Properties for Composite Material Analysis**

The computational framework performs a composite analysis of the bridge, thus each material must be described in terms of plies to work with the program. Even those materials that are homogeneous (such as the girder steel) are defined as composite materials. The homogeneous materials are created as almost entirely matrix with a very small amount of fiber of the same material contained within them. The actual composite materials, namely the reinforced concrete bridge deck, are defined in terms of several plies, thinner ones near the top of the bridge deck (the location of interest). There are five materials described in the third file, which pertain to the five material types assigned to the nodes in the creation of the finite element model.

Each material is defined by a matrix which contains a variety of information. The matrix for material 1 (the reinforced concrete bridge deck) is shown below.

LTYPE	1	24	3					
PLY	1	1	70.00	70.0	0.0	0.	0.100	
PLY	2	1	70.00	70.0	0.0	0.	0.100	
PLY	3	1	70.00	70.0	0.0	0.	0.100	
PLY	4	1	70.00	70.0	0.0	0.	0.100	
PLY	5	1	70.00	70.0	0.0	0.	0.100	
PLY	6	1	70.00	70.0	0.0	0.	0.200	
PLY	7	1	70.00	70.0	0.0	0.	0.300	
PLY	8	1	70.00	70.0	0.0	0.	0.500	
PLY	9	1	70.00	70.0	0.0	0.	0.500	
PLY	10	1	70.00	70.0	0.0	0.	0.500	
PLY	11	1	70.00	70.0	0.0	0.	0.500	
PLY	12	2	70.00	70.0	0.0	0.	0.500	
PLY	13	3	70.00	70.0	0.0	90.	0.500	
PLY	14	1	70.00	70.0	0.0	0.	0.620	
PLY	15	1	70.00	70.0	0.0	0.	0.620	
PLY	16	1	70.00	70.0	0.0	0.	0.620	
PLY	17	1	70.00	70.0	0.0	0.	0.620	
PLY	18	1	70.00	70.0	0.0	0.	0.620	
PLY	19	2	70.00	70.0	0.0	0.	0.500	
PLY	20	3	70.00	70.0	0.0	90.	0.500	
PLY	21	1	70.00	70.0	0.0	0.	0.350	
PLY	22	1	70.00	70.0	0.0	0.	0.350	
PLY	23	1	70.00	70.0	0.0	0.	0.350	
PLY	24	1	70.00	70.0	0.0	0.	0.350	
MATCRD	1CNCFCNC	.300	.01	CNCFCNC	0.0	.60	.03	
MATCRD	2RBSFCNC	.050	.01	CNCFCNC	0.0	.60	.03	
MATCRD	3RBSFCNC	.050	.01	CNCFCNC	0.0	.60	.03	

The first line in each layered material properties type (LTYPE) definition provides three numbers; the LTYPE number (corresponding with those listed in the description of the nodal coordinates), the number of layers (plies) defined in the LTYPE, and the number of materials (MATCRD). Each MATCRD line defines proportions of “matrices” and “fibers” from the databank used in the material of a layer. For the sake of clarity, the materials described in the databank will be referred to as constituent-materials. For this LTYPE, the next twenty-four lines identify the twenty-four different plies assigned to the material. From left to right, the columns in this matrix contain the ply number, material (MATCRD) number, usage temperature, cure temperature, moisture content, orientation of the layer (PLY) coordinates with respect to the x-axis (in degrees), and the thickness of the ply. The units of this matrix are inches and degrees Fahrenheit. The temperature and moisture distributions were determined in Task 3 and the corresponding layer-by-layer values computed.

Let’s take a closer look at each of these columns. The first, as mentioned previously, contains the ply number. The second, the material (MATCRD) number, will be discussed shortly. The third and fourth columns contain the usage and cure temperatures, respectively. A

uniform temperature of 70°F was applied to both columns for all plies in the bridge. The next column, moisture content, was set to 0 in all cases because it will require the results of Task 3 to be completed. In the fifth column, the ply orientation is defined. Since the concrete is treated as homogeneous, there is no orientation applied to the plies corresponding to concrete. However, plies 12, 13 and 19, 20 contain reinforcing steel. The primary steel reinforcement (plies 13 and 20) has a fiber orientation of 90° because it runs perpendicular to the x-axis. However, the secondary (T&S) steel reinforcement (plies 12 and 19) has an orientation of 0° because it runs parallel to the x-axis. The last column contains the thickness of the ply, ranging from 0.1 inch to 0.62 inches for this example, depending on the desired level of refinement for calculation.

Now back to the constituent-materials. The last three lines defining material 1 describe the properties of and proportions of the three constituent-materials contained within it. The first column is the material (MATCRD) number, corresponding to the materials listed in the corresponding layers with the ply information. The second column is the constituent-material names, which corresponds to the combination of names in the databank. Third, the fiber volume ratio is listed. Notice that for the concrete it is a very small number. As explained earlier, even those materials considered to be homogeneous must still be defined as a composite material and will thus be given a very small fiber ratio. The second and third MATCRD lines represent the concrete deck layers with main reinforcement and T&S reinforcement, respectively. Each have rebar steel as a constituent. For this example the longitudinal and transverse reinforcements are assumed isotropic according to the current NYSDOT practice as #4 bars at 8" spacing.

The fourth column in this sub-material matrix represents the void ratio of the constituent fiber material. The last four columns in this matrix contain information about the secondary composite system in each MATCRD material (name, secondary material ratio, fiber ratio, void ratio), but since there are none in this case, the secondary material ratio for each of these is set to zero and the rest of the values become irrelevant.

After the completion of the five material specifications, the file FOR085.ORG contains all of the information about the geometry of the model, which is currently obtained by a preprocessor as outlined in Task 7 report. Previously, the CBRAN input file was obtained from the file created by the Matlab program. In addition to this, another matrix was created which defined the boundary conditions for each of the nodes in the model. There are six degrees of freedom at each node; translation along the x-, y-, and z-axes, as well as rotation about each of these axes. Slave nodes are already fully bound since they are fixed to move with their master nodes. The degrees of freedom to be fixed for the remainder of the nodes are determined based on the expected behavior of the bridge. The last portion of the FOR085.ORG file contains loading information and then instructs the computational framework to calculate the displacement, stress, and strain at each node on the bridge. See Appendix 1; Making Software Operational, for details.

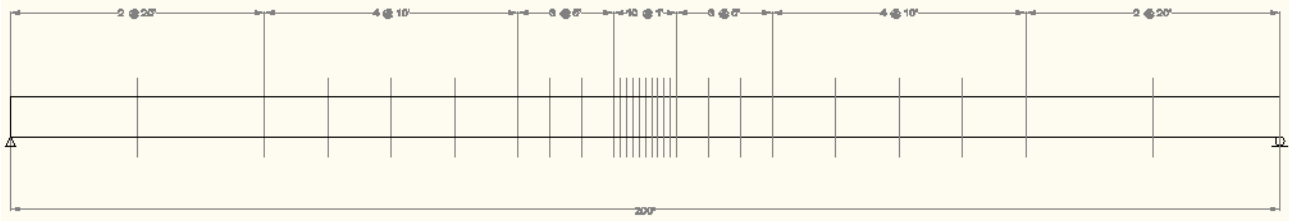


Figure 2-6 - Elevation Image (not to scale) of an 850 Node Two-Span Continuous Finite Element Model

### 2.5 Use of Tying Equations Instead of Duplicate Nodes for Improved Accuracy

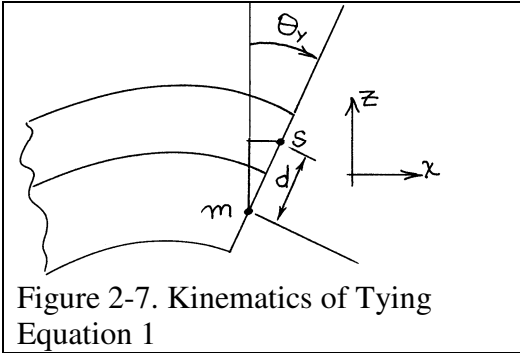


Figure 2-7. Kinematics of Tying Equation 1

The model was first constructed by duplicate node assignments had a kinematic inconsistency. TWG member Ryan Lund pointed out that the duplicate node assignments of stacked layers would result in a deformation pattern that would produce discontinuity of normal strains at the top and bottom boundaries of stacked elements. To solve the problem a new model of the two-span deck-girder replaced duplicate node assignments with tying equations. Each master-slave node combination was assigned six tying equations for the six degrees of freedom ( $\Delta_x$ ,  $\Delta_y$ ,  $\Delta_z$ ,  $\Theta_x$ ,  $\Theta_y$ ,  $\Theta_z$ ). The

following tying equations were used: 1)  $\Delta_{xs} = \Delta_{xm} + \Theta_{ym} * (z_s - z_m)$ ; 2)  $\Delta_{ys} = \Delta_{ym}$ ; 3)  $\Delta_{zs} = \Delta_{zm}$ ; 4)  $\Theta_{xs} = \Theta_{xm}$ ; 5)  $\Theta_{ys} = \Theta_{ym}$ ; 6)  $\Theta_{zs} = \Theta_{zm}$ . Figure 2-7 shows the resulting kinematics due to tying equation 1. In Figure 2-7 and in the tying equations m indicates the master node and s indicates the slave node. The difference in the z coordinates of the slave and master nodes is denoted as “d” in Figure 2-7. The six tying equations simulate an effective “rigid link” between the nodes of stacked elements within the definition of small displacement. The tying equations for each node are input according to the MHOST Users’ Manual Section D.3 (Nakazawa et al 1987). The example below shows the first set of tying equations that in addition to providing rotational compatibility relate the x components of connected node displacements to the rotation about the y axis.

```

*TYING
      3      5      1      6      1      6      5
1.00000  2.00000
      2      5      2      6      2
1.00000
      2      5      3      6      3
1.00000
      2      5      4      6      4
1.00000
      2      5      5      6      5
1.00000
      2      5      6      6      6
1.00000
      .
      .
      .

```

Results of the model with tying equations described above indicate that strains and stresses are consistent across the top and bottom stacked element boundaries.

## 2.6 Improvement of the Tying Equations Model

After obtaining the above results it was decided to improve the tying equations by adding compatibility of  $\Delta_y$  and  $\theta_x$ . This was done by adding the tying equation  $\Delta_{ys} = \Delta_{ym} - \Theta_{xm} * (z_s - z_m)$ . The negative sign is because a positive  $\Theta_{xm}$  will produce a negative  $\Delta_{ys}$  if  $z_s$  is above  $z_m$ . This addition makes the tying equations equivalent to a rigid link. The input data for the tying equations was modified as shown below. The resulting stresses and strains were changed slightly and are given next. The stress data prior to the addition of the  $\Delta_y$  and  $\theta_x$  compatibility equation is left in the report for reference.

```

*TYING
      3      5      1      6      1      6      5
1.00000  2.00000
      3      5      2      6      2      6      4
1.00000 -2.00000
      2      5      3      6      3
1.00000
      2      5      4      6      4
1.00000
      2      5      5      6      5
1.00000
      2      5      6      6      6
1.00000
      .
      .

```

Next, stresses and strains in the top flange of the girder with corrected lateral tying equations including the compatibility equation  $\Delta_{ys} = \Delta_{ym} - \Theta_{xm} * (z_s - z_m)$  are given. Improved stress and strain results after correction of tying Equation on lateral displacements are shown below:

```

      870
IPASS=    1 IHOST=    1
PLY NO., SIG11,      SIG22,      SIG12,      SIG13,      SIG23,      EPS11,      EPS22

                                NODE NUMBER= 428
  1  0.7443E+01  0.6716E-01 -0.1939E-09  0.5668E-16  0.1333E-17  0.1683E-05 -0.3221E-06
  2  0.7160E+01  0.5285E-01 -0.1966E-09  0.1639E-15  0.3854E-17  0.1683E-05 -0.3221E-06
  3  0.6876E+01  0.3854E-01 -0.1992E-09  0.2628E-15  0.6180E-17  0.1683E-05 -0.3221E-06
  4  0.6593E+01  0.2423E-01 -0.2019E-09  0.3535E-15  0.8313E-17  0.1683E-05 -0.3221E-06
  5  0.6026E+01 -0.4380E-02 -0.2072E-09  0.5101E-15  0.1200E-16  0.1683E-05 -0.3221E-06
  6 -0.1287E+00  0.7225E+01  0.3173E-06  0.1506E-16 -0.6404E-15  0.1683E-05 -0.3221E-06
  7  0.5849E+01 -0.4420E-01 -0.2515E-09  0.6997E-15  0.1646E-16  0.1683E-05 -0.3221E-06
  8  0.4680E+01 -0.7234E-01 -0.2197E-09  0.7500E-15  0.1764E-16  0.1683E-05 -0.3221E-06
  9  0.4255E+01 -0.9380E-01 -0.2237E-09  0.7871E-15  0.1851E-16  0.1683E-05 -0.3221E-06
 10  0.3830E+01 -0.1153E+00 -0.2277E-09  0.8056E-15  0.1895E-16  0.1683E-05 -0.3221E-06
 11  0.3405E+01 -0.1367E+00 -0.2317E-09  0.8056E-15  0.1895E-16  0.1683E-05 -0.3221E-06
 12  0.3478E+01 -0.1719E+00 -0.2738E-09  0.7893E-15  0.1856E-16  0.1683E-05 -0.3221E-06
 13 -0.2906E+00  0.3543E+01  0.1649E-06  0.1790E-16 -0.7610E-15  0.1683E-05 -0.3221E-06
 14  0.2200E+01 -0.1975E+00 -0.2429E-09  0.7049E-15  0.1658E-16  0.1683E-05 -0.3221E-06
 15  0.1350E+01 -0.2404E+00 -0.2509E-09  0.5441E-15  0.1280E-16  0.1683E-05 -0.3221E-06
 16  0.2166E+00 -0.2977E+00 -0.2615E-09  0.2143E-15  0.5041E-17  0.6254E-07 -0.7656E-07

```

```

      870
IPASS=    1 IHOST=    1
PLY NO., SIG11,      SIG22,      SIG12,      SIG13,      SIG23,      EPS11,      EPS22

                                NODE NUMBER= 438
  1 -0.4902E+01 -0.2902E+01 -0.6078E-09  0.2168E-14 -0.4586E-15 -0.1404E-06 -0.4886E-07
  2 -0.6764E+01 -0.3201E+01 -0.5438E-09  0.2168E-14 -0.4586E-15 -0.2022E-06 -0.3968E-07

```

Ply 1 stresses across the width of the deck with improved tying equations are printed below:

PLY 1 STRESSES on DECK (PSI)			
NODE	SIG11,	SIG22,	SIG12
421	0.5821574E+01	-.8279170E-02	-.7515657E-09
422	0.5960223E+01	0.1960551E-01	-.7372806E-09
423	0.6135999E+01	0.4170931E-01	-.8210187E-09
424	0.6566391E+01	0.1732731E+00	-.9669387E-09
425	0.6899488E+01	0.2981124E+00	-.1007943E-08
426	0.7391953E+01	-.2009299E+00	-.2880378E-09
427	0.7556217E+01	-.3886477E-01	-.2418264E-09
428	0.7442990E+01	0.6715600E-01	-.1939033E-09
429	0.7556217E+01	-.3886477E-01	-.2418278E-09
430	0.7391953E+01	-.2009299E+00	-.2880401E-09
431	0.6899488E+01	0.2981124E+00	-.1007942E-08
432	0.6566391E+01	0.1732731E+00	-.9669384E-09
433	0.6135999E+01	0.4170931E-01	-.8210191E-09
434	0.5960223E+01	0.1960551E-01	-.7372808E-09
435	0.5821574E+01	-.8279170E-02	-.7515660E-09

PLY 1 STRESSES in GIRDER (PSI)			
NODE	SIG11,	SIG22,	SIG12
436	-.7959401E+01	-.1771099E+01	-.2221700E-09
437	-.7207082E+01	-.2571885E+01	-.4149807E-09
438	-.4901697E+01	-.2902350E+01	-.6077929E-09
439	-.7207082E+01	-.2571885E+01	-.4149777E-09
440	-.7959401E+01	-.1771099E+01	-.2221683E-09
441	-.1187560E+02	-.1134400E+02	-.3727024E-11
442	-.3674272E+02	-.1921736E+02	-.1735729E-10
443	-.6414128E+02	-.3322184E+02	-.1665908E-10
444	-.9818880E+02	-.6433944E+02	-.1437024E-10
445	-.1543080E+03	-.9680000E+02	-.2641304E-10
446	-.1260238E+03	-.1637893E+02	-.9167910E-11
447	-.1218274E+03	-.1912634E+02	-.8221980E-11
448	-.1364100E+03	-.2756939E+02	-.7277530E-11
449	-.1218274E+03	-.1912634E+02	-.8209040E-11
450	-.1260238E+03	-.1637893E+02	-.9139430E-11

First ply stresses on the deck are now in the range of 5.8 to 7.6 psi instead of 5.7 psi to 7.7 psi. The change is relatively small but the improvement in accuracy can be more obvious in general.

## ***2.7 Integrated girder plus deck finite element model***

Next, we developed an alternative model where the girder and the part of the deck immediately above the girder are integrated into a single element using the tying equations to connect it to the overhanging part of the deck. For this model the girder web is expanded to be as wide as the top flange by assigning equivalent properties to the web, similar to composite beam analysis. That is the stiffness and strength properties of the web are multiplied by the web thickness and divided by the flange width and the web is assumed to be as wide as the flange. The

resulting material properties are designated as WBSF/WBSM and added to the databank. The purpose of this model is to verify that the change of the results would be toward Euler beam theory. Additionally, this model will be used to verify the results of subsequent tasks for the direct computation of residual stresses. The resulting stresses and strains are shown in the next page for node 218 (center node above the continuous support). As in the previous case PLY STRESSES AND STRAINS ARE IN LOCAL PLY COORDINATES (Local ply x coordinate is in the direction of reinforcement). We note that ply 1 stresses are slightly reduced, moving toward Euler beam results. Euler beam stresses at top and bottom of integrated beam are computed in Appendix 2 for reference. Also, the neutral plane has shifted downwards toward the Euler beam neutral axis. Strains and stresses are of course continuous since there is no break in the element modeling from top to bottom. Ply 1 stresses of nodes over the continuous support vary between 6.1 to 7.2 psi, closer to the Euler beam results.

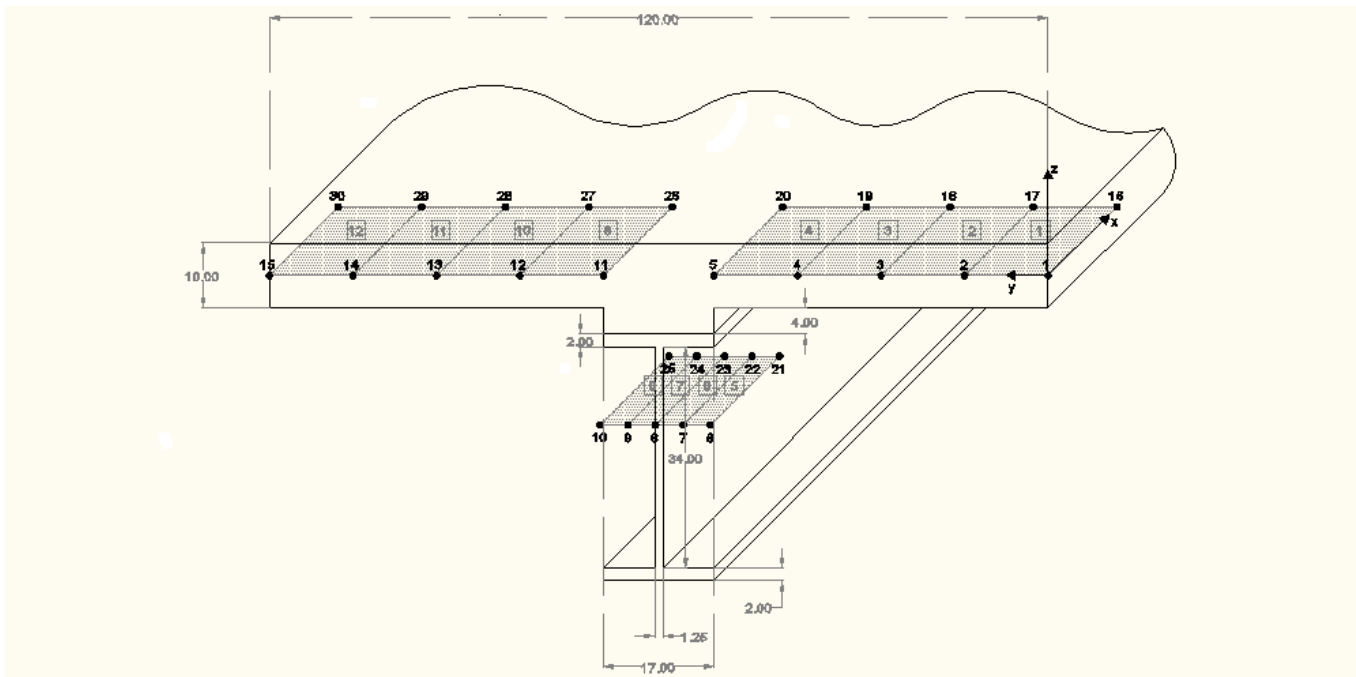


Figure 2-8. Node Numbering for Integrated Deck with Girder Finite Element Model

Input data to define the material properties through the thickness of the integrated girder and deck system replace the separate LTYP definitions for the girder elements and the part of the deck with haunch above the girder. The integrated system is subdivided to 34 layers by appending to the deck and haunch representation the additional “plies” associated with girder elements as shown below:

LTYP	2	34	5			
PLY	1	1	70.00	70.0	0.0	0. 0.100
PLY	2	1	70.00	70.0	0.0	0. 0.100

PLY	3	1	70.00	70.0	0.0	0.0	0.100	
PLY	4	1	70.00	70.0	0.0	0.0	0.100	
PLY	5	1	70.00	70.0	0.0	0.0	0.100	
PLY	6	1	70.00	70.0	0.0	0.0	0.200	
PLY	7	1	70.00	70.0	0.0	0.0	0.300	
PLY	8	1	70.00	70.0	0.0	0.0	0.500	
PLY	9	1	70.00	70.0	0.0	0.0	0.500	
PLY	10	1	70.00	70.0	0.0	0.0	0.500	
PLY	11	1	70.00	70.0	0.0	0.0	0.500	
PLY	12	2	70.00	70.0	0.0	0.0	0.500	
PLY	13	3	70.00	70.0	0.0	90.0	0.500	
PLY	14	1	70.00	70.0	0.0	0.0	0.620	
PLY	15	1	70.00	70.0	0.0	0.0	0.620	
PLY	16	1	70.00	70.0	0.0	0.0	0.620	
PLY	17	1	70.00	70.0	0.0	0.0	0.620	
PLY	18	1	70.00	70.0	0.0	0.0	0.620	
PLY	19	2	70.00	70.0	0.0	0.0	0.500	
PLY	20	3	70.00	70.0	0.0	90.0	0.500	
PLY	21	1	70.00	70.0	0.0	0.0	0.350	
PLY	22	1	70.00	70.0	0.0	0.0	0.350	
PLY	23	1	70.00	70.0	0.0	0.0	0.350	
PLY	24	1	70.00	70.0	0.0	0.0	0.350	
PLY	25	1	70.00	70.0	0.0	0.0	2.000	
PLY	26	1	70.00	70.0	0.0	0.0	2.000	
PLY	27	4	70.00	70.0	0.0	0.0	0.500	
PLY	28	4	70.00	70.0	0.0	0.0	0.500	
PLY	29	5	70.00	70.0	0.0	0.0	8.500	
PLY	30	5	70.00	70.0	0.0	0.0	8.500	
PLY	31	5	70.00	70.0	0.0	0.0	8.500	
PLY	32	5	70.00	70.0	0.0	0.0	8.500	
PLY	33	4	70.00	70.0	0.0	0.0	0.500	
PLY	34	4	70.00	70.0	0.0	0.0	0.500	
MATCRD	1	CNCFCNC	.300	.01	CNCFCNC	0.0	.60	.03
MATCRD	2	RBSFCNC	.05000	.01	CNCFCNC	0.0	.60	.03
MATCRD	3	RBSFCNC	.05000	.01	CNCFCNC	0.0	.60	.03
MATCRD	4	GRSFGRDS	.30	.00	GRSFGRDS	0.0	.02	.03
MATCRD	5	WBSFWBSM	.30	.00	WBSFWBSM	0.0	.02	.03

ENDN

Ply stresses computed by the integrated deck plus girder finite element model are given below. The first ply stresses across the surface of the deck also show a smooth variation of the stress pattern indicating that the tying equations for the compatibility of  $\Delta_x$  with  $\theta_y$  as well as rotational compatibilities are imposed between the adjacent overhanging deck and integrated deck with girder elements.

NODE NUMBER= 218 Ply Stresses (psi) and Normal Strains Through the Thickness

PLY NO.,	SIG11,	SIG22,	SIG12,	SIG13,	SIG23,	EPSXX,	EPSYY
1	0.723E+01	-0.602E-01	-0.323E-09	0.162E-16	0.218E-15	0.164E-05	-0.341E-06
2	0.698E+01	-0.611E-01	-0.311E-09	0.481E-16	0.648E-15	0.158E-05	-0.330E-06
3	0.673E+01	-0.621E-01	-0.299E-09	0.794E-16	0.107E-14	0.153E-05	-0.319E-06

4	0.647E+01	-0.631E-01	-0.287E-09	0.110E-15	0.148E-14	0.147E-05	-0.307E-06
5	0.596E+01	-0.650E-01	-0.263E-09	0.169E-15	0.228E-14	0.135E-05	-0.285E-06
6	-0.175E+00	0.723E+01	0.319E-06	0.309E-14	-0.229E-15	-0.261E-06	0.123E-05
7	0.589E+01	-0.622E-01	-0.259E-09	0.263E-15	0.354E-14	0.116E-05	-0.247E-06
8	0.476E+01	-0.695E-01	-0.206E-09	0.300E-15	0.403E-14	0.108E-05	-0.231E-06
9	0.438E+01	-0.710E-01	-0.189E-09	0.338E-15	0.454E-14	0.994E-06	-0.214E-06
10	0.400E+01	-0.724E-01	-0.171E-09	0.374E-15	0.504E-14	0.908E-06	-0.197E-06
11	0.361E+01	-0.739E-01	-0.153E-09	0.409E-15	0.551E-14	0.822E-06	-0.180E-06
12	0.377E+01	-0.765E-01	-0.159E-09	0.440E-15	0.593E-14	0.743E-06	-0.165E-06
13	-0.153E+00	0.393E+01	0.176E-06	0.629E-14	-0.467E-15	-0.151E-06	0.671E-06
14	0.253E+01	-0.779E-01	-0.102E-09	0.501E-15	0.674E-14	0.578E-06	-0.132E-06
15	0.177E+01	-0.808E-01	-0.665E-10	0.559E-15	0.752E-14	0.405E-06	-0.984E-07
16	0.756E+00	-0.847E-01	-0.188E-10	0.627E-15	0.843E-14	0.175E-06	-0.532E-07
17	0.121E+00	-0.871E-01	0.110E-10	0.664E-15	0.893E-14	0.314E-07	-0.250E-07
18	-0.133E+00	-0.880E-01	0.229E-10	0.677E-15	0.911E-14	-0.261E-07	-0.137E-07
19	-0.242E+01	-0.967E-01	0.130E-09	0.771E-15	0.104E-13	-0.544E-06	0.879E-07
20	-0.674E+01	-0.113E+00	0.333E-09	0.804E-15	0.108E-13	-0.152E-05	0.280E-06
21	-0.111E+02	-0.129E+00	0.535E-09	0.649E-15	0.874E-14	-0.250E-05	0.472E-06
22	-0.154E+02	-0.146E+00	0.738E-09	0.306E-15	0.412E-14	-0.348E-05	0.664E-06
23	-0.177E+02	-0.154E+00	0.845E-09	0.481E-16	0.648E-15	-0.399E-05	0.765E-06
24	-0.179E+02	-0.155E+00	0.857E-09	0.162E-16	0.218E-15	-0.405E-05	0.777E-06

PLY	1 STRESSES (psi) ACROSS WIDTH OF DECK			
NODE	SIG11,	SIG22,		SIG12
211	0.6121520E+01	-.4184792E-01		-.7939430E-09
212	0.6287134E+01	0.9794557E-02		-.7670593E-09
213	0.6395843E+01	-.4111659E-01		-.8597942E-09
214	0.7089766E+01	0.1832595E+00		-.1034945E-08
215	0.7181243E+01	0.3768138E+00		-.1090367E-08
216	0.7006587E+01	-.7103253E-01		-.3299302E-09
217	0.7183756E+01	-.5279652E-01		-.3271472E-09
218	0.7234588E+01	-.6017816E-01		-.3226132E-09
219	0.7183756E+01	-.5279652E-01		-.3271473E-09
220	0.7006587E+01	-.7103253E-01		-.3299297E-09
221	0.7181243E+01	0.3768138E+00		-.1090366E-08
222	0.7089766E+01	0.1832595E+00		-.1034945E-08
223	0.6395843E+01	-.4111659E-01		-.8597944E-09
224	0.6287134E+01	0.9794557E-02		-.7670593E-09
225	0.6121520E+01	-.4184792E-01		-.7939432E-09

First ply stresses on the deck are now in the range of 6.1 to 7.2 psi instead of 5.8 to 7.6 psi for the corresponding case of the separate deck and girder elements model with the full set of tying equations. With the integrated deck girder model the spread of ply 1 stresses is smaller. However, the average stress at the top of the deck is the same. The integrated deck-girder model is preferred for the direct computation of residual stresses due to temperature and shrinkage effects.

## ***2.8 Conclusions of Part 2***

A computational framework has been developed and demonstrated to compute consistent stress and strain levels across the thickness of a composite bridge deck. The methodology was improved in response to the requests of the technical working group (TWG) after the February 12, 2009 meeting in Albany. Duplicate node assignments have been replaced by tying equations relating the dependencies of individual degrees of freedom. Resulting strain and stress gradients are smooth and compare reasonably with Euler beam theory approximations.

## **Part 3. Development of mathematical models for temperature and moisture gradients and shrinkage in the deck slab**

Mathematical models for the determination of the temperature and moisture gradients and shrinkage in the deck slab are described. Task 3 results comprise a necessary background for Task 4 where the temperature variation, moisture loss, autogenous and drying shrinkage models are used to predict the thermal and shrinkage strains in bridge deck. These strains are to be added to the strains from creep and mechanical loads and applied to an elasto-plastic damage approach to quantify the damage and stresses in deck slab. Finally the damage and the stresses are to be used in Task 4 to quantify the crack width. A meeting was held with the TWG on August 12, 2009. Meeting location was Clarkson University.

Task 3 Deliverable: At the end of this task, the PI shall deliver an interim report documenting the mathematical models developed for temperature and moisture gradients in the deck slab to the NYSDOT Project Manager. The PI shall first submit a draft report to the NYSDOT Project Manager and review comments shall be addressed to his/her satisfaction before it is made final. After it is finalized, the PI shall submit two hard copies of the report and a CD with report in electronic format (Word and PDF) to the NYSDOT Project Manager.

### ***3.1 Effect of temperature rise during curing of concrete deck:***

During the TWG meeting on February 12, 2009 in Albany it was clarified that the residual stresses because of the rising of concrete temperature during curing play a very important role in the development of deck cracking. Temperature differential between the deck concrete and the supporting beam at the time when they start acting as a composite section is the critical temperature to consider. Temperature rise after that point will not contribute to the restrained shrinkage due thermal effects. Determination of thermal residual stresses requires knowledge of concrete temperatures as a function of time from the initial placement of concrete. The Initial placement temperature, the concrete mix design as well as the change in the ambient temperature have significant influence on the temperature time-history. In addition, these are some of the factors we actually could change or control during the construction operation. The designer will benefit from the use the computational tool if they can use it to establish construction control that will reduce the cracking tendencies of the deck for the structure type and expected time of placement of the deck.

To compute the time-history temperature profile of the bridge deck a one-dimensional thermal analysis finite element approach was used. The analysis requires thermal conductivity and specific heat values, and hydration heat generated per unit volume as a function of time. In general, convective heat transfer coefficient for heat transfer from concrete surface to air is also a time variable. However, the curing process for NYSDOT bridge deck construction involves placing wet burlap over the bridge decks almost immediately after pouring (within 30 minutes). The burlap is kept wet with soaker hoses. As a result the heat transfer away from the deck is not just by convection. It would be appropriate to just define the surface temperature while the deck surface is covered with wet burlap.

Mathematical models for the convective heat transfer coefficient  $h$  and the hydration heat generated  $Q$  were obtained by calibrating appropriate models using test data. The calibration process is outlined in the next two sections.

### 3.2 Determining time history of the convective heat transfer coefficient, $h$ :

The convective heat transfer coefficient was investigated for the case of heat transfer from an open concrete surface to the atmosphere. Convective heat transfer modeling is applicable to determine the amount of heat transfer between the concrete surface and the atmosphere prior to the placement of wet burlap. After setting of concrete, NYSDOT practice is to cover the deck with wetted burlap for a week, convective heat transfer model will not be applicable while the wet burlap covers the concrete surface. According to TWG comments, it may be more appropriate to specify the surface temperature as a function of time. The section on convective heat transfer coefficient is left in the report in case a thermal analysis is required after the removal of wet burlap.

The convective heat transfer coefficient,  $h$ , is not a constant, but a value that changes due to some property. Based on graphs from Lee et. al., it was concluded that  $h$  shows no obvious correlation to temperature change within the concrete. It is most likely that  $h$  is mainly a function of surface moisture. In order to incorporate  $h$  into our finite element model for the time-dependent temperature change of a concrete bridge deck,  $h$  was determined as a function of time. To do this, a line was fit to the data points shown in Figure 3-1 (Lee et. al. (2009)).

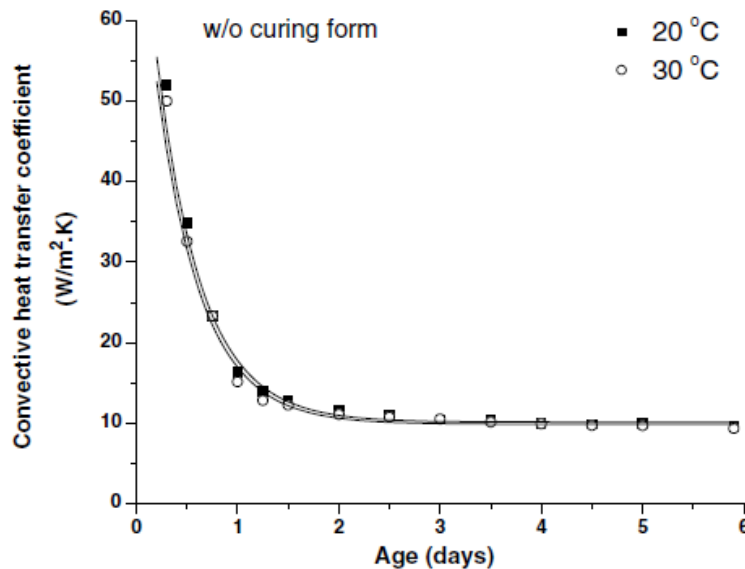


Figure 3-1 – Convective heat transfer coefficients  $h$  with ambient temperature and curing condition without wet burlap and (wind velocity of 0.0 m/s)

Once the units of the above graph were corrected to agree with the traditional US engineering units being used elsewhere in the analysis, Microsoft Excel was used to fit a line to

the data points through a trial-and-error process. The line that fit best out of the several that were tested was

$$h_j(t) = \frac{13.7}{t^2} + 0.039625 \quad (1)$$

The plot of this line superimposed on the data points is shown in Figure 3-2. The units of the convective heat transfer coefficient  $h$  used in this study are Btu/(hr.°F.in<sup>2</sup>).

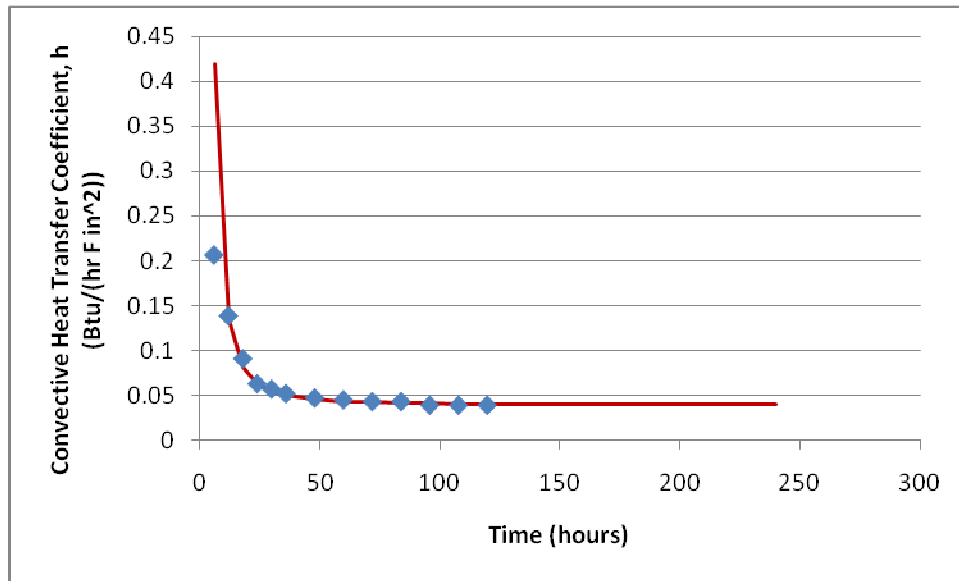


Figure 3-2 – Plot of convective heat transfer coefficient data with best fit line

The “+ 0.039625” appearing at the end of the equation shifts the graph upward so that as the age ( $t$ ) approaches infinity, the convective heat transfer coefficient,  $h$ , will approach a value of 10 W/(m<sup>2</sup>·K) (0.039625 Btu/(hr.°F.in<sup>2</sup>)), as it appears to be in Figure 3-1 (and Figure 3-2). This value will be referred to as the asymptotic value  $h_0$  for the remainder of this report.

Looking at the plot in Figure 3-2, it is obvious that, prior to approximately 0.5 days (12 hours), the chosen model does not fit the data well. To correct the initial values of  $h$  immediately after the placement of concrete, an interpolation is performed to form an equation representative of this early age behavior. This interpolation is similar to the inelastic column buckling equation from the American Institute of Steel Construction (AISC) Manual. It has been interpreted in this situation to yield the following:

$$h(t) = \left[ 0.658 \left( \frac{h_m - h_0}{h_j(t)} \right) \right] (h_m - h_0) + h_0 \quad (2)$$

where  $h_m$  is the approximate value of  $h$  at time zero (taken here to be  $0.23775 \text{ Btu}/(\text{hr}\cdot^\circ\text{F}\cdot\text{in}^2)$  to match the test data by ), and all other values are as defined previously. Substituting in all the appropriate values, this equation yields

$$h(t) = \left[ 0.658 \frac{\frac{0.198}{13.7}}{t^2 + 0.039625} \right] (0.198) + 0.039625 \quad (3)$$

In order to construct an overall model capable of predicting the convective heat transfer at any time,  $t$ , it is necessary to determine when  $h(t)$  is appropriate and when  $h_j(t)$  becomes the more fitting model. The point of intersection of  $h(t)$  and  $h_j(t)$  was determined by solving the two equations simultaneously. It was found to occur at 10.84811 hours. So, the model for convective heat transfer coefficient,  $h$ , becomes

$$h(t) = \begin{cases} \left[ 0.658 \frac{\frac{0.198}{13.7}}{t^2 + 0.039625} \right] (0.198) + 0.039625 & 0 < t < 10.84811 \\ \frac{13.7}{t^2} + 0.039625 & 10.84811 \leq t \end{cases} \quad (4)$$

The graph of this joint model superimposed on the original data is shown in Figure 3-3.

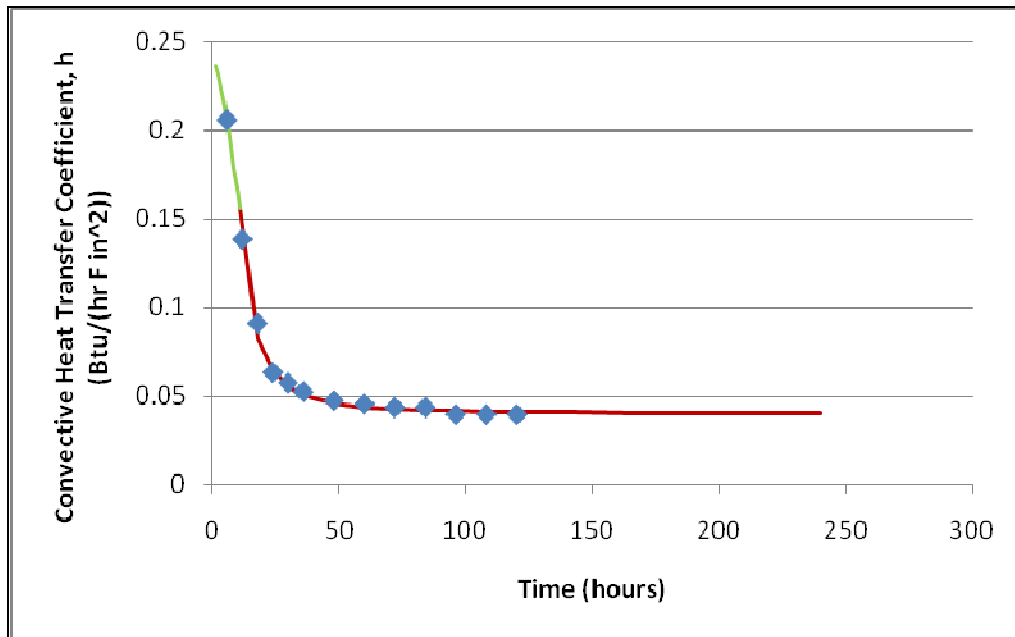


Figure 3-3 – Final convective heat transfer coefficient model

### 3.3 Determining heat generation, $Q_t$ :

Similar to the convective heat transfer coefficient, the heat generation was determined by fitting a model to a graph taken from previous work. In this case, the following graph, taken from Wojcik and Fitzjarrald (2001), was used to generate this model. This particular set of data was chosen for fitting because it follows the smoothest path and because it demonstrates the closest agreement between predicted and measured values, compared to the other data sets available.

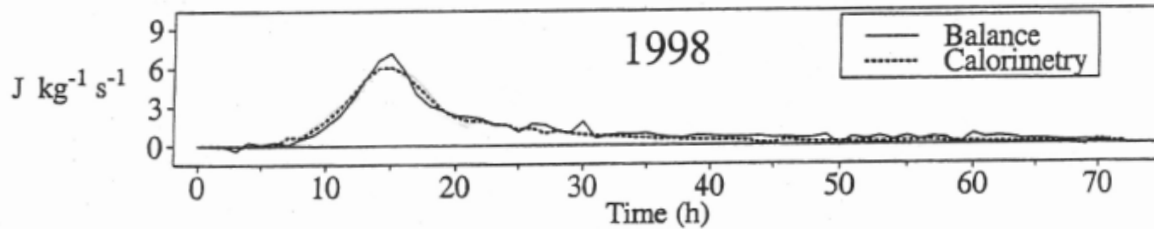


Figure 3-4 – Heat generation curve as taken from Wojcik and Fitzjarrald (2001)

The test data indicates the practical absence of heat generation during the first seven hours after placement. This phenomenon may be explained by examination of the concrete hydration reaction kinetics, as follows. Portland cement consists of five major compounds and a few minor compounds. The composition of a typical portland cement is listed by weight percentage in Table 1.

Cement Compound	Weight Percentage	Chemical Formula
Tricalcium silicate	50 %	$\text{Ca}_3\text{SiO}_5$ or $3\text{CaO}\cdot\text{SiO}_2$
Dicalcium silicate	25 %	$\text{Ca}_2\text{SiO}_4$ or $2\text{CaO}\cdot\text{SiO}_2$
Tricalcium aluminate	10 %	$\text{Ca}_3\text{Al}_2\text{O}_6$ or $3\text{CaO}\cdot\text{Al}_2\text{O}_3$
Tetracalcium aluminoferrite	10 %	$\text{Ca}_4\text{Al}_2\text{Fe}_2\text{O}_{10}$ or $4\text{CaO}\cdot\text{Al}_2\text{O}_3\cdot\text{Fe}_2\text{O}_3$
Gypsum	5 %	$\text{CaSO}_4\cdot 2\text{H}_2\text{O}$

Table 3.1 - Composition of typical portland cement with chemical composition and weight percent.

When water is added to cement, each of the compounds undergoes hydration and contributes to the final concrete product. Only the calcium silicates contribute to strength. Tricalcium silicate is responsible for most of the early strength (first 7 days). Dicalcium silicate, which reacts more slowly, contributes only to the strength at later times. Stages of hydration of tricalcium silicate will be discussed in detail.

Tricalcium silicate + Water  $\rightarrow$  Calcium silicate hydrate + Calcium hydroxide + heat



Upon the addition of water, tricalcium silicate rapidly reacts to release calcium ions, hydroxide ions, and a large amount of heat. The pH quickly rises to over 12 because of the release of alkaline hydroxide ( $\text{OH}^-$ ) ions. This reaction usually occurs during the delivery of concrete in the truck mixer before the concrete is placed. If the distance between the concrete plant and the construction site is short, the tail end of the initial hydrolysis heat may also be observed immediately after placement. This initial hydrolysis slows down quickly after it starts, resulting in a decrease in heat evolved. For a number of hours the reaction heat is reduced to a negligible level. The length of this dormant phase can be adjusted by adding admixtures to the concrete mix. During that time the reaction slowly continues producing calcium and hydroxide ions until the system becomes saturated. Once this occurs, the calcium hydroxide starts to crystallize. Simultaneously, calcium silicate hydrate begins to form. Ions precipitate out of solution accelerating the reaction of tricalcium silicate to calcium and hydroxide ions. (Le Chatelier's principle). The evolution of heat is then dramatically increased. For the example depicted in Figure 3-4 the dormant stage lasts approximately 7 hours. The second stage of the reaction is observed to peak after approximately 15 hours from initial placement.

The formation of the calcium hydroxide and calcium silicate hydrate crystals provide "seeds" upon which more calcium silicate hydrate can form. The calcium silicate hydrate crystals grow thicker making it more difficult for water molecules to reach the unhydrated tricalcium silicate. The speed of the reaction is now controlled by the rate at which water molecules diffuse through the calcium silicate hydrate coating. This coating thickens over time causing the production of calcium silicate hydrate to become slower and slower. This stage corresponds to the quadratic decline of the heat of hydration from its peak value.

Wojcik and Fitzjarrald (2001) describe the hydration process in terms of four unique phases, as shown in Figure 3-5.

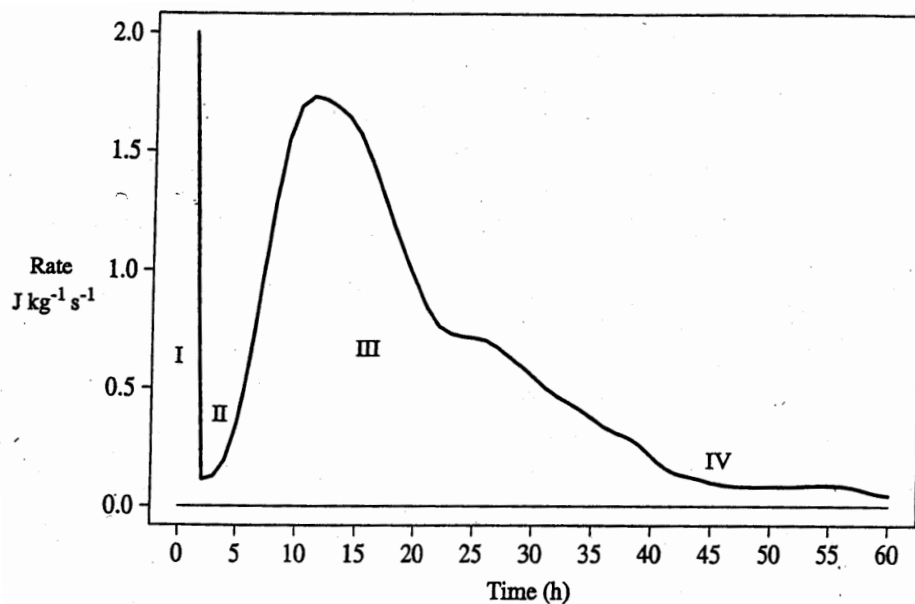


Figure 3-5 – Hydration phases during concrete curing (Wojcik and Fitzjarrald, 2001)

The first phase of this model deals with the period during which reactions occur on the surface of cementitious particles to form a “gel”. According to Wojcik and Fitzjarrald, this phase lasts about 30 minutes, but other sources indicate that the process can occur in under 15 minutes. During this phase, a significant amount of heat is produced. The gel formed on the cement particles in Phase I inhibits the diffusion of water into these particles, slowing the hydration process. This slowing down occurs during Phase II, and it lasts for several hours. As water breaks through the gel barrier and reaches the unhydrated cement particles, Phase III begins. As the hydration reactions occur, the concrete stiffens and heat generation occurs once again. After the peak heat generation is reached, the hydration process slows again. This is represented by Phase IV and it continues on for years.

The experimental data on the heat of hydration depicted in Figure 3-4 has segments with different characteristics that would be best represented by multiple equations. By inspection, it was determined that, in this particular case, the hydration heat generation is practically zero until a time of 7 hours after placement of concrete, so the first portion of the model states that

$$Q_i(t) = 0; \quad 0 \leq t < 7 \quad (5)$$

The next portion of the model represents the heat generation from a time of 7 hours to the time of the peak heat generation, which is at 15 hours. Data points were extracted from the graph in Figure 3-4 and, using Microsoft Excel, a best fit linear line was generated (again after converting to the proper units), as shown in Figure 3-6.

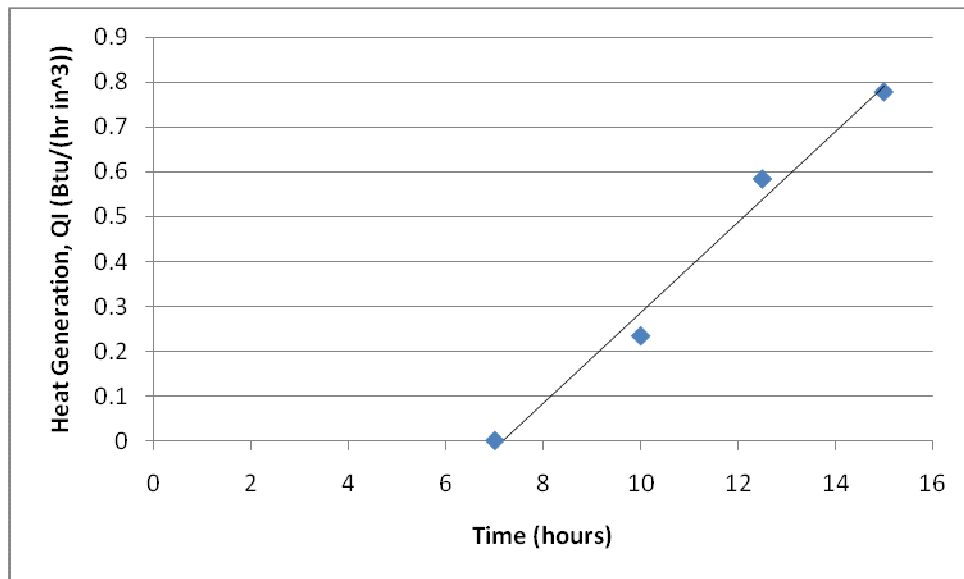


Figure 3-6 –  $Q_1$  data from time of 7 to 15 hours with best fit linear line

Although the heat generation in this time range differs slightly from a linear behavior, a straight line fit was considered to be sufficiently accurate for the purposes of this model. The linear fit gives an over-approximation between about 7 and 11 hours, and an under-approximation from 11 to 15 hours. Thus, the overall value generated during this time period is considered to be close to the actual value. The equation of the linear line shown in Figure 3-6 is

$$Q_I(t) = 0.1012t - 0.7262 \quad (6)$$

Next, the right side of the graph, covering the time period from 15 hours on, was investigated. Again, a curve was loosely fit to the data, which took the form

$$Q_{IR}(t) = \frac{78}{(t-5)^2} \quad (7)$$

The plot of this function with the data being fitted is shown in Figure 3-7.

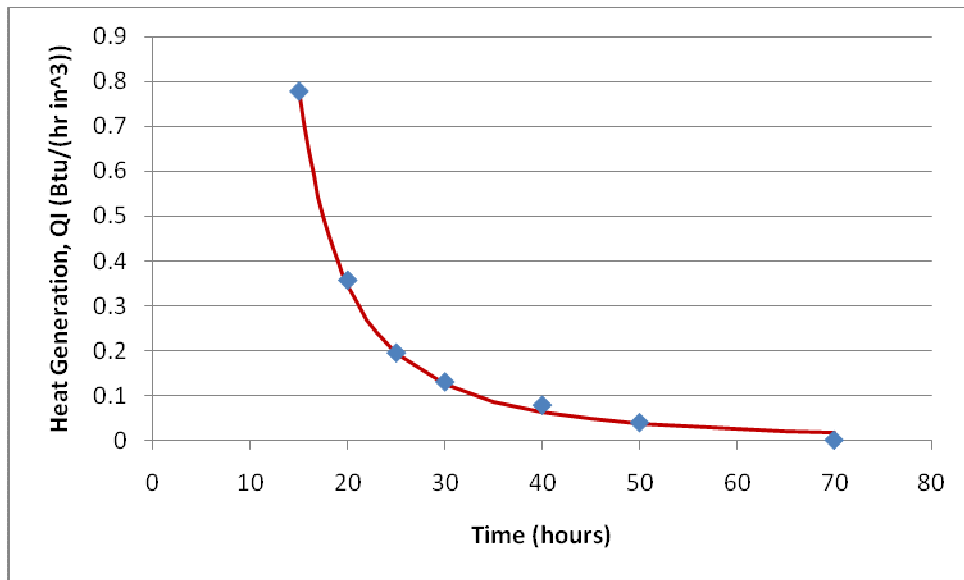


Figure 3-7 – Heat generation model for time  $t > 15$  hours

Assembling this with the model for the first 15 hours, the following model depicted in Figure 3-8 is created for the entire time period of the test data.

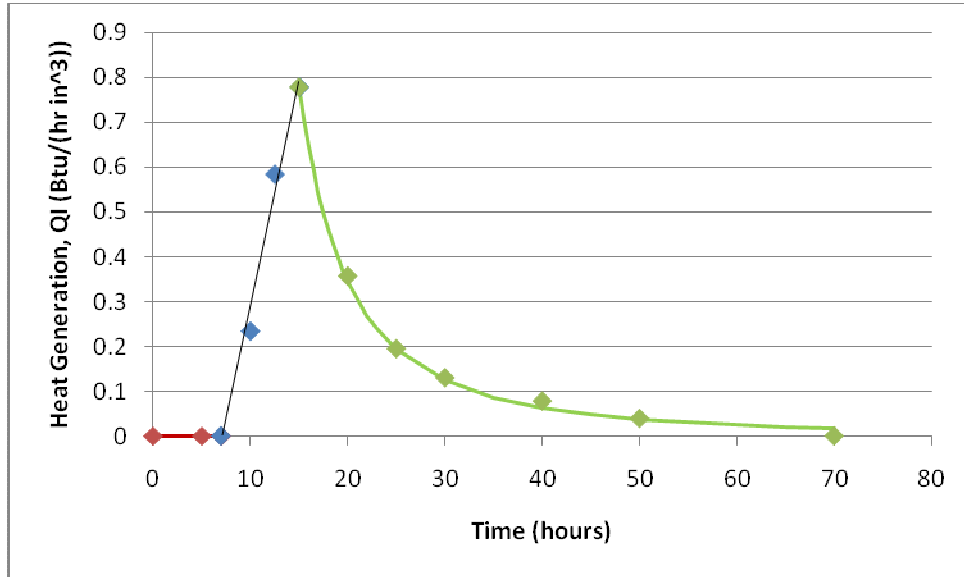


Figure 3-8 – Complete heat generation model

The above model is represented by the following equations.

$$Q_1(t) = \begin{cases} 0 & 0 \leq t < 7 \\ 0.1012t - 0.7262 & 7 \leq t \leq 15 \\ \frac{78}{(t-5)^2} & t > 15 \end{cases} \quad (8)$$

The above model demonstrates adequate fit to the data for the specific material investigated Wojcik and Fitzjarrald (2001). However, the heat generation behavior is expected to vary

by significantly depending on the composition of the concrete. Additionally, the initial dormant time may decrease because of delay of the concrete mix truck in transit. It was reasonably assumed that, for any cement, the shape of the heat generation curve would be similar. Therefore, the above equations were generalized in terms of  $t_1$  (the time at which the heat generation starts to occur after placement of concrete),  $t_2$  (the time at which the heat generation peaks), and  $Q_p$  (the peak heat generation, occurring at time  $t_2$ ). The generalized model takes the following form.

$$Q_I(t) = \begin{cases} 0 & 0 \leq t < t_1 \\ \left( \frac{Q_p}{t_2 - t_1} \right) (t - t_1) & t_1 \leq t \leq t_2 \\ \frac{100 * Q_p}{(t - (t_2 - 10))^2} & t > t_2 \end{cases} \quad (9)$$

This generalized model was tested with a variety of data sets and, in each case, it exhibited a good fit to the data points.

### 3.4 Thermal Conductivity and Specific Heat Capacity of Concrete:

The thermal conductivity was taken to be  $k=0.0818$  BTU/(in-hr-°F) or  $1.7$  W/(m-°K) and the heat capacity  $c=0.210$  BTU/(lb-°F) or  $880$  J/(Kg-°K). Time history thermal analysis of the 10" thick concrete bridge deck used in Task 2 was conducted for three cases. In case 1, both the top and bottom surfaces of the deck were open to the atmosphere. It should be noted that Case 1 was simulated to test the program in general and does not correspond to an actual deck placement and curing method. A diagram of this trial case with node and element numbers, nodal coordinates, and initial and boundary conditions is shown in Figure 3-9. It is acknowledged the standard NYSDOT deck thickness is currently 9.5 in (240 mm) and will be used in the next task.

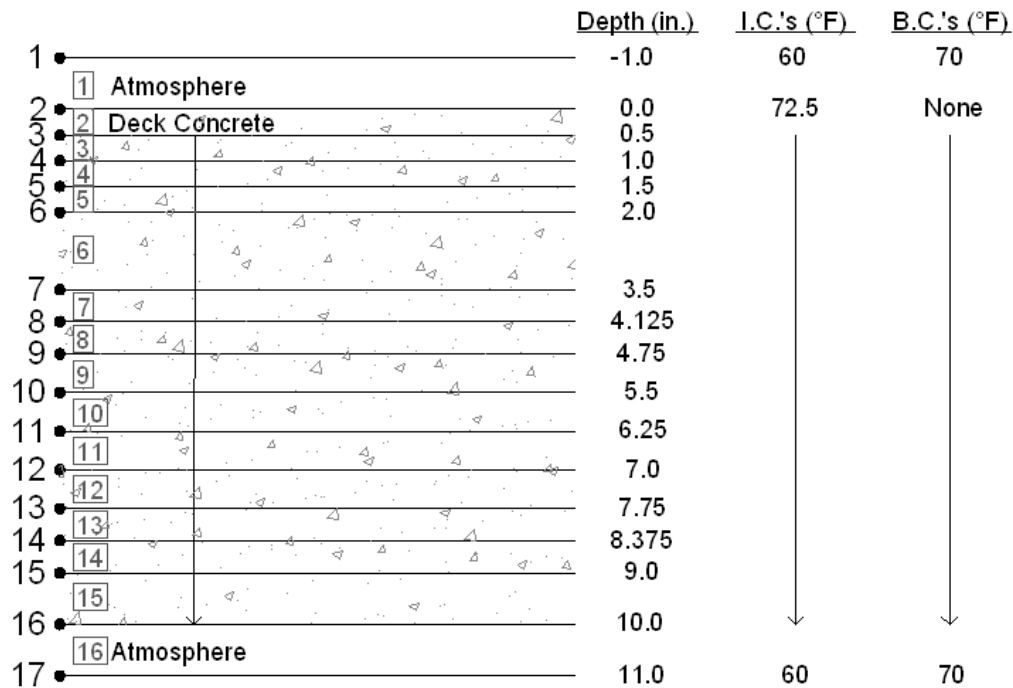


Figure 3-9 – Thermal Finite Element model for Deck Curing Case 1 from Task 3

Case 1 also demonstrates the capability to simulate a concrete bridge deck with removable forms with the bottom surface of the deck directly exposed to the atmosphere.

NYSDOT option of using removable forms will be simulated by combining case 1 with Case 3 that is presented later in this report.

In case 2 only the top surface was open to the air and the bottom was covered with a thin steel formwork with styrofoam insulation between the steel formwork and the concrete. A diagram of this trial case is shown in Figure 3-10.

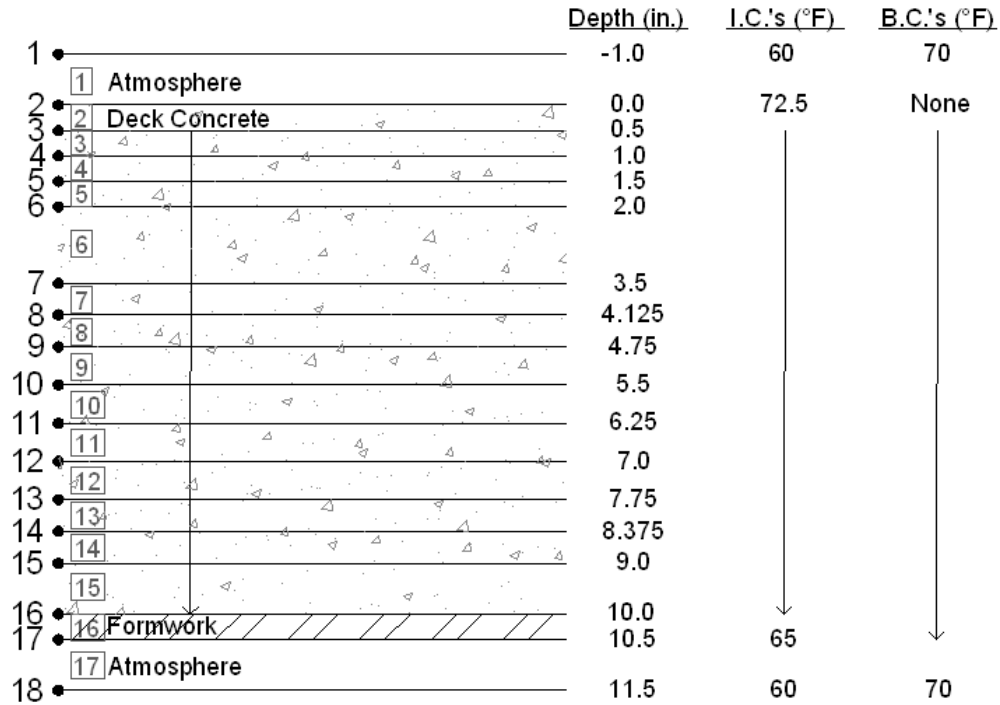


Figure3-10 – Thermal Finite Element model for Deck Curing Case 2 from Task 3

Case 3 was designed to include wetted burlap on the surface of the concrete deck in order to accommodate standard practice by the New York State Department of Transportation. To do this, the air layer above the deck was removed and the temperature at the top node of the deck and air temperature at the bottom of the formwork were defined. A diagram of this trial case is shown in Figure 3-11.

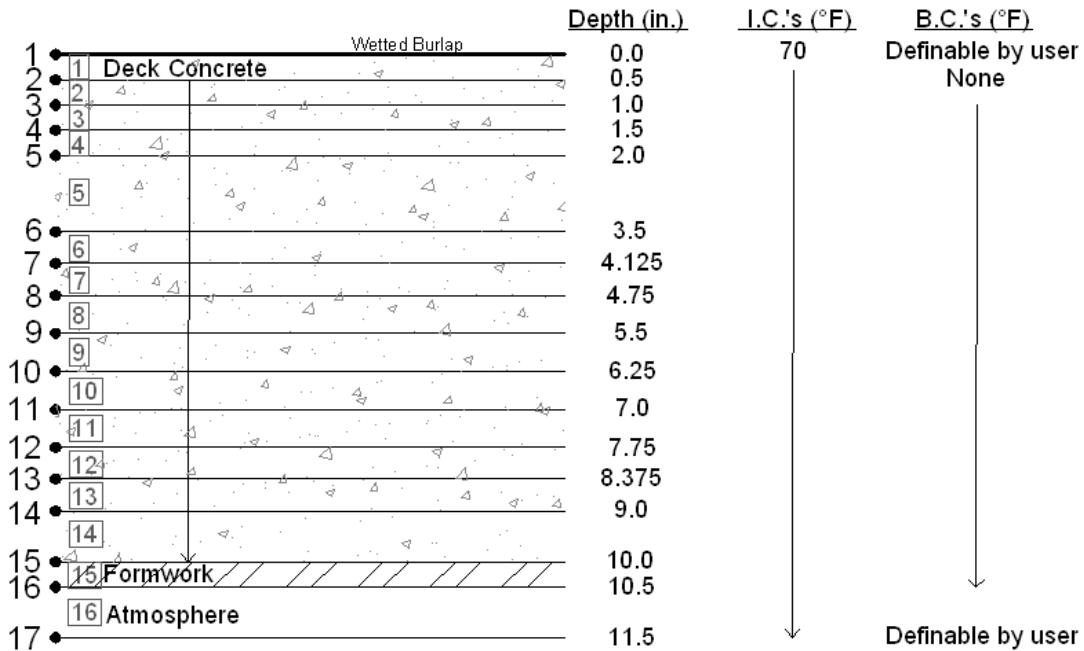


Figure 3-11 – Thermal Finite Element model for Deck Curing Case 3 from Task 3

In case 3(a), the surface temperature was kept constant over the 36 hour analysis period. In case 3(b), the surface temperature was varied with time to simulate the changing atmospheric conditions throughout a typical day. In all three cases, the thermal finite element dimensions in the bridge deck were based on the layer thicknesses used in Task 2 to discretize the deck for composite stress analysis. After comments from the TWG the program was generalized to include variation of concrete deck top surface temperature and air temperature under the formwork. Case 3b considers reasonable variation of top surface and bottom air temperatures. One dimensional thermal analysis was considered to be adequate since reasonable variations of the boundary conditions did not produce a significant effect on the peak temperatures and their locations.

### 3.5 Incorporation of Temperature Models into Thermal Finite Element Analysis Program:

Computation of the time-history temperature profile of the bridge deck was done using a one-dimensional thermal analysis finite element approach. The finite element analysis was performed by a computer program written in FORTRAN. The program implements a standard one-dimensional time-history finite element analysis as described by Desai (1979). The time-dependent changes in convective heat transfer coefficient and heat generation are taken into account for each time step by coding Equations 4 and 9, respectively for  $h$  and  $Q_t$ , as time functions that are referenced at each time step. The program recalculates the convective heat transfer coefficient and the heat generation at each time step in the analysis. The computer code for this one-dimensional finite element analysis program can be found in Appendix 3A.

### **3.6 Input Data for Thermal Finite Element Analysis across the Concrete Deck Thickness:**

The thermal finite element analysis program is designed to read information from an available input file. The file includes everything from node and element data to material properties and conditions acting on the bridge deck system. This file is constructed in a specific format in order to be compatible with the program. The format is outlined in Appendix 3B. A unique file is created for each problem or case investigated by the program.

The first line of the input file contains the problem number and title. Next, the file provides the basic parameters of the problem, such as the type of problem and the number of nodes, materials, and time intervals. The next lines in the file include the material properties of each material in the model. There is a unique line for each material. In appendices C-F listing the input files for thermal analysis, material type 1 is air, type 2 is concrete, type 3 is insulated formwork (if present), and type 4 is included as a spare but not used. The model is further described by listing the nodal point data, including the location of each node and the appropriate boundary conditions for the model. Again, there is a unique line for each node in the model. Similarly, the input file contains a unique line for each element in the model, located immediately following the nodal point data in the file. The element data describes the element connectivity and the material type assigned to each element.

The next two lines in the input file define the areas of the elements in the model. The first line contains one number, specifying whether the areas are uniform over all elements, or if they vary either linearly or arbitrarily. The other line gives a specific value or values for the area of the elements. Following these lines, there is a group of lines that describes the heat generation at the concrete deck elements in the system. There is an individual line in the input file for each element with active heat generation. Since this is known to be a function of time according to Eq. 9, these values are changed at each time step during the analysis.

The next line in the input file contains information regarding the desired time steps for the analysis, including the time increment and the total time to be investigated. This line also specifies whether the initial conditions in the system (temperatures or pressures) are uniform across all nodes, or if they vary, either linearly or arbitrarily, from node to node. Appropriately, the next two lines of the file are used to list the desired output time levels of the analysis and the initial conditions in the system, respectively. The last two lines are used to specify the surface temperatures at the top of deck and the ambient air temperatures below the formwork, respectively. These two temperatures are specified for each time step in the analysis. Finally, the input file is concluded with a blank line.

For Case 1 (without formwork) and Case 2 (with insulated steel formwork), and Cases 3(a) and 3(b) introduced previously in this report, the input files of the above format were constructed in Microsoft Notepad. After discussions with the Project Manager and TWG members, Case 3(b) was adopted as the most appropriate for this research as it takes into account the presence of wet burlap that regulates the surface temperature of the deck for the first 14 days. The input file for Case 3(b) is shown in Appendix 3C. Initial temperature of the concrete mix at the time of placement is specified by the user in the input files.

### **3.7 Results of Thermal Time-History Finite Element Analysis across the Concrete Deck Thickness:**

Upon running the thermal finite element analysis program, a new file is created within the same directory as the input file. This file contains all of the information pertaining to the analysis. First of all, it restates all of the problem parameters as read from the input file described in the previous section. The output file also contains the results of the analysis run by the program. For each time step listed in the input file, there is a list of temperatures at each node. In all four cases, the peak temperature occurred 16 hours after placement of concrete. It should be noted that the significant drop in temperature within the last two nodes for Cases 2, 3(a), and 3(b) is due to the fact that these two nodes represent the insulated formwork attached to the bottom surface of the bridge deck. For Case 1, the highest temperature node is in the middle of the deck thickness. For Cases 2, 3(a), and 3(b), the hottest node is the last one before the insulated bottom formwork. It was known that the temperature reaches a peak value that is about 45°F above where it began. This information was used to verify the temperatures determined by the analysis. It is interesting to note that, under the conditions imposed for these trial cases, there was virtually no difference between the peak heat generation in Cases 3(a) and 3(b). The insulation between the steel formwork and bottom concrete surface was sufficient to prevent a significant change in the concrete temperature with reasonable variations in ambient air temperatures. The results are expected to differ noticeably with the removal of the insulation layer above the formwork. The program provides the flexibility to make this change.

### **3.8 Development of Moisture Model for Curing Concrete Bridge Deck:**

Standard practice in bridge construction includes moist curing of the concrete bridge deck. Drying of the concrete starts to occur once moist curing has ended (i.e. removal of wetted burlap from surface of concrete deck). The purpose of the moisture model is to clarify the drying shrinkage of concrete that would begin after the removal of the wet burlap from the deck. Autogenous shrinkage is to be considered independently. It has been determined that autogenous shrinkage can happen at relatively high water-cement ratios above 0.35 when the concrete mix is rich in very fine particles. CUNY study shows that there is significant autogenous shrinkage in class HP concretes used for bridge decks (Subramaniam and Agrawal 2009).

Moisture diffusivity of concrete is usually a smooth function of drying time. Therefore it is possible to derive a mathematical model for moisture as a function of time and depth directly from test data. According to Neithalath et. al. (2005), the moisture content of the bridge deck can be modeled in terms of both drying time in hours,  $t$ , and depth,  $x$ , from the drying face by the following model:

$$H(x,t) = H_l - (H_l - H_s) \cdot \left[ \operatorname{erfc} \left[ \frac{x}{2\sqrt{D_M t}} \right] \right] \quad (10)$$

where  $H(x,t)$  represents the relative humidity (moisture content) as a function of  $x$  and  $t$ .  $H_I$  and  $H_s$  are the relative humidities at the interior of a sealed concrete and at the surface of the deck, respectively.  $\text{erfc}$  is the complementary error function, and  $D_M$  is the aging moisture diffusion coefficient of concrete. The value of  $H_s$  is taken to be 50%, which is a typical value in New York State for the summertime relative humidity in the atmosphere. Change in the atmospheric humidity will change the surface moisture boundary of concrete deck.  $H_I$  is defined as the relative humidity in the interior of a sealed concrete. Based on the interpretation of test data,  $H_I$  is determined to be a function of time, approximately described by the following equation:

$$H_I(t) = -0.0078125t + 100 \quad (11)$$

Again,  $t$  is given in hours. The value of  $H_I$  is decreased from 100 percent due to loss of moisture to hydration of the concrete mix. The time coefficient in Equation 11 may be modified as a function of the concrete mix. Equation (11) is applicable for the first 192 hours (8 days) of drying after the removal of wetted burlap. If the moisture model needs to be extended beyond 8 days, the following model will be used for  $H_I$ :

$$H_I(t) = -0.0032894737(t - 192) + 98.5 \quad (12)$$

$D_M$  was measured experimentally as a function of concrete specimen age, as shown in Figure 3-12.

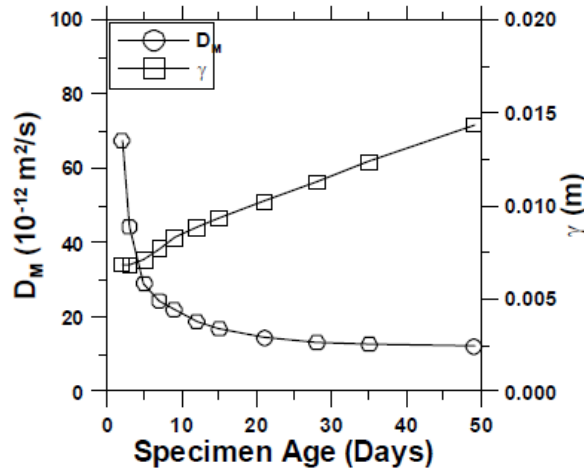


Figure 3-12 – Illustration of Time Dependent Variations in the Moisture Diffusion Coefficient and Gamma (Neithalath et. al. (2005))

The value gamma, which is defined as  $\gamma = 2(D_M t)^{0.5}$ , is determined corresponding to each measured value of  $D_M$ . The behavior of gamma can be reasonably described as a linear function, which takes the following form:

$$\gamma(t) = 0.000279 t + 0.236 \quad (13)$$

It should be noted that gamma is in units of inches and, once again, time is in hours.

In order to verify the moisture model, especially considering the unit conversions made throughout the different portions of the model, a plot was created using Microsoft Excel

demonstrating the updated model, as shown in Figure 3-13(b). This graph was compared to the illustration of the original model, as given in Neithalath et. al (2005).

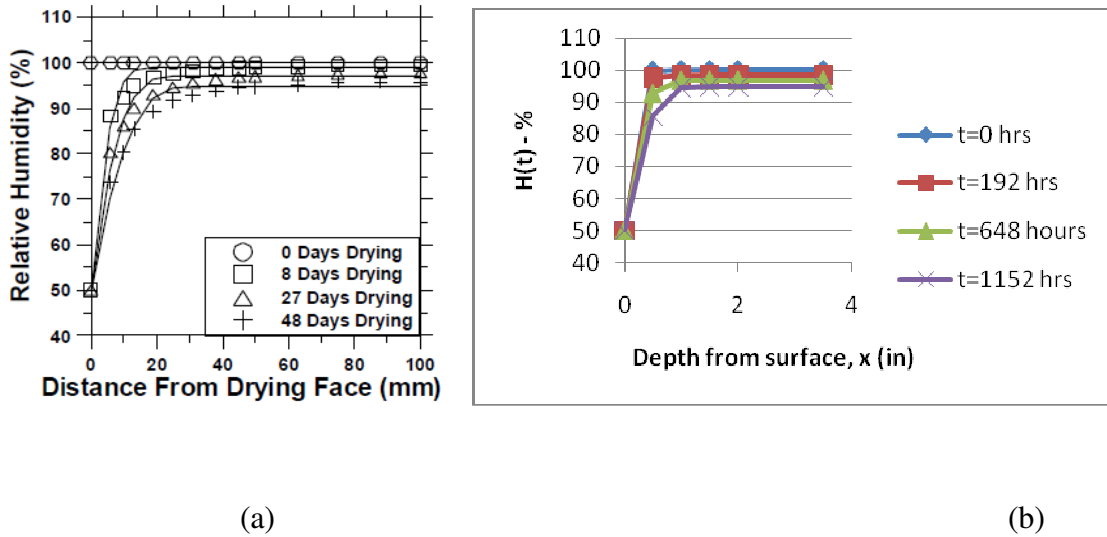


Figure 3-13– (a) Illustration of the Fit Between Moisture Model and Experimental Observations (Neithalath et. al. (2005)). (b) Illustration of moisture model with units updated for this project.

It was decided that the model with the updated units demonstrated sufficient likeness to the original model to consider it a good model. Figure 3-14 shows the changes in moisture content over time for five different concrete depths,  $x$ , as determined using the model described above.

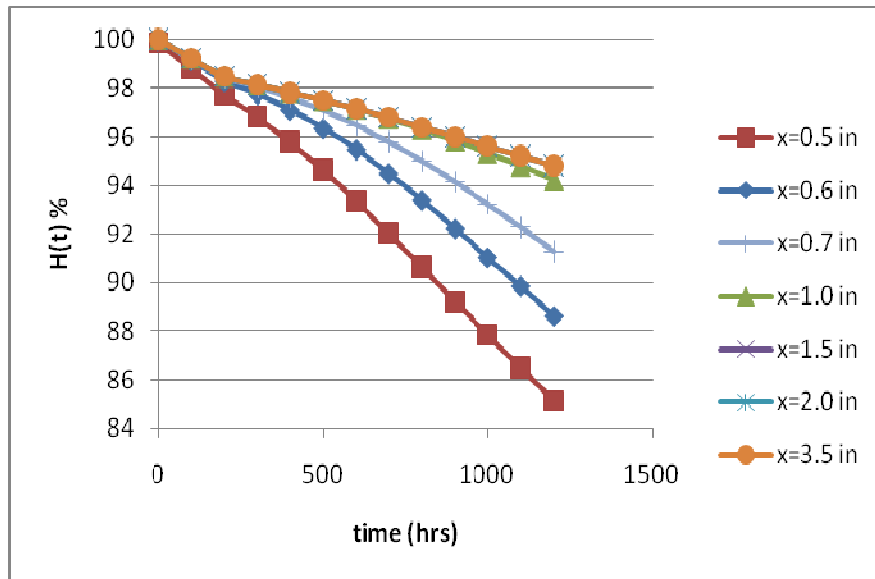


Figure 3-14 – Change in moisture content with time at five different depths from the curing surface

### 3.9 Development of Shrinkage Models for Concrete Bridge Deck:

It was decided that the most practical way to determine the shrinkage due to moisture loss experienced during the curing of a reinforced concrete bridge deck would be to fit a model to existing data on shrinkage. To allow for flexibility of the model, the autogenous shrinkage and drying shrinkage are treated separately. This allows for the beginning of drying shrinkage to be delayed until exposure of the drying surface (i.e. at the time of wetted burlap removal), while still allowing the autogenous shrinkage to begin immediately after the mixing of the concrete.

The graph shown below in Figure 3-15 was taken from the report by Subramaniam and Agrawal (2009) and it contains data describing both the autogenous and total shrinkage strains experienced in three different regions of the New York State Department of Transportation. These values are shown as a function of time.

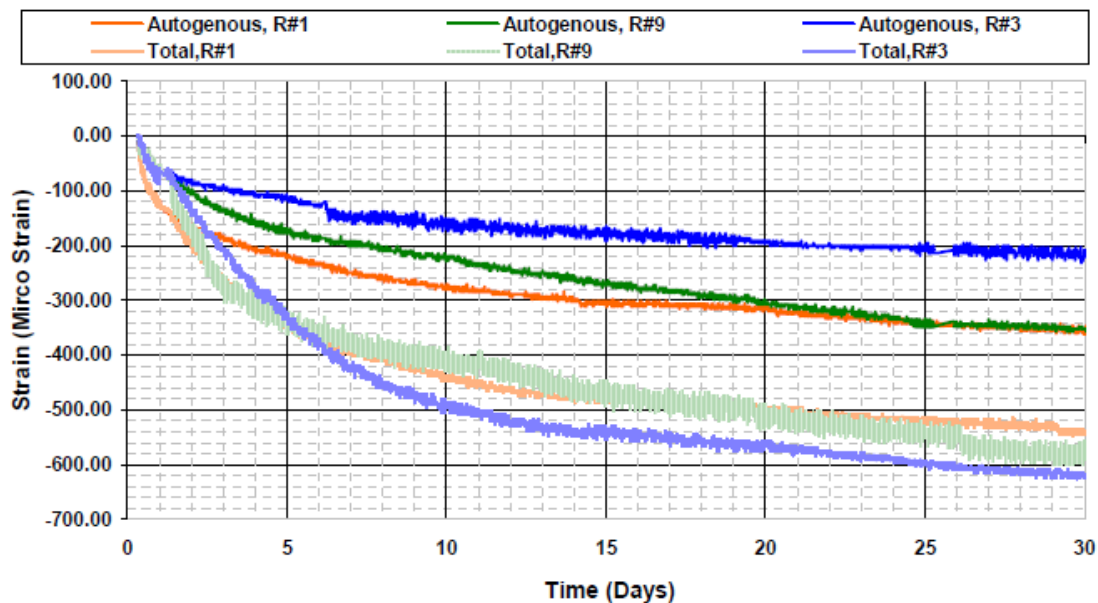


Figure 3-15 – Total and Autogenous shrinkage strains for Regions 1, 3, and 9 (Subramaniam and Agrawal, 2009)

The total shrinkage strain in the Subramaniam and Agrawal (2009) report is defined as the summation of the autogenous and drying shrinkage. Thus, in order to find the drying shrinkage strain at any given time, the autogenous strain is subtracted from the corresponding total shrinkage strain. Looking at the graph in Figure 15, Regions 1 and 9 were chosen to average and fit a model to since they showed very similar results. The averaged data for autogenous shrinkage strains is shown in Figure 3-16 below.

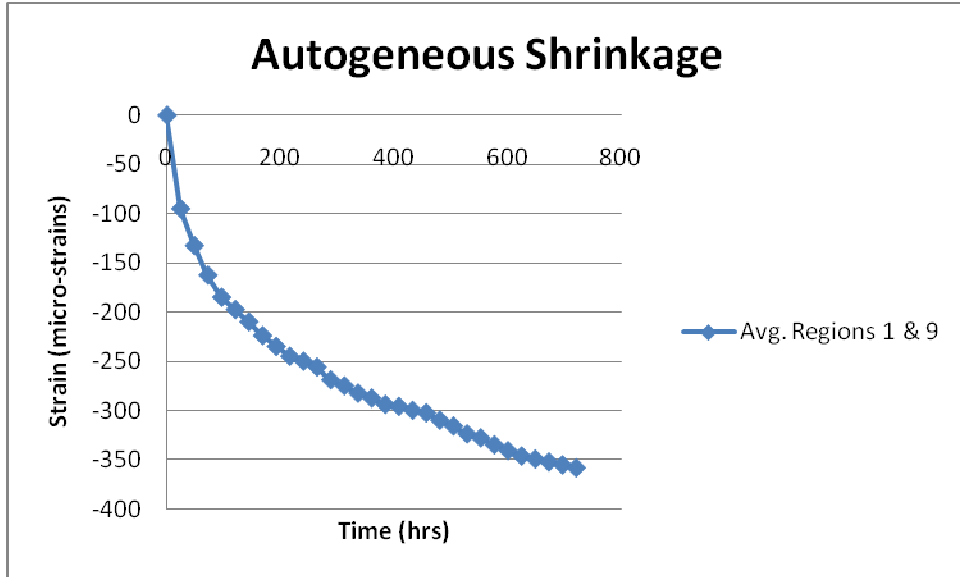


Figure 3-16 – Average autogeneous shrinkage strains for Regions 1 and 9

Through trial and error, the following equation was found to demonstrate a good fit to a majority of the data in Figure 3-16.

$$S_A = \frac{S_{AM}}{2} * \log(0.075t) \quad (14)$$

In this equation,  $S_{AM}$  represents the maximum autogeneous shrinkage strain reached by the system (Note: this should be a negative value), and  $t$  is the curing time. Plotting this equation versus time along with the data shown in Figure 3-16 yields the following graph

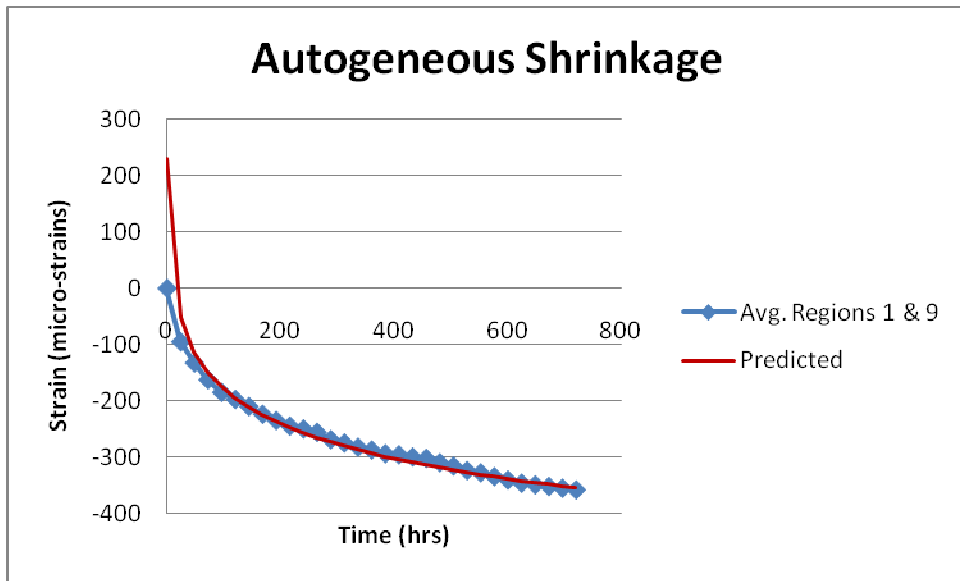


Figure 3-17 – Base model for autogeneous shrinkage strains on a reinforced concrete bridge deck

Upon inspection, equation (14) shows a very good fit to the data, except during the first 24 hours of curing. The data in this range follows a reasonably linear pattern, starting from a shrinkage strain value of zero from time zero. The linear line fit to this range is described by the following equation.

$$S_A = \frac{S_{AM}}{48} \cdot \log(1.8) \cdot t \quad (15)$$

Thus, the overall model for autogeneous shrinkage strain becomes

$$S_A = \begin{cases} \frac{S_{AM}}{48} \cdot \log(1.8) \cdot t & 0 \leq t \leq 24 \\ \frac{S_{AM}}{2} \cdot \log(0.075t) & t > 24 \end{cases} \quad (16)$$

Figure 3-18 shows a plot of the model in equation (16) along with the data points from Figure 3-15.

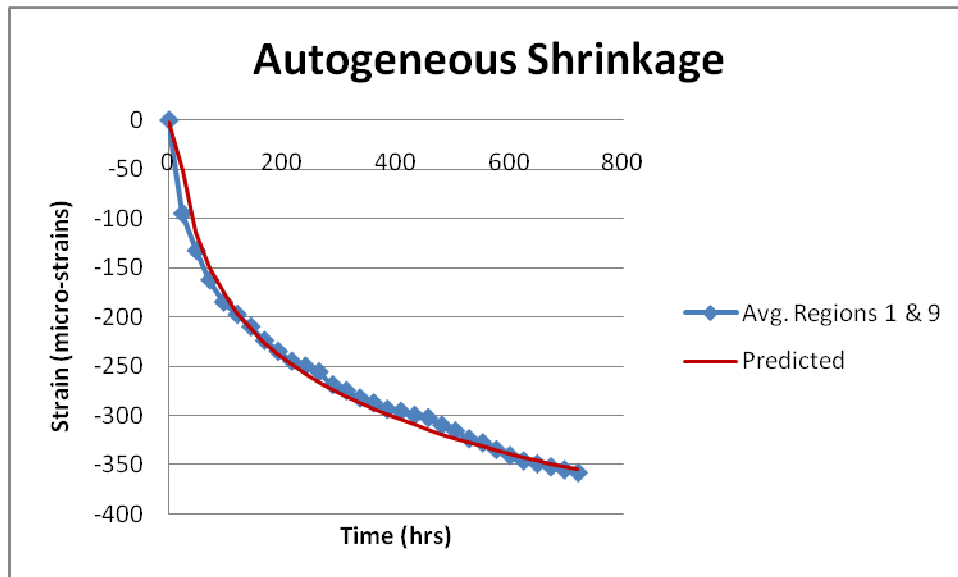


Figure 3-18 – Model for autogeneous shrinkage strains on a reinforced concrete bridge deck

The model for drying shrinkage strain was derived using a similar process to the autogeneous shrinkage strain model. As stated previously, the values for drying shrinkage were

determined by subtracting the autogeneous shrinkage from the total shrinkage, determined from the graph in Figure 3-15. The extracted data was plotted, as shown in Figure 3-19.

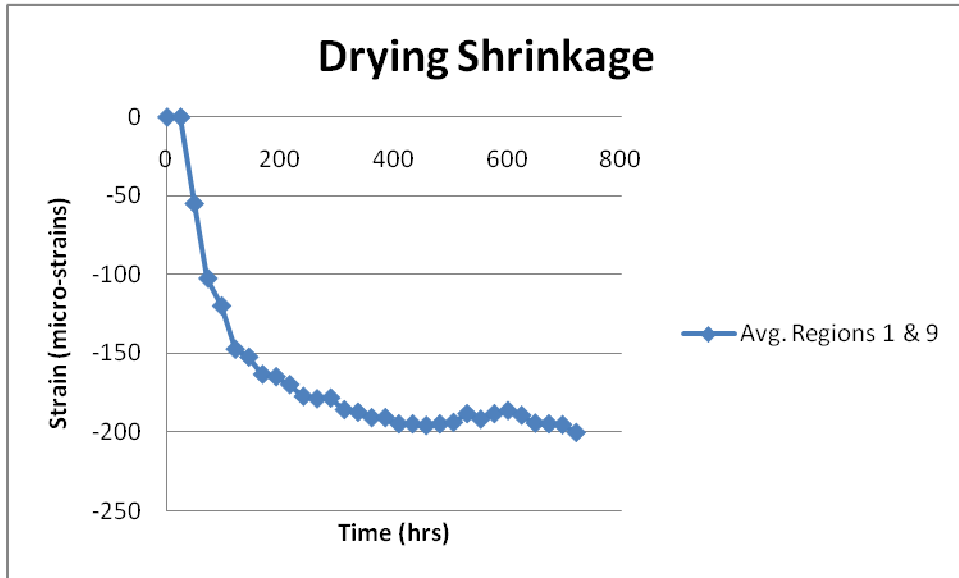


Figure 3-19 – Average drying shrinkage strains for Regions 1 and 9

It was noted from this data that, in the case of drying shrinkage, no strain is developed in approximately the first 24 hours of drying when the wet burlap is removed. This makes sense if the surface is damp when drying is begun; for example from excess bleed water or from moisture remaining on the surface upon removal of wetted burlap. Thus, the first part of the drying shrinkage model dictates that the strain will be zero until some time,  $t_i$ .

Trial and error was again used to determine an equation that followed a reasonably close path to the data after the time  $t_i$  (taken to be 24 hours in this case). The overall model is given in equation (17)

$$S_D = \begin{cases} 0 & 0 \leq t \leq t_i \\ \frac{2}{5} S_{DM} \cdot \log(0.55(t - t_i)) & t > t_i \end{cases} \quad (17)$$

where  $S_{DM}$  is the maximum drying shrinkage strain (again, this should be a negative number). Figure 3-20 shows a plot of the model from equation (17) along with the data from Figure 3-15.

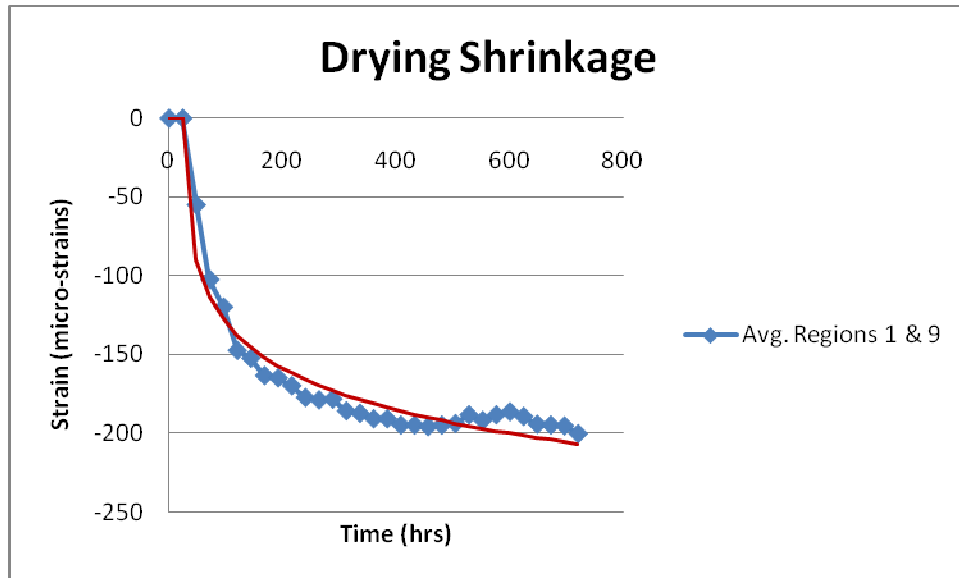


Figure 3-20 – Model for drying shrinkage strains on a reinforced concrete bridge deck

Since the drying shrinkage model from Subramaniam and Agrawal (2009) does not discriminate between the surface layers and interior of the deck, it could only be used to describe the overall through the thickness drying shrinkage. To evaluate layer by layer time history drying strains the approach given by Neithalath et al (2005), as depicted in Figures 3-12, 3-13, and 3-14 was used. Calibration of Neithalath’s model in conjunction with Subramaniam and Agrawal’s data on NYSDOT HP concrete deck shrinkage strain measurements is in Task 4 Report and also summarized in Part 4 of this report on page 57.

### 3.6 Summary and Conclusions of Part 3

Surface convective heat transfer coefficient and internal heat generation time functions have been defined based on test data. These functions are implemented in a one-dimensional time-history finite element analysis to compute the time-history internal temperatures of a typical concrete bridge deck as described in Task 2. The time history relative moisture content of a concrete deck is also expressed as a function of the distance from drying surface and time, calibrated based on test data. Mathematical functions for autogenous shrinkage with time after the placement of concrete and drying shrinkage with time after the exposure of the deck surface to the atmosphere are also derived based on test data. Next step is Task 4 where the functions and numerical methods implemented in Task 3 are to be incorporated into the computational infrastructure developed in Task 2 for the implementation of the formulated theoretical framework in finite element progressive cracking simulation software.

## **Part 4. Implementation of the formulated theoretical framework in finite element progressive cracking simulation software**

In this task the mathematical models for temperature and shrinkage and concrete stiffness developed in Task 3 are implemented into the computational framework from Task 2. Creep strains based on the current thermal and shrinkage (T&S) stresses are also taken into account. The T&S strains and the concrete modulus of elasticity are incrementally analyzed by the computational model. The simulation begins from the time when concrete begins to cure. The time increment may be adjusted. For the first 24 hours it may be appropriate to use one hour increments of time. Once the curing temperatures have been dissipated the time increment can be increased to 24 hours or longer. Thermal finite element simulations indicate that curing temperatures are completely dissipated after 14 days. The time increments for the output of thermal finite element analysis were selected as follows: every hour for the first 36 hours, then at 48 hours, followed by at the end of each 24 hour period up to 158 hours (7 days), then at 14 days, 21 days, and 28 days. Additionally, a plane strain finite element was used for the local analysis of crack opening and determination of crack spacing because of T&S residual stresses.

**Task 4 Deliverable:** At the end of this task, the PI shall deliver an interim report documenting the FEA based composite bridge deck cracking simulation software as well as source and executable files on a CD-ROM for personal computer (PC) with theoretical and user's manuals including an analysis example to the NYSDOT Project Manager. The PI shall first submit a draft report/documentation and the software to the NYSDOT Project Manager and review comments shall be addressed to his/her satisfaction before it is made final. After it is finalized, the PI shall submit two hard copies of the report with the software documentation and a CD with report and documentation in electronic format (Word and PDF) and the software source and executable files to the NYSDOT Project Manager.

### **Corrections to Task 4 Report:**

The draft report for Task 4 was discussed during a meeting held at Clarkson University on October 25, 2010 with presence of the Project Manager from NYSDOT and the PI from Clarkson University. TWG members also participated in the meeting by teleconferencing. It was agreed that Task 4 report is generally acceptable as it addresses all items of temperature and shrinkage effects to compute residual stresses in the bridge deck. The following corrections to Task 4 report were made as a result of the meeting on October 25, 2010.

- 1) The TIMARY and CODEXE subroutines were not included in the task 4 draft report. These subroutines are added as items (2a) and (2b) to the corrected Task 4 report.
- 2) A flow diagram for the CEBRAN program was considered to be very helpful for the user to understand the flow of the program. A flow diagram prepared by TWG member Ryan Lund was added to the corrected Task 4 report.

- 3) In the October 25, 2010 meeting a question was raised on whether or not the steel girder thermal characteristics are included in the thermal finite element analysis (Task 3 related questions). The steel girder properties are included as material type 4 in the thermal finite element analysis program carried out in Task 4. To clarify this point the thermal analysis input file FE3A\_NEW.DAT and the output file FE3A\_NEW.OUT are added to the corrected Task 4 report as items 2c) and 2d).
- 4) In the function DEPSCR, the modulus was calculated inside the function as  $57000*\sqrt{6000}$ . In the corrected report, subroutine INCTET and function DEPSCR are modified to use the time dependent modulus calculated in function ETIME.
- 5) Page 9 of the draft Task 4 report states that: "The computation is coded as function SAUTO that is referenced by subroutine DSHEPS." This statement is clarified on page 70 of the corrected report as "The computation is coded as function SAUTO, which is called by EPSSH, while EPSSH is called by DSHEPS.
- 6) In subroutine UPDBK, should the tensile and compressive strengths of the concrete also be updated with the modulus, as a function of time? The program does not use tensile and compressive strengths for the computation of residual stresses. The tensile and compressive strengths in the databank are the 28-day strengths. However, a function can be used to evaluate the strengths with time to compare the computed stresses with strengths and alert the user if a strength level is exceeded by the corresponding stress. In Task 5 a function that is fitted to compute concrete strength S as a function of time (in days) and the 28-day strength  $S_{28}$  will be written as:
 
$$S = 0.1429 t S_{28} \text{ for } t \leq 3 \text{ days}$$

$$S = C \log_{10} t S_{28} \text{ for } t \geq 3 \text{ days where } C = 0.6925 \text{ if } t > 7 \text{ days and } C = 1.052 - 0.05116 t \text{ if } 3 \text{ days} < t < 7 \text{ days.}$$
- 7) On page 6 of the Task 4 draft report, in subroutine TEMPRD, the comments indicated that "FE3A.out" will be read, but "FE3A\_NEW.out" is read in program. The corrected Task 4 report indicates on page 3 and page 7 that FE3A\_NEW.OUT file is read by subroutine TEMPRD.

It was further agreed that the following improvements will be made in Task 5 model calibration and software validation stage:

- 1) The Thermal Finite Element Analysis Program that is currently a separate code will be made a module of CBRAN and will be called by the main program.
- 2) In general, it may be easier for the user if input parameters are defined in one file, with their definitions, and then these could be passed to other subroutines and functions. This way the program would not have to be recompiled as often as parameters change. For example should Zcoord for concrete be defined in a global input file to define the z coordinates for the concrete deck? Currently it is defined inside of function SHSTR, which is a shrinkage strain function. It was agreed that all input data will be consolidated into appropriate input files with definitions in Task 5.
- 3) In Task 5 the PI will help install the developed software in a Personal Computer running X-windows at the NYSDOT offices in Albany, including the source and executable codes with the ability to make changes and run the code.
- 4) During the October 25, 2010 meeting it was pointed out that the crack size may be underestimated due to the assumption of crack arrest at the top longitudinal

reinforcement. The surface crack is likely to extend through the deck thickness. It was agreed that in Task 5 local analysis for crack size and spacing will be changed to take into account extension of crack to the bottom of the deck using the complete residual stress data through the deck thickness.

#### **Work Done in Task 4:**

Structural analysis uses the Composite BRidge ANalysis (CBRAN) code that was assembled at the end of Task 2 for analysis of vehicle loads. To integrate the temperature and shrinkage effects into the code, the time history from placement of concrete is subdivided into a number of time increments that begin as small as one hour during the first 24 hours and increase gradually as the heat of hydration dissipates. At the beginning of each time increment the following computations are carried out:

1. Input materials databank file is updated with the current modulus of elasticity of concrete. Subroutine UPDBK writes the concrete modulus of elasticity at time  $t$  to material properties databk.
2. CBRAN input file is updated with the “use” and “cure” temperatures where the use temperature is for the current time increment and the cure temperature is in the previous time increment. Subroutine TEMPRD reads the layer temperatures for all time levels from the FE3A\_NEW.OUT results of the thermal finite element analysis and writes a new file TEMPS.LYR that contains the time and associated layer temperatures. The thermal finite element analysis code was presented in the Task 3 interim report and Appendix 3A of this report.
3. The incremental shrinkage strain  $\Delta\varepsilon$  is also accounted for using the same software tool i.e.  $\Delta t_{\text{equivalent}} = \Delta\varepsilon/\alpha$  where  $\alpha$  is the coefficient of thermal expansion.
4. The incremental creep strains are subtracted at each step. Creep strains for HP concrete between the current and previous time increments are computed using empirical data on the creep coefficient of HP bridge deck.
5. CBRAN incremental simulation results for  $\Delta t$  at time  $t$  are stored in a data file. If the cumulative concrete stresses at time  $t+\Delta t$  exceed the modulus of rupture  $f_t$  a message is printed and the program pauses for user options.
6. The crack size and crack spacing are determined using a local plane-strain finite element analysis to zoom into the cracked region. The plane strain analysis assumes the crack is arrested by the top longitudinal T&S rebars.



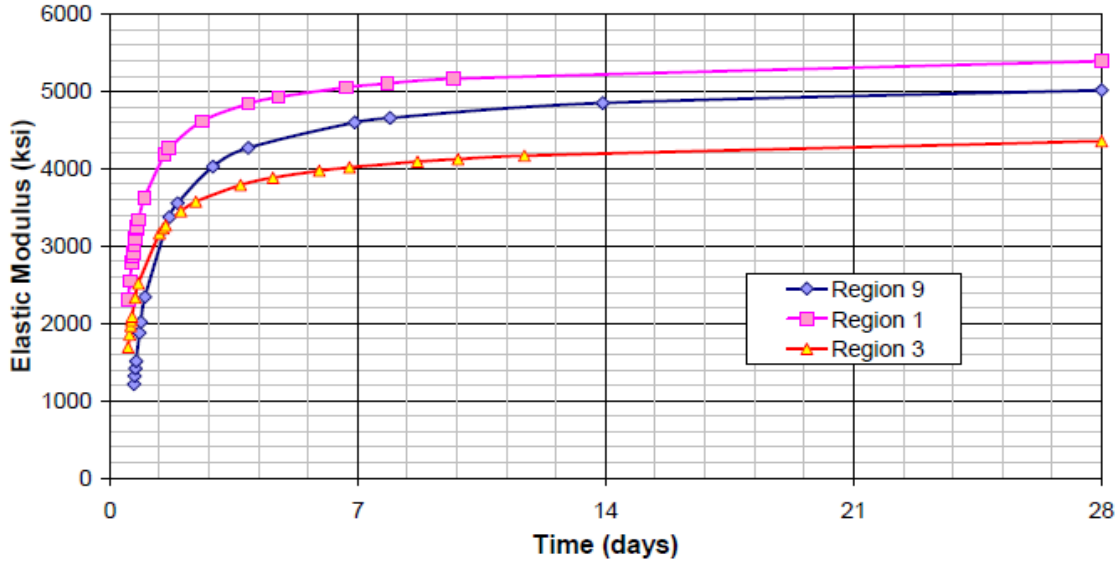


Figure 4-1. Development of Elastic Modulus with age (Subramaniam and Agrawal, 2009)

Additional data, taken from Lee et al. (2009) was used to construct the graph shown in Figure 4-2. The two lines in this plot represent moist cured and dry cured conditions, as indicated by the legend to the right.

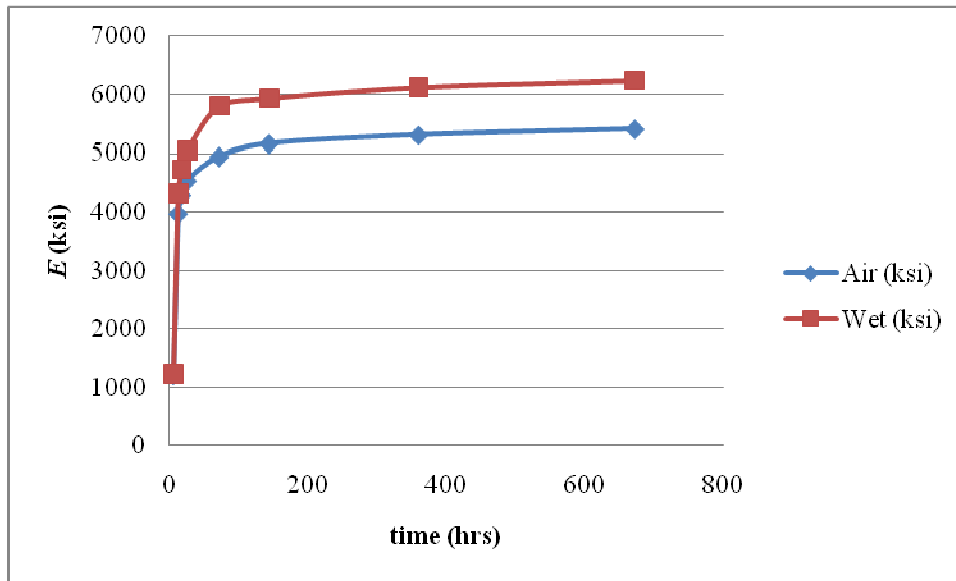


Figure 4-2. Modulus of Elasticity data plotted versus age of concrete (Lee et al., 2009)

A model was fit to the data for modulus of elasticity,  $E$ , in order to represent this property of the concrete versus its age. The equation that was determined to best represent the data provided takes the following form:

$$E(t) = 0.71 \cdot E_{28} \cdot t^{1/19} \tag{4.1}$$

where  $E_{28}$  is the value of  $E$  at 28 days of age. The plot of this model with the original data shown in Figure 4-2 is given in Figure 4-3.

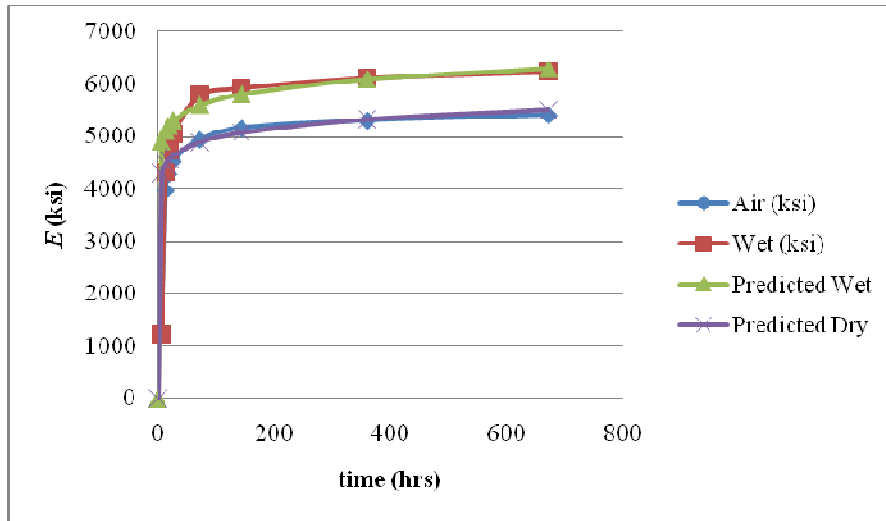


Figure 4-3. Model for Modulus of Elasticity plotted with original data from Lee et al. (2009)

The model given above has been tested with various other data and has been determined to be a reasonable fit. Subroutine UPDBK with the help of function ETIME is used to update the databank properties. A listing of subroutine UPDBK is given in Appendix 4-1

2. Subroutine TEMPRD was added to the CBRAN program. It is called by the main program and reads the thermal analysis output file FE3A\_NEW.OUT and writes a new file TEMPS.LYR that contains the times and associated layer temperatures. The CBRAN program uses the TEMPS.LYR data for each time step to compute the thermal stress increments in unit 77 and accumulated sums of thermal stresses for each layer in unit 91 (file named FOR091.DAT). A listing of subroutine TEMPRD is found in Appendix 4-2.

2b) Subroutine CODEXE is adapted from a composite durability analysis code. It has many additional features for damage progression tracking that are not used in the current application. Subroutine CODEXE functions as the main subroutine that controls the execution of the CBRAN program.

2c) To clarify that the steel girder properties are included in the thermal analysis the input data FE1A\_NEW.DAT to FE1 program as detailed in the Task 3 report, (and in Appendix 3C of this Final Report) is added where the steel girder is included as material type 4.

2d) The output of FE1 program as detailed in the Task 3 report, gives the FE3A\_NEW.OUT file with computed temperatures of concrete and steel layers for each designated time

The main program was updated to carry out the computational flow of the CBRAN code to include T&S and creep effects. A listing of the final MAIN program is in Appendix 4-3.

3. The amounts of autogeneous shrinkage and drying shrinkage strains are computed by the mathematical models developed in Task 3 report. Subroutine DSHEPS evaluates the shrinkage strains. It calls subroutine SHSTR that in turn calls subroutine EPSSH to evaluate drying shrinkage strain at time  $t$  at each layer of the concrete deck. The auxiliary function HIN computes the interior moisture of a sealed concrete as a function of time using Equations 11 and 12 on page 19 of Task 3 report. The function ERFC computes the complementary error function that is used in the drying shrinkage model defined by Equation 10 on page 18 of the Task 3 report. Equation 13 from the Task 3 report was modified to represent the value of  $\gamma$  more consistently with the NYSDOT HP concrete behavior. Using shrinkage data from the CUNY report a graph was constructed that plots the value of  $\gamma$  with time,  $t$  (in hours). The plot is shown in Figure 4-4.

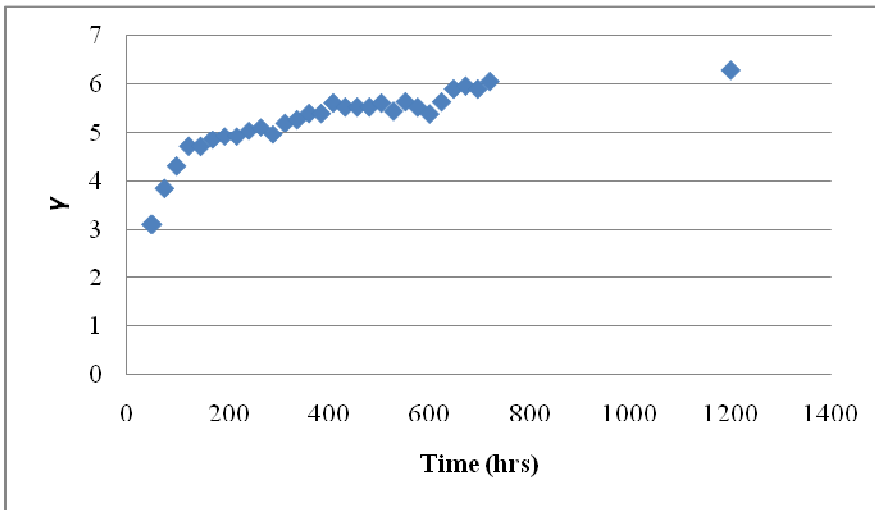


Figure 4-4. Plot of  $\gamma$  values over the curing time, as specific to HP concrete from CUNY report

Including the nonlinear portion of the graph from the first 100 hours of drying, the value of  $\gamma$  is computed as:

$$\gamma = 0.0826 \cdot t - 0.0003591 \cdot t^2 \quad \text{for } t < 116 \text{ hours}$$

$$\gamma = 0.0017 \cdot t + 4.6692 \quad \text{for } t \geq 116 \text{ hours}$$

The autogeneous shrinkage strain is computed by Equation 16 from page 23 of the Task 3 report. The computation is coded as function SAUTO, which is called by EPSSH, while EPSSH is called by DSHEPS.

Simulation with the code shows that initially as the concrete and the top flange of the beam begin to cool down and the girder's thermally induced negative curvature is reduced, concrete stresses are compressive at the surface and tensile in the interior. This effect lasts as long as the wet burlap is present on the surface. However, as soon as the wet burlap is removed and the drying shrinkage begins, tensile stresses appear at the surface of the concrete deck. Simulations show that the T&S stresses at the surface of the deck reach 590 psi after 336 hours (14 days), 605 psi after 672 hours (28 days), and 625 psi after 2020 hours (84.2 days). The modulus of rupture may

be estimated as  $f_t = 7.5(f_c')^{0.5}$ . If we substitute  $f_c' = 6000$  psi then  $f_t = 581$  psi, indicating that cracks may develop due to T&S as early as 14 days. The above simulations do not take into account creep. Shrinkage is computed in subroutine DSHEPS with additional routines a listing of which is given in Appendix 4-4.

- HP concrete used for composite bridge decks has relatively low creep compared to ordinary concrete. Nevertheless the small amount of creep provides a measurable relief of the T&S induced stresses in concrete. Therefore the computational model needs to take creep into account. A new function DEPSCR was coded to compute the incremental creep strains using empirical data on bridge deck HP concretes (deLarrard and Acker 1990). The DEPSCR function is appended to subroutine INCTET that writes the incremental input file to CBRAN with thermal, shrinkage, and creep effects. The incremental creep strain  $\Delta\varepsilon$  during a time increment  $\Delta t$  of stress  $\sigma$  is computed by:

$$\Delta\varepsilon = K_{t_0}(\sigma/E)(\Delta t)^{0.5}/(B + \Delta t)^{0.5}$$

Where  $\Delta t$  is measured in days,  $K_{t_0}$  is the creep coefficient and  $B$  is a parameter indicative of the kinetics of the creep phenomenon for a given concrete. The value of  $B$  may be assumed 1.7 for HP concrete protected from drying. The value of  $B$  may increase to 11 when the HP concrete is not protected from drying. Variation of the creep coefficient depends on the relative humidity (RH). When the HP concrete is covered with wetted burlap  $RH=100\%$  and the lower curve shown in Figure 4-5 below is in effect (deLarrard and Acker 1990).

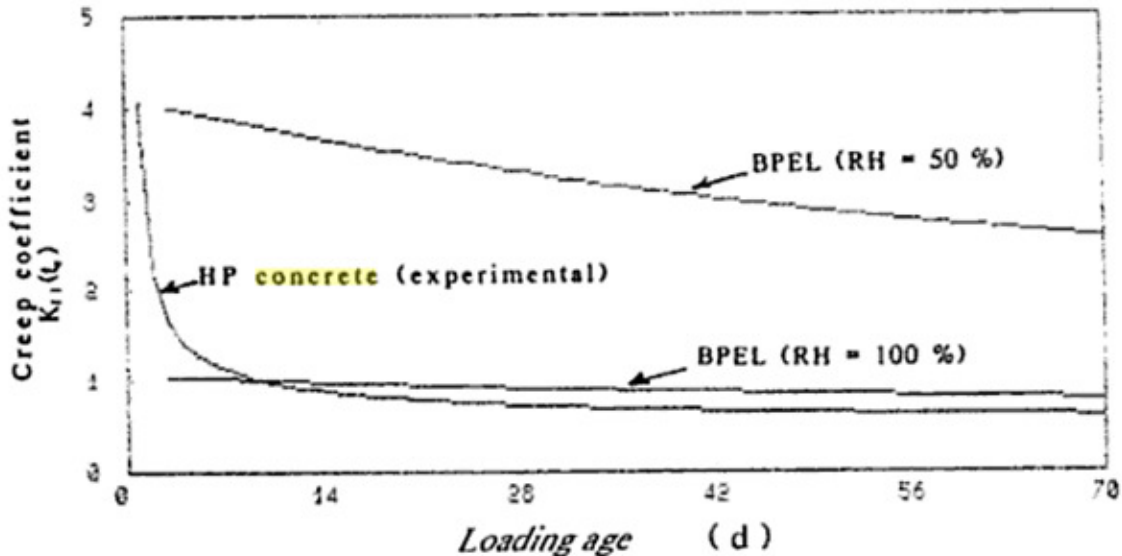


Figure.4-5 Variation of the creep coefficient with time (deLarrard and Acker 1990).

Using two smoothing functions the creep coefficient  $K_{t_0}$  at  $RH=100\%$  is given by:

$K_{t_0} = 4.1$	if $t < 0.9256$ days
$K_{t_0} = 0.2719 \pi^2/t^2 + 0.9681$	if $0.9256 \text{ days} < t < 9.17$ days
$K_{t_0} = 3.5542 \pi^2/t^2 + 0.5828$	if $9.17 \text{ days} < t$

Where  $t$  is the age of HP concrete in days.

After the removal of the wet burlap at time  $t_2$ , the creep coefficient  $K_{t_0}$  at RH=50% is given by:

$$K_{t_0} = 4.1 - (2.4t/70) + 0.000142857t^2$$

Simulations including creep effects with T&S stresses show that at the surface of the deck concrete stresses reach 581 psi after 336 hours (14 days), 592 psi after 672 hours (28 days), and 605 psi after 2020 hours (84.2 days). The effects of creep on T&S tensile stresses is negligible because during the initial times of high creep coefficient, wet burlap covers the deck, and surface stresses remain compressive. In the above simulations it was assumed that the wetted burlap was removed after  $t_2=7$  days. Creep strains are computed by function DEPSCR that is found with subroutine INCTET that does the incremental time-history residual stress analysis. A listing of subroutine INCTET, including the function DEPSCR is given in Appendix 4-5.

5. Simulation of crack size and spacing: To compute the crack size and spacing due to T&S stresses a global-local approach was used. The original MHOST finite element code (OMHOST) was used with a plain strain finite element model above the top longitudinal reinforcement (Nakazawa et al 1987). The OMHOST code is the original standalone version of the same finite element code as that incorporated as an integrated module in the CBRAN code for composite bridge system analysis. Rectangular plane strain elements were used for local simulation. Strain data from the global simulation was used to prescribe the displacement boundary conditions for local analysis. A schematic of the local plane strain analysis region is shown in Figure 4-6.

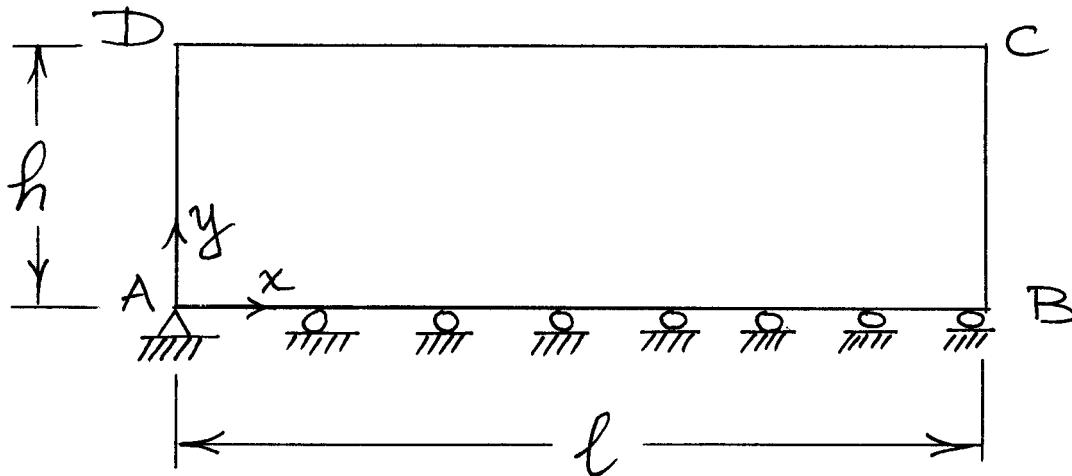


Figure 4-6 Schematic of local analysis region for crack opening and spacing

At point A both the  $x$  and  $y$  components of displacement are restrained. Along the edge AB the displacement in the  $y$  direction is prevented and the displacement along the  $x$  direction is proportional to the distance from point A, or  $u=\epsilon x$  where  $\epsilon$  is the constant

strain of rebar along AB. Along edge BC the displacement along the x axis varies according to the layered strains computed in the global analysis, from  $\epsilon l$  at point B to  $\epsilon l + \Delta\epsilon l$  at point C. Edge BC is not restrained in the y direction except at point B. Edge CD is not restrained in any direction. Edge AD is not restrained in any direction except at point A. Finite element analysis computes the displacement of point D that is interpreted as half the crack opening and the location along the top edge DC where the longitudinal normal stress reaches the modulus of rupture  $f_r$  for the formation of a new crack. The distance from the location of the new crack to point D is interpreted as the crack spacing.

A program named WPSMHM was written to write the plane strain OMHOST model for local analysis. WPSMHM uses depth of the top rebar ( $DC=h$ ), a tentative length from a crack along the girder ( $AL=l$ ), the number of vertical finite element subdivisions (NV), the number of horizontal finite element subdivisions (NL), and rebar strain  $\epsilon$ . A listing of WPSMHM program is given in Appendix 4-6.

Results of local plane strain analysis indicates that because of T&S residual stresses, after 28 days of concrete placement, crack width will be 0.00364 inch and crack spacing will be 5 inches. Loading effects are not included in the crack size and spacing calculations. Development of wider cracks with larger spacing is expected with repeated vehicle load applications.

## Discussion

Computational simulations indicate that after hydration of concrete, low levels of tensile stresses are mainly developed in the interior part of the deck. Longitudinal stresses at the surface of the deck remain compressive until the removal of the wetted burlap. The interior tensile stresses are due to combination of autogeneous shrinkage and thermal contraction of the concrete with the top flange of the girder. The compressive stresses of the surface are mainly due to the loss of the negative curvature of girders that is present during hydration heating because of the thermal gradient between the top and bottom flanges of the girders. After the removal of wetted burlap, drying shrinkage begins that produces the longitudinal tensile stresses at the surface as well as increasing tensile stresses at the interior of the deck and transverse cracks appear. Sealing the concrete surface immediately after removal of the wetted burlap should be considered for the prevention of cracking. Other possible construction practices to reduce cracking are to be investigated in subsequent tasks of this research project. Possible approaches to reduce residual tensile stresses include the following: Selection of girder size with sufficient moment of inertia would lower the neutral axis of the composite section to help reduce tensile stresses in the deck after it cools down from hydration temperatures. Refrigerating the lower flange of the girder at negative moment regions during concrete hydration would increase the compressive stresses at the surface of deck after dissipation of the hydration heat and mitigate tensile stresses due to drying shrinkage.

## Part 5. Model calibration and software validation

The model-based simulation using available models developed in tasks 2, 3, 4, and data gathered from the literature in Task 1 was verified by comparison with experimental results from Task 6. The current experimental results reported on Task 6 were not used to change the model parameters that have been established based on the more detailed and thoroughly reviewed test results from the CUNY Report (Subramaniam and Agrawal 2009). To ensure an acceptable performance before full-scale implementation, the developed software was validated by comparison with the new test data that combined a deck and girder system. NYSDOT Project Manager and the TWG provided input based on bridge deck cracking observations. Key parameters were evaluated to validate the model. A meeting was held on May 19 with the NYSDOT Project Manager, the TWG, and the PIs in Albany during Task 5 and 6. Another meeting was held in Watertown on July 20, 2011

Task 5 Deliverables: At the end of this task, the PI shall deliver an interim report documenting and comparing the software simulations with experimental data to the NYSDOT Project Manager. The PI shall first submit a draft report to the NYSDOT Project Manager and review comments shall be addressed to his/her satisfaction before it is made final. After it is finalized, the PI shall submit two hard copies of the report and a CD with report in electronic format (Word and PDF) to the NYSDOT Project Manager.

The following aspects of the software were compared with test data:

1. Thermal finite element analysis of deck/girder system. Comparison of measured temperatures with computed values.
2. Strains and residual stresses developed due to thermal expansion and shrinkage.
3. Load levels to produce cracking.
4. Crack width and crack spacing.

**1. Thermal finite element model:** The FE3A\_NEW.DAT input data file was used for thermal analysis of the deck/girder test specimen. Thermal finite element sizes are coordinated with deck layer thicknesses for structural analysis. Deck surface temperature is assumed to be kept at 70°F by the wet burlap. Thermal analysis is conducted up to 720 hours after placement of concrete. Hydration reaction is assumed to begin seven hours after the placement of concrete. A mistake in setting the nodal coordinates was corrected due to observation by Ryan Lund during the July 20, 2011 meeting followed by written request.

The output from thermal analysis is given by the FE3A\_NEW.OUT file. The CBRAN structural analysis software parses the file to obtain the more compact TEMPRTRS.LYR file that provides the layer temperatures for each designated time step as shown in Appendix 5-1.

To verify the computed temperature rise with test data we compare the computed results with Task 6 laboratory test report's Figure 27 Thermocouple Temperature Profile. Gage T9 is approximately at the center of the deck and corresponds to finite element node 16. We plot the simulated temperatures at node 16 for the first 120 hours or 5 days. The corrections to thermal analysis increased the simulated temperatures by no more than 0.3°F. The maximum temperature rise is computed as 40°F. In the test case the concrete temperature was initially measured at 68°F(20°C). Test data shows an initial drop of thermocouple temperature from 21.5°C room temperature to as low as 10°C due to wetting of the formwork with cold water just before the placement of concrete, then it rises to 41°C (105.8°F) at its peak. The concrete temperature rose by 19.5°C (35.1°F) from the room temperature and by 21°C (37.8°F) from initial concrete temperature. It may be assumed that a small amount of the hydration heat was used to bring the concrete temperature up to the room temperature. Dissipation of heat is slower for the test case compared to the simulation. This is most likely due to higher temperature of the wetted burlap in the test and the higher ambient temperature. In both the simulation and the test results the concrete temperatures approach the ambient temperature within the five days.

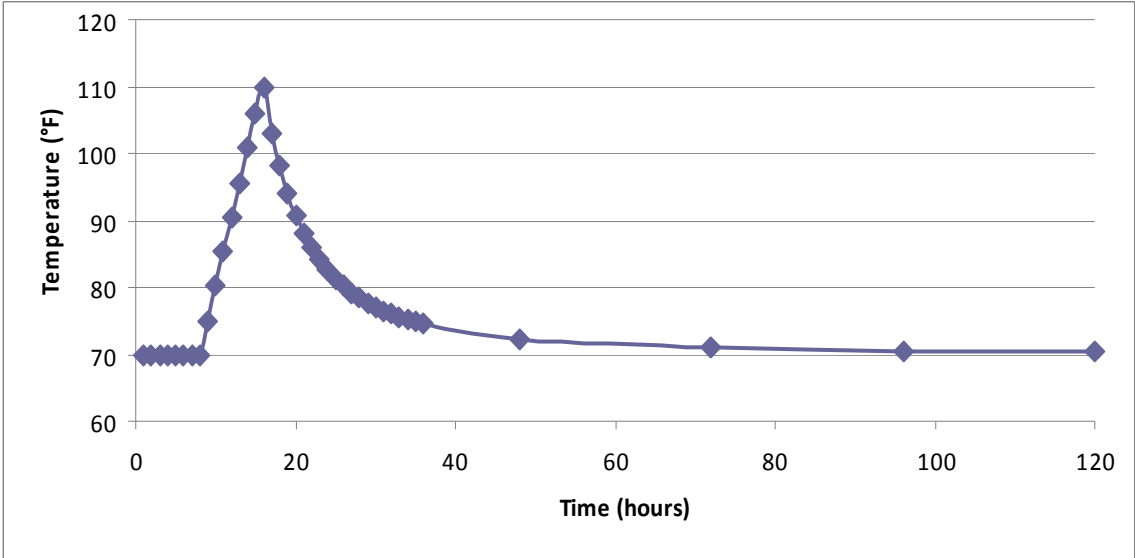
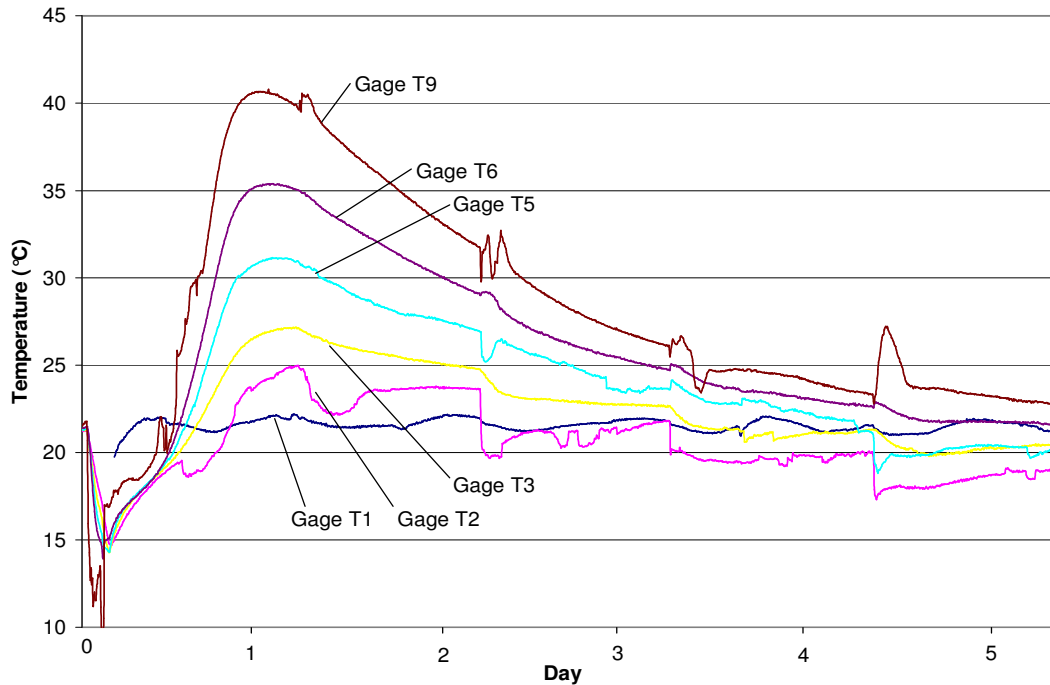


Figure 5-1- Computed temperature at node 16 corresponding to location of gage T9

**Thermocouple Temperature Profile (1st 5 days)**



Test Figure 1: Thermocouple Temperature Profile (Test)

## 2. Strains and residual stresses developed due to thermal expansion and shrinkage

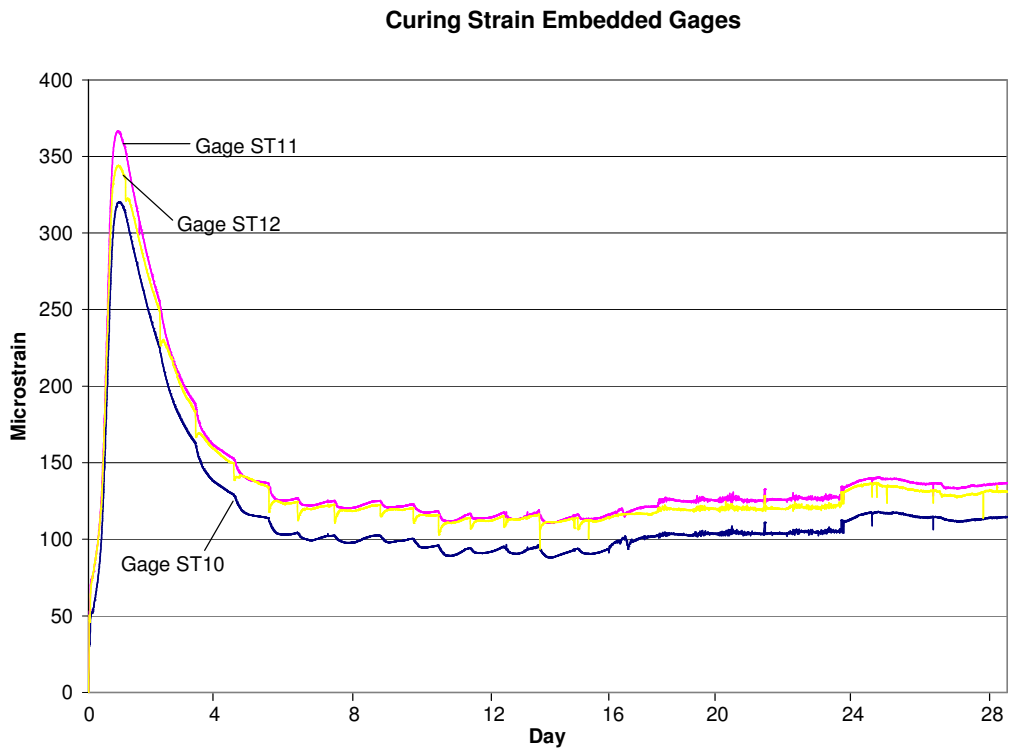
Comparison of measured total strains to software prediction:

It is noted that the measured total strains are the algebraic sum of initial strains due to temperature changes with shrinkage/creep and also elastic strains that produce stresses.

$$\epsilon_{\text{total}} = \epsilon_{\text{initial}} + \epsilon_{\text{elastic}}$$

Measured strains during the initial hydration of concrete are mainly initial strains due to thermal expansion as the hydration reaction takes place. For comparison of test data with computer simulations we consider the embedded strain gages ST11 and ST12 that are between the bottom rebar and the top flange of the girder (Figure 41 from test report copied here for convenience). ST11 and ST12 are at approximately node 24 of thermal FEM at the bottom of the concrete deck. The initial strains  $\epsilon_{\text{initial}}$  due to temperature rise are  $\epsilon_{\text{initial}} = \alpha_t \Delta T$  where  $\alpha_t$  is the coefficient of thermal expansion for concrete. The residual stresses  $\sigma$  that develop correspond to the elastic strains  $\epsilon_{\text{elastic}} = \sigma/E$ . It is noted that the test strains begin at approximately 50 microstrains at time zero. This is because the girder is not supported at its right end and the weight of concrete

produces an initial negative curvature of the girder. The VW strain gages are attached to the girder through the reinforcing cage and therefore register this initial strain. However, this initial strain does not affect the residual stresses developed due to temperature and shrinkage since the concrete is initially in liquid form. Figure 5-2 shows the thermal expansion strains during the hydration of concrete. The maximum strain in Figure 5-2 is 237 microstrains as compared to the measured strain of approximately 350 microstrains (average of gages ST11 and ST12). Part of the difference (approximately 50 microstrains) may be attributed to the initial loading of the girder by the pumping of concrete and the remainder of the difference (approximately 63 microstrains) may be attributed to the larger temperature rise of VW gage from its lowest temperature (10°C) to the highest temperature (41°C), a total of 31°C. The computed temperature rise was from 70°F (21.1°C) to 110°F (43.3°C), for a total of 40°F (22.22°C). The computed temperature rise was 72 percent of the tested temperature rise of the VW gage and the computed initial thermal strain (230  $\mu\epsilon$ ) is approximately 77 percent of the estimated test initial thermal strain (300  $\mu\epsilon$ ). The computed residual stresses at layer 24 at the bottom of the deck (9.5 inches from the top of the deck) due to temperature and shrinkage are shown in Figure 5-3. The effect of drying shrinkage after 14 days (336 hours) is visible. The initial rise of the compressive stresses is due to thermal expansion of concrete that is restrained by the cooler steel girder.



Test report's Figure 2: Curing Strain Embedded Gages

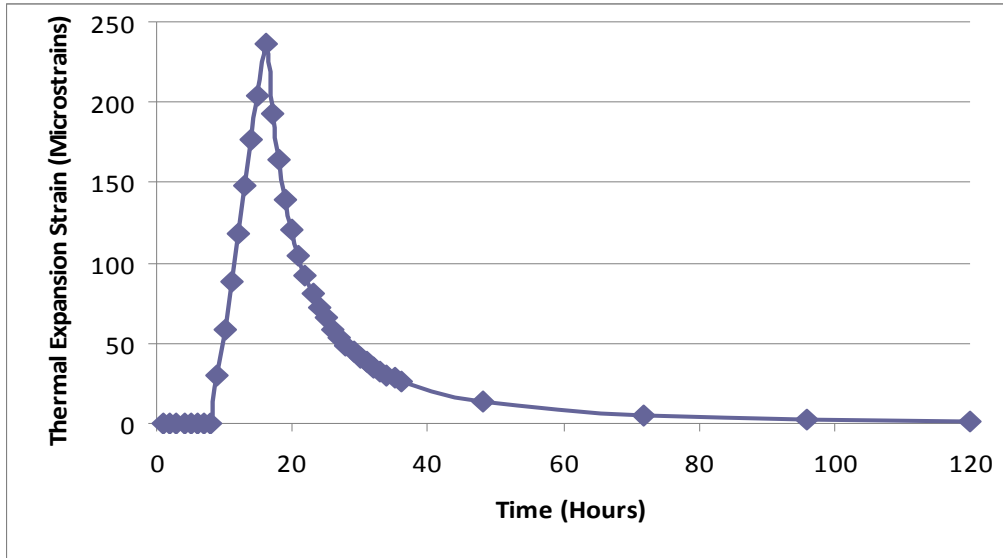


Figure 5-2. Thermal Expansion Strains during Hydration of Concrete

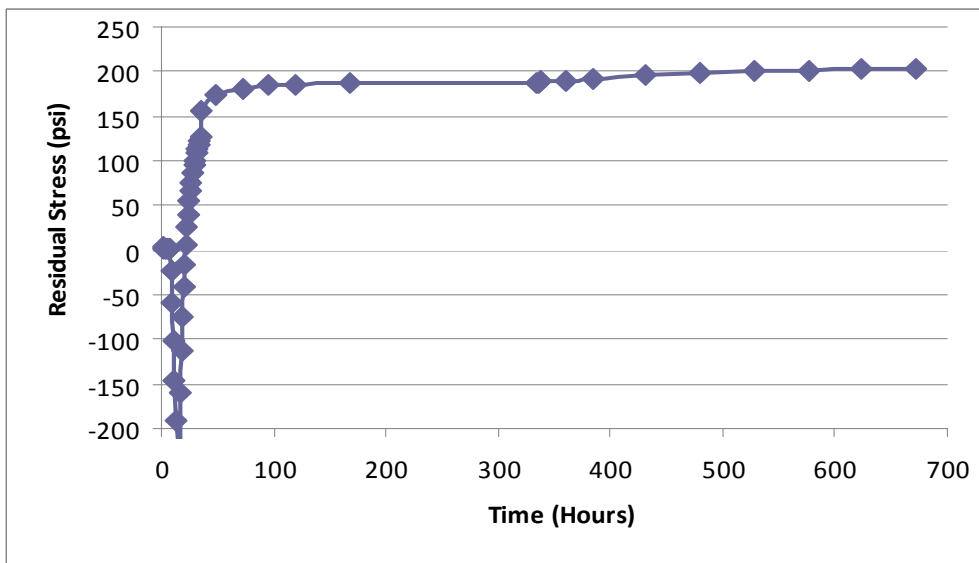


Figure 5-3 Computed Residual Stresses in Concrete at bottom of deck due to Temperature and Shrinkage

**3. Load levels to produce cracking:** In the test case the first crack was formed under a 14,000 lbs load applied at the right end of the girder. Computational simulation showed that under the 14,000 lbs load longitudinal tensile stresses above the top reinforcement bars of the deck exceeded 800 psi. That is well above the modulus of rupture of 581 psi. However stresses at

the top longitudinal reinforcement bar level were 605 psi and the stresses below the top rebars were below the modulus of rupture. Here, we should consider that the deck stresses near the surface are strongly affected by drying shrinkage. Our computer model assumed a 35 percent constant relative humidity that was measured initially near the test specimen. Due to fluctuation of humidity between day 14 and day 28 it is likely that drying shrinkage may have been slower. For example if the relative humidity were 45 percent, the tensile stresses at the surface of the concrete deck would have been reduced by approximately 100 psi. In any case, the test showed no visible cracking below the 14,000 lbs load level. When the tensile stresses at the top longitudinal reinforcement approached the modulus of rupture, the deck cracked, rebars debonded at the crack, and the load dropped. There may have been previous microcracking above the top rebars, but if present such microcracks were not observed by sight. If these observations are correct, it may be concluded that the critical stress levels at the top rebar are the most pertinent for the formation of transverse cracks. The residual stresses near the surface are very strongly affected by drying shrinkage. The CUNY report did not provide through the thickness variation of drying shrinkage strains. A model of drying shrinkage was used from the literature based on tests conducted at Purdue University (Neithalath et al 2005). During our meeting on July 20, 2011 it was suggested adjusting the drying shrinkage model to take into account the lower porosity of HP concrete. Tests with the software show that it takes a very large reduction in the aging coefficient  $\gamma$  (i.e. reducing  $\gamma$  to 10 percent of its specified value) in subroutine DSHEPS to reflect in a substantial decrease in the residual stresses due to shrinkage.

#### **4. Crack opening and spacing:**

Computational simulation with the corrected software shows an initial crack opening of 0.0026 in. and a crack spacing of 141 in. for the formation of secondary cracks under the same load. In the test the crack width under the 14,000 lbs loading was estimated as 0.004 in. Since the available concrete deck was much shorter, the load needed to increase to 22,000 lbs for the formation of a second crack approximately 9.5 inches from the first crack. At the location of the second crack the load induced stresses under the 14,000 lbs load that produced the first crack were only 140 psi. With the addition of 125 psi temperature and shrinkage stresses the stress level was 265 psi. The additional 8,000 lbs increased the stress levels at the location of the second crack so that the stresses at the top longitudinal rebar level exceeded the modulus of rupture and the second crack was formed. We recall that 14,000 lbs was needed to raise the tensile stresses from 125 psi to 581 psi, or 0.33 psi per pound of loading. For the second crack, 8,000 lbs additional load was needed to raise the stresses from 265 psi to 581 psi or 0.040 psi per lb loading. In the formation of the second crack, part of the loading was expanded into widening the first crack.

## **Part 6. Integration with Structural Health Monitoring (SHM): Experimental Testing of Early Age Transverse Cracking of Composite Bridge Decks**

Experimental testing of early age transverse cracking of composite bridge decks was conducted as part of development of a structural health monitoring (SHM) methodology to detect and track the evolution of cracking in bridge decks. Early age transverse cracking of composite bridge decks was investigated by building an experimental bridge deck model that conformed to the features of a real deck construction. Testing included monitoring the curing phase of the concrete by using thermocouples, thermistors, and strain gages. A secondary test was performed after the curing by loading the bridge until cracks formed. During the secondary test, strain and cracking data was collected. The testing provides methodologies for software coordinated SHM to give better insight into the performance of the prototype bridges. During Tasks 5 and 6 meeting with the NYSDOT Project Manager, the TWG, and the PIs were held in Albany on May 19, 2011 in Watertown on July 20, 2011.

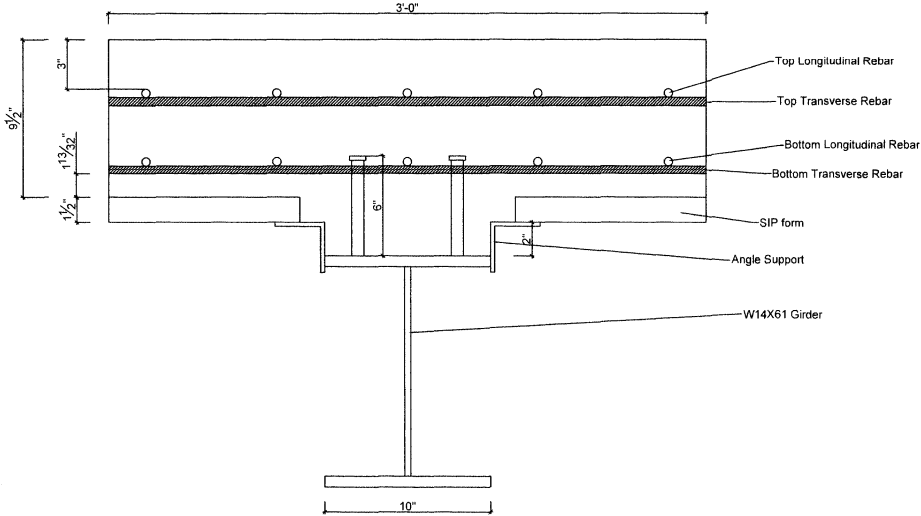
Task 6 Deliverables: At the end of this task, the PI shall deliver to the NYSDOT Project Manager an interim report documenting the software coordinated experimental testing and related results. The PI shall first submit a draft report to the NYSDOT Project Manager and review comments shall be addressed to his/her satisfaction before it is made final. After it is finalized, the PI shall submit two hard copies of the report and a CD with the report in electronic format (Word and PDF) to the NYSDOT Project Manager.

The following summarizes the test girder-deck model and results conducted under Task 6. Task 6 report is based on the Masters of Science thesis of Matthew LaPlante who served as the Graduate Research Assistant for this phase of the project.

A bridge deck model was designed based on NYSDOT specification as much as it was possible for laboratory testing. The bridge deck model was designed based on decisions to obtain the most reliable and accurate model possible. The objective was to experimentally analyze the model bridge during curing and during a loading sequence. The model was instrumented with thermocouples and vibrating wire strain gages. The temperatures and strains of the model were measured during the curing phase. During the loading phase, the strains were recorded. The displacement was increased and the cracking of the concrete was observed, measured and documented. All of the data was then analyzed to help determine why transverse cracking was occurring on composite bridge decks at an early age.

The testing of the concrete was done when it was fresh to determine initial properties. Cylinders were made to better understand the strength of HP concrete as it cured. The temperatures were measured during the twenty-eight day curing period. The maximum temperature was reached in about twenty-four hours after initial placement then decreased

eventually to ambient temperature. The strains were also measured during the curing period and its maximum was reached when the temperature was at its peak.



Cross Section of Bridge Model



Figure 6-1 Reinforcement on Model

After the 28 day curing period, the bridge model was loaded by a hydraulic universal testing machine. The load was applied at the right end of the girder. The composite deck-girder

center was supported at midspan. The left end of the girder was anchored down by two bolts through the flanges as shown in the picture. During the loading, the deflection, strain, and cracking were all measured. The beam was then analyzed to determine when it lost its elasticity. Finally, the cracks were examined to determine the crack widths and the changes that occurred.



Figure 6-2 Left End Support



Figure 6-3 Center Support

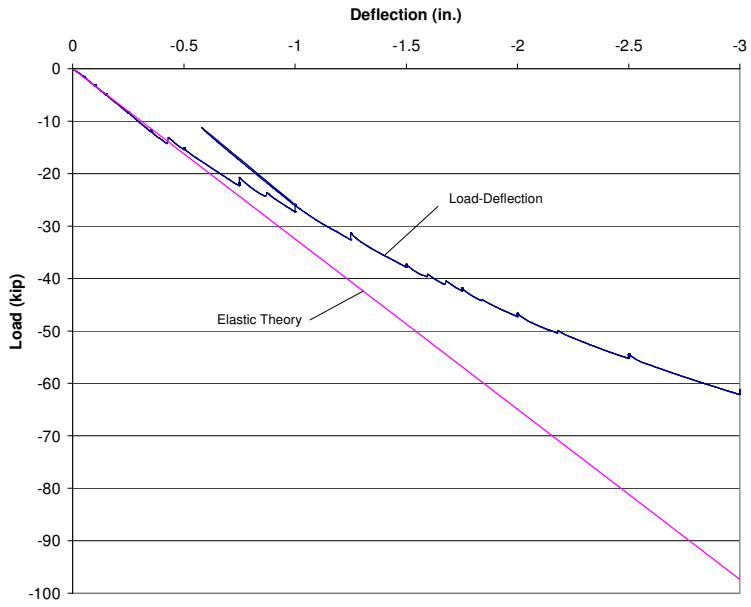


Figure 6-4 Load Deflection Curve



Figure 6-5 Actuator Loading on right end of Girder

## **Part 7. Implementation and technology transfer with recommendations for bridge deck cracking mitigation**

The research team conducted a one-day training course in Albany for NYSDOT engineers on August 3, 2011 to communicate the research findings and recommendations as well as provide training for the use of the developed software. Based on the literature search and the model-based simulations, recommendations to mitigate transverse cracking in composite bridge decks of newly constructed bridges in terms of materials selection, design details and construction practices were identified and recommended for implementation. A meeting will be held with the TWG in Albany on August 19, 2011 to discuss and evaluate results of this project.

**Task 7 Deliverables:** At the end of this task, the PI shall deliver a one day training course to the NYSDOT personnel. The PI shall first submit a draft plan of the one day training course and associated materials as well as a draft report on recommendations to avoid/mitigate transverse cracking to the NYSDOT Project Manager and review comments shall be addressed to his/her satisfaction before they are made final. After it is finalized, the PI shall submit twenty-five (25) copies of printed and electronic training materials and recommendations to mitigate transverse cracking to the NYSDOT Project Manager.

Developed software components run either in the Absoft Development Command Shell or MS-DOS Command window (start/Run/cmd). Compilation of the software is carried out in the Absoft Development Command Shell. A commercial/government Absoft license was purchased by Clarkson University on June 24, 2011 for use by NYSDOT to compile the developed software source. The following procedures for data preparation and running the software were covered in the one day training workshop on August 3, 2011:

1. Generation of data for the CBRAN structural analysis program and writing the input file FOR085.ORG with the help of a short preprocessor. Example fortran preprocessor programs are in the directory CBRAN INPUT GENERATOR. The MDL\_TY.FOR file generates the structural analysis model for a two-span continuous bridge. This model is named as “mdl\_in\_t.dat” that is renamed as FOR085.ORG to run with CBRAN. TESTL\_TY.FOR file generates the CBRAN input file “test\_m\_t.dat” for the laboratory test bridge of Task 6. The WATFOR77.EXE fortran interpreter with the accompanying CONFIG.COM file are used to run the fortran preprocessor files to generate models by using the command WATFOR77 TESTL\_TY.FOR or WATFOR77 MDL\_TY.FOR in the Development Command Shell or the MS-DOS Command window. The WATFOR77 fortran interpreter can also be used to generate preprocessor executable files. For example, using the command watfor77/exe mdl\_ty will produce the mdl\_ty.exe file that can be run to generate the input data file for a two span continuous bridge with 100’ spans.
2. Preparation of nodal coordinates for the FE3A thermal analysis input file FE3A\_NEW.DAT. Nodal coordinates may be obtained by running the PREAD.FOR program in the THERMAL\_ANALYSIS\THERMAL\_ANALYSIS\_NODAL\_COORDINATES\_GENE

RATOR directory. The PREAD.FOR program uses information from the CBRAN input file FOR085.ORG generated in step 1 and parametr.dat file.

3. Prepare the FE3A\_NEW.DAT thermal analysis input file using the nodal coordinates generated in step 2. Format of the FE3A\_NEW.DAT input file is documented in the Task 3 report. Run the FE3A thermal analysis program in the THERMAL\_ANALYSIS directory.
4. Copy the results of step 3 FE3A\_NEW.OUT file into the CBRAN\SRC\LAB\_TEST or DECK\_TEST directory. Also include FOR085.ORG, databk.org, parametr.dat, cbran.exe, and prep.bat files in the same directory. First issue the prep.bat command, then run CBRAN with the command cbran > cbran.out. The cbran.out file will contain all screen dump of debugging statements. Stresses for each time step will be summarized through the thickness in FOR091.DAT file for the designated structural node. Layer by layer stresses are printed up to 672 hours (28 days) and after the application of a loading that is expected to produce cracking.
5. To determine the cracking width and spacing a local plane strain finite element model is used. The input data file is prepared in the OMHOST\DATA\_prep directory. Running the WPSMHM.FOR file requires an estimated value of the crack depth. Discussions during TWG meetings had concluded that cracks extend the total depth of the deck. During the laboratory experiment, cracks appeared to extend close to the bottom of the deck at the edges. Assuming that crack depth is 9.5 inches, we enter the stress level at layer 24 of 195.2 psi into WPSMHM.FOR to compute strains at the bottom of the crack to generate the OMHOST input file crack.dat. Then we copy crack.dat into the OMHOST\_CODE directory to run OMHOST. The output shows the displacement of one side of the crack to be 0.0013 inch, making the crack width estimate 0.0026 in. In comparison, test crack was compared with crack gage to be approximately 0.004 in. From the CRACK.OUT results file crack spacing under the same loading is estimated to be 140 inches. This is based on the growth of surface stresses as we move away from the stress relief of the crack opening. There is no experimental comparison because the test deck was not long enough.

## Results of Part 7:

Residual stresses due to temperature and shrinkage are accumulated and listed for each time step in the FOR091.DAT file. During the TWG meeting on August 19, 2011 Ryan Lund pointed out that autogeneous shrinkage strains were being computed but not being accumulated in subroutine DSHEPS for the computation of residual stresses. Further investigation indicated an additional decimal point mistake in evaluating shrinkage strains. The corrections were made to subroutine DSHEPS and results were reevaluated.

For the laboratory test bridge, a support was provided at midspan of the 12 ft long composite girder-deck system. A tie down was installed on the left end of the girder 10 ft from the middle support. Layered models were used for (1) deck only, (2) integrated deck and girder, (3) girder only for the end extensions. Appendix 7-1a shows listing of the TESTL\_TY.FOR preprocessor program to generate the CBRAN input file. After 28 days a concentrated load was applied at the right end as detailed in the Task 6 Report. The first crack was heard and observed under a 14,000 lbs load. The new results matched the laboratory test results from Task 6 fairly

well. Analysis showed that after 28 days residual tensile stresses were raised to 313 psi that is well below the estimated modulus of rupture of 581 psi. After the application of the 14,000 lbs loading tensile stresses above the top rebars were raised to 633 lbs that produce cracking. Appendix 7-1b shows stresses at the critical node after 28 days and after the application of the 14,000 lbs loading as printed in the FOR091.DAT file.

For the two-span continuous bridge with a 36" steel girder, after 672 hours (28 days) the stresses above the top longitudinal rebars were raised to 248 psi that are well below the estimated modulus of rupture of 581 psi. However, stresses are raised to 598 psi that is slightly higher than the level of modulus of rupture when HS25 trucks pass over the bridge spans. Appendix 7-2a shows the representation of layered structure from the beginning of the FOR085.ORG structural analysis input file. The preprocessor program MDL\_TY.FOR that generates the CBRAN input file is given in Appendix 7-2b. Appendix 7-2c shows stresses at the critical node after 28 days and after the application of HS25 truck loadings as printed in the FOR091.DAT file.

Next, for the same two span bridge model the girder depth was increased by fifty percent to 55". The input data file MDL2\_INT.DAT was generated using the MDL2\_TY.FOR preprocessor as outlined in Step 1 above. The CBRAN input file layer structure is shown in Appendix 7-3a. Thermal analysis was also updated to the deeper girder. In this case the residual stresses due to temperature and shrinkage were approximately 320 psi after 672 hours (28 days). The increased stress level is due to the additional restraint imposed by the larger girder. However, when HS25 trucks were critically placed over both bridge spans, the stresses were raised to approximately 509 psi that is below the modulus of rupture of 581 psi. Therefore the results indicate that even though the temperature and shrinkage residual stresses increase with the girder depth, the live load stresses are substantially reduced to avoid cracking. Appendix 7-3b shows stresses at the critical node after 28 days and after the application of HS25 truck loadings as printed in the FOR091.DAT file for the deeper girder bridge.

### ***Alternate Model of Deck with Thin Steel Rebar Layers***

During the TWG meeting on August 19, 2011 it was suggested that an alternative model with a thin steel layer for each rebar level may be more appropriate to clarify the distinction of steel rebar and concrete properties. Appendix 7-4a shows the layer structure with thin steel rebar layers used for the bridge deck with the 36" composite girder. In this model 0.025" steel layers represent #4@8" rebars for longitudinal or transverse rebars top or bottom. The CBRAN input file with thin steel rebar layers was generated by the preprocessor program MDL\_TY\_N.FOR listed in Appendix 7-4b. The residual stresses accumulated after 28 days and the additional HS25 live load stresses from the FOR091.DAT file are given in Appendix 7-4c. It is noted that stresses computed by the thin rebar layers model are somewhat higher than those computed by the previous composite rebar and concrete layers. Further experience is needed to test the reliability of the new model with thin steel rebar layers.

## Conclusions

A computer program has been developed and implemented to compute the time-history residual stresses due to temperature and shrinkage. The program also adds HS25 vehicle loads after 28 days from the placement of concrete. Cracking is predicted if tensile stresses developed in the bridge deck exceed the modulus of rupture of concrete. After the formation of a crack, crack width and spacing are evaluated using a local plane strain finite element model with displacement boundary conditions derived from strains computed by the global structural analysis. Results indicate that the effects of autogeneous and drying shrinkage are the most significant in building up the residual tensile stresses in a bridge deck. Temperature effects due to the heat of hydration are less significant. It is possible to further mitigate temperature effects by controlling girder temperatures during the first four days after placement of concrete. Keeping the bottom flange of the girder significantly cooler than the top flange during hydration of concrete would help reduce the residual stresses due to the cooling down of concrete from hydration temperatures. The bottom flange of the girder would be allowed to warm up gradually as the concrete cools down. This would produce an additional positive curvature of the deck and reduce the tensile stresses at the surface. Autogeneous and drying shrinkage are more difficult to mitigate. Drying shrinkage may be reduced by coating the deck with a moisture barrier. Autogeneous shrinkage may be mitigated by addition of expansive cements in the HP concrete mix. Vehicle loads add more tensile stresses to the top of deck in negative moment regions and are usually the initiator of cracking. Increasing the girder depth increases residual stresses in concrete due to shrinkage. This is because a larger girder provides more constraint that resists the concrete shrinkage. However, increasing the girder depth reduces live load stresses in the concrete deck. Computational simulations show that increasing the girder depth improves the overall cracking resistance of deck.

## References

- ACI Committee 224 (2001), "Control of Cracking in Concrete Structures (ACI 224R-01)," American Concrete Institute, Farmington Hills, MI
- AISC Steel Construction Manual (2005). 13th. American Institute of Steel Construction
- ASTM Standard C143, 2010, "Standard Test Method for Slump of Hydraulic Cement Concrete" ASTM International, West Conshohocken, PA, 2010, DOI: 10.1520/C00143\_C00143M-10A, [www.astm.org](http://www.astm.org).
- ASTM Standard C231, 2010, "Standard Test Method for Air Content of Freshly Mixed Concrete by the Pressure Method" ASTM International, West Conshohocken, PA, 2010, DOI: 10.1520/C00231\_C00231M-10, [www.astm.org](http://www.astm.org).
- ASTM Standard C496, 2004e1, "Standard Test Method for Splitting Tensile Strength of Cylindrical Concrete Specimens" ASTM International, West Conshohocken, PA, 2004, DOI: 10.1520/C00496\_C00496M-10, [www.astm.org](http://www.astm.org).
- ASTM Standard C496, 2010a, "Standard Test Method for Compressive Strength of Concrete Cylinders Cast in Place in Cylindrical Molds" ASTM International, West Conshohocken, PA, 2010, DOI: 10.1520/C00873\_C0873M-10A, [www.astm.org](http://www.astm.org).
- ASTM Standard C496, 2010, "Standard Practice for Making Test Cylinders and Prisms for Determining Strength and Density of Preplaced-Aggregate Concrete in the Laboratory" ASTM International, West Conshohocken, PA, 2010, DOI: 10.1520/C0943-10, [www.astm.org](http://www.astm.org).
- ASTM Standard C78, 2010, "Standard Test Method for Flexural Strength of Concrete" ASTM International, West Conshohocken, PA, 2010, DOI: 10.1520/C0078\_C0078M-10, [www.astm.org](http://www.astm.org).
- Curtis, R. H. and White H. (2007). "NYSDOT Bridge Deck Task Force Evaluation of Bridge Deck Cracking on NYSDOT Bridges." New York State Department of Transportation Internal Report.
- Frosch, R., Blackman, D., and Radabaugh, R. (2003). "Investigation of Bridge Deck Cracking in Various Bridge Superstructure Systems." *Report Number FHWA/IN/JTRP-2002/25*, Indiana Department of Transportation, Division of Research, West Lafayette, IN.
- Miller, R., Mirmiran, A., Ganesh, P., and Sappro, M. (2006) "Transverse Cracking of High Performance Concrete Bridge Decks After One Season or Six to Eight Months" Report Number FHWA/OH-2006/6, Ohio Department of Transportation.
- Alampalli, S., and Owens, F. T. (2000). "Improved Performance of New York State Bridge Decks." *HPC bridge Views*, Issue No. 7.
- Chung, W., and Sotelino, E. D. (2005). "Nonlinear Finite-Element Analysis of Composite Steel Girder Bridges." *Journal of Structural Engineering*, 131(2), 304-313.

- Curtis, R. H. and White H. (2007). "NYSDOT Bridge Deck Task Force Evaluation of Bridge Deck Cracking on NYSDOT Bridges." New York State Department of Transportation Internal Report.
- D'Ambrosia, M. D., Lange, D. A., and Grasley, Z. C. (2004). "Measurement and Modeling of Concrete Tensile Creep and Shrinkage at Early Age." ACI SP 220, 99-112.
- deLarrard, F., Acker, P. "Creep in high and very high performance concrete," L.C.P.C., Paris, France, from Chapter 7 of High Performance Concrete: From material to structure. Edited by Yves Malier, E&FN SPON, Chapman&Hall, 1990, ISBN 0 419 17600 4
- Desai, C. S. (1979). *Elementary Finite Element Method*. Englewood Cliffs, N.J.: Prentice-Hall, Inc.
- Fanous, F., Wu, H., and Pape, J. (2000). "Impact of deck cracking on durability." Center for Transportation Research and Education, Iowa State University, Ames, IA.
- French, C., Eppers, L., Le, Q., and Hajjar, J. F. (1999), "Transverse Cracking in Concrete Bridge Decks," Transportation Research Record No. 1688, TRB, National Research Council, Washington, D.C.
- Frosch, R., Blackman, D., and Radabaugh, R. (2003). "Investigation of Bridge Deck Cracking in Various Bridge Superstructure Systems." *Report Number FHWA/IN/JTRP-2002/25*, Indiana Department of Transportation, Division of Research, West Lafayette, IN.
- Gilbert, R. I. (2008). "Control of Flexural Cracking in Reinforced Concrete." *ACI Structural Journal*, 105(3), 301-307.
- Goel, R., Kumar, R., Parkash, S., and Paul, D. K. (2006). "Prediction of Creep and Shrinkage Strains in Prestressed Concrete Bridges." *Advances in Bridge Engineering*, March 24-25, 2006, 543-554.
- Huang, D., and Minnetyan, L. (1998). "Damage progression in carbon-fiber reinforced plastic I-beams." *ASCE Journal of Composites for Construction*, 2(1), 38-45.
- Huo, X. S., Zhu, P., Ung, F., and Wasserman, E. P. (2006). "Case Study of a High-Performance Concrete Bridge in Tennessee." *Practice Periodical on Structural Design and Construction*, 11(4), 229-237.
- Kapila, D., Falkowsky, J., and Plawsky, J. L. (1997). "Thermal Effects During the Curing of Concrete Pavements." *ACI Materials Journal*, 94(2), 119-128.
- Krauss, P. D., and Rogalla, E. A. (1997). "Transverse cracking in newly constructed bridge decks." *Rep. No. NCHRP Report 380*, Transportation Research Board, National Research Council, Washington, D.C.
- Kwak, H. G., Seo, Y. J., and Jung, C. M. (2000). "Effects of the slab casting sequences and the drying shrinkage of concrete slabs on the short-term and long-term behavior of composite steel box girder bridges. Part 2." *Engineering Structures*, 23(2000), 1467-1480.

- Lee, Y., Choi, M.-S., Yi, S.-T., and Kim, J.-K. (2009). "Experimental study on the convective heat transfer coefficient of early-age concrete." *Cement & Concrete Composites*, 31, 60-71.
- Miller, R., Mirmiran, A., Ganesh, P., and Sappro, M. (2006) "Transverse Cracking of High Performance Concrete Bridge Decks After One Season or Six to Eight Months" Report Number FHWA/OH-2006/6, Ohio Department of Transportation.
- Minnetyan, L., and Abdi, F. (2004). "Dynamic impact loading damage propagation in composite structures." *Proceedings of the 45<sup>th</sup> AIAA/ASME/ASCE/AHS/ASC SDM Conference*, Palm Springs, California, 19-22 April 2004, Paper No. AIAA 2004-1688, p.8.
- Minnetyan, L., and Assamany, A. (2004). "Serviceability of high performance concrete." Presented at the Central New York ASCE, ASME, IEEE, NSPE Engineering Expo, Syracuse, NY, November 15, 2004.
- Minnetyan, L., Murthy, P. L. N., and Chamis, C. C. (1992). "Progressive fracture in composites subjected to hygrothermal environment." *International Journal of Damage Mechanics*, 1(1), 60-79.
- Minnetyan, L., Murthy, P. L. N., and Chamis, C. C. (1990). "Composite structure global fracture toughness via computational simulation." *Computers & Structures*, 37(2), 75-180.
- Murthy, P. L. N., and Chamis, C. C. (1986). "Integrated Composite Analyzer (ICAN) users and programmers manual." NASA-TP-2515, 1986, p.75.
- Nakazawa, S., Dias, J. B., and Spiegel, M. S. (1987). *MHOST Users I Manual*, Prepared for NASA Lewis Research Center by MARC Analysis Research Corp., April 1987.
- Neithalath, N., Pease, B., Moon, J.-H., Rajabipour, F., Weiss, J., and Attiogbe, E. (2005). "Considering Moisture Gradients and Time-Dependent Crack Growth in Restrained Concrete Elements Subjected to Drying." *High-Performance Cement-Based Concrete Composites*, Special Publication, 279-289.
- New York State Department of Transportation (NYSDOT) (2006), 4th, "Bridge Manual"
- New York State Department of Transportation (NYSDOT) (2006), "Standard Specifications"
- Oh, B. H., and Kim, S. H. (2007). "Advanced Crack Width Analysis of Reinforced Concrete Beams under Repeated Loads." *Journal of Structural Engineering*, 133(3), 411-420.
- Okui, Y., and Nagai, M. (2007). "Block FEM for Time-Dependent Shear-Lag Behavior in Two I-Girder Composite Bridges." *Journal of Bridge Engineering*, 12(1), 72-79.
- Ruiz, J. M., Rasmussen, R. O., Chang, G. K., Dick, J. C., Nelson, P. K., and Ferragut, T. R. (2005). "Computer-Based Guidelines for Concrete Pavements Volume I – Project Summary." *Report Number FHWA-HRT-04-121*, Office of Infrastructure Research and Development, Federal Highway Administration, McLean, VA.

- Saadeghvaziri, M. A., and Hadidi, R. (2002). "Cause and control of transverse cracking in concrete bridge decks." *Rep. No. FHWA-NJ-2002-19*, Federal Highway Administration, U.S. Department of Transportation, Washington, D.C.
- Saadeghvaziri, M. A., and Hadidi, R. (2005). "Transverse Cracking of Concrete Bridge Decks: Effects of Design Factors." *Journal of Bridge Engineering*, 10(5), 511-519.
- Shah, A. R., and Chamis, C. C. (1996). "Cyclic load effects on long term behavior of polymer matrix composites." *NASA-TM 107007*, March 1996.
- Sheban, M. A., Ababneh, A. N., and Fulton, S. R. (2006). "Numerical simulation of moisture diffusion in concrete." Joint International Conference on Computing *and Decision Making in Civil and Building Engineering*, June 14-16, 2006 – Montréal, Canada, 1015-1024.
- Soehardjono, A., Raka, I., and Suprobo, P. (2006). "Crack Width Prediction for Precast Reinforced Concrete Slabs under Repeated Loadings." International Civil Engineering Conference *Towards Sustainable Civil Engineering Practice*, August 25-26, 2006 – Surabaya.
- Streeter, D. A. (1999). "HPC in New York State Bridge Decks." *HPC bridge Views*, Issue No. 6.
- Subramaniam, K., Agrawal, A. K. (2009) "Concrete Deck Material Properties," Final Report, SPR Project C-02-03, New York State Department of Transportation, TIRC 1 – Cornell University Research Consortium.
- Wiegrink, K., Marikunte, S., and Shah, S. P. (1996). "Shrinkage cracking of high-strength concrete." *ACI Materials Journal*, 93(5), 409-415.
- Wojcik, G. S., and Fitzjarrald, D. R. (2001). "Energy Balances of Curing Concrete Bridge Decks." *Journal of Applied Meteorology*, 40(11), 2003-2025.
- Xia, P. Q., and Brownjohn, J. M. (2004). "Bridge Structural Condition Assessment Using Systematically Validated Finite-Element Model." *Journal of Bridge Engineering*, 9(5), 418-423.
- Yazdani, N., Filsaime, M., and Islam, S. (2007). "Accelerated Curing of Silica Fume Concrete." *TRB 2007 Annual Meeting CD-ROM*.
- Zhang, H., and Minnetyan, L. (2007). "Prediction of effective stiffness in [0m/90n]s laminates due to transverse cracking." *Journal of Composite Materials*, 41(1), 89-109.

## **APPENDIX 1: Making Software Operational on PC:**

The software modules that are used in the development of the computational framework were originally developed on a SUN Sparcstation and IBM RS6000 workstations. These modules were ported and made operational on a PC using the Absoft compiler.

To run the software the following source files are needed:

### Source Files:

Fortran source files containing the finite element module. The source files contain the routines from the MHOST finite element program, ICAN composite mechanics module, and an executive module that provides the interface between finite element analysis and composite mechanics. Source files need to be compiled using the Absoft compiler to produce an executable file.

### Materials Databank:

DATABK or Databank file for constituent material properties: This is currently a Fortran direct access file with a fixed record length that needs to be in your directory. At the beginning of time history analysis of residual stresses the databk.org file is copied using the prep.bat command into the databk file that is modified as the concrete properties change with curing. The current DATABK file format is defined as described in the ICAN User's Manual (Murthy and Chamis 1986). A schematic of databank properties is given below:

### Fiber Properties:

FP	$N_f$	$d_f$	$\rho_f$			
FE	$E_{f11}$	$E_{f22}$	$\nu_{f22}$	$\nu_{f23}$	$G_{f12}$	$G_{f23}$
FT	$\alpha_{f11}$	$\alpha_{f22}$	$K_{f11}$	$K_{f22}$	$C_f$	
FS	$S_{fT}$	$S_{fC}$				

### Matrix Properties:

MP	$\rho_m$						
ME	$E_m$	$\nu_m$	$\alpha_m$				
MT	$K_m$	$C_m$					
MS	$S_{mT}$	$S_{mC}$	$S_{mS}$	$\epsilon_{mT}$	$\epsilon_{mC}$	$\epsilon_{mS}$	$\epsilon_{mTOR}$
MV	$K_v$	$T_{gdr}$					

where the following notations are used:

$N_f$  = number of fibers per end

$d_f$  = fiber diameter

$\rho_f$  = fiber density

$E_{f11}$  = fiber longitudinal elastic modulus

$E_{f22}$  = fiber transverse elastic modulus

$\nu_{f12}$  = fiber Poisson's ratio in a longitudinal-transverse plane

$v_{f23}$  = fiber Poisson's ratio in a transverse-normal plane  
 $G_{f12}$  = fiber shear modulus in a longitudinal-transverse plane  
 $G_{f23}$  = fiber shear modulus in a transverse-normal plane  
 $\alpha_{f11}$  = fiber coefficient of thermal expansion in longitudinal direction  
 $\alpha_{f22}$  = fiber coefficient of thermal expansion in transverse direction  
 $K_{f11}$  = fiber longitudinal thermal conductivity  
 $K_{f22}$  = fiber transverse thermal conductivity  
 $C_f$  = fiber heat capacity  
 $S_{fT}$  = fiber tensile strength  
 $S_{fC}$  = fiber compressive strength

Matrix Properties:

$\rho_m$  = matrix density  
 $E_m$  = matrix elastic modulus  
 $\nu_m$  = matrix Poisson's ratio  
 $\alpha_m$  = matrix coefficient of thermal expansion  
 $K_m$  = matrix thermal conductivity  
 $C_m$  = matrix heat capacity  
 $S_{mT}$  = matrix tensile strength  
 $S_{mC}$  = matrix compressive strength  
 $S_{mS}$  = matrix shear strength  
 $\epsilon_{mT}$  = matrix tensile strain limit  
 $\epsilon_{mC}$  = matrix compressive strain limit  
 $\epsilon_{mS}$  = matrix shear strain limit  
 $\epsilon_{mTOR}$  = matrix torsional strain limit  
 $K_v$  = matrix thermal conductivity  
 $T_{gdr}$  = Matrix glass transition or melting temperature

The software could be converted to a sequential access databank file in the future for easier interpretation and compatibility with commercial software such as GENOA or NASTRAN-Multidisciplinary. Subroutine BANKRD needs to be rewritten to convert the databank to a sequential format. The databank information using the sequential access format compatible with the commercial software GENOA is included here describing the constituent properties of deck and girder elements:

```

FIBER PROPERTIES
RBSF  REBAR STEEL (FIBER)
$(The Material Property used in C-06-37 Deck #5 rebars)
$(REBAR Fy=60 ksi, Fu=90 ksi)
$
NUMBER OF FIBERS           Nf           1.000E+00      --
DIAMETER                   Df           6.250E-01      INCHES
WEIGHT DENSITY             Rhof         2.836E-01      LB/IN**3
MELTING TEMPERTURE        Tempmf       2.500E+03      DEG. F
NORMAL MODULUS (11)       Ef11         2.900E+07      PSI
NORMAL MODULUS (22)       Ef22         2.900E+07      PSI
POISSON'S RATIO (12)     Nuf12        3.000E-01      --
  
```

POISSON'S RATIO (23)	Nuf23	3.000E-01	--
SHEAR MODULUS (12)	Gf12	1.120E+07	PSI
SHEAR MODULUS (23)	Gf23	1.120E+07	PSI
COEF. THERMO. EXP. (11)	Alfaf11	6.500E-06	IN/IN/F
COEF. THERMO. EXP. (22)	Alfaf22	6.500E-06	IN/IN/F
THERMAL CONDUCTIVITY (11)	Kf11	4.028E+00	BTU/HR/F/IN
THERMAL CONDUCTIVITY (22)	Kf22	4.028E+00	BTU/HR/F/IN
HEAT CAPACITY	Cf	1.001E-01	BTU/LB
TENSION STRENGTH (11)	Sf11T	6.000E+04	PSI
COMPRESSION STRENGTH (11)	Sf11C	6.000E+04	PSI
TENSION STRENGTH (22)	Sf22T	6.000E+04	PSI
COMPRESSION STRENGTH (22)	Sf22C	6.000E+04	PSI
TORSION STRENGTH (12)	Sf12S	3.600E+04	PSI
TORSION STRENGTH (23)	Sf23S	3.600E+04	PSI

GRSF GIRDER STEEL (FIBER)

\$(The Material Property used in C-06-37 girders)

\$(GIRDER Fy=50 ksi, Fu=65 ksi)

\$

NUMBER OF FIBERS	Nf	1.000E+03	--
DIAMETER	Df	6.250E-03	INCHES
WEIGHT DENSITY	Rhof	2.836E-01	LB/IN**3
MELTING TEMPERTURE	Tempmf	2.500E+03	DEG. F
NORMAL MODULUS (11)	Ef11	2.900E+07	PSI
NORMAL MODULUS (22)	Ef22	2.900E+07	PSI
POISSON'S RATIO (12)	Nuf12	3.000E-01	--
POISSON'S RATIO (23)	Nuf23	3.000E-01	--
SHEAR MODULUS (12)	Gf12	1.120E+07	PSI
SHEAR MODULUS (23)	Gf23	1.120E+07	PSI
COEF. THERMO. EXP. (11)	Alfaf11	6.500E-06	IN/IN/F
COEF. THERMO. EXP. (22)	Alfaf22	6.500E-06	IN/IN/F
THERMAL CONDUCTIVITY (11)	Kf11	4.028E+00	BTU/HR/F/IN
THERMAL CONDUCTIVITY (22)	Kf22	4.028E+00	BTU/HR/F/IN
HEAT CAPACITY	Cf	1.001E-01	BTU/LB
TENSION STRENGTH (11)	Sf11T	5.000E+04	PSI
COMPRESSION STRENGTH (11)	Sf11C	5.000E+04	PSI
TENSION STRENGTH (22)	Sf22T	5.000E+04	PSI
COMPRESSION STRENGTH (22)	Sf22C	5.000E+04	PSI
TORSION STRENGTH (12)	Sf12S	3.000E+04	PSI
TORSION STRENGTH (23)	Sf23S	3.000E+04	PSI

CNCF CONCRETE PROPERTIES (FIBER)

\$(The Material Property used in C-06-37 HP concrete deck)

\$(fc'=6 ksi)

\$

NUMBER OF FIBERS	Nf	1.000E+03	--
DIAMETER	Df	6.250E-03	INCHES
WEIGHT DENSITY	Rhof	8.391E-02	LB/IN**3
MELTING TEMPERTURE	Tempmf	2.500E+03	DEG. F
NORMAL MODULUS (11)	Ef11	4.463E+06	PSI
NORMAL MODULUS (22)	Ef22	4.463E+06	PSI
POISSON'S RATIO (12)	Nuf12	2.000E-01	--
POISSON'S RATIO (23)	Nuf23	2.000E-01	--
SHEAR MODULUS (12)	Gf12	1.724E+06	PSI
SHEAR MODULUS (23)	Gf23	1.724E+06	PSI

COEF. THERMO. EXP. (11)	Alfaf11	5.500E-06	IN/IN/F
COEF. THERMO. EXP. (22)	Alfaf22	5.500E-06	IN/IN/F
THERMAL CONDUCTIVITY (11)	Kf11	1.489E-01	BTU/HR/F/IN
THERMAL CONDUCTIVITY (22)	Kf22	1.489E-01	BTU/HR/F/IN
HEAT CAPACITY	Cf	2.006E-01	BTU/LB
TENSION STRENGTH (11)	Sf11T	5.809E+02	PSI
COMPRESSION STRENGTH (11)	Sf11C	6.000E+03	PSI
TENSION STRENGTH (22)	Sf22T	5.809E+02	PSI
COMPRESSION STRENGTH (22)	Sf22C	6.000E+03	PSI
TORSION STRENGTH (12)	Sf12S	1.549E+02	PSI
TORSION STRENGTH (23)	Sf23S	1.549E+02	PSI

WBSF GIRDER WEB STEEL (FIBER) (1/13.6)\*STEEL PROPERTIES  
\$(The Material Property used in C-06-37 girder webs integral)  
\$(GIRDER Fy=50 ksi/13.6, Fu=65/13.6 ksi)  
\$

NUMBER OF FIBERS	Nf	1.000E+03	--
DIAMETER	Df	6.250E-03	INCHES
WEIGHT DENSITY	Rhof	2.085E-02	LB/IN**3
MELTING TEMPERTURE	Tempmf	2.500E+03	DEG. F
NORMAL MODULUS (11)	Ef11	2.132E+06	PSI
NORMAL MODULUS (22)	Ef22	2.132E+06	PSI
POISSON'S RATIO (12)	Nuf12	3.000E-01	--
POISSON'S RATIO (23)	Nuf23	3.000E-01	--
SHEAR MODULUS (12)	Gf12	8.235E+05	PSI
SHEAR MODULUS (23)	Gf23	8.235E+05	PSI
COEF. THERMO. EXP. (11)	Alfaf11	6.500E-06	IN/IN/F
COEF. THERMO. EXP. (22)	Alfaf22	6.500E-06	IN/IN/F
THERMAL CONDUCTIVITY (11)	Kf11	2.962E-01	BTU/HR/F/IN
THERMAL CONDUCTIVITY (22)	Kf22	2.962E-01	BTU/HR/F/IN
HEAT CAPACITY	Cf	0.736E-02	BTU/LB
TENSION STRENGTH (11)	Sf11T	3.676E+03	PSI
COMPRESSION STRENGTH (11)	Sf11C	3.676E+03	PSI
TENSION STRENGTH (22)	Sf22T	3.676E+03	PSI
COMPRESSION STRENGTH (22)	Sf22C	3.676E+03	PSI
TORSION STRENGTH (12)	Sf12S	2.206E+03	PSI
TORSION STRENGTH (23)	Sf23S	2.206E+03	PSI

OVER FIBER PROPERITIES  
MATRIX PROPERTIES

CONC CONCRETE MATRIX.  
\$(The Material Property used in C-06-37 Concrete Deck)  
\$(Concrete fc'=6000 psi)  
\$

WEIGHT DENSITY	Rhom	8.391E-02	LB/IN**3
NORMAL MODULUS	Em	4.463E+06	PSI
POISSON'S RATIO	Num	2.000E-01	--
COEF. THERMO. EXP.	Alfam	5.500E-06	IN/IN/F
THERMAL CONDUCTIVITY	Km	1.489E-01	BTU/HR/F/IN
HEAT CAPACITY	Cm	2.006E-01	BTU/LB
TENSION STRENGTH	SmT	5.809E+02	PSI
COMPRESSION STRENGTH	SmC	6.000E+03	PSI
SHEAR STRENGTH	SmS	1.549E+02	PSI
TENSION STRAIN	EpsmT	1.312E-04	--
COMPRESSION STRAIN	EpsmC	3.000E-03	--
SHEAR STRAIN	EpsmS	8.814E-05	--

TORSION STRAIN	EpsmTOR	8.814E-05	--
VOID THERMO. COND.	Kvoid	2.250E-01	BTU/HR/F/IN
MELTING TEMPERTURE	Tempmm	2.500E+03	DEG. F

RBRS REBAR STEEL MATRIX.

\$(The Material Property used in C-06-37 Deck rebars)

\$(REBAR Fy=60 ksi, Fu=90 ksi)

\$

WEIGHT DENSITY	Rhom	2.836E-01	LB/IN**3
NORMAL MODULUS	Em	2.900E+07	PSI
POISSON'S RATIO	Num	2.900E-01	--
COEF. THERMO. EXP.	Alfam	6.500E-06	IN/IN/F
THERMAL CONDUCTIVITY	Km	4.028E+00	BTU/HR/F/IN
HEAT CAPACITY	Cm	1.001E-01	BTU/LB
TENSION STRENGTH	SmT	6.000E+04	PSI
COMPRESSION STRENGTH	SmC	6.000E+04	PSI
SHEAR STRENGTH	SmS	3.600E+04	PSI
TENSION STRAIN	EpsmT	2.069E-03	--
COMPRESSION STRAIN	EpsmC	2.069E-03	--
SHEAR STRAIN	EpsmS	3.214E-03	--
TORSION STRAIN	EpsmTOR	3.214E-03	--
VOID THERMO. COND.	Kvoid	2.250E-01	BTU/HR/F/IN
MELTING TEMPERTURE	Tempmm	2.500E+03	DEG. F

GRDS GIRDER STEEL MATRIX.

\$(The Material Property used in C-06-37 Girders)

\$(Fy=50 ksi, Fu=65 ksi)

\$

WEIGHT DENSITY	Rhom	2.836E-01	LB/IN**3
NORMAL MODULUS	Em	2.900E+07	PSI
POISSON'S RATIO	Num	2.900E-01	--
COEF. THERMO. EXP.	Alfam	6.500E-06	IN/IN/F
THERMAL CONDUCTIVITY	Km	4.028E+00	BTU/HR/F/IN
HEAT CAPACITY	Cm	1.001E-01	BTU/LB
TENSION STRENGTH	SmT	5.000E+04	PSI
COMPRESSION STRENGTH	SmC	5.000E+04	PSI
SHEAR STRENGTH	SmS	3.000E+04	PSI
TENSION STRAIN	EpsmT	1.724E-03	--
COMPRESSION STRAIN	EpsmC	1.724E-03	--
SHEAR STRAIN	EpsmS	2.679E-03	--
TORSION STRAIN	EpsmTOR	2.679E-03	--
VOID THERMO. COND.	Kvoid	2.250E-01	BTU/HR/F/IN
MELTING TEMPERTURE	Tempmm	2.500E+03	DEG. F

WBSM GIRDER STEEL MATRIX.

\$(The Material Property used in C-06-37 Girders)

\$(Fy=50 ksi/13.6, Fu=65 ksi/13.6)

\$

WEIGHT DENSITY	Rhom	2.085E-02	LB/IN**3
NORMAL MODULUS	Em	2.132E+06	PSI
POISSON'S RATIO	Num	2.900E-01	--
COEF. THERMO. EXP.	Alfam	6.500E-06	IN/IN/F
THERMAL CONDUCTIVITY	Km	2.962E-01	BTU/HR/F/IN
HEAT CAPACITY	Cm	0.736E-02	BTU/LB
TENSION STRENGTH	SmT	3.676E+03	PSI

COMPRESSION STRENGTH	SmC	3.676E+03	PSI
SHEAR STRENGTH	SmS	2.206E+03	PSI
TENSION STRAIN	EpsmT	1.724E-03	--
COMPRESSION STRAIN	EpsmC	1.724E-03	--
SHEAR STRAIN	EpsmS	2.679E-03	--
TORSION STRAIN	EpsmTOR	2.679E-03	--
VOID THERMO. COND.	Kvoid	2.250E-01	BTU/HR/F/IN
MELTING TEMPERTURE	Tempmm	2.500E+03	DEG. F

OVER MATRIX PROPERITIES  
INTERFACE PROPERTIES  
OVER INTERFACE PROPERITIES  
PLY PROPERTIES  
OVER PLY PROPERITIES

### Input Data:

An input data file is needed to define the composite structure, geometry, and thermal environment during manufacturing and service, the initial finite element model, boundary conditions, and loading. The computational framework is more general compared to what is needed to describe the requisite structural analysis of this project and therefore not all input data lines are used in the current version. The input data lines with their required format are outlined as follows:

Line 1: (4L6,F6.3,3L6,5I6) BRICK, SHELL, PLOTS, OPTIM, FACT,  
RSTART, RSAVE, MODANL, NODWPD, IDPLY1, IDPLY2, IDMG1, IDMG2

BRICK (Boolean): True if 3-D brick elements are to be used. SHELL (Boolean): True if thick shell elements are to be used. PLOTS (Boolean): If deformed shape plot file (unit 75) created. OPTIM (Boolean): Use optimization Scheme in the MHOST module. FACT (Real): Factor to be used in Subroutine LDINCR  
RSTART (Boolean): If this is a restart of a previous run.  
RSAVE (Boolean): If the restart file (unit 76) is to be created.  
MODANL (Boolean): If the Eigen analyses are to be performed to determine the free vibration and buckling stability properties.  
NODWPD (Integer): Node number with initial ply damage.

IDPLY1 (Integer): First ply with initial damage.  
IDPLY2 (Integer): Last ply with initial damage.  
IDMG1 (Integer): Initial damage mode No.1  
IDMG2 (Integer): Initial damage mode No.2

Notes: BRICK and SHELL cannot be true simultaneously.  
OPTIM is not compatible with the generation of vibration mode and buckling mode eigenvectors by MHOST. If IDMG1 and IDMG2 are both set equal to 1, all 14 modes of damage are prescribed.

Line 2: (10X,6I6,5L6) NUMTRB, NADDWD, NADDWF, MIHOST, IPLYST,  
ITHRS1, DEBOND, DMGINW, DEBOLT, GLUED, LECHNL

NUMTRB (Integer): Number of nodes where nonzero displacements are prescribed for a displacement controlled loading. This option requires nonzero displacement boundary conditions for the first load increment. If there are no prescribed nonzero displacement boundary conditions then NUMTRB must be set equal to zero.

NADDWD (Integer): Number of additional nodes allowed to sustain damage during a structural analysis step within a load increment, prior to the through-the-thickness fracture of any node.

NADDWF (Integer): Number of additional nodes allowed to sustain damage during a structural analysis step within a load increment, after the through-the-thickness fracture of any node.

MIHOST (Integer): Maximum number of finite element analyses allowed within a CBRAN run.

IPLYST (Integer): Ply number for which the ply stresses are to be output to unit 88.

ITHRS1 (Integer): Node number where all ply stresses will be printed out to unit 77.

DE BOND (Logical): If true, duplicate nodes will be separated when one of the joined components sustains damage.

DMGINW (Logical): If true, the damage index will be printed out to default output (unit 6).

DEBOLT (Logical): If true, duplicate nodes will be separated when both components of in-plane normal stress of the laminate are tensile.

GLUED (Logical): If true, stacked laminate modeling is used for layers of adhesive and the joined laminates.

LECHNL (Logical): If true, Lekhnitskii's solution for stretch stress due to bending of a curved laminate is added to interlaminar normal stress.

Next NUMTRB lines each have a node number (integer) where a nonzero displacement is prescribed, and the tributary width of the node (real) perpendicular to the direction of loading.

Next line (10X,I10,G10.0,I10,2L6,I6,2L6): NUMCRT, VOLSTR, NDISPL, IDISPL, PRTHRU, SYMLOD, ICNDBG, YIELD, DELEM2

NUMCRT (Integer): Is the number of nodes passing through a critical section, through which the force transfer is to be computed. This is a development tool to enable computation of force transfer through any section.

VOLSTR (Real): Volume of structure (cubic inches). Is used to compute the percent damage that is printed to unit 28.

IFORCO (Integer): Degree of freedom direction number for which the summation of all forces will be printed to unit 28.

PRTHRU (Boolean): If true, ply stresses for all plies will be printed out at selected nodes. The node selection method is described below.

SYMLOD (Boolean): If true, loading is symmetrical, only the

positive loads will be summed up for printout to the fort.73 codhist2 file (unit 73).

ICNDBG (Integer): A debugging tool. Should be set to zero for normal execution. If anything other than zero, the full ICAN output will be dumped to fort.96 for the node number contained in the ICNDBG variable.

YIELD If .TRUE. the simulation will consider yielding of the material via the accumulation of generalized strains rather than the generalized stresses. Set it to • FALSE. for polymer matrix composites.

DELEM2 If • TRUE. then elements will be deleted if any two contiguous nodes fail on a given element. Use DELEM2 = .TRUE. for standard CBRAN simulation.

Next line (1018): ( NDISPL(I), IDISPL(I), I = 1, 5 )  
 NDISPL(I) is the node number where a coordinate displacement is to be written to unit 26 after each equilibrium.  
 IDISPL(I) is the corresponding coordinate direction number for writing the displacement component to unit 26.  
 Note: the coordinate direction numbers are limited to 1, 2, and 3, corresponding to the translations.

Next NUMCRT lines each have a node number (integer) through the critical section, and the tributary width of the node (real) perpendicular to the direction of force transfer.

If PRTHRU=.TRUE. then the next line must contain three integers (free format) as follows: 1) the first node number where all ply stresses are to be printed out, 2) the last node number where all ply stresses are to be printed out, and 3) the number of nodes to be skipped in progressing from the first to the last node that are printed to unit 77.

If LECHNL=.TRUE. then the next line must contain the radius of curvature to the laminate mid-plane and two node numbers defining the range of nodes for which Lekhnitskii's solution for stretch stress due to bending is to be computed.

Next Line: Consists of the keyword "ICAN" in the first four spaces. Indicates that subsequent lines contain data for the ICAN module. It is recommended that a copy of the ICAN Users Manual (ref. 6) be available when using CBRAN.

After the keyword ICAN, the subsequent lines specify the layered composite properties for as many laminate types (LTYP) as required. If there are variations in the composite properties, the properties may be specified separately for each laminate type. The laminate type number for each node is later assigned when the nodal coordinates are written.

The first line after the keyword ICAN is formatted as (A4,4X,3I8) where the first four characters consist of the keyword LTYP. The first integer specifies the laminate type number. The first LTYP number should be 1. For additional laminate types, sequential integer numbers in increasing order should be used. The second integer is the number of plies for the given laminate type. The third integer is the number of composite material cards used to specify the laminate.

After the LTYP line, the properties of each ply are specified using an (A8,2I8,5E8.3) format as indicated in the ICAN users manual. For each ply, the ply number, the material type number, temperature during loading (degrees Fahrenheit, typical), curing temperature, percentage of moisture, orientation angle of the ply, and the thickness of the ply (inches, typical) are entered. These input parameters are explained in detail in the ICAN User's Manual (2).

After the laminate properties are specified, the material properties for each material type are given on a separate line using an (A8,I8,2A4,2E8.2,2A4,3E8.2) format. Each material card describes a material system to be used. After the keyword MATCRD and the material identification number, the primary composite code names for fiber and matrix are given. The code names identify the properties from the composite databank file (named databk) that are to be used. The next two real entries are the primary fiber volume ratio and the primary void volume ratio. The next two keywords refer to the secondary composite system for the case of a hybrid composite ply. They should be the same as the primary fiber/matrix code names for standard composite systems. The next entry is the secondary composite system volume ratio. This is zero for standard composite systems.

The last two entries are the fiber volume ratio and the void volume ratio for the secondary composite system. These values are entered when applicable.

After all material property lines are entered, the keyword ENDN indicates the end of ICAN input data for the laminate type. If there are more than one laminate types, other laminate types are defined beginning with a line that starts with the LTYP keyword and proceeding with subsequent laminate definition lines as for the first laminate type. After all needed laminate types are defined, the line after the last ENDN keyword starts with the keyword MHOST, indicating that initial data for the MHOST module is to follow. (The input data to the MHOST module is modified by CBRAN as necessary during analysis.) After the MHOST keyword, the subsequent line contains an arbitrary title to be used by the MHOST module to label its output. The current version of CBRAN uses MHOST version 4.2 (supplied by Sverdrup Corporation on June 14, 1991) as the analysis module. It is recommended that the CBRAN user obtain a copy of the MHOST version 4.2 User's Manual and Examples Manual to become familiar with the MHOST input requirements. MHOST input data is organized into three blocks as: 1) Parameter Data, 2) Model Data, and 3) Incremental Data. The Parameter Data block specifies the

number of elements, the element type, the keyword "COMPOSITE", number of nodes, maximum number of boundary conditions, and the maximum number of forces, as shown in the example data files. In general, MHOST input statements start with an asterisk placed in the first space of the data line. The keyword \*END indicates the end of the Parameter Data block and the beginning of the Model Data block.

The Model Data block contains the maximum number of increments in MHOST (Specified as 0 for static analysis because the load increments are controlled by the CBRAN executive module via subroutine LDINCR). Iteration parameters follow the \*ITERATIONS keyword and are given as the maximum number of iterations (integer), Maximum allowable relative error in the residuals (real), Maximum allowable absolute error in the residuals (real), Maximum allowable relative error in the root-mean-square of the displacements (real), and Maximum allowable relative error in the root-mean-square of strain energy associated with the residuals (real). The \*PROPERTIES keyword with the finite element number (75 for thick shell element) precedes the nodal properties of the structure. Nodal properties are given with two integers indicating the range of nodes followed by N real entries (N=5 for MHOST element type 75). The real entries are sequentially, the thickness of the shell, Young's modulus, Poisson's ratio, the coefficient of thermal expansion, and the mass density. Most of these properties are ignored for composite durability analysis and the composite laminate properties are computed in CBRAN. (The current version of MHOST as modified by Sverdrup requires a second line of data that starts with the mass density, followed by three additional real numbers after the nodal properties data line. The last three real numbers do not have any meaning but the code stops with an error message if this redundant data line is excluded.)

The keyword \*COOR precedes the definition of geometry for the composite structure. After the \*COOR keyword, each line (formatted I8,4E17.8,I4) contains a node number, then the x, y, z coordinates, the shell thickness at that node, and the laminate type number. After all nodal coordinates are entered, the keyword \*ELEM 75 precedes the connectivity data for the finite elements. For each element, the element number and the four node numbers are given. The node numbers are defined in the counterclockwise sense for each element when observed from the tip of the positive local z axis. After the element connectivity data is entered, the \*DUPLICATENODE keyword precedes the duplicate node designations if there are duplicate node definitions. After the \*DUPLICATENODE keyword, each additional line contains a slave node number and the corresponding master node number using 2I5 format.

The keyword \*LAMINATE is necessary to signal the need to generate the composite laminate properties at each node. The keyword \*BOUNDARYCONDITIONS precedes the specification of the displacement boundary conditions. Each individual boundary condition takes a separate line with the node number and degree of freedom direction number that is restrained. For homogeneous displacement boundary conditions the node number and the fixed degree of freedom number are given using 2I9 format. When there is a nonzero prescribed displacement, the node number, the degree of

freedom number, and the amount of prescribed displacement must be given using 2I9,1PE22.9 format. After the specification of the boundary conditions, the keyword \*FORCE precedes the specification of nodal forces. After the \*FORCE keyword, each line contains a node number, a degree of freedom direction number, and the magnitude of the applied force in the global coordinate system, using I5,I2,F18.9 format. The keyword \*PRINT precedes items that are desired to be output in the MHOST lineprinter or MHOST6 file (unit 36). The nodal displacements and generalized nodal stresses may be required for debugging purposes when new capabilities of CBRAN are explored. Otherwise, these lines are started with the letter "C" so as to be ignored by MHOST. The keyword \*END indicates the end of model data. There is no MHOST incremental data for static CBRAN analysis. Thus the next keyword is \*STOP indicating the end of MHOST data. This also indicates the end of CBRAN input data. Most numerical results are summarized in the usual Fortran output file (unit 6). When a job is submitted, this file should be redirected to a filename derived from the particular job, such as <jobname>.out. In addition to the console output file, other files are also generated. The following files contain useful information as outlined:

codhist2 or FOR073.DAT (unit 73): Provides a summary of the total loading applied at each finite element analysis and a summary of the state of damage in the composite structure.

femsplot or FOR088.DAT (unit 88): Contains the finite element models and the generalized stresses. Data is first written to this file before the application of loading.

hostin05: FOR055.DAT (unit 55): contains MHOST input data at the time of program termination. May be valuable for debugging purposes.

mhost6: FOR036.DAT (unit 36): contains lineprinter output from the last MHOST analysis. May be useful for debugging purposes. This file also contains computational error estimates including the mean square displacement and mean square energy errors.

FOR077.DAT (unit 77): Contains ply stresses through-the-thickness of the laminate at selected nodes.

The input file FOR085.ORG for the example with 435 nodes is shown here in characteristic parts for reference:

```

      F      T      F      F 0.50      F      F      F      0      1      2      1      1
PRESCRIBED      0      1      1      1      1      218      F      T      F      F      F
CRITICALSE      0      0.7200      3      F      F      0      F      F      F      F      F
              8      3      8      3      8      3      8      3      8      3
ICAN
LTYP          1      24      3
  PLY         1      1  70.00  70.0      0.0      0. 0.100
  PLY         2      1  70.00  70.0      0.0      0. 0.100
  PLY         3      1  70.00  70.0      0.0      0. 0.100

```

PLY	4	1	70.00	70.0	0.0	0.	0.100	
PLY	5	1	70.00	70.0	0.0	0.	0.100	
PLY	6	1	70.00	70.0	0.0	0.	0.200	
PLY	7	1	70.00	70.0	0.0	0.	0.300	
PLY	8	1	70.00	70.0	0.0	0.	0.500	
PLY	9	1	70.00	70.0	0.0	0.	0.500	
PLY	10	1	70.00	70.0	0.0	0.	0.500	
PLY	11	1	70.00	70.0	0.0	0.	0.500	
PLY	12	2	70.00	70.0	0.0	0.	0.500	
PLY	13	3	70.00	70.0	0.0	90.	0.500	
PLY	14	1	70.00	70.0	0.0	0.	0.620	
PLY	15	1	70.00	70.0	0.0	0.	0.620	
PLY	16	1	70.00	70.0	0.0	0.	0.620	
PLY	17	1	70.00	70.0	0.0	0.	0.620	
PLY	18	1	70.00	70.0	0.0	0.	0.620	
PLY	19	2	70.00	70.0	0.0	0.	0.500	
PLY	20	3	70.00	70.0	0.0	90.	0.500	
PLY	21	1	70.00	70.0	0.0	0.	0.350	
PLY	22	1	70.00	70.0	0.0	0.	0.350	
PLY	23	1	70.00	70.0	0.0	0.	0.350	
PLY	24	1	70.00	70.0	0.0	0.	0.350	
MATCRD	1CNCFCNC		.300	.01	CNCFCNC	0.0	.60	.03
MATCRD	2RBSFCNC		.050	.01	CNCFCNC	0.0	.60	.03
MATCRD	3RBSFCNC		.050	.01	CNCFCNC	0.0	.60	.03
LTYP	2	34		5				
PLY	1	1	70.00	70.0	0.0	0.	0.100	
PLY	2	1	70.00	70.0	0.0	0.	0.100	
PLY	3	1	70.00	70.0	0.0	0.	0.100	
PLY	4	1	70.00	70.0	0.0	0.	0.100	
PLY	5	1	70.00	70.0	0.0	0.	0.100	
PLY	6	1	70.00	70.0	0.0	0.	0.200	
PLY	7	1	70.00	70.0	0.0	0.	0.300	
PLY	8	1	70.00	70.0	0.0	0.	0.500	
PLY	9	1	70.00	70.0	0.0	0.	0.500	
PLY	10	1	70.00	70.0	0.0	0.	0.500	
PLY	11	1	70.00	70.0	0.0	0.	0.500	
PLY	12	2	70.00	70.0	0.0	0.	0.500	
PLY	13	3	70.00	70.0	0.0	90.	0.500	
PLY	14	1	70.00	70.0	0.0	0.	0.620	
PLY	15	1	70.00	70.0	0.0	0.	0.620	
PLY	16	1	70.00	70.0	0.0	0.	0.620	
PLY	17	1	70.00	70.0	0.0	0.	0.620	
PLY	18	1	70.00	70.0	0.0	0.	0.620	
PLY	19	2	70.00	70.0	0.0	0.	0.500	
PLY	20	3	70.00	70.0	0.0	90.	0.500	
PLY	21	1	70.00	70.0	0.0	0.	0.350	
PLY	22	1	70.00	70.0	0.0	0.	0.350	
PLY	23	1	70.00	70.0	0.0	0.	0.350	
PLY	24	1	70.00	70.0	0.0	0.	0.350	
PLY	25	1	70.00	70.0	0.0	0.	2.000	
PLY	26	1	70.00	70.0	0.0	0.	2.000	
PLY	27	4	70.00	70.0	0.0	0.	0.500	
PLY	28	4	70.00	70.0	0.0	0.	0.500	
PLY	29	5	70.00	70.0	0.0	0.	8.500	
PLY	30	5	70.00	70.0	0.0	0.	8.500	
PLY	31	5	70.00	70.0	0.0	0.	8.500	
PLY	32	5	70.00	70.0	0.0	0.	8.500	
PLY	33	4	70.00	70.0	0.0	0.	0.500	
PLY	34	4	70.00	70.0	0.0	0.	0.500	
MATCRD	1CNCFCNC		.300	.01	CNCFCNC	0.0	.60	.03
MATCRD	2RBSFCNC		.05000	.01	CNCFCNC	0.0	.60	.03
MATCRD	3RBSFCNC		.05000	.01	CNCFCNC	0.0	.60	.03
MATCRD	4GRSFGRDS		.30	.00	GRSFGRDS	0.0	.02	.03

```

MATCRD      5WBSFWBSM .30 .00 WBSFWBSM 0.0 .02 .03
ENDN
MHOST
A TEST OF COMPOSITE DECK SIMULATION
*ELEMENT      336
  75
*COMPOSITE
*NODES      435
*LOUB 3 1 3
*FORCE  12
*TYING      348      3
*BOUNDARYCONDITIONS  20
C*OPTIMIZE
*CONSTITUTIVE 0
*DISPL
*END
*INCR
0
*ITERATION
  2      0.05      0.05      0.05      0.05
*PROPERTIES 75
  1  435  1.00000  0.00001  0.00001  0.00001
      0.1      0.0      0.0      0.0
*COOR
  1  -1200.00000000      0.00000000      -5.00000000      10.00000000      1
  2  -1200.00000000      12.87500000      -5.00000000      10.00000000      1
  3  -1200.00000000      25.75000000      -5.00000000      10.00000000      1
  4  -1200.00000000      38.62500000      -5.00000000      10.00000000      1
  5  -1200.00000000      51.50000000      -5.00000000      10.00000000      1
  6  -1200.00000000      51.50000000      -26.00000000      52.00000000      2
  7  -1200.00000000      55.75000000      -26.00000000      52.00000000      2
  8  -1200.00000000      60.00000000      -26.00000000      52.00000000      2
  9  -1200.00000000      64.25000000      -26.00000000      52.00000000      2
 10  -1200.00000000      68.50000000      -26.00000000      52.00000000      2
 11  -1200.00000000      68.50000000      -5.00000000      10.00000000      1
 12  -1200.00000000      81.37500000      -5.00000000      10.00000000      1
 13  -1200.00000000      94.25000000      -5.00000000      10.00000000      1
 14  -1200.00000000     107.12500000      -5.00000000      10.00000000      1
 15  -1200.00000000     120.00000000      -5.00000000      10.00000000      1
 16   -960.00000000      0.00000000      -5.00000000      10.00000000      1
 17   -960.00000000     12.87500000      -5.00000000      10.00000000      1
 18   -960.00000000     25.75000000      -5.00000000      10.00000000      1
 19   -960.00000000     38.62500000      -5.00000000      10.00000000      1
 20   -960.00000000     51.50000000      -5.00000000      10.00000000      1
  .
  .
  .
  .
  .
 207  -12.00000000     81.37500000      -5.00000000      10.00000000      1
 208  -12.00000000     94.25000000      -5.00000000      10.00000000      1
 209  -12.00000000    107.12500000      -5.00000000      10.00000000      1
 210  -12.00000000    120.00000000      -5.00000000      10.00000000      1
 211   0.00000000      0.00000000      -5.00000000      10.00000000      1
 212   0.00000000     12.87500000      -5.00000000      10.00000000      1
 213   0.00000000     25.75000000      -5.00000000      10.00000000      1
 214   0.00000000     38.62500000      -5.00000000      10.00000000      1
 215   0.00000000     51.50000000      -5.00000000      10.00000000      1
 216   0.00000000     51.50000000     -26.00000000      52.00000000      2
 217   0.00000000     55.75000000     -26.00000000      52.00000000      2
 218   0.00000000     60.00000000     -26.00000000      52.00000000      2
 219   0.00000000     64.25000000     -26.00000000      52.00000000      2
 220   0.00000000     68.50000000     -26.00000000      52.00000000      2
 221   0.00000000     68.50000000      -5.00000000      10.00000000      1
 222   0.00000000     81.37500000      -5.00000000      10.00000000      1
 223   0.00000000     94.25000000      -5.00000000      10.00000000      1

```

224	0.00000000	107.12500000	-5.00000000	10.00000000	1
225	0.00000000	120.00000000	-5.00000000	10.00000000	1
226	12.00000000	0.00000000	-5.00000000	10.00000000	1
227	12.00000000	12.87500000	-5.00000000	10.00000000	1
228	12.00000000	25.75000000	-5.00000000	10.00000000	1
229	12.00000000	38.62500000	-5.00000000	10.00000000	1
230	12.00000000	51.50000000	-5.00000000	10.00000000	1
231	12.00000000	51.50000000	-26.00000000	52.00000000	2
232	12.00000000	55.75000000	-26.00000000	52.00000000	2
233	12.00000000	60.00000000	-26.00000000	52.00000000	2
234	12.00000000	64.25000000	-26.00000000	52.00000000	2
235	12.00000000	68.50000000	-26.00000000	52.00000000	2
236	12.00000000	68.50000000	-5.00000000	10.00000000	1
237	12.00000000	81.37500000	-5.00000000	10.00000000	1
.	.	.	.	.	.
.	.	.	.	.	.
424	1200.00000000	38.62500000	-5.00000000	10.00000000	1
425	1200.00000000	51.50000000	-5.00000000	10.00000000	1
426	1200.00000000	51.50000000	-26.00000000	52.00000000	2
427	1200.00000000	55.75000000	-26.00000000	52.00000000	2
428	1200.00000000	60.00000000	-26.00000000	52.00000000	2
429	1200.00000000	64.25000000	-26.00000000	52.00000000	2
430	1200.00000000	68.50000000	-26.00000000	52.00000000	2
431	1200.00000000	68.50000000	-5.00000000	10.00000000	1
432	1200.00000000	81.37500000	-5.00000000	10.00000000	1
433	1200.00000000	94.25000000	-5.00000000	10.00000000	1
434	1200.00000000	107.12500000	-5.00000000	10.00000000	1
435	1200.00000000	120.00000000	-5.00000000	10.00000000	1

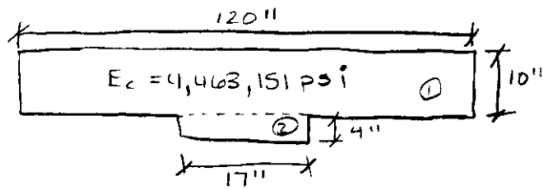
\*ELEM 75

1	2	1	16	17
2	3	2	17	18
3	4	3	18	19
4	5	4	19	20
5	7	6	21	22
6	8	7	22	23
7	9	8	23	24
8	10	9	24	25
9	12	11	26	27
10	13	12	27	28
11	14	13	28	29
12	15	14	29	30
13	17	16	31	32
14	18	17	32	33
15	19	18	33	34
16	20	19	34	35
17	22	21	36	37
18	23	22	37	38
19	24	23	38	39
20	25	24	39	40
21	27	26	41	42
.	.	.	.	.
.	.	.	.	.
322	403	402	417	418
323	404	403	418	419
324	405	404	419	420
325	407	406	421	422
326	408	407	422	423
327	409	408	423	424
328	410	409	424	425
329	412	411	426	427
330	413	412	427	428
331	414	413	428	429
332	415	414	429	430

333	417	416	431	432		
334	418	417	432	433		
335	419	418	433	434		
336	420	419	434	435		
*LAMINATE						
*TYING						
3	5	1	6	1	6	5
1.00000	21.00000					
3	5	2	6	2	6	4
1.00000	-21.00000					
2	5	3	6	3		
1.00000						
2	5	4	6	4		
1.00000						
2	5	5	6	5		
1.00000						
2	5	6	6	6		
1.00000						
3	11	1	10	1	10	5
1.00000	21.00000					
3	11	2	10	2	10	4
1.00000	-21.00000					
2	11	3	10	3		
1.00000						
2	11	4	10	4		
1.00000						
2	11	5	10	5		
1.00000						
2	11	6	10	6		
1.00000						
.	.					
3	431	1	430	1	430	5
1.00000	21.00000					
3	431	2	430	2	430	4
1.00000	-21.00000					
2	431	3	430	3		
1.00000						
2	431	4	430	4		
1.00000						
2	431	5	430	5		
1.00000						
2	431	6	430	6		
1.00000						
*BOUNDARYCONDITIONS						
6	3					
7	3					
8	2					
8	3					
9	3					
10	3					
216	3					
217	3					
218	1					
218	2					
218	3					
219	3					
220	3					
425	3					
426	3					
427	3					
428	2					
428	3					

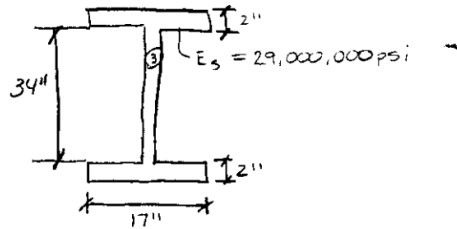
```
429      3
430      3
*PRINT
TOTALDISPLACEM
STRESS
STRAIN
*END
*STOP
```

**Appendix 2: Manual computation of bending stress using beam diagram from AISC manual and strength of materials (for reference)**



$$A_{(1)} = 10(120) = 1200 \text{ in}^2$$

$$A_{(2)} = 4(17) = 68 \text{ in}^2$$

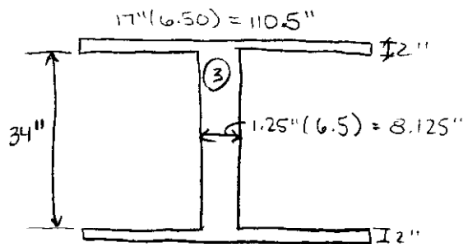


$$A_{(3)} = 2(2)(17) + 1.25(34) = 110.5 \text{ in}^2$$

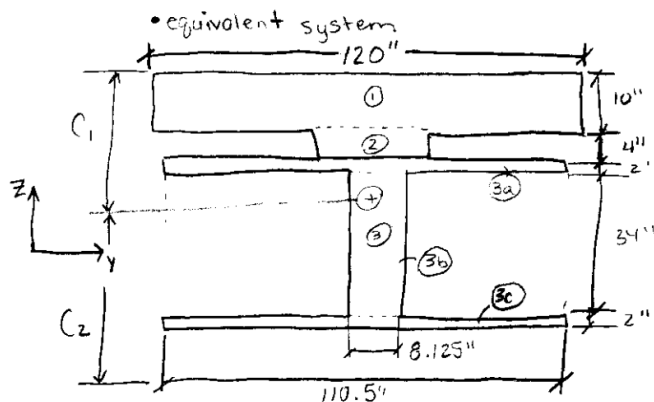
\* equivalent system, based on  $E_c$

$$n = \frac{E_s}{E_c} = \frac{29,000,000}{4,463,151} = 6.50$$

• equivalent steel



$$A_{(3)} = 2(110.5(2)) + 8.125(34) = 718.25 \text{ in}^2$$



$$\bar{z}_{(1)} = 5''$$

$$\bar{z}_{(2)} = 12''$$

$$\bar{z}_{(3)} = 33''$$

$$\bar{z}_{(3a)} = 15''$$

$$\bar{z}_{(3b)} = 33''$$

$$\bar{z}_{(3c)} = 51''$$

• centroid

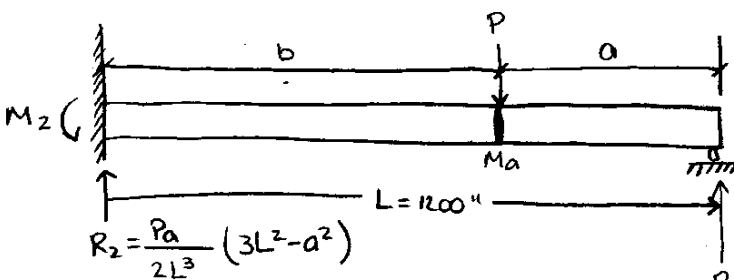
$$\bar{z} = \frac{1200 \text{ in}^2 (5'') + 68 \text{ in}^2 (12'') + 718.25 \text{ in}^2 (33'')}{(1200 + 68 + 718.25) \text{ in}^2}$$

$$\bar{z} = 15.365''$$

$$c_1 = 15.365''$$

$$c_2 = 52'' - 15.365'' = 36.635''$$

\* Moment @ fixed end



$$a = 40 \text{ ft} = 480''$$

$$b = 60 \text{ ft} = 720''$$

$$P = 1000 \text{ lb}$$

$$R_2 = \frac{Pa}{2L^3} (3L^2 - a^2)$$

$$R_1 = \frac{Pb^2}{2L^3} (a + 2L)$$

$$M_a = \frac{Pab^2}{2L^3} (a + 2L)$$

$$M_2 = \frac{Pab}{2L^2} (a + L)$$

$$M_a = \frac{1000(480')(720'')^2}{2(1200'')^3} (480'' + 2(1200''))$$

$$M_2 = \frac{1000(480'')(720'')}{2(1200'')^2} (480'' + 1200'')$$

$$M_2 = \underline{201600 \text{ lb-in}}$$

$$M_a = 207360 \text{ lb-in}$$

\* stresses on cross section (@ fixed end)

•  $I_t$  for equivalent system

$$I_t = \sum \left( \frac{1}{12} bh^3 + Ad^2 \right)$$

$$d = \bar{z} - \bar{z}_c$$

$$I_{t\text{①}} = \frac{1}{12} (120'')(10'')^3 + 1200 \text{ in}^2 (10.365'')^2 = \underline{138919.87 \text{ in}^4}$$

$$d = 15.365'' - 5'' = 10.365''$$

$$I_{t\text{②}} = \frac{1}{12} (17'')(4'')^3 + 68 \text{ in}^2 (3.365'')^2 = \underline{860.65 \text{ in}^4}$$

$$d = 15.365'' - 12'' = 3.365''$$

$$I_{(a)} = \frac{1}{12}(110.5'')(2'')^3 + 2''(110.5'')(0.365'')^2 = \underline{103.11 \text{ in}^4}$$

$$d = 15.365'' - 15'' = 0.365''$$

$$I_{(b)} = \frac{1}{12}(8.125'')(34'')^3 + 8.125''(34'')(17.635'')^2 = \underline{112523.96 \text{ in}^4}$$

$$d = 15.365'' - 33'' = -17.635''$$

$$I_{(c)} = \frac{1}{12}(110.5'')(2'')^3 + 2''(110.5'')(35.635'')^2 = \underline{280711.23 \text{ in}^4}$$

$$d = 15.365'' - 51'' = -35.635''$$

$$I_t = 138919.87 \text{ in}^4 + 860.65 \text{ in}^4 + 103.11 \text{ in}^4 + 112523.96 \text{ in}^4 + 280711.23 \text{ in}^4$$

$$\underline{I_t = 533118.82 \text{ in}^4}$$

• stress calculations

$$\sigma_{x_T} = \frac{-M(c_1)}{I_t} = \frac{-201600 \text{ lb-in}(15.365'')}{533118.82 \text{ in}^4} = -5.81 \text{ psi}$$

$$\sigma_{x_B} = \frac{-M(c_2)n}{I_t} = \frac{-201600 \text{ lb-in}(-36.635'')(6.5)}{533118.82 \text{ in}^4} = -90.05 \text{ psi}$$

## Appendix 3A: Thermal Finite Element Analysis Program Listing

```

C PROGRAM FE1
C *****
C FINITE ELEMENT CODE FOR ONE-DIMENSIONAL DEFORMATION, FLOW,
C TEMPERATURE AND CONSOLIDATION
C PROGRAM NAME DFT/C-IDFC
C PROGRAM FE1
C *****
C FINITE ELEMENT CODE FOR ONE-DIMENSIONAL DEFORMATION, FLOW,
C TEMPERATURE AND CONSOLIDATION
C PROGRAM NAME DFT/C-IDFC
C DEVELOPED BY C.S.DESAI
C *****
      IMPLICIT DOUBLE PRECISION (A-H,O-Z)
      DIMENSION A(41,3), AK(41,3), AP(41,3), H(41), R(41), QK(2,2),
      *QP(2,2), Q(2), LP(2), TIM(56), Y(41), IE(40,3), VLY(41),
      *PROP(10), AREAEL(34), DENS(10), KODE(41), ALL(41), TY(34),
      *KEL(34), RO(10), AMV(10), UINIT(41), TITLE(18), RSUM(41),
      *SURTMP(72), AIRTMP(72)
C *****
C *** STAGE 1 *** INPUT QUANTITIES
C *****
C FOR EXPLANATION OF VARIOUS STAGES SEE CHAPTER 6
C *** INPUT SET 1 ***
      OPEN (5, file='FE3A_NEW.DAT', status='old')
      OPEN (6, file='FE3A_NEW.OUT', status='unknown')

      20 READ (5,920) NPROB,TITLE
      IF (NPROB.LE.0) GO TO 910
      WRITE (6,930) NPROB,TITLE
      WRITE (6,940)
      WRITE (6,950)
      READ (5,'(3E10.3)') TIME1, TIME2, QPEAK
      WRITE(6,'('' TIME1 (HR) TIME2 (HR) QPEAK (BTU/(HR-IN^3))''')
      WRITE(6,'(3E12.3)') TIME1, TIME2, QPEAK
      WRITE(6,*) ' '

C *** PROBLEM PARAMETERS
      READ (5,960) NNP,NMAT,NSLC,NBODY,NOPT,IBAND,NTIME
      WRITE (6,970) NNP,NMAT,NSLC,NBODY,NOPT,IBAND,NTIME
C *** MATERIAL PROPERTIES
      WRITE (6,990)
      DO 30 I=1,NMAT
      READ (5,980) PROP(I),AMV(I),RO(I),DENS(I)
30 CONTINUE
      WRITE (6,1000) (I,PROP(I),AMV(I),RO(I),DENS(I),I=1,NMAT)
C *** INPUT SET 2
C *** NODAL POINT DATA
      WRITE (6,1010)
      N=1
40 READ (5,1020) M,KODE(M),Y(M),VLY(M)
      IF (M-N) 50,80,60
50 CONTINUE
      WRITE (6,1030) M
      GO TO 910
C *** AUTOMATIC GENERATION OF NODAL POINT DATA ***
60 DF=M+1-N
      RY=(Y(M)-Y(N-1))/DF
70 KODE(N)=0
      Y(N)=Y(N-1)+RY
      VLY(N)=0.0
80 IF (N.EQ.1) GO TO 100
C *** COMPUTE ELEMENT LENGTH ***

```

```

90  ALL(N-1)=Y(N)-Y(N-1)                                MAIN 480
100 CONTINUE                                           MAIN 490
    WRITE (6,1040) N,KODE(N),Y(N),VLY(N)              MAIN 500
    N=N+1                                              MAIN 510
    IF (M-N) 110,90,70                                MAIN 520
110  IF (N.LE.NNP) GO TO 40
C    *****
C          *** INPUT SET 3
C          *** ELEMENT DATA
C    *****
    WRITE (6,1050)
    NEL=NNP-1
    N=0
120  READ (5,960) M, (IE(M,I),I=1,3)
130  N=N+1
    IF (M-N) 140,160,150
140  WRITE (6,1060) M
    GO TO 910
150  IE(N,1)=IE(N-1,1)+1
    IE(N,2)=IE(N-1,2)+1
    IE(N,3)=IE(N-1,3)
160  IF (M-N) 170,170,130
170  IF (NEL-N) 180,180,120
180  CONTINUE
C    INPUT ELEMENT AREAS
    READ(5,960) IAREA
    GOTO (190,210,230), IAREA
190  READ(5,980) AREAEL(1)
    DO 200 I=1,NEL
200  AREAEL(I)=AREAEL(1)
    GO TO 240
210  READ(5,980) AREAEL(1), AREAEL(NEL)
    AL=Y(NNP)-Y(1)-(ALL(1)+ALL(NEL))/2.0
    SLOPE=(AREAEL(NEL)-AREAEL(1))/AL
    NEL1=NEL-1
    DISTY=0.0
    DO 220 I=2,NEL1
    DISTY=DISTY+(ALL(I-1)+ALL(I))/2.0
    AREAEL(I)=AREAEL(1)+SLOPE*DISTY
220  CONTINUE
    GO TO 240
230  READ (5,980) (AREAEL(I),I=1,NEL)
240  CONTINUE
    DO 250 M=1,NEL
250  WRITE (6,1070) M, IE(M,1), IE(M,2), IE(M,3), AREAEL(M)
C    *****
C          INPUT SET 4
C          SURFACE TRACTION CARDS
C    *****
    IF (NSLC.EQ.0) GO TO 280
    WRITE(6,1080)
    DO 260 I=1,NSLC
260  READ(5,1090) KEL(I),TY(I)
    DO 270 I=1,NSLC
270  WRITE(6,1100) I,KEL(I),TY(I)
280  CONTINUE
C    *****
C          ***INPUT SET 5
C          ***DATA FOR TIME DEPENDENT PROBLEM
C    *****
    IF (NOPT.LT.3) GO TO 370
    WRITE (6,1110)
    READ (5,1120) DT,TOTIM,INOPT

```

```

WRITE (6,1130) DT,TOTIM,INOPT
WRITE (6,1140)
READ (5,980) (TIM(I),I=1,NTIME)
DO 290 I=1,NTIME
290 WRITE(6,1150) I,TIM(I)
C   INOPT =1 UNIFORM INITIAL CONDITIONS,=2 LINEAR,=3 ARBITRARY
WRITE (6,1160)
GO TO (300,320,340), INOPT
300 READ (5,980) UUNIT(1)
DO 310 I=1,NNP
310 UUNIT(I) = UUNIT(1)
GO TO 350
320 READ (5,980) UUNIT(1),UUNIT(NNP)
NNP1= NNP-1
DO 330 I=2,NNP1
AL = Y(NNP)-Y(1)
SLOPE = (UUNIT(NNP)-UUNIT(1))/AL
330 UUNIT(I)=UUNIT(1)+SLOPE*Y(I)
GO TO 350
340 READ(5,980) (UUNIT(I),I=1,NNP)
350 CONTINUE
DO 360 I=1,NNP
360 WRITE(6,1170) I,UUNIT(I)
WRITE(6,*)

c   READ(5,980) (SURTMP(I),I=1,NTIME)
c   READ(5,980) (AIRTMP(I),I=1,NTIME)
c   WRITE(6,*) ' SURFACE TEMPERATURES FOR EACH HOUR'
c   WRITE(6,980) (SURTMP(I),I=1,NTIME)
c   WRITE(6,*)
c   WRITE(6,*) ' AMBIENT AIR TEMPERATURES FOR EACH HOUR'
c   WRITE(6,980) (AIRTMP(I),I=1,NTIME)
c   WRITE(6,*)
C   write (*,*)' NTIME=',ntime
CAUTION HARDWIRES: 36 was inserted instead of NTIME
READ(5,980) (SURTMP(I),I=1,36)
READ(5,980) (AIRTMP(I),I=1,36)
WRITE(6,*) ' SURFACE TEMPERATURES FOR EACH HOUR'
WRITE(6,980) (SURTMP(I),I=1,36)
WRITE(6,*)
WRITE(6,*) ' AMBIENT AIR TEMPERATURES FOR EACH HOUR'
WRITE(6,980) (AIRTMP(I),I=1,36)
WRITE(6,*)

C*****
C                               ***STAGE 2*** INITIALIZE
C*****
370 CONTINUE
NCT=0
TIME=0.0

375 CONTINUE
C Preceding 375 CONTINUE statement added to include stages 3 & 4 in time loop
C 5/7/2009 GO TO 375 will replace GO TO 530 for temperature problems
C will recompute the h (convectivity or surface factor) and QI heat flux
C for each time increment
DO 373 I=1,NNP
373 RSUM(I)=0.0

DO 380 I=1,NNP
IF (NOPT.LT.3) UUNIT(I)=0.0
C added block if to modify surface and air temperatures with time
IF (I .EQ. 1 .and. NCT .GT. 0) THEN

```

```

CAUTION HARDWIRE
  IF (NCT .LE. 36) THEN
    VLY(I)=SURTMP(NCT)
  ELSEIF (MOD(NCT,24) .EQ. 0) THEN
    VLY(I) = SURTMP(24)
  ELSE
    VLY(I)=SURTMP( MOD (INT(TIME),24) )
  ENDIF

  ELSEIF (I .EQ. NNP .and. NCT .GT. 0) THEN

CAUTION HARDWIRE
  IF (NCT .LE. 36) THEN
    VLY(I)=AIRTMP(NCT)
  ELSEIF (MOD(NCT,24) .EQ. 0) THEN
    VLY(I) = AIRTMP(24)
  ELSE
    VLY(I)=AIRTMP( MOD (INT(TIME),24) )
  ENDIF

  ENDIF

  H(I)=UNIT(I)

  R(I)=0.0
  DO 380 J=1,IBAND

C initialization of a(i,j) made only in the first step
  IF (TIME .lt. 0.1D-5) THEN
    A(I,J)=0.

    AK(I,J)=0.
    AP(I,J)=0.
  ENDIF

380 CONTINUE

  DO 520 M=1,NEL
    II1=IE(M,1)
    II2=IE(M,2)
    ALEN=ABS(Y(II1)-Y(II2))
    MT=IE(M,3)
    DO 390 I=1,2
      Q(I)=0.0
      DO 390 J=1,2
        QK(I,J)=0.
        QP(I,J)=0.
      IF (NOPT.LT.4) GO TO 410
C FOR CONSOLIDATION (OF LAYERED MEDIA) FIND TIME FACTOR ON THE
C BASIS OF AVERAGE CV, THIS IS AN APPROXIMATION, ALTERNATIVELY
C THIS CAN BE DONE ON THE BASIS OF ONE OF THE LAYERS
      ANEL=NEL
      CV=0.0
      DO 400 MM=1,NEL
        MTT=IE(MM,3)
400 CV=CV+PROP(MTT)/(RO(MTT)*AMV(MTT))
      CVA=CV/ANEL
      HH=(Y(NNP)-Y(1))/2.0
      TFF=CVA/(HH*HH)
410 CONTINUE
C
C ***** MAIN1710
C *** STAGE 3*** COMPUTE ELEMENT MATRICES

```

```

C          *****
C          IF (NOPT .LT.3) GO TO 450
C          IF (NOPT .EQ. 4) GO TO 420
C          TEMPERATURE PROBLEM
C          IF MT=1 (surface to air layer) recompute PROP(1) using Jess's equation
C          IF (MT .EQ. 1) THEN
C              PROP(1)=HCONVC(TIME)
C          ENDIF
C DR1 and DR2 appear to be the scalar multipliers to assemble Eq 5-33
C          DR1=(AREAEL(M)*PROP(MT))/ALEN
C          DR2=(AMV(MT)*RO(MT)*ALEN)/DT
C          GO TO 440
C          CONSOLIDATION PROBLEM
420         DR1=PROP(MT)/(RO(MT)*ALEN)
C          DR2=(AMV(MT)*ALEN)/DT
C          TUINIT=0.0
430         DO 430 I=1,NNP
C          TUINIT=TUINIT+UINIT(I)
440         CONTINUE
C          QK(1,1)=DR1
C          QK(2,2)=QK(1,1)
C          QK(1,2)=-QK(1,1)
C          QK(2,1)=QK(1,2)
C          QP(1,1)=DR2*(1.0/3.0)
C          QP(1,2)=QP(1,1)/2.
C          QP(2,2)=QP(1,1)
C          QP(2,1)=QP(1,2)
C          GO TO 500 STATEMENT REPLACED BY THE NEXT STATEMENT 5-8-09
C          GO TO 455
C          the next block is for steady state problems
450         CF=(AREAEL(M)*PROP(MT))/ALL(M)
C          QK(1,1)=CF
C          QK(2,2)=CF
C          QK(1,2)=-CF
C          QK(2,1)=-CF
C          *****
C          *** STAGE 4*** ASSEMBLE
C          *****
455         CONTINUE
C          PREVIOUS STATEMENT 455 ADDED TO COMPUTE FLUX FOR THERMAL PROBLEM
C          IF (NSLC .EQ. 0) GO TO 480
C          COMPUTE ELEMENT FORCE VECTOR Q DUE TO TRACTION OR FLUX
C          DO 460 IM=1,NSLC
C              MK=KEL(IM)
C              IF (MK.EQ.M) GO TO 470
460         CONTINUE
470         GO TO 480
C          RECOMPUTE THE FLUX ACCORDING TO JESS'S EQUATION
C          Assume all layers have the same heat generation. This is not exact since
C          the layers with steel will have less heat generation. We can correct later
C          Concrete material type is 2
C          IF (IE(M,3) .LT. 3) THEN
C              TY(IM)= QIFLUX(TIME, TIME1, TIME2, QPEAK)
C          ELSE
C              TY(IM)=0.
C          ENDIF
C          Q(1)=Q(1)+(TY(IM)*ALL(MK))/2.0
C          Q(2)=Q(2)+Q(1)
480         CONTINUE

```

```

C      ADD FORCING VECTOR DUE TO BODY FORCE OR FLUX TO ELEMENT LOAD VECTOMAIN2140
      IF (NBODY.NE.1) GO TO 490                                          MAIN2150
      GWT=(AREAEL(M)*ALL(M)*DENS(MT))/2.0                               MAIN216
      Q(1)=Q(1)+GWT                                                    MAIN2170
      Q(2)=Q(2)+GWT                                                    MAIN2180
490    CONTINUE                                                         MAIN2190
500    CONTINUE                                                         MAIN2200
      LP(1)=M                                                           MAIN2210
      LP(2)=M+1                                                         MAIN2220
      DO 510 LL=1,2
      I=LP(LL)
C      ADDED NEXT STATEMENT TO COMPUTE R at TIME 5-7-09
      RSUM(I)=RSUM(I)+Q(LL)

      R(I)=R(I)+Q(LL)

      DO 510 MM=1,2
      J=LP(MM)-I+1
      IF (J.LE.0) GO TO 510
C if condition added to next statement
      IF (TIME .LT. 0.1D-5) AK(I,J)=AK(I,J)+QK(LL,MM)
      IF (NOPT.LT.3) GO TO 510
Cdebug if condition added to next statement
      IF (TIME .LT. 0.1D-5) AP(I,J)=AP(I,J)+QP(LL,MM)
510    CONTINUE
520    CONTINUE
530    NCT=NCT+1
      IF (NOPT.GE.3) TIME=TIME+DT
      IF (NOPT.EQ.4) TF=TFF*TIME
      DO 540 I=1,NNP
      DO 540 J=1,IBAND
C      **** IMPORTANT NOTE **** IF NO (TIME DEPENDENT) FORCING
C      ELEMENT PARAMETERS SUCH AS FLUX ARE APPLIED, THEN INITIALIZE VECTO
C      R AT THE START OF EACH TIME STEP** IF TIME DEPENDENT FORCING
C      PARAMETERS ARE APPLIED THEN STAGES 3 AND 4 SHOULD BE PERFORMED
C      AT EACH TIME LEVEL AND THE ELEMENT CONTRIBUTIONS ADDED TO R
C      CONCENTRATED TIME DEPENDENT FORCES CAN HOWEVER BE APPLIED
C      IF (NOPT.GE.3) R(I)=0.0
C preceding statement commented out because initialization is in step 2
      IF (NOPT.GE.3) R(I)=RSUM(I)
540    A(I,J)=AK(I,J)
C      *****
C      *** STAGE 5***CONCENTRATED FORCES
C      ADD CONCENTRATED FORCES TO ASSEMBLAGE LOAD VECTOR R
C      *****
      DO 550 I=1,NNP
      IF (KODE(I).NE.0) GO TO 550
      R(I)=R(I)+VLY(I)

550    CONTINUE
C      *****
C      *** STAGE 6*** BOUNDARY CONDITIONS
C      *****
C      ADD K(ALPHA) + K(T)
      DO 560 I=1,NNP
      DO 560 J=1,IBAND
      A(I,J)=A(I,J)+AP(I,J)
560    CONTINUE
      DO 600 N=1,NNP
      IF (KODE(N).EQ.0) GO TO 590
      BOUND=VLY(N)
      DO 580 M=2,IBAND
      K=N-M+1

```

```

      IF (K.LE.0) GO TO 570
      R(K)=R(K)-A(K,M)*BOUND
      A(K,M)=0.0
      AP(K,M)=0.0
570    K=N+M-1
      IF (K.GT.NNP) GO TO 580
      R(K)=R(K)-A(N,M)*BOUND
      A(N,M)=0.0
      AP(N,M)=0.0
580    CONTINUE
      A(N,1)=1.0
      AP(N,1)=0.0
      R(N)=BOUND
590    CONTINUE
600    CONTINUE
C      *****
C                                     *** STAGE 7*** TIME INTEGRATION
C      *****
      IF (NOPT.LT.3) GO TO 650
      DO 640 I=1,NNP
      BB=0.
      IF (I.EQ.1) GO TO 620
      IP=I-1
      DO 610 KK=1,IP
      JJ=I+1-KK
C      COMPUTE RIGHT HAND SIDE 'EQUIVALENT LOAD' K(T)* R(T)
      IF (JJ.GT.IBAND) GO TO 610
      BB=BB+AP(KK,JJ)*H(KK)
610    CONTINUE
620    CONTINUE
      DO 630 J=1,IBAND
      II=I+J-1
      IF (II.GT.NNP) GO TO 630
      BB=BB+AP(I,J)*H(II)
630    CONTINUE
      R(I)=R(I)+BB

640    CONTINUE
650    CONTINUE
C      *****
C                                     *** STAGE 8*** SOLVE EQUATIONS           MAIN3180
C      EQUATION SOLVER - GAUSS-DOOLITTLE ELIMINATION PROCEDURE           MAIN3090
C      *****MAIN3100
      NRS=NNP-1
      NR=NNP
      DO 670 N=1,NRS
      M=N-1
      MR=MIN0 (IBAND, NR-M)
      PIVOT=A(N,1)
      DO 670 L=2,MR
      C=A(N,L)/PIVOT
      I=M+L
      J=0
      DO 660 K=L,MR
      J=J+1
660    A(I,J)=A(I,J)-C*A(N,K)
670    A(N,L)=C
      DO 680 N=1,NRS
      M=N-1
      MR=MIN0 (IBAND, NR-M)
      C=R(N)
      R(N)=C/A(N,1)
      DO 680 L=2,MR

```

```

      I=M+L
680  R(I)=R(I)-A(N,L)*C
      R(NR)=R(NR)/A(NR,1)
      DO 690 I=1,NRS
      N=NR-I
      M=N-1
      MR=MIN0(IBAND,NR-M)
      DO 690 K=2,MR
      L=M+K
690  R(N)=R(N)-A(N,K)*R(L)
C*****
C          *** STAGE 9 *** SET R(T) = H( ) = R(T+DT)
C*****
      DO 700 I=1,NNP
700  H(I) = R(I)
C*****
C          *** STAGE 10 *** OUTPUT QUANTITIES
C*****
      IF (NOPT.GE.3) GO TO 710
      WRITE (6,1180)
710  CONTINUE
      GO TO (720,750,780,830), NOPT
C          *** OUTPUT FOR SRESS-DEFORMATION PROBLEM ***
720  WRITE (6,1190)
      WRITE (6,1200)
      DO 730 I=1,NNP
730  WRITE (6,1250) I,R(I)
C      COMPUTE STRESSES
      WRITE (6,1210)
      DO 740 L=2,NNP
      MT=IE(L-1,3)
      STRESS=(R(L)-R(L-1))*PROP(MT)/ALL(L-1)
      L1=L-1
740  WRITE (6,1230) L1,STRESS
      GO TO 890
C      PRINT OUT RESULTS FOR FLOW PROBLEM//)
C          *** OUTPUT FOR FLOW
750  WRITE (6,1240)
      WRITE (6,1270)
      DO 760 I=1,NNP
760  WRITE (6,1250) I,R(I)
C      COMPUE VELOCITIES
      WRITE (6,1220)
      DO 770 L=2,NNP
      MT=IE(L-1,3)
      VELO=(R(L)-R(L-1))*PROP(MT)/ALL(L-1)
      VELO=-VELO
      L1=L-1
770  WRITE(6,1230) L1,VELO
      GO TO 890
C          **** OUTPUT FOR TRANSIENT TEMPERATURE ****
C      IF DT IS CHOSEN TO BE LESS THAN 0.0001, CHANGE TOLER
780  TOLER=0.0001
      IF (TIME.GT.DT) GO TO 790
      WRITE (6,1180)
      WRITE (6,1280)
790  CONTINUE
      IF (TIME.GT.TOTIM) GO TO 900
      DO 800 I=1,NTIME
      DIF=ABS(TIME-TIM(I))
      IF (DIF.LT.TOLER) GO TO 810
800  CONTINUE
C      GO TO 530 replaced with GO TO 375 to recompute element matrices

```

```

      GO TO 375
810  WRITE (6,1260) TIME
      WRITE (6,1290)
      DO 820 I=1,NNP
820  WRITE (6,1250) I,R(I)
C    GO TO 530 replaced with GO TO 375 to recompute element matrices
      GO TO 375
C
      ***** OUTPUT FOR CONSOLIDATION
830  TOLER=0.0001
      IF (TIME.GT.DT) GO TO 840
      WRITE (6,1180)
      WRITE (6,1300)
840  CONTINUE
      IF (TIME.GT.TOTIM) GO TO 900
      DO 850 I=1,NTIME
      DIF=ABS(TIME-TIM(I))
      IF (DIF.LT.TOLER) GO TO 860
850  CONTINUE
      GO TO 530
860  CONTINUE
      USUM=0.0
      DO 870 I=1,NNP
      UZ=R(I)/TUINIT
870  USUM=USUM+UZ
      UAV=1.-USUM
      WRITE (6,1310) TIME,TF,UAV
C    PRINT OUT NODAL PORE PRESSURES
      WRITE (6,1320)
      DO 880 I=1,NNP
880  WRITE (6,1330) I,R(I)
      IF (UAV.GE.0.98) GO TO 900
      GO TO 530
890  CONTINUE
900  CONTINUE
      GO TO 20
      910 CONTINUE
      WRITE(6,1340)
      STOP
C    *****
C
920  FORMAT(I5,3X,18A4)
930  FORMAT(//1H1,10X,8HPROBLEM=,I5,3H..,18A4////)
940  FORMAT(10X,16HINPUT QUANTITIES////)
950  FORMAT(10X,38HINPUT TABLE 1A .. PROBLEM PARAMETERS//)
960  FORMAT(16I5)
970  FORMAT (5X,39HNUMBER OF NODE POINTS          ...=,I5/5X,39HNUM
1BER OF MATERIALS          ...=,I5/5X,39HNUMBER OF TRACTION C
2ARDS          ...=,I5/5X,39HOPTION FOR BODY FORCE =0 OR 1      ..
3.=,I5/5X,39HOPTION FOR PROBLEM TYPE          ...=,I5/5X,39HSEMI-
4BAND WIDTH          ...=,I5/5X,39HNUMBER OF OUTPUT TIME
5LEVELS          ...=,I5)
980  FORMAT(8E10.3)
990  FORMAT (////10X,36HINPUT TABLE 1B...MATERIAL PROPERTIES//5X,55H M
1AT          K          C OR MV RO/DEN OF WAT          MAIDENS//)
1000  FORMAT (5X,I5,2X,E10.3,2X,E10.3,2X,E13.3,2X,E10.3)
1010  FORMAT (////10X,33HINPUT TABLE 2 .. NODAL POINT DATA//5X,40H NODE
1 KODE          Y-COORD          DISP/FORCE/)
1020  FORMAT (2I5,2E10.3)
1030  FORMAT (10X,19HERROR IN NODE CARD=,I5)
1040  FORMAT (5X,I5,2X,I5,2X,E10.3,2X,E12.3)
1050  FORMAT (////10X,30HINPUT TABLE 3 .. ELEMENT DATA//5X,40HEL NO NO
1DE I NODE J MTYPE          AREA/)
1060  FORMAT (5X,21HERROR IN ELEMENT CARD,I5)

```

```

1070 FORMAT (5X,I5,2I8,2X,I6,2X,E10.3)
1080 FORMAT (////10X,35HINPUT TABLE 4 .. SURFACE TRACTIONS//5X,26HNUMB
1ER ELEM TRACTION/)
1090 FORMAT (I5,E10.3)
1100 FORMAT (5X,I6,2X,I5,2X,E10.3)
1110 FORMAT (////10X,51HINPUT TABLE 5A .. DATA FOR TIME DEPENDENT PROB
1LEMS//)
1120 FORMAT (2E10.3,I5)
1130 FORMAT (5X,15HTIME INCREMENT=,E10.3,2X,20HTOTAL SOLUTION TIME=,E10MAIN4630
1.3,5X,7HOPTION=,I5)
1140 FORMAT (////10X,44HINPUT TABLE 5B.. DATA FOR OUTPUT TIME LEVELS//5MAIN4650
1X,26HNUMBER OUTPUT TIME/)
1150 FORMAT (5X,I6,10X,E12.3)
1160 FORMAT (////10X,37HINPUT TABLE 5C.. INITIALS CONDITIONS //5X,25HNO MAIN468
1DE TEMP/PRES/)
1170 FORMAT (5X,I4,10X,E10.3)
1180 FORMAT (/1H1,10X,18HOUTPUT QUANTITIES)
1190 FORMAT (////10X,46HOUTPUT TABLE 1 .. STRESS-DEFORMATION PROBLEM /MAIN4720
1/)
1200 FORMAT (/5X,27H NODE DISPLACEMENT/)
1210 FORMAT (/5X,24HELEM STRESS)
1220 FORMAT (/5X,27HELEM VELOCITY/)
1230 FORMAT (5X,I4,10X,E10.3)
1240 FORMAT (////10X,32HOUTPUT TABLE 1 .. FLOW PROBLEM//)
1250 FORMAT (5X,I5,10X,E12.3)
1260 FORMAT (/10X,14HELAPSED TIME =,E10.3//)
1270 FORMAT (/5X,24HNODE POTENTIAL)
1280 FORMAT (////10X,38HOUTPUT TABLE 1 .. TEMPERATURE PROBLEM//)
1290 FORMAT (/5X,28H NODE TEMPERATURE//)
1300 FORMAT (////10X,52HOUTPUT TABLE 1 .. RESULTS FOR CONSOLIDATION PRMAIN4840
1OBLEM/)
1310 FORMAT (5X,13HELAPSED TIME=,E10.3,2X,12HTIME FACTOR=,E10.3,2X
1,24HDEGREE OF CONSOLIDATION=,E10.3//)
1320 FORMAT (/10X,28H NODE PORE PRESSURE//)
1330 FORMAT (10X,I5,10X,E13.4)
1340 FORMAT (////17H ** JOB END ** )
END

```

```

C Function to compute the convective heat transfer coefficient h
C units of h are (BTU/(hr.F.in^2)

```

```

DOUBLE PRECISION FUNCTION HCONVC(TIME)
IMPLICIT DOUBLE PRECISION (A-H,O-Z)
IF (ABS(TIME-0.0) .LT. 0.1E-6) THEN
H=0.198+0.039625
ELSEIF (TIME .LT. 12.47 ) THEN
H=(0.658**(0.198/(13.7/TIME**2+0.039625)))*0.198+0.039625
ELSEIF (TIME .GE. 12.47 ) THEN
H= 13.7/TIME**2 + 0.039625
ENDIF
HCONVC=H
RETURN
END

```

```

C Function to compute heat generation QI in the concrete
C units are (BTU/(hr.in^3)

```

```

C REAL FUNCTION QIFLUX(TIME)
C REAL TIME
DOUBLE PRECISION FUNCTION QIFLUX(TIME, TIME1, TIME2, QPEAK)
IMPLICIT DOUBLE PRECISION (A-H,O-Z)
IF (TIME .LT. 1.0) THEN
QI= 0.0
ELSEIF (TIME .LE. TIME1) THEN
QI=0.0
ELSEIF (TIME .GT. TIME1 .AND. TIME .LE. TIME2) THEN
QI= QPEAK*(TIME-TIME1)/(TIME2-TIME1)

```

```

ELSEIF (TIME .GT. TIME2 ) THEN
  QI= 100.0*QPEAK/(TIME-(TIME2-10.0))**2
ENDIF
QIFLUX=QI

RETURN
END

C   REAL FUNCTION AMBTMP(TIME)
C   DIMENSION T(24)
C   DATA T /13.5,13.8,14.4,15.0,15.5,16.1,16.6,17.1,17.5,17.1,
C   & 16.6,16.1,15.6,15.1,14.8,14.7,14.6,14.5,14.4,14.2,14.0,13.8,
C   & 13.7,13.6/
C   ITIME=IFIX(TIME+1.0)
C   AMBTMP=T(ITIME)*9.0/5.0+32.0
C   RETURN
C   END

```

## Appendix 3B: Format for Input File for Thermal Finite Element Analysis Program

Problem number and title:  
 FORMAT (I5,3X,18A4)

NPROB		Blank	TITLE															
1	5 6	8 9																80

Basic parameters:

FORMAT (16I5)

NNP	NMAT	NSLC	NBODY	NOPT	IBAND	NTIME						
1	5 6	10 11	15 16	20 21	25 26	30 31	35					

Material properties:

FORMAT (8E10-3)

Input as many cards as NMAT.

PROP	AMV	RO	DENS						
1	10 11	20 21	30 31	40					

Nodal point data:

FORMAT (2I5,2E10-3)

N.P.NO.	KODE	Y-COORD	VLY						
1	5 6	10 11	20 21	30					

Element data:

FORMAT (16I5)

M	IE(M,1)	IE(M,2)	IE(M,3)						
1	5 6	10 11	15 16	20					

See note 2 on page 143 for automatic generation of element data.

Areas of elements:

Option for variation  
 FORMAT (16I5)

IAREA					
1	5				

- = 1 for constant areas
- = 2 for linearly varying areas
- = 3 for different areas for each element

Values of areas:

FORMAT (8E10-3)

AREAEL (1)	AREAEL (2)	...					
1	10 11	20 21					

- If area is constant, input only one value AREAEL (1).
- If areas vary linearly, input values for the first and the last elements.
- If areas have different values in each element, input all values.

Surface tractions:

FORMAT (15,E10-3)

KEL	TY											
1	5 6	15										

Input as many cards as NSLC.

For time-dependent problems only:

Time increment, total time, and option for variation of initial conditions:

FORMAT (2E10-3,15)

DT	TOTIM	INOPT	
1	10 11	20 21	25

INOPT = 1 for constant values of initial conditions  
= 2 for linear variation  
= 3 for different values at each node

Selected output time levels:

FORMAT (8E10-3)

TIM(1)	TIM(2)	. . .
1	10 11	20 21

Input as many as NTIME values.

Initial conditions:

FORMAT (8E10-3)

UINIT(1)	UINIT(2)	UINIT(3)	. . .
1	10 11	20 21	30 31

If initial values constant, input one value UINIT(1).  
If linear variation, input values for the first and the last node.  
If values different at each node, input all values.

Surface Temperatures top of deck (°F):

FORMAT (8E10.3)

SURTMP(1)	SURTMP(2)	. . .
1	10 11	20 21

Input as many as NTIME values.

Ambient Air Temperatures below the formwork (°F):

FORMAT (8E10.3)

AIRTMP(1)	AIRTMP(2)	. . .
1	10 11	20 21

Input as many as NTIME values.

Blank Card
------------

Input at the end of each run. Each run can contain more than one problem, NPROB. Blank card required only at the end of all problems.

**NOTATION for input Data Parameters**(all page and equation numbers refer to Desai, 1971)

AMV =  $c$  = specific heat (BTU/lbm/°F) (p. 108)

**A** = Assemblage matrix which is set equal to **AK**; only once for stress deformation and steady flow but at every time step for transient flow.

**AK** = Assemblage matrix which is computed only once. This matrix corresponds to **[K]** [Eqs. (3-32), (4-13) or (5-33)].

**ALL** = Length of each element.

**AP** = Assemblage matrix corresponds to **[K<sub>α</sub><sup>\*</sup>]** [Eq. (5-33)].

**AREAEL** = Area of elements. If **IAREA** = 1, input one value of uniform area, = 2 input first and last values, = 3 input all values.

**DENS** = Density (unit weight) for different materials.

**DT** = Time increment [Eqs. (5-23) and (5-33)].

**GWT** = Contribution of gravity or body force at an element node.

**H** = Vector that stores initial values of temperature (or pore pressure) and also  $R_{t+\Delta t}$  computed at  $t + \Delta t$  time level for use as  $R_t$  for the subsequent time level.

**IAREA** = Option for specifying areas of elements:

= 1: for uniform area over all elements.

= 2: for linearly varying areas; input values for only the first and last elements.

= 3: for arbitrary variation, that is, input area for each element.

**IBAND** = Semibandwidth. Set 2 for the one-dimensional problem with linear approximation.

**IE(M,1)** = Node 1 of element *M*.

**IE(M,2)** = Node 2 of element *M*.

**IE(M,3)** = Material type of element *M*.

**INOPT** = Option for initial conditions:
 

- = 1: uniform temperature or pressure at all nodes.
- = 2: linearly varying temperature or pressure; input values only for the first and the last nodes.
- = 3: arbitrary; input values for all nodes.

**KEL** = Element(s) on which surface tractions (TY) are applied.

**KODE** = Code for boundary conditions:
 

- = 1: specified displacement, potential, temperature, or pore pressure.
- = 0: free node where concentrated force can be applied.

**NBODY** = 0 for no body force, = 1 if body force specified.

**NCT** = Step of time increment; can be printed out if desired.

**NMAT** = Number of materials.

**NNP** = Number of nodes.

**NOPT** = 1 stress deformation, = 2 steady flow, = 3 transient temperature, = 4 consolidation.

**NPROB** = Problem number; if = 0, program exits from the computer.

**NSLC** = Number of surface traction cards.

**NTIME** = Number of time levels at which output is desired.

**PROP** = Material property:
 

- = *E*, elastic modulus for stress deformation.
- = *k*, coefficient of permeability for flow.
- =  $\alpha$ , thermal diffusivity for temperature (for homogeneous medium).
- =  $c_v$ , coefficient of consolidation (for homogeneous medium). For layered media, see Table 6-1.

**QK** = Element matrix [*k*] in Eqs. (3-28) and (4-9) and [*k<sub>α</sub>*] in Eq. (5-21).

**QP** = Element matrix [*k<sub>r</sub>*] in Eq. (5-21).

**R** = Assemblage forcing vector {*R*} in Eqs. (3-32), (4-13), and (5-33). Computed nodal displacements, potential, temperature, or pressure are stored in this vector after Gaussian elimination.

**RO** = Mass density of material.

**TF** = Time factor.

**TIM** = Selected time levels at which output is desired.

**TIME** = Elapsed time.

**TITLE** = Title and description of problem.

**TUINIT** = Total of initial values = (sum of initial pore pressures) × (number of nodes).

**TY** = Applied surface traction load.

**UAV** = Average degree of consolidation at a given time.

**UINIT** = Values of initial temperature or pore pressure at time  $\leq 0$ .

**USUM** = Average dissipation of pore pressure at a given time.

**VLV** = Value of applied boundary condition. If **KODE** = 1, it implies specified displacement, potential, temperature, or pressure; if **KODE** = 0, it implies free node where forcing parameters (concentrated load) can be specified.

**Y** = *y* coordinate for stress deformation (of vertical column and strut) and for consolidation.
 

- = *x* coordinate for flow and temperature.

## Appendix 3C: Input File for Thermal Finite Element Analysis Case 3(b) of Bridge Deck Curing

```

1 Heat flow in concrete deck
7.000E-00 0.150E+02 0.780E-00
35 5 34 0 3 2 53
2.376E-01 2.006E+01 4.335E-05 4.335E-05
8.185E-02 2.102E-01 8.391E-02 8.391E-02
1.589E-08 3.296E-08 8.391E-02 8.391E-02
0.207E+01 1.075E-01 2.741E-01 2.741E-01
1.300E-01 3.296E-01 8.391E-02 8.391E-02
1 1 0.000E+00 0.700E+02
2 0 1.000E-01 0.000E+00
3 0 2.000E-01 0.000E+00
4 0 3.000E-01 0.000E+00
5 0 4.000E-01 0.000E+00
6 0 5.000E-01 0.000E+00
7 0 7.000E-01 0.000E+00
8 0 1.000E+00 0.000E+00
9 0 1.500E+00 0.000E+00
10 0 2.000E+00 0.000E+00
11 0 2.500E+00 0.000E+00
12 0 3.000E+00 0.000E+00
13 0 3.500E+00 0.000E+00
14 0 4.000E+00 0.000E+00
15 0 4.620E+00 0.000E+00
16 0 5.240E+00 0.000E+00
17 0 5.860E+00 0.000E+00
18 0 6.480E+00 0.000E+00
19 0 7.100E+00 0.000E+00
20 0 7.600E+00 0.000E+00
21 0 8.100E+00 0.000E+00
22 0 8.450E+00 0.000E+00
23 0 8.800E+00 0.000E+00
24 0 9.150E+00 0.000E+00
25 0 9.500E+00 0.000E+00
26 0 1.150E+01 0.000E+00
27 0 1.350E+01 0.000E+00
28 0 1.450E+01 0.000E+00
29 0 1.550E+01 0.000E+00
30 0 3.250E+01 0.000E+00
31 0 4.950E+01 0.000E+00
32 0 6.650E+01 0.000E+00
33 0 8.350E+01 0.000E+00
34 0 8.450E+01 0.000E+00
35 1 8.550E+01 7.000E+01
1 1 2 2
2 2 3 2
3 3 4 2
4 4 5 2
5 5 6 2
6 6 7 2
7 7 8 2
8 8 9 2
9 9 10 2
10 10 11 2
11 11 12 2
12 12 13 2
13 13 14 2
14 14 15 2
15 15 16 2

```

16	16	17	2						
17	17	18	2						
18	18	19	2						
19	19	20	2						
20	20	21	2						
21	21	22	2						
22	22	23	2						
23	23	24	2						
24	24	25	2						
25	25	26	2						
26	26	27	2						
27	27	28	4						
28	28	29	4						
29	29	30	4						
30	30	31	4						
31	31	32	4						
32	32	33	4						
33	33	34	4						
34	34	35	4						
3									
0.100E+01									
0.100E+01									
0.100E+01									
0.278E+00	0.278E+00	0.278E+00	0.278E+00	0.104E-01	0.104E-01	0.104E-01	0.104E-01	0.104E-01	0.104E-01
0.278E+00	0.278E+00								
1	0.000E-00								
2	0.000E-00								
3	0.000E-00								
4	0.000E-00								
5	0.000E-00								
6	0.000E-00								
7	0.000E-00								
8	0.000E-00								
9	0.000E-00								
10	0.000E-00								
11	0.000E-00								
12	0.000E-00								
13	0.000E-00								
14	0.000E-00								
15	0.000E-00								
16	0.000E-00								
17	0.000E-00								
18	0.000E-00								
19	0.000E-00								
20	0.000E-00								
21	0.000E-00								
22	0.000E-00								
23	0.000E-00								
24	0.000E-00								
25	0.000E-00								
26	0.000E-00								
27	0.000E-00								
28	0.000E-00								
29	0.000E-00								
30	0.000E-00								
31	0.000E-00								
32	0.000E-00								
33	0.000E-00								
34	0.000E-00								
0.100E+01	0.768E+03	1							
0.100E+01	0.200E+01	0.300E+01	0.400E+01	0.500E+01	0.600E+01	0.700E+01	0.800E+01		
0.900E+01	0.100E+02	0.110E+02	0.120E+02	0.130E+02	0.140E+02	0.150E+02	0.160E+02		
0.170E+02	0.180E+02	0.190E+02	0.200E+02	0.210E+02	0.220E+02	0.230E+02	0.240E+02		

0.250E+02 0.260E+02 0.270E+02 0.280E+02 0.290E+02 0.300E+02 0.310E+02 0.320E+02  
0.330E+02 0.340E+02 0.350E+02 0.360E+02 0.480E+02 0.720E+02 0.960E+02 0.120E+03  
0.168E+03 0.335E+03 0.336E+03 0.337E+03 0.360E+03 0.384E+03 0.432E+03 0.480E+03  
0.528E+03 0.576E+03 0.624E+03 0.672E+03 0.720E+03  
0.700E+02  
0.700E+02 0.700E+02 0.700E+02 0.700E+02 0.700E+02 0.700E+02 0.700E+02 0.700E+02  
0.700E+02 0.700E+02 0.700E+02 0.700E+02 0.700E+02 0.700E+02 0.700E+02 0.700E+02  
0.700E+02 0.700E+02 0.700E+02 0.700E+02 0.700E+02 0.700E+02 0.700E+02 0.700E+02  
0.700E+02 0.700E+02 0.700E+02 0.700E+02  
0.700E+02 0.700E+02 0.700E+02 0.700E+02 0.700E+02 0.700E+02 0.700E+02 0.700E+02  
0.700E+02 0.700E+02 0.700E+02 0.700E+02 0.700E+02 0.700E+02 0.700E+02 0.700E+02  
0.700E+02 0.700E+02 0.700E+02 0.700E+02 0.700E+02 0.700E+02 0.700E+02 0.700E+02  
0.700E+02 0.700E+02 0.700E+02 0.700E+02  
0.700E+02 0.700E+02 0.700E+02 0.700E+02

Results of the thermal finite element analysis are given in the FE3A\_NEW.OUT file that is read by the CBRAN structural analysis program that considers the time history deck temperatures during the curing process in computing the residual stresses due to temperature and shrinkage.

## Appendix 4-1 Subroutine UPDBK is used to update DATABANK properties

```

C      Subroutine to update the databank for the concrete
C      modulus of elasticity for incremental
C      thermal stress analysis.
C      units are hours for time and psi for modulus of elasticity
C23456789*123456789*123456789*123456789*123456789*123456789*123456789*12
C
      SUBROUTINE UPDBK(TIME, TIME1)
C      IMPLICIT DOUBLE PRECISION (A-H,O-Z)
      CHARACTER*82 BUF
      IO90=90
      IO98=98
      OPEN (UNIT=IO90,STATUS='OLD',ACCESS='DIRECT',FORM='FORMATTED',RECL
1=82,FILE='databk.org')
      OPEN (UNIT=IO98,STATUS='OLD',ACCESS='DIRECT',FORM='FORMATTED',RECL
1=82,FILE='databk')
      ECONC=ETIME(TIME,TIME1)
C      SCONCT=Strength of concrete in tension
C      SCONCC=Strength of concrete in compression
      SCONCC=SCONC(TIME,TIME1)
      SCONCT=7.5*SQRT(SCONCC)
C this next block points to locations where strengths are to be updated
      IF (TIME .GT. 672.) THEN
C update the strengths for CONC
      READ (IO90,'(A80)', REC=513) BUF
      WRITE (BUF(4:13),'(E10.3)') SCONCT
      WRITE (BUF(14:23),'(E10.3)') SCONCC
      WRITE (IO98,'(A80)', REC=513) BUF
C update the strengths for CNCF
      READ (IO90,'(A80)', REC=526) BUF
      WRITE (BUF(4:13),'(E10.3)') SCONCT
      WRITE (BUF(14:23),'(E10.3)') SCONCC
      WRITE (IO98,'(A80)', REC=526) BUF
      ENDIF
C
C update the modulus of elasticity for CONC
      READ (IO90,'(A82)', REC=511) BUF
      WRITE (BUF(4:13),'(E10.3)') ECONC
      WRITE (IO98,'(A82)', REC=511) BUF
C update the modulus of elasticity for CNCF
      READ (IO90,'(A82)', REC=524) BUF
      WRITE (BUF(4:23),'(2E10.3)') ECONC, ECONC
      WRITE (IO98,'(A82)', REC=524) BUF
      CLOSE (IO98)
      CLOSE (IO90)
      RETURN
      END

C      Function ETIME to compute modulus of elasticity E in the concrete
C      as a function of time (hours), units of E are psi
C      TIME1 is the time from pouring when the concrete begins to hydrate
C
C23456789*123456789*123456789*123456789*123456789*123456789*123456789*12
C
      REAL FUNCTION ETIME(TIME, TIME1)
C      IMPLICIT DOUBLE PRECISION (A-H,O-Z)
      E28=0.446E+7
      IF (TIME .LT. 1.0) THEN
          ET= 10.0
      ELSEIF (TIME .LE. TIME1+1) THEN

```

```

    ET=10.0
ELSEIF (TIME .GT. TIME1+1) THEN
    ET= 0.710*E28*(TIME-TIME1)**(1/19)
    ET=ET*(1.0-1.0/(TIME-TIME1)**(0.333))
ELSE
    WRITE(*,*) ' ERROR in function ETIME, TIME=', TIME
    STOP 100
ENDIF
ETIME=ET
RETURN
END

C    Function SCONC to compute strength S of the concrete
C    as a function of time (hours), units of S are psi
C    TIME1 is the time from pouring when the concrete begins to set
C    SCONC is called by UPDBK to update the databank with concrete tensile
C    and compressive stresses
C23456789*123456789*123456789*123456789*123456789*123456789*123456789*12
REAL FUNCTION SCONC(TIME, TIME1)
C    SCONC will compute fc' as a function of time from hydration
C    IMPLICIT DOUBLE PRECISION (A-H,O-Z)
S28=6000.0
C    T=time from curing (days)
T=(TIME-TIME1)/24.0
IF (T .LE. 0.0) THEN
    S= 10.0
ELSEIF (T .LE. 3.0) THEN
    S= 0.1429*T*S28
ELSEIF (T .GT. 3.0 .AND. T .LT. 7.0 ) THEN
    C=1.052-0.05116*T
    S=C*alog10(T)*S28
ELSEIF (T .GE. 7.0) THEN
    C=0.6925
    S=C*alog10(T)*S28
ELSE
    WRITE(*,*) ' ERROR in function SCONC, TIME=', TIME
    STOP 100
ENDIF
SCONC=S
RETURN
END

```

## Appendix 4-2 Listing of subroutine TEMPRD

```
C      Subroutine to read the nodal temperatures from FE3A_NEW.OUT
C      to be used by CBRAN to write the input data files of layer
C      temperatures for incremental thermal stress analysis.
C      units are degrees F
C23456789*123456789*123456789*123456789*123456789*123456789*123456789*12
C
      SUBROUTINE TEMPRD(TEMPL, NLAYER)
      IMPLICIT DOUBLE PRECISION (A-H,O-Z)
      CHARACTER*80 BUF
      DIMENSION TEMPL(NLAYER)
      DIMENSION TEMP(35)
      iinput=11
      ioutpt=81
      OPEN (iinput,FILE='FE3A_NEW.OUT',status='OLD')
      OPEN (ioutpt,FILE='TEMPRTRS.LYR',status='unknown')
      rewind iinput
      rewind ioutpt
1     READ (iinput,'(A80)') BUF
      IF (BUF(11:48).EQ.'OUTPUT TABLE 1 .. TEMPERATURE PROBLEM')THEN
          GO TO 2
      ELSE
          GO TO 1
      ENDIF
2     READ (iinput,'(A80)',END=3) BUF
      IF (BUF(11:24).EQ.'ELAPSED TIME =')THEN
Cdebug      write (*,'(A80)') BUF
          READ (BUF(25:34),'(E10.3)') TIME
          READ (iinput,'(A80)') BUF
          DO 4 i=1, NLAYER+1
              READ (iinput,'(I10,12X,E10.3)') IREAD, TEMP(I)
Cdebug      write (*,'(I10,12X,E10.3)') IREAD, TEMP(I)
              IF (I .NE. IREAD) THEN
                  WRITE(*,*) ' ERROR in TEMPRD - STOP'
                  STOP 111
              ENDIF
4         CONTINUE
          DO 5 i=1, nlayer
              TEMPL(i)=0.5d0*(TEMP(i)+TEMP(i+1))
5         CONTINUE
          WRITE (ioutpt,('ELAPSED TIME =',E10.3)) TIME
          WRITE (ioutpt,'(8E10.3)') (TEMPL(I),I=1,NLAYER)
Cdebug      WRITE (*,'('ELAPSED TIME =',E10.3)') TIME
Cdebug      WRITE (*,'(8E10.3)') (TEMPL(I),I=1,NLAYER)
      ENDIF
      GO TO 2
3     CLOSE (iinput)
      CLOSE (ioutpt)
Cdebug      WRITE (*,*) ' Returning from TEMPRD'
      RETURN
      END
```



```

Cdebug      IF (TIME .GT. 337. ) STOP 1111
WRITE (*,*)' TIME=', TIME,' HOURS'
Cdebug      write (*,*)' Before UPDBK NLayer=', NLayer
CALL UPDBK(TIME, TIME1)
C          call INCTET to read the layer temperatures from TEMPS.LYR
C          and update the CBRAN input file IO85 with the
C          incremental temperatures of the layers for incremental
C          thermal stress analysis.
Cdebug      write (*,*)' Before INCTET NLayer=', NLayer
CALL INCTET (TEMPL, TEMPL1, TIMES(I), TIMES(I+1), TIME1, TIME2,
& SIG11, EPSINI, NLayer, HS,TD,BD,DTHICK)
C23456789*123456789*123456789*123456789*123456789*123456789*123456789*12
C          Call the executive module "CODEXE".  COD00140
C          COD00150

      IO77 = 77
      REWIND IO77
      write(*,*)' CALLING CODEXE I=', I
Cdebug      write (*,*)' Before CODEXE NLayer=', NLayer
CALL CODEXE (WKAREA, ISIZE, CODARA, ISIZE2)          COD00160
C          call STREAD to obtain and add the thermal stresses
Cdebug      write (*,*)' Before STREAD NLayer=', NLayer
C          IF (TIME-TIME1 .GT. 8.0) THEN
CALL STREAD (SIG11, SIG22, SIG12, SIG13, SIG23, EPS11, EPS22, EPSINI,
& TIME, TIME1, NLayer, ICRACK)
      WRITE (*,*) ' ICRACK=', ICRACK
C          ENDIF
C          672 hours=28 days
      IF (ABS(TIME-672.0) .LT. 0.10E-5)GO TO 2
C          IF (I.GT.10) STOP
      1 CONTINUE
      2 CONTINUE
C do analysis under loading
C 14000 lbs loading on cantilevered right end for the lab test
C HS25 loading 14 ftx14 ft LOADING ON ONE SPAN for 2-span bridge
C write input file FOR085.DAT with loading
      REWIND IO77
      IF (LABTST) THEN
CALL LB1485(ICRACK)
      write(*,*)' CALLING CODEXE 14K LOADING ON RIGHT'
CALL CODEXE (WKAREA, ISIZE, CODARA, ISIZE2)
      WRITE (91,*)
      WRITE (91,*) ' 14000 lbs LOADING RESULTS after', TIME,' HOURS =',
& TIME/24.0,' DAYS'
CALL STREAD (SIG11, SIG22, SIG12, SIG13, SIG23, EPS11, EPS22,
& EPSINI, TIME, TIME1, NLayer,
& ICRACK)
      WRITE (*,*) ' ICRACK=', ICRACK
      ELSE
CALL HS2585(ICRACK)
      write(*,*)' CALLING CODEXE HS25 14 ftx14 ft LOADING ON ONE SPAN'
CALL CODEXE (WKAREA, ISIZE, CODARA, ISIZE2)
      WRITE (91,*)
      WRITE (91,*) ' HS25 14 ftx14 ft LOADING RESULTS after', TIME,
& ' HOURS =', TIME/24.0,' DAYS'
CALL STREAD (SIG11, SIG22, SIG12, SIG13, SIG23, EPS11, EPS22,
& EPSINI, TIME, TIME1, NLayer,
& ICRACK)
      WRITE (*,*) ' ICRACK=', ICRACK
      ENDIF
C
      CALL FLUSH(85)
      STOP          COD00170
      END          COD00180

```

## Appendix 4-4 Computation of shrinkage strains

```
      SUBROUTINE DSHEPS(DESH, TIME, TIMNXT, TIME1, TIME2, NLYR,
& HS,TD,BD,DTHICK)
C   DSHEPS computes incremental shrinkage strains (microstrains)
C23456789*123456789*123456789*123456789*123456789*123456789*123456789*12
      DIMENSION ESH(26), ESH1(26), DESH(NLYR)
C       TIME=1344.0
C       TIME1=7.0
C       TIME2=192.0
C       NLYR=24
C   Initialize the ESH array (Shrinkage strains)
C   Compute the shrinkage strains in the current and next time step
      CALL SHSTR (ESH, TIME, TIME1, TIME2, NLYR,HS,TD,BD,DTHICK)
      CALL SHSTR (ESH1, TIMNXT, TIME1, TIME2, NLYR,HS,TD,BD,DTHICK)
C   Compute the incremental shrinkage strains
      DO I =1, NLYR
          DESH(I)=ESH1(I)-ESH(I)
      ENDDO
      RETURN
      END

      SUBROUTINE SHSTR (ESH,TIME,TIME1,TIME2,NLAYER,HS,TD,BD,DTHICK)
      DIMENSION ZCOOR(26), ESH(NLAYER)
C       HS=35.0
C       TD=1.0
C       BD=0.0
C       DTHICK=9.5
C
C       ZCOOR(1)=0.05
C       ZCOOR(2)=0.15
C       ZCOOR(3)=0.25
C       ZCOOR(4)=0.35
C       ZCOOR(5)=0.45
C       ZCOOR(6)=0.6
C       ZCOOR(7)=0.85
C       ZCOOR(8)=1.25
C       ZCOOR(9)=1.75
C       ZCOOR(10)=2.25
C       ZCOOR(11)=2.75
C       ZCOOR(12)=3.25
C       ZCOOR(13)=3.75
C       ZCOOR(14)=4.31
C       ZCOOR(15)=4.93
C       ZCOOR(16)=5.55
C       ZCOOR(17)=6.17
C       ZCOOR(18)=6.79
C       7.1 in
C       ZCOOR(19)=7.35
C       ZCOOR(20)=7.85
C       8.1 in (layers 19 and 20 include rebars)
C       ZCOOR(21)=8.275
C       ZCOOR(22)=8.625
C       ZCOOR(23)=8.975
C       ZCOOR(24)=9.325
C       9.5 in
C       ZCOOR(25)=10.50
C       ZCOOR(26)=12.50
C       13.5 in at bottom of haunch

      OPEN (3,FILE='zcoords.dsh',status='unknown')
      do i=1,nlayer
```

```

        read (3,'(i5,e10.3)')iread, zcoor(i)
        if (iread.ne.i) then
            write (*,*) ' iread=',iread, ' i=',i, ' zcoor(i)=' ,zcoor(i)
            write (*,*) ' Error in DSHEPS: STOP 999'
            STOP 999
        endif
    enddo
close (3)
CALL EPSSH(TIME, TIME1, TIME2, HS,TD,BD,DTHICK,ZCOOR,ESH,NLAYER)
RETURN
END
C23456789*123456789*123456789*123456789*123456789*123456789*123456789*12
C
    SUBROUTINE EPSSH(TIME,TIME1,TIME2,HS,TD,BD,DTHICK,ZCOOR,ESH,
& NLAYER)
    CHARACTER*82 BUF
    DIMENSION ZCOOR(NLAYER), ESH(NLAYER)
    T=TIME-TIME2
C    T1=TIME-TIME1
    SAU=SAUTO(TIME, TIME1)
    WRITE(*,*) 'Msg from dsheps.f: SAUTO=', SAU
    IF (T .LT. 48.) THEN
C        GAMA=3.0
        GAMA=0.0826*T-0.0003591*T*T
    ELSEIF (T .LT. 116.) THEN
        GAMA=0.0826*T-0.0003591*T*T
    ELSE
        GAMA=0.0017*T+4.6692
    ENDIF
Cdebug    WRITE(*,*) ' TIME-TIME2=T=', T
Cdebug    WRITE(*,*) ' GAMA=', GAMA
    WRITE(*,*) 'Msg from dsheps.f;epssh: TIME=',TIME,' TIME2=',TIME2

    WRITE(*,*) 'Msg from dsheps.f;epssh: T=', T
    IF ( T .LT. 24.0) THEN
        DO 1 I=1, NLAYER
            ESH(I)=0.0+SAU
1    CONTINUE
    ELSE
        DO 2 I=1, NLAYER
            ERCATD=ZCOOR(I)/GAMA
            ERCABD=(DTHICK-ZCOOR(I))/GAMA
            HI=HIN(TIME,TIME2)

C            ESH(I)=-200.0*(100.0-HI+TD*(HI-HS)*ERFC(ERCATD)+BD*(HI-HS)*
C            & ERFC(ERCABD))/100.0

            HXT=HI-TD*(HI-HS)*ERFC(ERCATD)-BD*(HI-HS)*ERFC(ERCABD)

            ESH(I)=-200.0*(100.0-HXT)/100.
            ESH(I)=ESH(I)+SAU

            WRITE(*,*) 'MSG from dsheps.f: ESH(',I,')=',ESH(I)
2    CONTINUE
        ENDIF
    RETURN
    END

C    Function HIN to compute the interior moisture of a sealed concrete
C    as a function of time (hours), units of E are psi
C    TIME1 is the time from pouring when the concrete begins to set
C    TIME2 is when the wetted burlap is removed
C23456789*123456789*123456789*123456789*123456789*123456789*123456789*12

```

C

```
REAL FUNCTION HIN(TIME,TIME2)

IF (TIME .LE. TIME2+24.) THEN
  HI = 100.0
ELSEIF (TIME .GT. TIME2+24. .AND. TIME .LE. TIME2+24+192.0) THEN
  HI = -0.0078125*(TIME-TIME2-24.)+100.0
ELSEIF (TIME .GT. TIME2+24+192.0) THEN
  HI = -0.0032894737*(TIME-TIME2-192.0-24.)+98.5
ELSE
  WRITE(*,*) ' ERROR in function HIN, TIME=', TIME
  STOP
ENDIF
HIN=HI
RETURN
END
```

```
REAL FUNCTION ERFC(X)
ERFC=1.0-ERF(X)
RETURN
END
REAL FUNCTION ERF(X)
pi=3.141592654
a=0.140012
ERF=(X/ABS(X))*SQRT(1.0-exp(-1.0*X**2*((4.0/pi+a*X**2)/
&(1.0+a*X**2) ) ) )
RETURN
END
```

```
REAL FUNCTION SAUTO(TIME, TIME1)
C   T=TIME-TIME1 -8.
   T=TIME-TIME1
C   IF (T.LT. 0.0E-5 ) THEN
C     IF (T.LT. 48. ) THEN
C       SA=0.0
C       GO TO 1
C     ENDIF
C     SAM=-370.0
C     SAM=-341.0
C     IF (T .LE. 24.0) THEN
C       SA = SAM*ALOG10(1.8)*T/48.0
C     ELSEIF (T .GT. 24.0) THEN
C       SA=0.5*SAM*ALOG10(0.075*T)
C     ELSE
C       WRITE(*,*) ' ERROR in function SAUTO, TIME-TIME1=', T
C       STOP
C     ENDIF
1 CONTINUE
SAUTO=SA
RETURN
END
```

```
REAL FUNCTION SDRY(TIME, TIME2)
T=TIME-TIME2
IF (T .LT. 24.0) THEN
  SD=0.0
ELSE
  SDM=-201.0
  SD=0.4*SDM*ALOG10(0.55*(T-24.))
ENDIF
SDRY=SD
RETURN
END
```

## Appendix 4-5 Incremental time history residual stress analysis with creep

```

C      Subroutine to read the layer temperatures from TEMPS.LYR
C      and update the CBRAN input file IO85 with
C      the incremental temperatures of the layers for incremental
C      thermal stress analysis.
C      units are degrees F
C23456789*123456789*123456789*123456789*123456789*123456789*123456789*12
C
      SUBROUTINE INCTET(TEMPL, TEMPL1, TIME, TIMNXT, TIME1, TIME2,
& SIG11, EPSINI, N_LAYER, HS, TD, BD, DTHICK)
C      IMPLICIT DOUBLE PRECISION (A-H,O-Z)
      CHARACTER*80 BUF
      DIMENSION DESH(26)
      DIMENSION TEMPL(N_LAYER), TEMPL1(N_LAYER), SIG11(N_LAYER),
& EPSINI(N_LAYER)
Cdebug      WRITE (*,*)' N_LAYER=', N_LAYER
Cdebug      WRITE (*,*)' TIME=', TIME,' TIMNXT=',TIMNXT
      NLYR26=26
C      CTE=0.55E-5 read from databk
      IO98=98
      OPEN (UNIT=IO98,STATUS='OLD',ACCESS='DIRECT',FORM='FORMATTED',RECL
1=82,FILE='databk')
      READ (IO98,'(A80)', REC=511) BUF
      READ (BUF(24:33),'(E10.3)') CTE
      CLOSE (IO98)
      write (*,*)' inctet: CTE=',CTE
      TMPBTM=70.0
      iunit1=81
      io85=85
      io95=95
      OPEN (iunit1,FILE='TEMPRTRS.LYR',status='OLD')
      OPEN (io85,FILE='FOR085.DAT', status='OLD')
      OPEN (io95,FILE='FOR095.DAT', status='UNKNOWN')
      rewind iunit1
      rewind io85
      rewind io95
C read the temperature data for the TIME indicated and the subsequent time
1 READ (iunit1,'(A80)') BUF
  IF (BUF(1:14).EQ.'ELAPSED TIME =')THEN
    READ (BUF(15:24),'(E10.3)') EXTIME
    IF (ABS(EXTIME-TIME) .LT. 0.10E-4) THEN
      READ(iunit1,'(8E10.3)') (TEMPL(I),I=1,N_LAYER)
      READ(iunit1,'(14X,E10.3)') TIMNXT
      READ(iunit1,'(8E10.3)') (TEMPL1(I),I=1,N_LAYER)
      GO TO 11
    ENDIF
  ENDIF
  GO TO 1
11 CONTINUE
  CALL DSHEPS(DESH, TIME, TIMNXT, TIME1, TIME2, NLYR26,
& HS,TD,BD,DTHICK)
2 READ (io85,'(A80)') BUF
  WRITE (io95,'(A80)') BUF
  IF (BUF(1:4).EQ.'ICAN')GO TO 3
  GO TO 2

3 READ (io85,'(A80)') BUF
  READ (BUF(9:32),'(3I8)') NLAM, NLYR, NMAT
  WRITE (io95,'(A80)') BUF

```

```

      IF (NLAM .EQ. 1) THEN
Cdelete      IF (NLYR .NE. NLYR) THEN
Cdelete      WRITE (*,*) ' ERROR IN INCTET STOP'
Cdelete      STOP 100
Cdelete      ENDIF
      DO i=1, NLYR
        READ (io85,'(A80)') BUF
        READ (BUF(9:16),'(I8)') iread
        IF (iread .ne. i) THEN
          WRITE(*,*) ' ERROR in INCTET I=', I, ' IREAD=', iread
          STOP 111
        ENDIF
        READ (BUF(17:24),'(I8)') iread
        IF (iread .eq. 1) THEN
          DCREPS=DEPSCR(TIME, TIME1, TIMNXT, TIME2, SIG11(I))
          WRITE (BUF(25:31),'(F7.2)')TEMPL1(I)+
&              (1.0E-6*DESH(I)+DCREPS/1000.)/CTE

          WRITE (BUF(32:38),'(F7.1)')TEMPL(I)
        ELSE
          WRITE (BUF(25:31),'(F7.2)')TEMPL1(I)
          WRITE (BUF(32:38),'(F7.1)')TEMPL(I)
        ENDIF
        WRITE (io95,'(A80)') BUF
        DEPSI=CTE*(TEMPL1(I)-TEMPL(I))
        EPSINI(I)=EPSINI(I)+DEPSI

      ENDDO
      DO i=1, NMAT
        READ (io85,'(A80)') BUF
        WRITE (io95,'(A80)') BUF
      ENDDO
      GO TO 3
    ELSEIF (NLAM .EQ. 2) THEN
      IF (NLYR .NE. NLYR) THEN
&      WRITE (*,*) ' NLYR=', NLYR, ' NLYR=', NLYR,
        ' ERROR IN INCTET STOP'
&      STOP 100
      ENDIF
      DO i=1, NLYR
        READ (io85,'(A80)') BUF
        READ (BUF(9:16),'(I8)') iread
        IF (iread .ne. i) THEN
          WRITE(*,*) ' ERROR in INCTET I=', I, ' IREAD=', iread
          STOP 112
        ENDIF
        READ (BUF(17:28),'(I8)') iread
        IF (iread .eq. 1 .AND. I.LE.24) THEN
          DCREPS=DEPSCR(TIME, TIME1, TIMNXT, TIME2, SIG11(I))
          WRITE (BUF(25:31),'(F7.2)')TEMPL1(I)+
&              (0.1E-6*DESH(I)+DCREPS/1000.)/CTE

          WRITE (BUF(32:38),'(F7.1)')TEMPL(I)
        ELSEIF (I.LE. NLYR) THEN
          WRITE (BUF(25:31),'(F7.2)')TEMPL1(I)
          WRITE (BUF(32:38),'(F7.1)')TEMPL(I)
        ELSE
          WRITE(*,*) ' ERROR in INCTET I=', I
          STOP 114
        ENDIF
        WRITE (io95,'(A80)') BUF
      ENDDO
      DO i=1, NMAT

```

```

        READ (io85,'(A80)') BUF
        WRITE (io95,'(A80)') BUF
    ENDDO
ELSE
    WRITE(*,*)' ERROR in INCTET I=', I,' IREAD=', iread
    STOP 115
ENDIF

READ (io85,'(A80)') BUF
IF (BUF(1:4) .NE. 'ENDN' .AND. BUF(1:4) .NE. 'LTP') THEN
    WRITE(*,*)' ERROR in INCTET, expected ENDN but read',BUF
    STOP 117
ENDIF
WRITE (io95,'(A80)') BUF

4  READ (io85,'(A80)',END=5) BUF
   WRITE (io95,'(A80)') BUF
   GO TO 4
5  REWIND (IO85)
   REWIND (IO95)
6  READ (io95,'(A80)',END=7) BUF
   WRITE (io85,'(A80)') BUF
   GO TO 6
7  CONTINUE
   RETURN
END

```

```

REAL FUNCTION DEPSCR(TIME,TIME1,TIMNXT,TIME2,SIGMA)
C  Function to compute the creep coefficient and creep strain increment
C  E=57000.0*SQRT(6000.0)
E=ETIME(TIME,TIME1)
PI=3.141592654
DT=TIMNXT-TIME
T=TIME+0.5*DT
C  If the wetted burlap is present then
IF (TIME .LT. TIME1) THEN
    B=1.7
    AKT0= 1000.
ELSEIF (TIME .LT. TIME1+8.)THEN
    B=1.7
    AKT0=100.
ELSEIF (TIME/24.0 .LT. 0.9256) THEN
    B=1.7
    AKT0= 4.1
ELSEIF (TIME/24.0.LT.9.17) THEN
    B=1.7
    AKT0=PI*PI*0.271867/(T/24)**2+0.96809265
ELSEIF (TIME.LT.TIME2) THEN
    B=1.7
    AKT0=PI*PI*3.5542/(T/24)**2+0.582841
ELSE
    B=11.0
    AKT0=4.1-(2.4/70)*(T/24)+0.000142857*(T/24)**2
ENDIF
DEPSCR=AKT0*(SIGMA/E)*SQRT(DT/24.0)/(B+SQRT(DT/24.0))
RETURN
END

```

## **Appendix 4-6 WPSMHH preprocessor to write OMHOST plane strain local analysis input file to compute crack width and spacing**

```

C      Program WPSMHH(DC) to write a plane strain finite element input file to
C      determine crack width and crack spacing. Units are in inches.
C23456789*123456789*123456789*123456789*123456789*123456789*123456789*12
C      DC= depth of crack (in.)
C      AL= length of model (in.)
C      EPS= strain of rebar at bottom of model
C      ELNGTH= element length
C      EHGH= element height
C      NV= number of elements vertically
C      NL= number of elements along length
C      RBRSTR= rebar strain (or strain at bottom of deck)
C      SUBROUTINE WPSMHH(DC)
C      CHARACTER*80 BUF
C      DIMENSION TEMPL(NLAYER), TEMPL1(NLAYER)

C      DC=13.
C      DC=9.5
C      DC=7.35
C      NV=20
C      EHGH=DC/NV
C      NL=20
C      AL=100.0
C      ELNGTH=AL/NL
C      NELEM=NV*NL
C      NNODES=(NV+1)*(NL+1)
C      NBOUN=2.0*(NL+1)+NV
C      EC=4.46E+6
C      POISSON=0.2
C      ALPHA=0.55E-05
C      RHO=0.08681
C      SIG24=195.2
C      SIG24=130.3
C      RBRSTR=SIG24/(57000.*SQRT(6000.))
C      RBRSTR=0.010857763
C RBRSTR is the strain at the bottom of deck
C obtained by dividing the stress in layer 24
C by 57000*SQRT(6000)
C      RBRSTR=0.000019983
C      io55=55
C      OPEN (io55,FILE='crack.dat', status='UNKNOWN')
C      rewind io55
C write MHOST input file
C      WRITE (BUF(1:5),>('MHOST'))
C      WRITE (Io55,'(A80)')BUF
C      WRITE (Io55,
C      &(' PLANE STRAIN CRACK WIDTH AND SPACING SIMULATION'))
C      WRITE (Io55,('ELEMENT',I12)) NELEM
C      WRITE (Io55,(' 11'))
C      WRITE (Io55,('NODES',I10)) NNODES
C      WRITE (Io55,('LOUB 3 1 3'))
C      WRITE (Io55,('BOUNDARYCONDITIONS',I5)) NBOUN
C      WRITE (Io55,('CONSTITUTIVE 0'))
C      WRITE (Io55,('DISPL'))
C      WRITE (Io55,('END'))
C      WRITE (Io55,('INCR'))
C      WRITE (Io55,('0'))
C      WRITE (Io55,('ITERATION'))
C      WRITE

```

```

      &(Io55, '(' 2 0.05 0.05 0.05 0.05'))
C23456789*123456789*123456789*123456789*123456789*123456789*123456789*12
WRITE (Io55, ('*PROPERTIES 11'))
C DO 100 I=1, NNODES
WRITE (Io55, '(I5,I6,5E12.5)') 1, NNODES, 1.0, EC, POISSON, ALPHA, RHO
C WRITE (Io55, '(10X,E13.5)') RHO
C 100 CONTINUE
C write the input nodal coordinates
WRITE (Io55, ('*COORD'))
INODE=0
XCOOR=-ELNGTH

DO 1 INL=1, NL+1
XCOOR=XCOOR+ELNGTH
YCOOR=-EHGHT
DO 2 INV=1, NV+1
INODE=INODE+1
YCOOR=YCOOR+EHGHT
WRITE (Io55, '(I8,2F17.8)') INODE, XCOOR, YCOOR
2 CONTINUE
1 CONTINUE
C write the element connectivities
WRITE (Io55, ('*ELEM 11'))
IELEM=0
N1=0
DO 3 INL=1, NL
DO 4 INV=1, NV
IELEM=IELEM+1
N1=N1+1
N2=N1+(NV+1)
N3=N2+1
N4=N1+1
WRITE (Io55, '(I8,4I9)') IELEM, N1, N2, N3, N4
4 CONTINUE
N1=N1+1
3 CONTINUE
C write the boundary conditions
WRITE (Io55, ('*BOUNDARYCONDITIONS'))
INBOUN=1
WRITE (Io55, '(2I9)') INBOUN, 1
WRITE (Io55, '(2I9)') INBOUN, 2
DO 5 I=3, NBOUN-NV, 2
INBOUN=INBOUN+NV+1
DISPL=RBRSTR*(I-1)*ELNGTH
WRITE (Io55, '(2I9, E13.5)') INBOUN, 1, DISPL
WRITE (Io55, '(2I9, E13.5)') INBOUN, 2, 0.0
5 CONTINUE
C WRITE DISPLACEMENTS OF NODES ON A VERTICAL LINE AT DISTANCE AL
Considered as constant, an approximation
DO 6 I=NBOUN-NV+1, NBOUN
INBOUN=INBOUN+1
WRITE (Io55, '(2I9, E13.5)') INBOUN, 1, DISPL
6 CONTINUE
C write the printout commands
WRITE (Io55, ('*PRINT'))
WRITE (Io55, (' TOTALDISPLACEM'))
WRITE (Io55, (' STRESS'))
WRITE (Io55, (' STRAIN'))
WRITE (Io55, ('*END'))
WRITE (Io55, ('*STOP'))

C RETURN
END

```



0.804E+02 0.805E+02 0.805E+02 0.805E+02 0.805E+02 0.806E+02 0.806E+02 0.807E+02  
 0.804E+02 0.760E+02  
 ELAPSED TIME = 0.110E+02  
 0.703E+02 0.711E+02 0.718E+02 0.724E+02 0.731E+02 0.740E+02 0.753E+02 0.772E+02  
 0.791E+02 0.806E+02 0.817E+02 0.824E+02 0.826E+02 0.828E+02 0.832E+02 0.833E+02  
 0.835E+02 0.841E+02 0.846E+02 0.851E+02 0.853E+02 0.855E+02 0.856E+02 0.856E+02  
 0.857E+02 0.857E+02 0.857E+02 0.857E+02 0.858E+02 0.859E+02 0.860E+02 0.860E+02  
 0.854E+02 0.791E+02  
 ELAPSED TIME = 0.120E+02  
 0.705E+02 0.715E+02 0.724E+02 0.733E+02 0.741E+02 0.753E+02 0.771E+02 0.796E+02  
 0.821E+02 0.841E+02 0.857E+02 0.865E+02 0.868E+02 0.871E+02 0.876E+02 0.878E+02  
 0.880E+02 0.887E+02 0.894E+02 0.900E+02 0.904E+02 0.907E+02 0.908E+02 0.908E+02  
 0.908E+02 0.910E+02 0.910E+02 0.910E+02 0.911E+02 0.912E+02 0.913E+02 0.913E+02  
 0.906E+02 0.821E+02  
 ELAPSED TIME = 0.130E+02  
 0.706E+02 0.718E+02 0.730E+02 0.742E+02 0.752E+02 0.767E+02 0.789E+02 0.820E+02  
 0.851E+02 0.876E+02 0.896E+02 0.907E+02 0.911E+02 0.914E+02 0.920E+02 0.922E+02  
 0.925E+02 0.933E+02 0.943E+02 0.950E+02 0.955E+02 0.958E+02 0.960E+02 0.960E+02  
 0.961E+02 0.962E+02 0.962E+02 0.963E+02 0.963E+02 0.964E+02 0.965E+02 0.967E+02  
 0.958E+02 0.852E+02  
 ELAPSED TIME = 0.140E+02  
 0.708E+02 0.722E+02 0.736E+02 0.749E+02 0.762E+02 0.779E+02 0.807E+02 0.843E+02  
 0.882E+02 0.911E+02 0.935E+02 0.949E+02 0.953E+02 0.957E+02 0.963E+02 0.967E+02  
 0.970E+02 0.980E+02 0.992E+02 0.998E+02 0.101E+03 0.101E+03 0.101E+03 0.101E+03  
 0.101E+03 0.101E+03 0.101E+03 0.101E+03 0.102E+03 0.102E+03 0.102E+03 0.102E+03  
 0.101E+03 0.882E+02  
 ELAPSED TIME = 0.150E+02  
 0.708E+02 0.726E+02 0.742E+02 0.758E+02 0.772E+02 0.793E+02 0.825E+02 0.867E+02  
 0.912E+02 0.946E+02 0.974E+02 0.990E+02 0.995E+02 0.997E+02 0.101E+03 0.101E+03  
 0.102E+03 0.103E+03 0.104E+03 0.105E+03 0.106E+03 0.106E+03 0.106E+03 0.106E+03  
 0.106E+03 0.107E+03 0.107E+03 0.107E+03 0.107E+03 0.107E+03 0.107E+03 0.107E+03  
 0.106E+03 0.913E+02  
 ELAPSED TIME = 0.160E+02  
 0.710E+02 0.729E+02 0.748E+02 0.766E+02 0.783E+02 0.807E+02 0.843E+02 0.892E+02  
 0.942E+02 0.982E+02 0.101E+03 0.103E+03 0.104E+03 0.104E+03 0.106E+03 0.106E+03  
 0.106E+03 0.107E+03 0.109E+03 0.110E+03 0.111E+03 0.111E+03 0.112E+03 0.112E+03  
 0.112E+03 0.112E+03 0.112E+03 0.112E+03 0.112E+03 0.112E+03 0.113E+03 0.113E+03  
 0.111E+03 0.943E+02  
 ELAPSED TIME = 0.170E+02  
 0.708E+02 0.724E+02 0.740E+02 0.754E+02 0.768E+02 0.788E+02 0.818E+02 0.858E+02  
 0.899E+02 0.932E+02 0.958E+02 0.974E+02 0.978E+02 0.982E+02 0.991E+02 0.994E+02  
 0.997E+02 0.101E+03 0.102E+03 0.103E+03 0.104E+03 0.104E+03 0.104E+03 0.104E+03  
 0.104E+03 0.105E+03 0.105E+03 0.105E+03 0.105E+03 0.105E+03 0.105E+03 0.105E+03  
 0.104E+03 0.900E+02  
 ELAPSED TIME = 0.180E+02  
 0.707E+02 0.721E+02 0.733E+02 0.746E+02 0.758E+02 0.774E+02 0.799E+02 0.832E+02  
 0.868E+02 0.896E+02 0.918E+02 0.931E+02 0.934E+02 0.938E+02 0.944E+02 0.947E+02  
 0.950E+02 0.959E+02 0.971E+02 0.979E+02 0.984E+02 0.988E+02 0.989E+02 0.989E+02  
 0.989E+02 0.990E+02 0.991E+02 0.992E+02 0.993E+02 0.995E+02 0.996E+02 0.996E+02  
 0.986E+02 0.868E+02  
 ELAPSED TIME = 0.190E+02  
 0.706E+02 0.717E+02 0.728E+02 0.739E+02 0.749E+02 0.763E+02 0.784E+02 0.813E+02  
 0.843E+02 0.867E+02 0.885E+02 0.896E+02 0.899E+02 0.902E+02 0.908E+02 0.911E+02  
 0.913E+02 0.921E+02 0.931E+02 0.937E+02 0.942E+02 0.945E+02 0.946E+02 0.947E+02  
 0.947E+02 0.947E+02 0.948E+02 0.948E+02 0.950E+02 0.950E+02 0.952E+02 0.952E+02  
 0.944E+02 0.843E+02  
 ELAPSED TIME = 0.200E+02  
 0.705E+02 0.715E+02 0.725E+02 0.733E+02 0.742E+02 0.754E+02 0.772E+02 0.797E+02  
 0.823E+02 0.844E+02 0.859E+02 0.869E+02 0.872E+02 0.875E+02 0.879E+02 0.882E+02  
 0.884E+02 0.890E+02 0.898E+02 0.904E+02 0.908E+02 0.911E+02 0.913E+02 0.913E+02  
 0.913E+02 0.913E+02 0.914E+02 0.914E+02 0.915E+02 0.917E+02 0.917E+02 0.918E+02  
 0.911E+02 0.823E+02  
 ELAPSED TIME = 0.210E+02

0.704E+02 0.713E+02 0.721E+02 0.729E+02 0.737E+02 0.747E+02 0.763E+02 0.785E+02  
 0.807E+02 0.825E+02 0.839E+02 0.847E+02 0.850E+02 0.852E+02 0.856E+02 0.858E+02  
 0.860E+02 0.866E+02 0.873E+02 0.878E+02 0.882E+02 0.884E+02 0.885E+02 0.885E+02  
 0.886E+02 0.886E+02 0.886E+02 0.887E+02 0.888E+02 0.888E+02 0.889E+02 0.889E+02  
 0.883E+02 0.807E+02  
 ELAPSED TIME = 0.220E+02  
 0.704E+02 0.712E+02 0.718E+02 0.726E+02 0.733E+02 0.742E+02 0.756E+02 0.775E+02  
 0.794E+02 0.810E+02 0.822E+02 0.829E+02 0.832E+02 0.834E+02 0.838E+02 0.839E+02  
 0.841E+02 0.846E+02 0.853E+02 0.857E+02 0.859E+02 0.862E+02 0.863E+02 0.863E+02  
 0.863E+02 0.863E+02 0.864E+02 0.864E+02 0.864E+02 0.865E+02 0.866E+02 0.867E+02  
 0.861E+02 0.794E+02  
 ELAPSED TIME = 0.230E+02  
 0.703E+02 0.710E+02 0.717E+02 0.723E+02 0.728E+02 0.737E+02 0.749E+02 0.766E+02  
 0.783E+02 0.797E+02 0.808E+02 0.815E+02 0.817E+02 0.818E+02 0.821E+02 0.823E+02  
 0.824E+02 0.829E+02 0.835E+02 0.838E+02 0.842E+02 0.843E+02 0.844E+02 0.844E+02  
 0.845E+02 0.845E+02 0.845E+02 0.846E+02 0.846E+02 0.846E+02 0.847E+02 0.847E+02  
 0.843E+02 0.784E+02  
 ELAPSED TIME = 0.240E+02  
 0.703E+02 0.709E+02 0.715E+02 0.721E+02 0.725E+02 0.733E+02 0.744E+02 0.759E+02  
 0.775E+02 0.787E+02 0.797E+02 0.803E+02 0.804E+02 0.806E+02 0.808E+02 0.810E+02  
 0.812E+02 0.815E+02 0.820E+02 0.823E+02 0.826E+02 0.828E+02 0.829E+02 0.829E+02  
 0.829E+02 0.829E+02 0.829E+02 0.829E+02 0.830E+02 0.831E+02 0.831E+02 0.832E+02  
 0.828E+02 0.774E+02  
 ELAPSED TIME = 0.250E+02  
 0.703E+02 0.708E+02 0.713E+02 0.718E+02 0.723E+02 0.729E+02 0.740E+02 0.753E+02  
 0.767E+02 0.778E+02 0.787E+02 0.792E+02 0.793E+02 0.794E+02 0.797E+02 0.799E+02  
 0.800E+02 0.804E+02 0.808E+02 0.811E+02 0.813E+02 0.814E+02 0.815E+02 0.815E+02  
 0.815E+02 0.816E+02 0.816E+02 0.817E+02 0.817E+02 0.818E+02 0.818E+02 0.818E+02  
 0.814E+02 0.767E+02  
 ELAPSED TIME = 0.260E+02  
 0.703E+02 0.708E+02 0.712E+02 0.717E+02 0.721E+02 0.727E+02 0.735E+02 0.748E+02  
 0.760E+02 0.771E+02 0.778E+02 0.783E+02 0.784E+02 0.786E+02 0.788E+02 0.789E+02  
 0.790E+02 0.793E+02 0.797E+02 0.800E+02 0.802E+02 0.804E+02 0.804E+02 0.804E+02  
 0.804E+02 0.805E+02 0.805E+02 0.805E+02 0.805E+02 0.806E+02 0.806E+02 0.807E+02  
 0.804E+02 0.760E+02  
 ELAPSED TIME = 0.270E+02  
 0.703E+02 0.707E+02 0.711E+02 0.715E+02 0.719E+02 0.724E+02 0.733E+02 0.743E+02  
 0.755E+02 0.764E+02 0.771E+02 0.775E+02 0.776E+02 0.778E+02 0.780E+02 0.781E+02  
 0.782E+02 0.785E+02 0.788E+02 0.791E+02 0.792E+02 0.793E+02 0.794E+02 0.794E+02  
 0.795E+02 0.795E+02 0.795E+02 0.795E+02 0.796E+02 0.796E+02 0.797E+02 0.797E+02  
 0.793E+02 0.754E+02  
 ELAPSED TIME = 0.280E+02  
 0.702E+02 0.706E+02 0.710E+02 0.713E+02 0.717E+02 0.722E+02 0.729E+02 0.740E+02  
 0.750E+02 0.758E+02 0.765E+02 0.768E+02 0.770E+02 0.771E+02 0.773E+02 0.774E+02  
 0.775E+02 0.777E+02 0.781E+02 0.783E+02 0.785E+02 0.785E+02 0.786E+02 0.786E+02  
 0.786E+02 0.787E+02 0.787E+02 0.787E+02 0.787E+02 0.788E+02 0.788E+02 0.788E+02  
 0.785E+02 0.750E+02  
 ELAPSED TIME = 0.290E+02  
 0.702E+02 0.706E+02 0.709E+02 0.713E+02 0.716E+02 0.720E+02 0.727E+02 0.737E+02  
 0.746E+02 0.753E+02 0.760E+02 0.763E+02 0.764E+02 0.765E+02 0.767E+02 0.767E+02  
 0.768E+02 0.771E+02 0.773E+02 0.776E+02 0.778E+02 0.778E+02 0.779E+02 0.779E+02  
 0.779E+02 0.779E+02 0.779E+02 0.779E+02 0.780E+02 0.780E+02 0.780E+02 0.781E+02  
 0.778E+02 0.746E+02  
 ELAPSED TIME = 0.300E+02  
 0.702E+02 0.705E+02 0.708E+02 0.712E+02 0.714E+02 0.718E+02 0.724E+02 0.733E+02  
 0.742E+02 0.749E+02 0.754E+02 0.758E+02 0.758E+02 0.760E+02 0.761E+02 0.762E+02  
 0.763E+02 0.764E+02 0.767E+02 0.770E+02 0.771E+02 0.772E+02 0.772E+02 0.772E+02  
 0.772E+02 0.773E+02 0.773E+02 0.773E+02 0.773E+02 0.773E+02 0.774E+02 0.774E+02  
 0.772E+02 0.742E+02  
 ELAPSED TIME = 0.310E+02  
 0.702E+02 0.704E+02 0.708E+02 0.711E+02 0.713E+02 0.717E+02 0.722E+02 0.730E+02  
 0.738E+02 0.745E+02 0.750E+02 0.753E+02 0.754E+02 0.755E+02 0.757E+02 0.757E+02  
 0.758E+02 0.759E+02 0.762E+02 0.764E+02 0.765E+02 0.767E+02 0.767E+02 0.767E+02





0.700E+02 0.700E+02 0.700E+02 0.700E+02 0.700E+02 0.700E+02 0.700E+02 0.700E+02  
0.700E+02 0.700E+02  
ELAPSED TIME = 0.720E+03  
0.700E+02 0.700E+02 0.700E+02 0.700E+02 0.700E+02 0.700E+02 0.700E+02 0.700E+02  
0.700E+02 0.700E+02

## Appendix 7-1a preprocessor to generate CBRAN input file for laboratory test specimen

```

C   program to write input file for structural analysis of test
c
    implicit real (a-h,o-z)
c
    character*80 buf
c    dimension islave(135)
    dimension x(16),y(15),t(3), TPLY(34), ISLAVE(58), MASTER(58)
C   spacing of x coordinates changed for testing machine loading
    data x / 0.0, 2.0, 4.0, 8.0, 12., 18., 24., 36., 48., 60., 72.,
    & 72., 84., 96., 108., 120. /
    data y / 0.0, 3.250625, 6.50125, 9.751875, 13.0025, 13.0025,
    & 15.50125, 18., 20.49875,
    & 22.9975, 22.9975, 26.248125, 29.49875, 32.749375, 36. /
    data t / 9.5, 26.89, 13.89 /
    data TPLY / 0.1, 0.1, 0.1, 0.1, 0.1, 0.2, 0.3, 0.5, 0.5, 0.5,0.5,
    & 0.5, 0.5, 0.62, 0.62,0.62,0.62,0.62,0.5, 0.5, 0.35, 0.35, 0.35,
    & 0.35,
    & 1.75, 1.75, 0.3225,0.3225, 3.15, 3.15, 3.15, 3.15, 0.3225,0.3225/
c23456789*123456789*123456789*123456789*123456789*123456789*123456789*12
    open (12, file = 'test_m_t.dat',status='UNKNOWN')

C   nx1=# of nodes where deck is present
    nx1=11
    nx=16
    nx2=nx-nx1
C   ny1=# of nodes where girder is present
    ny1=5
    ny=15
    ny2=ny-ny1
c    open (11, file = 'MtrxSym.txt',
c    & status='OLD')

c    READ (11,'(a)') buf
c    READ (11,*) NNODES, NELEMS, NDUPL

C    nnodes = (nx+(nx-1))*ny
    nnodes = (nx1+(nx1-1))*ny + 2*nx2*ny1

C    nelems=(nx-1)*2*(ny-3)
    nelems=(nx1-1)*2*(ny-3) + (nx2-1)*2*(ny1-1)
c    ndupl=(nx+nx-1)*2
    ndupl=(nx1+nx1-1)*2 + 2*ny1

c   write the top of file
    write (buf,'(4L6,F5.2,1x,3L6,5i6)').FALSE.,.TRUE.,.FALSE.,
    & .FALSE., 0.5, .FALSE., .FALSE., .FALSE., 0, 1, 2, 1, 1
    write (12,'(a80)') buf
    write (buf,'(A10,6i6,5L6)') 'PRESCRIBED', 0,1,1,1,1,183,
    & .FALSE.,.TRUE.,.FALSE., .FALSE., .FALSE.
    write (12,'(a80)') buf
    write (buf,'(A10,i6,F10.4,i6,2L6,i6,5L6)') 'CRITICALSE',0,0.72,3,
    & .FALSE., .FALSE., 0, .FALSE.,.FALSE.,.FALSE., .FALSE., .FALSE.
    write (12,'(a80)') buf
    write (buf,'(10i8)') 8,3,8,3,8,3,8,3,8,3
    write (12,'(a80)') buf
    write (buf,'(A4)') 'ICAN'
    write (12,'(a80)') buf
    write (buf,'(A4,4x,3i8)') 'LTYP', 1, 24, 3

```

```

write (12,'(a80)') buf
do i=1,24
  if (i .eq. 13 .or. i .eq. 20) then
    angle=90.0
  else
    angle=0.0
  endif
  if (i .eq. 12 .or. i .eq. 19) then
    mtrl=2
  elseif(i .eq. 13 .or. i .eq. 20) then
    mtrl=3
  else
    mtrl=1
  endif
  write (buf,'(A8,2i8,f7.2,f7.1,f8.1,f9.0,f6.3)') '      PLY',i,
& mtrl, 70.,70.,0.0, ANGLE, TPLY(I)
  write (12,'(a80)') buf
enddo
c23456789*123456789*123456789*123456789*123456789*123456789*123456789*12

```

```

  write (buf,'(A8,i8,A8,2x,f6.5, 2x,f3.2,3x, A8, f5.1,5x,f3.2,5x,
& f3.2)')
& ' MATCRD', 1, 'CNCFCNC', 0.3, 0.01,'CNCFCNC', 0.0, 0.6, 0.03
  write (12,'(a80)') buf
  write (buf,'(A8,i8,A8,2x,f6.5, 2x,f3.2,3x, A8, f5.1,5x,f3.2,5x,
& f3.2)')
& ' MATCRD',
& 2, 'RBSFCNC', 0.05, 0.01,'CNCFCNC', 0.0, 0.6, 0.03
  write (12,'(a80)') buf
  write (buf,'(A8,i8,A8,2x,f6.5, 2x,f3.2,3x, A8, f5.1,5x,f3.2,5x,
& f3.2)')
& ' MATCRD',
& 3, 'RBSFCNC', 0.05, 0.01,'CNCFCNC', 0.0, 0.6, 0.03
  write (12,'(a80)') buf

```

```

  write (buf,'(A4,4x,3i8)') 'LTYP', 2, 34, 5
  write (12,'(a80)') buf
  do i=1,34
    if (i .eq. 13 .or. i .eq. 20) then
      angle=90.0
    else
      angle=0.0
    endif
    if (i .eq. 12 .or. i .eq. 19) then
      mtrl=2
    elseif(i .eq. 13 .or. i .eq. 20) then
      mtrl=3
    elseif(i.eq. 27 .or. i.eq.28.or. i .eq. 33.or. i .eq. 34) then
      mtrl=4
    elseif(i.eq. 29 .or. i.eq.30.or. i .eq. 31.or. i .eq. 32) then
      mtrl=5
    else
      mtrl=1
    endif
    write (buf,'(A8,2i8,f7.2,f7.1,f8.1,f9.0,f6.3)') '      PLY',i,
& mtrl, 70.,70.,0.0, ANGLE, TPLY(I)
    write (12,'(a80)') buf
  enddo
  write (buf,'(A8,i8,A8,2x,f6.5, 2x,f3.2,3x, A8, f5.1,5x,f3.2,5x,
& f3.2)')
& ' MATCRD',
& 1, 'CNCFCNC', 0.3, 0.01,'CNCFCNC', 0.0, 0.6, 0.03
  write (12,'(a80)') buf

```

```

write (buf,'(A8,i8,A8,2x,f6.5, 2x,f3.2,3x, A8, f5.1,5x,f3.2,5x,
& f3.2)')
& ' MATCRD',
& 2, 'RBSFCONC', 0.05, 0.01,'CNCFCONC', 0.0, 0.6, 0.03
write (12,'(a80)') buf
write (buf,'(A8,i8,A8,2x,f6.5, 2x,f3.2,3x, A8, f5.1,5x,f3.2,5x,
& f3.2)')
& ' MATCRD',
& 3, 'RBSFCONC', 0.05, 0.01,'CNCFCONC', 0.0, 0.6, 0.03
write (12,'(a80)') buf
write (buf,'(A8,i8,A8,2x,f6.5, 2x,f3.2,3x, A8, f5.1,5x,f3.2,5x,
& f3.2)')
& ' MATCRD',
& 4, 'GRSFGRDS', 0.3, 0.0,'GRSFGRDS', 0.0, 0.02, 0.03
write (12,'(a80)') buf
write (buf,'(A8,i8,A8,2x,f6.5, 2x,f3.2,3x, A8, f5.1,5x,f3.2,5x,
& f3.2)')
& ' MATCRD',
& 5, 'WBSFWBSM', 0.3, 0.0,'WBSFWBSM', 0.0, 0.02, 0.03
write (12,'(a80)') buf

C
write (buf,'(A4,4x,3i8)') 'LTPY', 3, 8, 2
write (12,'(a80)') buf
do i=27,34

if(i.eq. 27 .or. i.eq.28.or. i .eq. 33.or. i .eq. 34) then
mtrl=1
elseif(i.eq. 29 .or. i.eq.30.or. i .eq. 31.or. i .eq. 32) then
mtrl=2
endif
write (buf,'(A8,2i8,f7.2,f7.1,f8.1,f9.0,f6.3)') ' PLY',
& i-26, mtrl, 70.,70.,0.0, ANGLE, TPLY(I)
write (12,'(a80)') buf

enddo

write (buf,'(A8,i8,A8,2x,f6.5, 2x,f3.2,3x, A8, f5.1,5x,f3.2,5x,
& f3.2)')
& ' MATCRD',
& 1, 'GRSFGRDS', 0.3, 0.0,'GRSFGRDS', 0.0, 0.02, 0.03
write (12,'(a80)') buf
write (buf,'(A8,i8,A8,2x,f6.5, 2x,f3.2,3x, A8, f5.1,5x,f3.2,5x,
& f3.2)')
& ' MATCRD',
& 2, 'WBSFWBSM', 0.3, 0.0,'WBSFWBSM', 0.0, 0.02, 0.03
write (12,'(a80)') buf

write (buf,'(A4)') 'ENDN'
write (12,'(a80)') buf
write (buf,'(A5)') 'MHOST'
write (12,'(a80)') buf
write (buf,'(A36)') ' A TEST OF COMPOSITE DECK SIMULATION'
write (12,'(a80)') buf
write (buf,'(A8,i12)') '*ELEMENT', NELEMS
write (12,'(a80)') buf
write (buf,'(i5)') 75
write (12,'(a80)') buf
write (buf,'(A10)') '*COMPOSITE'
write (12,'(a80)') buf
write (buf,'(A6,i10)') '*NODES', nnodes
write (12,'(a80)') buf
write (buf,'(A11)') '*LOUB 3 1 3'
write (12,'(a80)') buf

```



```

        ISLAVE (NDUPL) = inod
        MASTER (NDUPL) = inod+1
    ELSEIF (J.EQ. 10) THEN
        NDUPL = NDUPL+1
        ISLAVE (NDUPL) =inod+1
        MASTER (NDUPL) = inod
    ENDIF
2    CONTINUE
    ELSEIF (abs(i) .gt. nx1) then
        DO 21 j=6,10
            YCOOR = Y(j)
            THCK= t(3)
            LTYP=3
            Z=-0.5*t(3)-t(2)
            INOD=INOD+1
            WRITE (12,'(i8,4F17.8,i4)') INOD,XCOOR,YCOOR,Z,THCK,LTYP
            IF (i.eq. nx1+1) then
                ndupl=ndupl+1
                master(ndupl)=inod
                islave (NDUPL) = inod-11
            elseif (i.eq. -nx1-1)then
                ndupl=ndupl+1
                master(ndupl)=inod
                islave (NDUPL) = inod+9
            endif
21    CONTINUE
        ELSE
            stop 222
        ENDIF
1    CONTINUE
    write (*,*) ' nnodes=',inod, ' ndupl=', ndupl, ' ntying=',6*ndupl

    WRITE (12,(' '*ELEM 75'))
    IELEM=0
    DO 3 i= 1, (nx-1)+(nx-1)
C    nx1=11, nx2=5, ny1=5
        IF (I .LT. (nx2)) THEN
            do 42 j=1,ny1-1
                IELEM=IELEM+1
                NOD1=ny1*(i-1)+j+1
                NOD2=ny1*(i-1)+j
                NOD3=ny1*i+j
                NOD4=ny1*i+j+1
                WRITE (12,'(i8,4i9)') IELEM, NOD1,NOD2,NOD3,NOD4
42    continue
            ELSEIF (I .eq. nx2) then
                go to 3
            ELSEIF (I .gt. nx2 .and. I.lt. 2*(nx-1)-(nx2-1)) THEN
                DO 4 j=1, ny-1
                    IF (J .ne. 5 .and. j .ne. 10) THEN
                        IELEM=IELEM+1
                        NOD1=25+ny*(i-nx2-1)+j+1
                        NOD2=25+ny*(i-nx2-1)+j
                        NOD3=25+ny*(i-nx2)+j
                        NOD4=25+ny*(i-nx2)+j+1
                        WRITE (12,'(i8,4i9)') IELEM, NOD1,NOD2,NOD3,NOD4
                    ELSE
                        CONTINUE
                    ENDIF
4    CONTINUE
            ELSEIF (I.eq.2*(nx-1)-(nx2-1)) THEN
                go to 3

```

```

ELSEIF (I.GT. 2*(nx-1)-(nx2-1)) THEN
  do 44 j=1,ny1-1
    IELEM=IELEM+1
    NOD1=340+ny1*(i-nx2-2*nx1)+j+1
    NOD2=340+ny1*(i-nx2-2*nx1)+j
    NOD3=340+ny1*(i-nx2-2*nx1+1)+j
    NOD4=340+ny1*(i-nx2-2*nx1+1)+j+1
    WRITE (12,'(i8,4i9)') IELEM, NOD1,NOD2,NOD3,NOD4
44  continue
  ENDIF
3  CONTINUE
  WRITE (*,*) ' nelems=', ielem
  WRITE (12,(' '*LAMINATE'))
C   WRITE (12,(' '*DUPLICATENODE'))
  WRITE (12,(' '*TYING'))
C   CCOMB=distance to center of combined girder plus deck from center of deck

  DO 5 i=1, NDUPL
C   WRITE (12,'(2i8)') ISLAVE(i), MASTER(i)
    if (i.le. 5 .or. i .ge. ndupl-5) then
      CCOMB=0.5*(t(2)-t(3))
    else
      CCOMB=0.5*(t(2)-t(1))
    endif
    WRITE (12,'(8i8)') 3, islave(i), 1 ,master(i), 1, master(i), 5
    WRITE (12,'(2f10.5)') 1.0, CCOMB
    WRITE (12,'(8i8)') 3, islave(i), 2 ,master(i), 2, master(i), 4
    WRITE (12,'(2f10.5)') 1.0, -CCOMB
    WRITE (12,'(8i8)') 2, islave(i), 3 ,master(i), 3
    WRITE (12,'(2f10.5)') 1.0

    WRITE (12,'(8i8)') 2, islave(i), 4 ,master(i), 4
    WRITE (12,'(2f10.5)') 1.0
    WRITE (12,'(8i8)') 2, islave(i), 5 ,master(i), 5
    WRITE (12,'(2f10.5)') 1.0
    WRITE (12,'(8i8)') 2, islave(i), 6 ,master(i), 6
    WRITE (12,'(2f10.5)') 1.0

  5  CONTINUE
  WRITE (12,(' '*BOUNDARYCONDITIONS'))
  NBOUN=0
C  Write the first end boundary conditions
  DO 32 i=6, 10
    IF ( i .eq. 8) then
      NBOUN = NBOUN + 3
      WRITE (12,'(2i9)') i, 2
      WRITE (12,'(2i9)') i, 3
      WRITE (12,'(2i9)') i, 4
    ELSE
      NBOUN = NBOUN + 1
      WRITE (12,'(2i9)') i, 3
    ENDIF
  32 CONTINUE
  DO 33 i=181, 185
    IF ( i .eq. 183) then
      NBOUN = NBOUN + 4
      WRITE (12,'(2i9)') i, 1
      WRITE (12,'(2i9)') i, 2
      WRITE (12,'(2i9)') i, 3
      WRITE (12,'(2i9)') i, 4
    ELSE
      NBOUN = NBOUN + 1
      WRITE (12,'(2i9)') i, 3

```

```

        ENDIF
33 CONTINUE
    DO 34 i=361, 365
        IF ( i .eq. 363) then
            NBOUN = NBOUN + 2
            WRITE (12,'(2i9)') i, 2
            WRITE (12,'(2i9)') i, 4
        ELSE
            GO TO 34
        ENDIF
34 CONTINUE

        Write (*,*) ' nboun=', nboun
C Write the edge boundary conditions
c     DO 33 i=1, 450, 30
c     NBOUN=NBOUN+2
c     WRITE (12,'(2i9)') i, 4
c     WRITE (12,'(2i9)') i+14, 4
c 33 CONTINUE

C     WRITE (12,(' '*FORCE'))
C     FORCE = -5000.0
C     WRITE (12,'(2i8,f21.8)') 363, 3, force

WRITE (12,(' '*PRINT'))

WRITE (12,('' TOTALDISPLACEM'))
WRITE (12,('' STRESS'))
WRITE (12,('' STRAIN'))

WRITE (12,(' '*END'))

WRITE (12,(' '*STOP'))

write (*,*) ' NBOUN=', NBOUN

STOP

end

```

**Appendix 7-1b Residual stresses from FOR091.DAT file after 28 days for lab specimen**

TIME= 672.0 HOURS  
 NODE NUMBER= 183  
 PLY NO., SIG11, SIG22, SIG12  
 STRESSES ARE IN PSI UNITS; LAYER COORDINATES

1	0.1930E+03	0.1969E+03	0.8685E-07
2	0.2028E+03	0.2036E+03	0.8639E-07
3	0.2096E+03	0.2139E+03	0.8592E-07
4	0.2182E+03	0.2195E+03	0.8545E-07
5	0.2242E+03	0.2289E+03	0.8497E-07
6	0.2354E+03	0.2371E+03	0.8427E-07
7	0.2491E+03	0.2545E+03	0.8311E-07
8	0.2700E+03	0.2726E+03	0.8123E-07
9	0.2877E+03	0.2942E+03	0.7890E-07
10	0.3029E+03	0.3064E+03	0.7655E-07
11	0.3109E+03	0.3180E+03	0.7423E-07
12	0.1929E+03	0.2761E+03	0.7996E-07
13	0.1919E+03	0.2848E+03	-0.3062E-07
14	0.3207E+03	0.3247E+03	0.6692E-07
15	0.3170E+03	0.3243E+03	0.6404E-07
16	0.3161E+03	0.3200E+03	0.6113E-07
17	0.3102E+03	0.3174E+03	0.5823E-07
18	0.3072E+03	0.3110E+03	0.5534E-07
19	0.1768E+03	0.2735E+03	0.6666E-07
20	0.1707E+03	0.2688E+03	0.2530E-07
21	0.2894E+03	0.2960E+03	0.4841E-07
22	0.2870E+03	0.2903E+03	0.4675E-07
23	0.2820E+03	0.2884E+03	0.4512E-07
24	0.2782E+03	0.2812E+03	0.4347E-07
25	0.1547E+03	0.1578E+03	0.3856E-07
26	0.5745E+02	0.5467E+02	0.3040E-07
27	-0.1274E+04	-0.1300E+04	-0.7986E-06
28	-0.1291E+04	-0.1320E+04	-0.8934E-06
29	-0.5262E+02	-0.5362E+02	-0.5276E-07
30	-0.5998E+02	-0.6102E+02	-0.8769E-07
31	-0.6735E+02	-0.6844E+02	-0.1226E-06
32	-0.7472E+02	-0.7586E+02	-0.1575E-06
33	-0.2127E+04	-0.2158E+04	-0.4712E-05
34	-0.2120E+04	-0.2151E+04	-0.4808E-05

14000 lbs LOADING RESULTS after 672.000 HOURS = 28.0000 DAYS

TIME= 672.0 HOURS  
 NODE NUMBER= 183  
 PLY NO., SIG11, SIG22, SIG12  
 STRESSES ARE IN PSI UNITS; LAYER COORDINATES

1	0.6116E+03	0.1728E+03	-0.9968E+00
2	0.6168E+03	0.1796E+03	-0.9909E+00
3	0.6190E+03	0.1900E+03	-0.9850E+00
4	0.6230E+03	0.1957E+03	-0.9792E+00
5	0.6244E+03	0.2052E+03	-0.9733E+00
6	0.6287E+03	0.2136E+03	-0.9645E+00
7	0.6308E+03	0.2313E+03	-0.9498E+00
8	0.6333E+03	0.2497E+03	-0.9263E+00
9	0.6282E+03	0.2721E+03	-0.8970E+00
10	0.6204E+03	0.2848E+03	-0.8677E+00
11	0.6054E+03	0.2969E+03	-0.8383E+00
12	0.5907E+03	0.2496E+03	-0.8334E+00
13	0.1507E+03	0.5949E+03	0.8031E+00

14	0.5433E+03	0.3053E+03	-0.7468E+00
15	0.5111E+03	0.3056E+03	-0.7104E+00
16	0.4816E+03	0.3020E+03	-0.6740E+00
17	0.4472E+03	0.3000E+03	-0.6376E+00
18	0.4156E+03	0.2942E+03	-0.6012E+00
19	0.2962E+03	0.2512E+03	-0.5855E+00
20	0.1427E+03	0.3411E+03	0.5552E+00
21	0.3292E+03	0.2806E+03	-0.5141E+00
22	0.3108E+03	0.2753E+03	-0.4935E+00
23	0.2896E+03	0.2738E+03	-0.4730E+00
24	0.2697E+03	0.2670E+03	-0.4524E+00
25	0.9598E+02	0.1427E+03	-0.3908E+00
26	-0.8185E+02	0.4142E+02	-0.2881E+00
27	-0.3309E+04	-0.1645E+04	-0.1794E+01
28	-0.3486E+04	-0.1679E+04	-0.1645E+01
29	-0.1673E+03	-0.6977E+02	-0.3154E-01
30	-0.2333E+03	-0.8209E+02	0.2321E-01
31	-0.2993E+03	-0.9442E+02	0.7796E-01
32	-0.3654E+03	-0.1068E+03	0.1327E+00
33	-0.1074E+05	-0.3054E+04	0.4341E+01
34	-0.1089E+05	-0.3060E+04	0.4491E+01

**Appendix 7-2a Layer structure from FOR085.ORG input file for composite bridge deck with 36" girder**

	F	T	F	F	0.50	F	F	F	0	1	2	1	1
PRESCRIBED	0		1	1	1	1	218	F	T	F	F	F	F
CRITICALSE	0	0.7200	3	F	F	0	F	F	F	3	F	F	F
	8	3	8	3	8	3	8	3	8	3	8	3	3
ICAN													
L1	1	24	3										
PLY	1	1	70.00	70.0	0.0	0.0	0.100						
PLY	2	1	70.00	70.0	0.0	0.0	0.100						
PLY	3	1	70.00	70.0	0.0	0.0	0.100						
PLY	4	1	70.00	70.0	0.0	0.0	0.100						
PLY	5	1	70.00	70.0	0.0	0.0	0.100						
PLY	6	1	70.00	70.0	0.0	0.0	0.200						
PLY	7	1	70.00	70.0	0.0	0.0	0.300						
PLY	8	1	70.00	70.0	0.0	0.0	0.500						
PLY	9	1	70.00	70.0	0.0	0.0	0.500						
PLY	10	1	70.00	70.0	0.0	0.0	0.500						
PLY	11	1	70.00	70.0	0.0	0.0	0.500						
PLY	12	2	70.00	70.0	0.0	0.0	0.500						
PLY	13	3	70.00	70.0	0.0	90.0	0.500						
PLY	14	1	70.00	70.0	0.0	0.0	0.620						
PLY	15	1	70.00	70.0	0.0	0.0	0.620						
PLY	16	1	70.00	70.0	0.0	0.0	0.620						
PLY	17	1	70.00	70.0	0.0	0.0	0.620						
PLY	18	1	70.00	70.0	0.0	0.0	0.620						
PLY	19	2	70.00	70.0	0.0	0.0	0.500						
PLY	20	3	70.00	70.0	0.0	90.0	0.500						
PLY	21	1	70.00	70.0	0.0	0.0	0.350						
PLY	22	1	70.00	70.0	0.0	0.0	0.350						
PLY	23	1	70.00	70.0	0.0	0.0	0.350						
PLY	24	1	70.00	70.0	0.0	0.0	0.350						
MATCRD	1	CNCFCONC	.300	.01	CNCFCONC	0.0	.60	.03					
MATCRD	2	RBSFCONC	.050	.01	CNCFCONC	0.0	.60	.03					
MATCRD	3	RBSFCONC	.050	.01	CNCFCONC	0.0	.60	.03					
L2	2	34	5										
PLY	1	1	70.00	70.0	0.0	0.0	0.100						
PLY	2	1	70.00	70.0	0.0	0.0	0.100						
PLY	3	1	70.00	70.0	0.0	0.0	0.100						
PLY	4	1	70.00	70.0	0.0	0.0	0.100						
PLY	5	1	70.00	70.0	0.0	0.0	0.100						
PLY	6	1	70.00	70.0	0.0	0.0	0.200						
PLY	7	1	70.00	70.0	0.0	0.0	0.300						
PLY	8	1	70.00	70.0	0.0	0.0	0.500						
PLY	9	1	70.00	70.0	0.0	0.0	0.500						
PLY	10	1	70.00	70.0	0.0	0.0	0.500						
PLY	11	1	70.00	70.0	0.0	0.0	0.500						
PLY	12	2	70.00	70.0	0.0	0.0	0.500						
PLY	13	3	70.00	70.0	0.0	90.0	0.500						
PLY	14	1	70.00	70.0	0.0	0.0	0.620						
PLY	15	1	70.00	70.0	0.0	0.0	0.620						
PLY	16	1	70.00	70.0	0.0	0.0	0.620						
PLY	17	1	70.00	70.0	0.0	0.0	0.620						
PLY	18	1	70.00	70.0	0.0	0.0	0.620						
PLY	19	2	70.00	70.0	0.0	0.0	0.500						
PLY	20	3	70.00	70.0	0.0	90.0	0.500						
PLY	21	1	70.00	70.0	0.0	0.0	0.350						
PLY	22	1	70.00	70.0	0.0	0.0	0.350						
PLY	23	1	70.00	70.0	0.0	0.0	0.350						

PLY	24	1	70.00	70.0	0.0	0.0	0.350
PLY	25	1	70.00	70.0	0.0	0.0	2.000
PLY	26	1	70.00	70.0	0.0	0.0	2.000
PLY	27	4	70.00	70.0	0.0	0.0	0.500
PLY	28	4	70.00	70.0	0.0	0.0	0.500
PLY	29	5	70.00	70.0	0.0	0.0	8.500
PLY	30	5	70.00	70.0	0.0	0.0	8.500
PLY	31	5	70.00	70.0	0.0	0.0	8.500
PLY	32	5	70.00	70.0	0.0	0.0	8.500
PLY	33	4	70.00	70.0	0.0	0.0	0.500
PLY	34	4	70.00	70.0	0.0	0.0	0.500
MATCRD	1CNCFCNC	.300	.01	CNCFCNC	0.0	.60	.03
MATCRD	2RBSFCNC	.05000	.01	CNCFCNC	0.0	.60	.03
MATCRD	3RBSFCNC	.05000	.01	CNCFCNC	0.0	.60	.03
MATCRD	4GRSFGGRDS	.30	.00	GRSFGGRDS	0.0	.02	.03
MATCRD	5WBSFWBSM	.30	.00	WBSFWBSM	0.0	.02	.03

ENDN  
MHOST  
A TEST OF COMPOSITE DECK SIMULATION  
\*ELEMENT 336  
75  
\*COMPOSITE  
\*NODES 435  
\*LOUB 3 1 3  
\*FORCE 12  
\*TYING 348 3  
\*BOUNDARYCONDITIONS 20  
C\*OPTIMIZE

## Appendix 7-2b preprocessor to generate CBRAN input file for two-span composite bridge model

```

c      implicit double precision (a-h,o-z)
      implicit real (a-h,o-z)
c
c      character*80 buf
c      dimension islave(135)
      dimension x(15),y(15),t(2), TPLY(34), ISLAVE(58), MASTER(58)
C      data x / 0.0, 12.0, 24., 36., 48., 60., 120., 180., 240., 360.,
C      & 480., 600., 720., 960., 1200.0 /
C      spacing of x coordinates changed for 14'x14' HS25 loading
      data x / 0.0, 12.0, 24., 36., 48., 60., 120., 180., 240., 360.,
      & 432., 600., 768., 960., 1200.0 /
      data y / 0.0, 12.875, 25.75, 38.625, 51.5, 51.5, 55.75, 60.,
      & 64.25, 68.5, 68.5, 81.375, 94.25, 107.125, 120.0 /
      data t / 9.5, 49.5 /
      data TPLY / 0.1, 0.1, 0.1, 0.1, 0.1, 0.2, 0.3, 0.5, 0.5, 0.5,0.5,
      & 0.5, 0.5, 0.62, 0.62,0.62,0.62,0.62,0.5, 0.5, 0.35, 0.35, 0.35,
      & 0.35,
      & 2.0, 2.0, 0.5, 0.5, 8.5, 8.5, 8.5, 8.5, 0.5, 0.5 /
c23456789*123456789*123456789*123456789*123456789*123456789*123456789*12
      open (12, file = 'mdl_in_t.dat',status='UNKNOWN')

      nx=15
      ny=15
c      open (11, file = 'MtrxSym.txt',
c      & status='OLD')

c      READ (11,'(a)') buf
c      READ (11,*) NNODES, NELEMS, NDUPL
      nnodes = (nx+(nx-1))*ny
      nelems=(nx-1)*2*(ny-3)
      ndupl=(nx+nx-1)*2

c      write the top of file
      write (buf,'(4L6,F5.2,1x,3L6,5i6)').FALSE.,.TRUE.,.FALSE.,
      & .FALSE., 0.5, .FALSE., .FALSE., .FALSE., 0, 1, 2, 1, 1
      write (12,'(a80)') buf
      write (buf,'(A10,6i6,5L6)') 'PRESCRIBED', 0,1,1,1,1,218,
      & .FALSE.,.TRUE.,.FALSE., .FALSE., .FALSE.
      write (12,'(a80)') buf
      write (buf,'(A10,i6,F10.4,i6,2L6,i6,5L6)') 'CRITICALSE',0,0.72,3,
      & .FALSE., .FALSE., 0, .FALSE.,.FALSE.,.FALSE., .FALSE., .FALSE.
      write (12,'(a80)') buf
      write (buf,'(10i8)') 8,3,8,3,8,3,8,3,8,3
      write (12,'(a80)') buf
      write (buf,'(A4)') 'ICAN'
      write (12,'(a80)') buf
      write (buf,'(A4,4x,3i8)') 'LTYP', 1, 24, 3
      write (12,'(a80)') buf
      do i=1,24
      if (i .eq. 13 .or. i .eq. 20) then
      angle=90.0
      else
      angle=0.0
      endif
      if (i .eq. 12 .or. i .eq. 19) then
      mtrl=2
      elseif(i .eq. 13 .or. i .eq. 20) then

```

```

        mtrl=3
    else
        mtrl=1
    endif
    write (buf,'(A8,2i8,f7.2,f7.1,f8.1,f9.0,f6.3)') '    PLY',i,
& mtrl, 70.,70.,0.0, ANGLE, TPLY(I)
    write (l2,'(a80)') buf
    enddo
c23456789*123456789*123456789*123456789*123456789*123456789*123456789*12

    write (buf,'(A8,i8,A8,2x,f6.5, 2x,f3.2,3x, A8, f5.1,5x,f3.2,5x,
& f3.2)')
& ' MATCRD', 1, 'CNCFCNC', 0.3, 0.01,'CNCFCNC', 0.0, 0.6, 0.03
    write (l2,'(a80)') buf
    write (buf,'(A8,i8,A8,2x,f6.5, 2x,f3.2,3x, A8, f5.1,5x,f3.2,5x,
& f3.2)')
& ' MATCRD',
& 2, 'RBSFCNC', 0.05, 0.01,'CNCFCNC', 0.0, 0.6, 0.03
    write (l2,'(a80)') buf
    write (buf,'(A8,i8,A8,2x,f6.5, 2x,f3.2,3x, A8, f5.1,5x,f3.2,5x,
& f3.2)')
& ' MATCRD',
& 3, 'RBSFCNC', 0.05, 0.01,'CNCFCNC', 0.0, 0.6, 0.03
    write (l2,'(a80)') buf

    write (buf,'(A4,4x,3i8)') 'LTP', 2, 34, 5
    write (l2,'(a80)') buf
    do i=1,34
        if (i .eq. 13 .or. i .eq. 20) then
            angle=90.0
        else
            angle=0.0
        endif
        if (i .eq. 12 .or. i .eq. 19) then
            mtrl=2
        elseif(i .eq. 13 .or. i .eq. 20) then
            mtrl=3
        elseif(i.eq. 27 .or. i.eq.28.or. i .eq. 33.or. i .eq. 34) then
            mtrl=4
        elseif(i.eq. 29 .or. i.eq.30.or. i .eq. 31.or. i .eq. 32) then
            mtrl=5
        else
            mtrl=1
        endif
        write (buf,'(A8,2i8,f7.2,f7.1,f8.1,f9.0,f6.3)') '    PLY',i,
& mtrl, 70.,70.,0.0, ANGLE, TPLY(I)
        write (l2,'(a80)') buf
    enddo
    write (buf,'(A8,i8,A8,2x,f6.5, 2x,f3.2,3x, A8, f5.1,5x,f3.2,5x,
& f3.2)')
& ' MATCRD',
& 1, 'CNCFCNC', 0.3, 0.01,'CNCFCNC', 0.0, 0.6, 0.03
    write (l2,'(a80)') buf
    write (buf,'(A8,i8,A8,2x,f6.5, 2x,f3.2,3x, A8, f5.1,5x,f3.2,5x,
& f3.2)')
& ' MATCRD',
& 2, 'RBSFCNC', 0.05, 0.01,'CNCFCNC', 0.0, 0.6, 0.03
    write (l2,'(a80)') buf
    write (buf,'(A8,i8,A8,2x,f6.5, 2x,f3.2,3x, A8, f5.1,5x,f3.2,5x,
& f3.2)')
& ' MATCRD',
& 3, 'RBSFCNC', 0.05, 0.01,'CNCFCNC', 0.0, 0.6, 0.03
    write (l2,'(a80)') buf

```

```

write (buf,'(A8,i8,A8,2x,f6.5, 2x,f3.2,3x, A8, f5.1,5x,f3.2,5x,
& f3.2)')
& ' MATCRD',
& 4, 'GRSFGGRDS', 0.3, 0.0,'GRSFGGRDS', 0.0, 0.02, 0.03
write (12,'(a80)') buf
write (buf,'(A8,i8,A8,2x,f6.5, 2x,f3.2,3x, A8, f5.1,5x,f3.2,5x,
& f3.2)')
& ' MATCRD',
& 5, 'WBSFWBSM', 0.3, 0.0,'WBSFWBSM', 0.0, 0.02, 0.03
write (12,'(a80)') buf

write (buf,'(A4)') 'ENDN'
write (12,'(a80)') buf
write (buf,'(A5)') 'MHOST'
write (12,'(a80)') buf
write (buf,'(A36)') ' A TEST OF COMPOSITE DECK SIMULATION'
write (12,'(a80)') buf
write (buf,'(A8,i12)') '*ELEMENT', NELEMS
write (12,'(a80)') buf
write (buf,'(i5)') 75
write (12,'(a80)') buf
write (buf,'(A10)') '*COMPOSITE'
write (12,'(a80)') buf
write (buf,'(A6,i10)') '*NODES', nnodes
write (12,'(a80)') buf
write (buf,'(A11)') '*LOUB 3 1 3'
write (12,'(a80)') buf
write (buf,'(A6,i5)') '*FORCE', 10
write (12,'(a80)') buf
C write (buf,'(A5,i11)') '*DUPL', ndupl
write (buf,'(A,i14,i10)') '*TYING', 6*ndupl, 3
write (12,'(a80)') buf
nboun=20
write (buf,'(A19,i5)') '*BOUNDARYCONDITIONS', nboun
write (12,'(a80)') buf
write (buf,'(A10)') 'C*OPTIMIZE'
write (12,'(a80)') buf
write (buf,'(A15)') '*CONSTITUTIVE 0'
write (12,'(a80)') buf
write (buf,'(A6)') '*DISPL'
write (12,'(a80)') buf
write (buf,'(A4)') '*END'
write (12,'(a80)') buf
write (buf,'(A5)') '*INCR'
write (12,'(a80)') buf
write (buf,'(i1)') 0
write (12,'(a80)') buf
write (buf,'(A10)') '*ITERATION'
write (12,'(a80)') buf
write (buf,'(i5, 4f10.2)') 2,0.05,0.05,0.05,0.05
write (12,'(a80)') buf
write (buf,'(A15)') '*PROPERTIES 75'
write (12,'(a80)') buf
write (buf,'(i5,i6,4f10.5)')1,nnodes,1.,0.00001,0.00001,0.00001
write (12,'(a80)') buf
write (buf,'(A45)')
& ' ' 0.1 0.0 0.0 0.0'
write (12,'(a80)') buf
write (buf,'(A5)') '*COOR'
write (12,'(a80)') buf

WRITE (12,'('' MHOST FEM Model for composite bridge deck''))
WRITE (12,'(''*COOR''))

```

```

INOD=0
NDUPL=0
DO 1 i= -nx,nx,1
  IF (i .lt. -1) then
    XCOOR = -X(-i)
  ELSEIF (i .gt. 0) then
    XCOOR = X(i)
  ELSEIF (i.eq. -1 .or. i .eq. 0) THEN
    GOTO 1
  ELSE
    STOP 100
  ENDIF
DO 2 j= 1, ny
  YCOOR = Y(j)
  IF ( j.lt. 6 .or. j .gt. 10) then
    THCK= t(1)
    LTYP=1
    Z=-5.
  ELSE
    THCK=t(2)
    LTYP=2
    Z=-26.
  ENDIF
  INOD=INOD+1
  WRITE (12,'(i8,4F17.8,i4)') INOD,XCOOR,YCOOR,Z,THCK,LTYP
  IF (J .eq. 5) THEN
    NDUPL = NDUPL+1
    ISLAVE (NDUPL) = inod
    MASTER (NDUPL) = inod+1
  ELSEIF (J.EQ. 10) THEN
    NDUPL = NDUPL+1
    ISLAVE (NDUPL) =inod+1
    MASTER (NDUPL) = inod
  ENDIF
2 CONTINUE
1 CONTINUE
write (*,*) ' nnodes=',inod, ' ndupl=', ndupl, ' ntying=',6*ndupl

WRITE (12,'(''*ELEM 75''')')
IELEM=0
DO 3 i= 1, (nx-1)+(nx-1)
  DO 4 j=1, ny-1
    IF (J .ne. 5 .and. j .ne. 10) THEN
      IELEM=IELEM+1
      NOD1=ny*(i-1)+j+1
      NOD2=ny*(i-1)+j
      NOD3=ny*i+j
      NOD4=ny*i+j+1
      WRITE (12,'(i8,4i9)') IELEM, NOD1,NOD2,NOD3,NOD4
    ELSE
      CONTINUE
    ENDIF
4 CONTINUE
3 CONTINUE
WRITE (*,*) ' nelems=', ielem
WRITE (12,'(''*LAMINATE''')')
C WRITE (12,'(''*DUPLICATENODE''')')
WRITE (12,'(''*TYING''')')
C CCOMB=distance to center of combined girder plus deck from center of deck
CCOMB=0.5*(t(2)-t(1))
DO 5 i=1, NDUPL
C WRITE (12,'(2i8)') ISLAVE(i), MASTER(i)
WRITE (12,'(8i8)') 3, islave(i), 1 ,master(i), 1, master(i), 5

```

```

WRITE (12,'(2f10.5)') 1.0, CCOMB
WRITE (12,'(8i8)') 3, islave(i), 2 ,master(i), 2, master(i), 4
WRITE (12,'(2f10.5)') 1.0, -CCOMB
WRITE (12,'(8i8)') 2, islave(i), 3 ,master(i), 3
WRITE (12,'(2f10.5)') 1.0

WRITE (12,'(8i8)') 2, islave(i), 4 ,master(i), 4
WRITE (12,'(2f10.5)') 1.0
WRITE (12,'(8i8)') 2, islave(i), 5 ,master(i), 5
WRITE (12,'(2f10.5)') 1.0
WRITE (12,'(8i8)') 2, islave(i), 6 ,master(i), 6
WRITE (12,'(2f10.5)') 1.0

5 CONTINUE
WRITE (12,'('*BOUNDARYCONDITIONS*'))
NBOUN=0
C Write the first end boundary conditions
DO 32 i=6, 10
  IF ( i .eq. 8) then
    NBOUN = NBOUN + 2
    WRITE (12,'(2i9)') i, 2
    WRITE (12,'(2i9)') i, 3
  ELSE
    NBOUN = NBOUN + 1
    WRITE (12,'(2i9)') i, 3
  ENDIF
32 CONTINUE
DO 33 i=216, 220
  IF ( i .eq. 218) then
    NBOUN = NBOUN + 3
    WRITE (12,'(2i9)') i, 1
    WRITE (12,'(2i9)') i, 2
    WRITE (12,'(2i9)') i, 3
  ELSE
    NBOUN = NBOUN + 1
    WRITE (12,'(2i9)') i, 3
  ENDIF
33 CONTINUE
DO 34 i=425, 430
  IF ( i .eq. 428) then
    NBOUN = NBOUN + 2
    WRITE (12,'(2i9)') i, 2
    WRITE (12,'(2i9)') i, 3
  ELSE
    NBOUN = NBOUN + 1
    WRITE (12,'(2i9)') i, 3
  ENDIF
34 CONTINUE

  Write (*,*) ' nboun=', nboun
C Write the edge boundary conditions
c DO 33 i=1, 450, 30
c NBOUN=NBOUN+2
c WRITE (12,'(2i9)') i, 4
c WRITE (12,'(2i9)') i+14, 4
c 33 CONTINUE

C WRITE (12,'('*FORCE*'))
C WRITE (12,'(i5,i2,f19.9)') inode, idof, force
C FORCE = -200.0
C DO i=36, 40
C WRITE (12,'(i5,i2,f19.9)') i, 3, force
C ENDDO

```

```
C      DO i=396, 400
C          WRITE (12,'(i5,i2,f19.9)') i, 3, force
C      ENDDO
WRITE (12,'('*PRINT')')

WRITE (12,'(''      TOTALDISPLACEM'')')
WRITE (12,'(''      STRESS'')')
WRITE (12,'(''      STRAIN'')')

WRITE (12,'('*END')')

WRITE (12,'('*STOP')')

write (*,*) ' NBOUN=', NBOUN

STOP

end
```

**Appendix 7-2c Residual stresses from FOR091.DAT file after 28 days for composite bridge deck with 36" girder followed by HS25 loading**

```

TIME= 672.0 HOURS
NODE NUMBER= 218
PLY NO., SIG11, SIG22, SIG12
STRESSES ARE IN PSI UNITS; LAYER COORDINATES
 1 0.1096E+03 0.1109E+03 0.2805E-07
 2 0.1202E+03 0.1184E+03 0.2797E-07
 3 0.1278E+03 0.1296E+03 0.2790E-07
 4 0.1381E+03 0.1368E+03 0.2782E-07
 5 0.1450E+03 0.1473E+03 0.2774E-07
 6 0.1573E+03 0.1566E+03 0.2764E-07
 7 0.1736E+03 0.1766E+03 0.2747E-07
 8 0.1973E+03 0.1977E+03 0.2718E-07
 9 0.2185E+03 0.2228E+03 0.2680E-07
10 0.2363E+03 0.2377E+03 0.2645E-07
11 0.2483E+03 0.2533E+03 0.2611E-07
12 0.1222E+03 0.1713E+03 0.3243E-07
13 0.1248E+03 0.1869E+03 0.1133E-06
14 0.2694E+03 0.2717E+03 0.2500E-07
15 0.2700E+03 0.2756E+03 0.2453E-07
16 0.2735E+03 0.2759E+03 0.2409E-07
17 0.2732E+03 0.2789E+03 0.2364E-07
18 0.2738E+03 0.2762E+03 0.2320E-07
19 0.1456E+03 0.2089E+03 0.2968E-07
20 0.1449E+03 0.2119E+03 0.1305E-06
21 0.2677E+03 0.2733E+03 0.2213E-07
22 0.2675E+03 0.2698E+03 0.2189E-07
23 0.2651E+03 0.2707E+03 0.2163E-07
24 0.2646E+03 0.2668E+03 0.2138E-07
25 0.1420E+03 0.1443E+03 0.2054E-07
26 0.9931E+02 0.9716E+02 0.1910E-07
27 -0.4101E+03 -0.4222E+03 -0.5123E-06
28 -0.4113E+03 -0.4263E+03 -0.5172E-06
29 -0.3343E+02 -0.3422E+02 -0.4118E-07
30 -0.3895E+02 -0.3957E+02 -0.4715E-07
31 -0.4446E+02 -0.4492E+02 -0.5312E-07
32 -0.5196E+02 -0.5230E+02 -0.5910E-07
33 -0.7734E+03 -0.7780E+03 -0.8470E-06
34 -0.7499E+03 -0.7530E+03 -0.8519E-06

```

HS25 14 ftx14 ft LOADING RESULTS after 672.000 HOURS = 28.0000 DAYS

```

TIME= 672.0 HOURS
NODE NUMBER= 218
PLY NO., SIG11, SIG22, SIG12
STRESSES ARE IN PSI UNITS; LAYER COORDINATES
 1 0.5229E+03 0.7241E+02 0.4520E-08
 2 0.5307E+03 0.8013E+02 0.4664E-08
 3 0.5354E+03 0.9148E+02 0.4807E-08
 4 0.5429E+03 0.9885E+02 0.4954E-08
 5 0.5469E+03 0.1095E+03 0.5098E-08
 6 0.5550E+03 0.1191E+03 0.5335E-08
 7 0.5642E+03 0.1395E+03 0.5717E-08
 8 0.5765E+03 0.1613E+03 0.6318E-08
 9 0.5835E+03 0.1873E+03 0.7051E-08
10 0.5870E+03 0.2030E+03 0.7810E-08
11 0.5848E+03 0.2196E+03 0.8578E-08
12 0.5985E+03 0.1325E+03 0.1552E-07
13 0.6694E+02 0.5747E+03 0.1889E-04
14 0.5615E+03 0.2407E+03 0.1094E-07

```

15	0.5445E+03	0.2457E+03	0.1185E-07
16	0.5303E+03	0.2470E+03	0.1279E-07
17	0.5124E+03	0.2511E+03	0.1373E-07
18	0.4954E+03	0.2496E+03	0.1466E-07
19	0.4497E+03	0.1782E+03	0.2217E-07
20	0.1017E+03	0.4529E+03	0.1206E-04
21	0.4470E+03	0.2492E+03	0.1690E-07
22	0.4369E+03	0.2463E+03	0.1743E-07
23	0.4245E+03	0.2479E+03	0.1796E-07
24	0.4140E+03	0.2446E+03	0.1848E-07
25	0.2580E+03	0.1241E+03	0.2026E-07
26	0.1584E+03	0.8051E+02	0.2326E-07
27	-0.1719E+03	-0.5497E+03	-0.4574E-06
28	-0.3259E+03	-0.5608E+03	-0.4536E-06
29	-0.1282E+03	-0.4872E+02	-0.3069E-07
30	-0.3246E+03	-0.6279E+02	-0.2569E-07
31	-0.5211E+03	-0.7686E+02	-0.2068E-07
32	-0.7195E+03	-0.9296E+02	-0.1569E-07
33	-0.1123E+05	-0.1394E+04	-0.1775E-06
34	-0.1136E+05	-0.1376E+04	-0.1736E-06

**Appendix 7-3a Layer structure from FOR085.ORG input file for composite bridge deck with 55" girder**

LTYPE	1	24	3					
PLY	1	1	70.00	70.0	0.0	0.	0.100	
PLY	2	1	70.00	70.0	0.0	0.	0.100	
PLY	3	1	70.00	70.0	0.0	0.	0.100	
PLY	4	1	70.00	70.0	0.0	0.	0.100	
PLY	5	1	70.00	70.0	0.0	0.	0.100	
PLY	6	1	70.00	70.0	0.0	0.	0.200	
PLY	7	1	70.00	70.0	0.0	0.	0.300	
PLY	8	1	70.00	70.0	0.0	0.	0.500	
PLY	9	1	70.00	70.0	0.0	0.	0.500	
PLY	10	1	70.00	70.0	0.0	0.	0.500	
PLY	11	1	70.00	70.0	0.0	0.	0.500	
PLY	12	2	70.00	70.0	0.0	0.	0.500	
PLY	13	3	70.00	70.0	0.0	90.	0.500	
PLY	14	1	70.00	70.0	0.0	0.	0.620	
PLY	15	1	70.00	70.0	0.0	0.	0.620	
PLY	16	1	70.00	70.0	0.0	0.	0.620	
PLY	17	1	70.00	70.0	0.0	0.	0.620	
PLY	18	1	70.00	70.0	0.0	0.	0.620	
PLY	19	2	70.00	70.0	0.0	0.	0.500	
PLY	20	3	70.00	70.0	0.0	90.	0.500	
PLY	21	1	70.00	70.0	0.0	0.	0.350	
PLY	22	1	70.00	70.0	0.0	0.	0.350	
PLY	23	1	70.00	70.0	0.0	0.	0.350	
PLY	24	1	70.00	70.0	0.0	0.	0.350	
MATCRD	1	CNCFCONC	.300	.01	CNCFCONC	0.0	.60	.03
MATCRD	2	RBSFCONC	.050	.01	CNCFCONC	0.0	.60	.03
MATCRD	3	RBSFCONC	.050	.01	CNCFCONC	0.0	.60	.03
LTYPE	2	36	5					
PLY	1	1	70.00	70.0	0.0	0.	0.100	
PLY	2	1	70.00	70.0	0.0	0.	0.100	
PLY	3	1	70.00	70.0	0.0	0.	0.100	
PLY	4	1	70.00	70.0	0.0	0.	0.100	
PLY	5	1	70.00	70.0	0.0	0.	0.100	
PLY	6	1	70.00	70.0	0.0	0.	0.200	
PLY	7	1	70.00	70.0	0.0	0.	0.300	
PLY	8	1	70.00	70.0	0.0	0.	0.500	
PLY	9	1	70.00	70.0	0.0	0.	0.500	
PLY	10	1	70.00	70.0	0.0	0.	0.500	
PLY	11	1	70.00	70.0	0.0	0.	0.500	
PLY	12	2	70.00	70.0	0.0	0.	0.500	
PLY	13	3	70.00	70.0	0.0	90.	0.500	
PLY	14	1	70.00	70.0	0.0	0.	0.620	
PLY	15	1	70.00	70.0	0.0	0.	0.620	
PLY	16	1	70.00	70.0	0.0	0.	0.620	
PLY	17	1	70.00	70.0	0.0	0.	0.620	
PLY	18	1	70.00	70.0	0.0	0.	0.620	
PLY	19	2	70.00	70.0	0.0	0.	0.500	
PLY	20	3	70.00	70.0	0.0	90.	0.500	
PLY	21	1	70.00	70.0	0.0	0.	0.350	
PLY	22	1	70.00	70.0	0.0	0.	0.350	
PLY	23	1	70.00	70.0	0.0	0.	0.350	
PLY	24	1	70.00	70.0	0.0	0.	0.350	
PLY	25	1	70.00	70.0	0.0	0.	2.000	
PLY	26	1	70.00	70.0	0.0	0.	2.000	
PLY	27	4	70.00	70.0	0.0	0.	1.000	
PLY	28	4	70.00	70.0	0.0	0.	1.000	
PLY	29	5	70.00	70.0	0.0	0.	8.500	

PLY	30	5	70.00	70.0	0.0	0.	8.500	
PLY	31	5	70.00	70.0	0.0	0.	8.500	
PLY	32	5	70.00	70.0	0.0	0.	8.500	
PLY	33	5	70.00	70.0	0.0	0.	8.500	
PLY	34	5	70.00	70.0	0.0	0.	8.500	
PLY	35	4	70.00	70.0	0.0	0.	1.000	
PLY	36	4	70.00	70.0	0.0	0.	1.000	
MATCRD	1CNCFCNC		.300	.01	CNCFCNC	0.0	.60	.03
MATCRD	2RBSFCNC		.05000	.01	CNCFCNC	0.0	.60	.03
MATCRD	3RBSFCNC		.05000	.01	CNCFCNC	0.0	.60	.03
MATCRD	4GRSFGRDS		.30	.00	GRSFGRDS	0.0	.02	.03
MATCRD	5WBSFWBSM		.30	.00	WBSFWBSM	0.0	.02	.03

ENDN

**Appendix 7-3b Residual stresses from FOR091.DAT file after 28 days  
for composite bridge deck with 55" girder**

TIME= 672.0 HOURS  
 NODE NUMBER= 218  
 PLY NO., SIG11, SIG22, SIG12  
 STRESSES ARE IN PSI UNITS; LAYER COORDINATES

1	0.1801E+03	0.1848E+03	0.2565E-07
2	0.1895E+03	0.1945E+03	0.2564E-07
3	0.1977E+03	0.2029E+03	0.2563E-07
4	0.2065E+03	0.2119E+03	0.2562E-07
5	0.2144E+03	0.2201E+03	0.2561E-07
6	0.2258E+03	0.2317E+03	0.2559E-07
7	0.2428E+03	0.2491E+03	0.2556E-07
8	0.2657E+03	0.2727E+03	0.2552E-07
9	0.2893E+03	0.2969E+03	0.2546E-07
10	0.3064E+03	0.3144E+03	0.2540E-07
11	0.3202E+03	0.3286E+03	0.2534E-07
12	0.2357E+03	0.2934E+03	0.1994E-07
13	0.2463E+03	0.3064E+03	-0.4676E-07
14	0.3427E+03	0.3518E+03	0.2517E-07
15	0.3457E+03	0.3548E+03	0.2509E-07
16	0.3495E+03	0.3586E+03	0.2502E-07
17	0.3509E+03	0.3601E+03	0.2495E-07
18	0.3521E+03	0.3613E+03	0.2488E-07
19	0.2689E+03	0.3411E+03	0.2080E-07
20	0.2681E+03	0.3401E+03	-0.3577E-07
21	0.3508E+03	0.3600E+03	0.2472E-07
22	0.3504E+03	0.3596E+03	0.2467E-07
23	0.3498E+03	0.3589E+03	0.2464E-07
24	0.3490E+03	0.3581E+03	0.2460E-07
25	0.3363E+03	0.3451E+03	0.2446E-07
26	0.2351E+03	0.2411E+03	0.2424E-07
27	0.7962E+02	0.7887E+02	0.4273E-06
28	0.5828E+02	0.5695E+02	0.3960E-06
29	-0.3207E+01	-0.3438E+01	0.1820E-07
30	-0.1661E+02	-0.1708E+02	-0.1343E-08
31	-0.3002E+02	-0.3072E+02	-0.2089E-07
32	-0.4342E+02	-0.4436E+02	-0.4042E-07
33	-0.5681E+02	-0.5800E+02	-0.5998E-07
34	-0.7426E+02	-0.7571E+02	-0.7950E-07
35	-0.1166E+04	-0.1189E+04	-0.1230E-05
36	-0.1160E+04	-0.1183E+04	-0.1261E-05

HS25 14 ftx14 ft LOADING RESULTS after 672.000 HOURS = 28.0000 DAYS

TIME= 672.0 HOURS  
 NODE NUMBER= 218  
 PLY NO., SIG11, SIG22, SIG12  
 STRESSES ARE IN PSI UNITS; LAYER COORDINATES

1	0.3945E+03	0.1622E+03	0.1790E-07
2	0.4030E+03	0.1720E+03	0.1794E-07
3	0.4102E+03	0.1804E+03	0.1798E-07
4	0.4180E+03	0.1895E+03	0.1803E-07
5	0.4250E+03	0.1978E+03	0.1807E-07
6	0.4350E+03	0.2096E+03	0.1813E-07
7	0.4496E+03	0.2271E+03	0.1824E-07
8	0.4686E+03	0.2510E+03	0.1842E-07
9	0.4874E+03	0.2756E+03	0.1863E-07
10	0.4998E+03	0.2935E+03	0.1885E-07
11	0.5088E+03	0.3080E+03	0.1907E-07

12	0.5074E+03	0.2695E+03	0.1376E-07
13	0.2110E+03	0.5318E+03	0.1092E-04
14	0.5164E+03	0.3325E+03	0.1974E-07
15	0.5134E+03	0.3359E+03	0.2001E-07
16	0.5113E+03	0.3402E+03	0.2028E-07
17	0.5068E+03	0.3422E+03	0.2055E-07
18	0.5020E+03	0.3439E+03	0.2082E-07
19	0.4826E+03	0.3209E+03	0.1693E-07
20	0.2389E+03	0.5161E+03	0.8592E-05
21	0.4865E+03	0.3437E+03	0.2146E-07
22	0.4828E+03	0.3436E+03	0.2161E-07
23	0.4788E+03	0.3432E+03	0.2177E-07
24	0.4747E+03	0.3427E+03	0.2192E-07
25	0.4507E+03	0.3306E+03	0.2243E-07
26	0.3304E+03	0.2282E+03	0.2330E-07
27	0.9411E+03	0.4607E+02	0.4263E-06
28	0.8173E+03	0.2146E+02	0.3994E-06
29	0.1678E+02	-0.6985E+01	0.1996E-07
30	-0.6069E+02	-0.2230E+02	0.3114E-08
31	-0.1382E+03	-0.3762E+02	-0.1373E-07
32	-0.2156E+03	-0.5294E+02	-0.3056E-07
33	-0.2931E+03	-0.6826E+02	-0.4742E-07
34	-0.3747E+03	-0.8765E+02	-0.6424E-07
35	-0.5739E+04	-0.1364E+04	-0.1002E-05
36	-0.5835E+04	-0.1361E+04	-0.1029E-05

## Appendix 7-4a Layer structure for thin steel layer model of bridge deck with 36" girder

	F	T	F	F	0.50	F	F	F	0	1	2	1	1
PRESCRIBED	0		1	1	1	1	218		F	T	F	F	F
CRITICALSE	0		0.7200	3		F	F	0	F	F	F	F	F
	8	3	8	3		8	3		8	3	8	3	
ICAN													
LTYP	1		32		3								
PLY	1		1	70.00	70.0		0.0		0.	0.100			
PLY	2		1	70.00	70.0		0.0		0.	0.100			
PLY	3		1	70.00	70.0		0.0		0.	0.100			
PLY	4		1	70.00	70.0		0.0		0.	0.100			
PLY	5		1	70.00	70.0		0.0		0.	0.100			
PLY	6		1	70.00	70.0		0.0		0.	0.200			
PLY	7		1	70.00	70.0		0.0		0.	0.300			
PLY	8		1	70.00	70.0		0.0		0.	0.500			
PLY	9		1	70.00	70.0		0.0		0.	0.500			
PLY	10		1	70.00	70.0		0.0		0.	0.500			
PLY	11		1	70.00	70.0		0.0		0.	0.500			
PLY	12		1	70.00	70.0		0.0		0.	0.237			
PLY	13		2	70.00	70.0		0.0		0.	0.025			
PLY	14		1	70.00	70.0		0.0		0.	0.237			
PLY	15		1	70.00	70.0		0.0		0.	0.237			
PLY	16		3	70.00	70.0		0.0	90.	0.025				
PLY	17		1	70.00	70.0		0.0		0.	0.237			
PLY	18		1	70.00	70.0		0.0		0.	0.620			
PLY	19		1	70.00	70.0		0.0		0.	0.620			
PLY	20		1	70.00	70.0		0.0		0.	0.620			
PLY	21		1	70.00	70.0		0.0		0.	0.620			
PLY	22		1	70.00	70.0		0.0		0.	0.620			
PLY	23		1	70.00	70.0		0.0		0.	0.237			
PLY	24		2	70.00	70.0		0.0		0.	0.025			
PLY	25		1	70.00	70.0		0.0		0.	0.237			
PLY	26		1	70.00	70.0		0.0		0.	0.237			
PLY	27		3	70.00	70.0		0.0	90.	0.025				
PLY	28		1	70.00	70.0		0.0		0.	0.237			
PLY	29		1	70.00	70.0		0.0		0.	0.350			
PLY	30		1	70.00	70.0		0.0		0.	0.350			
PLY	31		1	70.00	70.0		0.0		0.	0.350			
PLY	32		1	70.00	70.0		0.0		0.	0.350			
MATCRD			1CNCFCNC	.300	.01	CNCFCNC	0.0		.60		.03		
MATCRD			2RBSFGRDS	.050	.01	CNCFCNC	0.0		.60		.03		
MATCRD			3RBSFGRDS	.050	.01	CNCFCNC	0.0		.60		.03		
LTYP	2		42		5								
PLY	1		1	70.00	70.0		0.0		0.	0.100			
PLY	2		1	70.00	70.0		0.0		0.	0.100			
PLY	3		1	70.00	70.0		0.0		0.	0.100			
PLY	4		1	70.00	70.0		0.0		0.	0.100			
PLY	5		1	70.00	70.0		0.0		0.	0.100			
PLY	6		1	70.00	70.0		0.0		0.	0.200			
PLY	7		1	70.00	70.0		0.0		0.	0.300			
PLY	8		1	70.00	70.0		0.0		0.	0.500			
PLY	9		1	70.00	70.0		0.0		0.	0.500			
PLY	10		1	70.00	70.0		0.0		0.	0.500			
PLY	11		1	70.00	70.0		0.0		0.	0.500			
PLY	12		1	70.00	70.0		0.0		0.	0.237			
PLY	13		2	70.00	70.0		0.0		0.	0.025			
PLY	14		1	70.00	70.0		0.0		0.	0.237			
PLY	15		1	70.00	70.0		0.0		0.	0.237			

PLY	16	3	70.00	70.0	0.0	90.	0.025	
PLY	17	1	70.00	70.0	0.0	0.	0.237	
PLY	18	1	70.00	70.0	0.0	0.	0.620	
PLY	19	1	70.00	70.0	0.0	0.	0.620	
PLY	20	1	70.00	70.0	0.0	0.	0.620	
PLY	21	1	70.00	70.0	0.0	0.	0.620	
PLY	22	1	70.00	70.0	0.0	0.	0.620	
PLY	23	1	70.00	70.0	0.0	0.	0.237	
PLY	24	2	70.00	70.0	0.0	0.	0.025	
PLY	25	1	70.00	70.0	0.0	0.	0.237	
PLY	26	1	70.00	70.0	0.0	0.	0.237	
PLY	27	3	70.00	70.0	0.0	90.	0.025	
PLY	28	1	70.00	70.0	0.0	0.	0.237	
PLY	29	1	70.00	70.0	0.0	0.	0.350	
PLY	30	1	70.00	70.0	0.0	0.	0.350	
PLY	31	1	70.00	70.0	0.0	0.	0.350	
PLY	32	1	70.00	70.0	0.0	0.	0.350	
PLY	33	1	70.00	70.0	0.0	0.	2.000	
PLY	34	1	70.00	70.0	0.0	0.	2.000	
PLY	35	4	70.00	70.0	0.0	0.	0.500	
PLY	36	4	70.00	70.0	0.0	0.	0.500	
PLY	37	5	70.00	70.0	0.0	0.	8.500	
PLY	38	5	70.00	70.0	0.0	0.	8.500	
PLY	39	5	70.00	70.0	0.0	0.	8.500	
PLY	40	5	70.00	70.0	0.0	0.	8.500	
PLY	41	4	70.00	70.0	0.0	0.	0.500	
PLY	42	4	70.00	70.0	0.0	0.	0.500	
MATCRD	1	CNCFCNC	.300	.01	CNCFCNC	0.0	.60	.03
MATCRD	2	RBSFGRDS	.05000	.00	CNCFCNC	0.0	.60	.03
MATCRD	3	RBSFGRDS	.05000	.00	CNCFCNC	0.0	.60	.03
MATCRD	4	GRSFGRDS	.30	.00	GRSFGRDS	0.0	.02	.03
MATCRD	5	WBSFWBSM	.30	.00	WBSFWBSM	0.0	.02	.03

ENDN  
MHOST  
A TEST OF COMPOSITE DECK SIMULATION  
\*ELEMENT 336  
75  
\*COMPOSITE  
\*NODES 435  
\*LOUB 3 1 3  
\*FORCE 10  
\*TYING 348 3  
\*BOUNDARYCONDITIONS 20  
C\*OPTIMIZE  
\*CONSTITUTIVE 0  
\*DISPL  
\*END  
\*INCR  
0  
\*ITERATION  
2 0.05 0.05 0.05 0.05  
\*PROPERTIES 75  
1 435 1.00000 0.00001 0.00001 0.00001  
0.1 0.0 0.0 0.0  
.  
.  
.  
.  
.

## **Appendix 7-4b preprocessor to generate CBRAN input file for two-span composite bridge model with thin rebar steel layers**

```

c      implicit double precision (a-h,o-z)
      implicit real (a-h,o-z)
c
c      character*80 buf
c      dimension islave(135)
c      dimension x(15),y(15),t(2), TPLY(42), ISLAVE(58), MASTER(58)
C      data x / 0.0, 12.0, 24., 36., 48., 60., 120., 180., 240., 360.,
C      & 480., 600., 720., 960., 1200.0 /
C spacing of x coordinates changed for 14'x14' HS25 loading
C      data x / 0.0, 12.0, 24., 36., 48., 60., 120., 180., 240., 360.,
C      & 432., 600., 768., 960., 1200.0 /
C      data y / 0.0, 12.875, 25.75, 38.625, 51.5, 51.5, 55.75, 60.,
C      & 64.25, 68.5, 68.5, 81.375, 94.25, 107.125, 120.0 /
C      data t / 9.5, 49.5 /
C      data TPLY / 0.1, 0.1, 0.1, 0.1, 0.1, 0.2, 0.3, 0.5, 0.5, 0.5,0.5,
C      & 0.2375, 0.025, 0.2375, 0.2375, 0.025, 0.2375,
C      & 0.62, 0.62, 0.62, 0.62, 0.62,
C      & 0.2375, 0.025, 0.2375, 0.2375, 0.025, 0.2375,
C      & 0.35, 0.35, 0.35, 0.35,
C      & 2.0, 2.0, 0.5, 0.5, 8.5, 8.5, 8.5, 8.5, 0.5, 0.5 /
c23456789*123456789*123456789*123456789*123456789*123456789*123456789*12
C      steel rebars are represented by very thin layers
C      according to the discussion with TWG on August 19, 2011
C      Steel layer thickness = bar area / bar spacing,
C      e.g. for #4 bars @ 8" spacing (0.20/8)=0.025 inch thick layer
C
C      This file generates the following steel bar layers
C      layer 13 = top longitudinal rebars
C      lrbr1=13
C      layer 16 = top transverse rebars
C      lrbr2=16
C
C      layer 24 = bottom longitudinal rebars
C      lrbr3=24
C      layer 27 = bottom transverse rebars
C      lrbr4=27
C
C      nlyr1 = 32
C      nlyr2 = 42
C
C      open (12, file = 'mdl_in_t.dat',status='UNKNOWN')
C
C      nx=15
C      ny=15
c      open (11, file = 'MtrxSym.txt',
c      & status='OLD')
c
c      READ (11,'(a)') buf
c      READ (11,*) NNODES, NELEMS, NDUPL
c      nnodes = (nx+(nx-1))*ny
c      nelems=(nx-1)*2*(ny-3)
c      ndupl=(nx+nx-1)*2
c
c      write the top of file
c      write (buf,'(4L6,F5.2,1x,3L6,5i6)').FALSE.,.TRUE.,.FALSE.,
c      & .FALSE., 0.5, .FALSE., .FALSE., .FALSE., 0, 1, 2, 1, 1
c      write (12,'(a80)') buf
c      write (buf,'(A10,6i6,5L6)') 'PRESCRIBED', 0,1,1,1,1,218,

```

```

& .FALSE.,.TRUE.,.FALSE., .FALSE., .FALSE.
write (12,'(a80)') buf
write (buf,'(A10,i6,F10.4,i6,2L6,i6,5L6)')'CRITICALSE',0,0.72,3,
& .FALSE., .FALSE., 0, .FALSE.,.FALSE.,.FALSE., .FALSE., .FALSE.
write (12,'(a80)') buf
write (buf,'(10i8)') 8,3,8,3,8,3,8,3,8,3
write (12,'(a80)') buf
write (buf,'(A4)') 'ICAN'
write (12,'(a80)') buf
write (buf,'(A4,4x,3i8)') 'LTYP', 1, NLYR1, 3
write (12,'(a80)') buf
do i=1,NLYR1
  if (i .eq. lrbr2 .or. i .eq. lrbr4) then
    angle=90.0
  else
    angle=0.0
  endif
  if (i .eq. lrbr1 .or. i .eq. lrbr3) then
    mtrl=2
  elseif(i .eq. lrbr2 .or. i .eq. lrbr4) then
    mtrl=3
  else
    mtrl=1
  endif
  write (buf,'(A8,2i8,f7.2,f7.1,f8.1,f9.0,f6.3)') '      PLY',i,
& mtrl, 70.,70.,0.0, ANGLE, TPLY(I)
  write (12,'(a80)') buf
enddo
c23456789*123456789*123456789*123456789*123456789*123456789*123456789*12

write (buf,'(A8,i8,A8,2x,f6.5, 2x,f3.2,3x, A8, f5.1,5x,f3.2,5x,
& f3.2)')
& ' MATCRD', 1, 'CNCFCONC', 0.3, 0.01,'CNCFCONC', 0.0, 0.6, 0.03
write (12,'(a80)') buf
write (buf,'(A8,i8,A8,2x,f6.5, 2x,f3.2,3x, A8, f5.1,5x,f3.2,5x,
& f3.2)')
& ' MATCRD',
& 2, 'RBSFCONC', 0.99, 0.01,'CNCFCONC', 0.0, 0.6, 0.03
write (12,'(a80)') buf
write (buf,'(A8,i8,A8,2x,f6.5, 2x,f3.2,3x, A8, f5.1,5x,f3.2,5x,
& f3.2)')
& ' MATCRD',
& 3, 'RBSFCONC', 0.99, 0.01,'CNCFCONC', 0.0, 0.6, 0.03
write (12,'(a80)') buf

write (buf,'(A4,4x,3i8)') 'LTYP', 2, NLYR2, 5
write (12,'(a80)') buf
do i=1,NLYR2
  if (i .eq. lrbr2 .or. i .eq. lrbr4) then
    angle=90.0
  else
    angle=0.0
  endif
  if (i .eq. lrbr1 .or. i .eq. lrbr3) then
    mtrl=2
  elseif(i .eq. lrbr2 .or. i .eq. lrbr4) then
    mtrl=3
C    next are the flange steel layers
  elseif(i.eq. 35 .or. i.eq.36.or. i .eq. 41.or. i .eq. 42) then
    mtrl=4
C    next are the web steel layers
  elseif(i.eq. 37 .or. i.eq.38.or. i .eq. 39.or. i .eq. 40) then
    mtrl=5

```

```

else
  mtrl=1
endif
write (buf,'(A8,2i8,f7.2,f7.1,f8.1,f9.0,f6.3)') '      PLY',i,
& mtrl, 70.,70.,0.0, ANGLE, TPLY(I)
write (12,'(a80)') buf
enddo
write (buf,'(A8,i8,A8,2x,f6.5, 2x,f3.2,3x, A8, f5.1,5x,f3.2,5x,
& f3.2)')
& ' MATCRD',
& 1, 'CNCFCONC', 0.3, 0.01,'CNCFCONC', 0.0, 0.6, 0.03
write (12,'(a80)') buf
write (buf,'(A8,i8,A8,2x,f6.5, 2x,f3.2,3x, A8, f5.1,5x,f3.2,5x,
& f3.2)')
& ' MATCRD',
& 2, 'RBSFCONC', 0.99, 0.01,'CNCFCONC', 0.0, 0.6, 0.03
write (12,'(a80)') buf
write (buf,'(A8,i8,A8,2x,f6.5, 2x,f3.2,3x, A8, f5.1,5x,f3.2,5x,
& f3.2)')
& ' MATCRD',
& 3, 'RBSFCONC', 0.99, 0.01,'CNCFCONC', 0.0, 0.6, 0.03
write (12,'(a80)') buf
write (buf,'(A8,i8,A8,2x,f6.5, 2x,f3.2,3x, A8, f5.1,5x,f3.2,5x,
& f3.2)')
& ' MATCRD',
& 4, 'GRSFGRDS', 0.3, 0.0,'GRSFGRDS', 0.0, 0.02, 0.03
write (12,'(a80)') buf
write (buf,'(A8,i8,A8,2x,f6.5, 2x,f3.2,3x, A8, f5.1,5x,f3.2,5x,
& f3.2)')
& ' MATCRD',
& 5, 'WBSFWBSM', 0.3, 0.0,'WBSFWBSM', 0.0, 0.02, 0.03
write (12,'(a80)') buf

write (buf,'(A4)') 'ENDN'
write (12,'(a80)') buf
write (buf,'(A5)') 'MHOST'
write (12,'(a80)') buf
write (buf,'(A36)') ' A TEST OF COMPOSITE DECK SIMULATION'
write (12,'(a80)') buf
write (buf,'(A8,i12)') '*ELEMENT', NELEMS
write (12,'(a80)') buf
write (buf,'(i5)') 75
write (12,'(a80)') buf
write (buf,'(A10)') '*COMPOSITE'
write (12,'(a80)') buf
write (buf,'(A6,i10)') '*NODES', nnodes
write (12,'(a80)') buf
write (buf,'(A11)') '*LOUB 3 1 3'
write (12,'(a80)') buf
write (buf,'(A6,i5)') '*FORCE', 10
write (12,'(a80)') buf
C write (buf,'(A5,i11)') '*DUPL', ndupl
write (buf,'(A,i14,i10)') '*TYING', 6*ndupl, 3
write (12,'(a80)') buf
nboun=20
write (buf,'(A19,i5)') '*BOUNDARYCONDITIONS', nboun
write (12,'(a80)') buf
write (buf,'(A10)') 'C*OPTIMIZE'
write (12,'(a80)') buf
write (buf,'(A15)') '*CONSTITUTIVE 0'
write (12,'(a80)') buf
write (buf,'(A6)') '*DISPL'
write (12,'(a80)') buf

```

```

write (buf,'(A4)') '*END'
write (12,'(a80)') buf
write (buf,'(A5)') '*INCR'
write (12,'(a80)') buf
write (buf,'(i1)') 0
write (12,'(a80)') buf
write (buf,'(A10)') '*ITERATION'
write (12,'(a80)') buf
write (buf,'(i5, 4f10.2)') 2,0.05,0.05,0.05,0.05
write (12,'(a80)') buf
write (buf,'(A15)') '*PROPERTIES 75'
write (12,'(a80)') buf
write (buf,'(i5,i6,4f10.5)')1,nnodes,1.,0.00001,0.00001,0.00001
write (12,'(a80)') buf
write (buf,'(A45)')
&      '          0.1          0.0  0.0  0.0'
write (12,'(a80)') buf
write (buf,'(A5)') '*COOR'
write (12,'(a80)') buf

C      WRITE (12,'('' MHOST FEM Model for composite bridge deck''))
C      WRITE (12,'('*COOR''))
INOD=0
NDUPL=0
DO 1 i= -nx,nx,1
  IF (i .lt. -1) then
    XCOOR = -X(-i)
  ELSEIF (i .gt. 0) then
    XCOOR = X(i)
  ELSEIF (i.eq. -1 .or. i .eq. 0) THEN
    GOTO 1
  ELSE
    STOP 100
  ENDIF
  DO 2 j= 1, ny
    YCOOR = Y(j)
    IF ( j.lt. 6 .or. j .gt. 10) then
      THCK=t(1)
      LTYP=1
      Z=-5.
    ELSE
      THCK=t(2)
      LTYP=2
      Z=-26.
    ENDIF
    INOD=INOD+1
    WRITE (12,'(i8,4F17.8,i4)') INOD,XCOOR,YCOOR,Z,THCK,LTYP
    IF (J .eq. 5) THEN
      NDUPL = NDUPL+1
      ISLAVE (NDUPL) = inod
      MASTER (NDUPL) = inod+1
    ELSEIF (J.EQ. 10) THEN
      NDUPL = NDUPL+1
      ISLAVE (NDUPL) =inod+1
      MASTER (NDUPL) = inod
    ENDIF
  2  CONTINUE
1  CONTINUE
write (*,*) ' nnodes=',inod, ' ndupl=', ndupl, ' ntying=',6*ndupl

WRITE (12,'('*ELEM 75''))
IELEM=0
DO 3 i= 1, (nx-1)+(nx-1)

```

```

DO 4 j=1, ny-1
  IF (J .ne. 5 .and. j .ne. 10) THEN
    IELEM=IELEM+1
    NOD1=ny*(i-1)+j+1
    NOD2=ny*(i-1)+j
    NOD3=ny*i+j
    NOD4=ny*i+j+1
    WRITE (12,'(i8,4i9)') IELEM, NOD1,NOD2,NOD3,NOD4
  ELSE
    CONTINUE
  ENDIF
4  CONTINUE
3  CONTINUE
  WRITE (*,*) ' nelems=', ielem
  WRITE (12,(' '*LAMINATE'))
C  WRITE (12,(' '*DUPLICATENODE'))
  WRITE (12,(' '*TYING'))
C  CCOMB=distance to center of combined girder plus deck from center of deck
  CCOMB=0.5*(t(2)-t(1))
  DO 5 i=1, NDUPL
C  WRITE (12,'(2i8)') ISLAVE(i), MASTER(i)
  WRITE (12,'(8i8)') 3, islave(i), 1 ,master(i), 1, master(i), 5
  WRITE (12,'(2f10.5)') 1.0, CCOMB
  WRITE (12,'(8i8)') 3, islave(i), 2 ,master(i), 2, master(i), 4
  WRITE (12,'(2f10.5)') 1.0, -CCOMB
  WRITE (12,'(8i8)') 2, islave(i), 3 ,master(i), 3
  WRITE (12,'(2f10.5)') 1.0

  WRITE (12,'(8i8)') 2, islave(i), 4 ,master(i), 4
  WRITE (12,'(2f10.5)') 1.0
  WRITE (12,'(8i8)') 2, islave(i), 5 ,master(i), 5
  WRITE (12,'(2f10.5)') 1.0
  WRITE (12,'(8i8)') 2, islave(i), 6 ,master(i), 6
  WRITE (12,'(2f10.5)') 1.0

5  CONTINUE
  WRITE (12,(' '*BOUNDARYCONDITIONS'))
  NBOUN=0
C  Write the first end boundary conditions
  DO 32 i=6, 10
    IF ( i .eq. 8) then
      NBOUN = NBOUN + 2
      WRITE (12,'(2i9)') i, 2
      WRITE (12,'(2i9)') i, 3
    ELSE
      NBOUN = NBOUN + 1
      WRITE (12,'(2i9)') i, 3
    ENDIF
32  CONTINUE
  DO 33 i=216, 220
    IF ( i .eq. 218) then
      NBOUN = NBOUN + 3
      WRITE (12,'(2i9)') i, 1
      WRITE (12,'(2i9)') i, 2
      WRITE (12,'(2i9)') i, 3
    ELSE
      NBOUN = NBOUN + 1
      WRITE (12,'(2i9)') i, 3
    ENDIF
33  CONTINUE
  DO 34 i=425, 430
    IF ( i .eq. 428) then
      NBOUN = NBOUN + 2

```

```

        WRITE (12,'(2i9)') i, 2
        WRITE (12,'(2i9)') i, 3
    ELSE
        NBOUN = NBOUN + 1
        WRITE (12,'(2i9)') i, 3
    ENDIF
34 CONTINUE

    Write (*,*) ' nboun=', nboun
C Write the edge boundary conditions
c   DO 33 i=1, 450, 30
c       NBOUN=NBOUN+2
c       WRITE (12,'(2i9)') i, 4
c       WRITE (12,'(2i9)') i+14, 4
c   33 CONTINUE

C       WRITE (12,'('*FORCE*'))
C       WRITE (12,'(i5,i2,f19.9)') inode, idof, force
C       FORCE = -200.0
C       DO i=36, 40
C           WRITE (12,'(i5,i2,f19.9)') i, 3, force
C       ENDDO
C       DO i=396, 400
C           WRITE (12,'(i5,i2,f19.9)') i, 3, force
C       ENDDO
WRITE (12,'('*PRINT*'))

WRITE (12,'(''      TOTALDISPLACEM''))
WRITE (12,'(''      STRESS''))
WRITE (12,'(''      STRAIN''))

WRITE (12,'('*END*'))

WRITE (12,'('*STOP*'))

write (*,*) ' NBOUN=', NBOUN

STOP

end

```

**Appendix 7-4c Residual stresses from FOR091.DAT file after 28 days for composite bridge deck with 36" girder and thin rebar steel layers**

```

TIME= 672.0 HOURS
NODE NUMBER= 218
PLY NO., SIG11, SIG22, SIG12
STRESSES ARE IN PSI UNITS; LAYER COORDINATES
 1 0.2020E+03 0.2071E+03 0.2622E-09
 2 0.2113E+03 0.2166E+03 0.2579E-09
 3 0.2203E+03 0.2258E+03 0.2533E-09
 4 0.2287E+03 0.2344E+03 0.2488E-09
 5 0.2362E+03 0.2421E+03 0.2443E-09
 6 0.2472E+03 0.2534E+03 0.2376E-09
 7 0.2628E+03 0.2695E+03 0.2262E-09
 8 0.2845E+03 0.2917E+03 0.2082E-09
 9 0.3061E+03 0.3139E+03 0.1856E-09
10 0.3220E+03 0.3302E+03 0.1630E-09
11 0.3330E+03 0.3414E+03 0.1406E-09
12 0.3393E+03 0.3479E+03 0.1240E-09
13 0.2114E+03 0.2126E+03 -0.1424E-07
14 0.3418E+03 0.3505E+03 0.1121E-09
15 0.3448E+03 0.3536E+03 0.1015E-09
16 0.1910E+03 0.1914E+03 0.5746E-07
17 0.3470E+03 0.3558E+03 0.8962E-10
18 0.3503E+03 0.3591E+03 0.7045E-10
19 0.3532E+03 0.3622E+03 0.4245E-10
20 0.3540E+03 0.3630E+03 0.1457E-10
21 0.3547E+03 0.3637E+03 -0.1356E-10
22 0.3526E+03 0.3616E+03 -0.4140E-10
23 0.3509E+03 0.3598E+03 -0.6076E-10
24 0.4703E+02 0.3997E+02 -0.1211E-07
25 0.3497E+03 0.3586E+03 -0.7255E-10
26 0.3499E+03 0.3587E+03 -0.8336E-10
27 0.2050E+02 0.2389E+02 0.2000E-06
28 0.3495E+03 0.3582E+03 -0.9493E-10
29 0.3479E+03 0.3567E+03 -0.1083E-09
30 0.3469E+03 0.3557E+03 -0.1239E-09
31 0.3459E+03 0.3546E+03 -0.1398E-09
32 0.3447E+03 0.3533E+03 -0.1554E-09
33 0.3311E+03 0.3394E+03 -0.2085E-09
34 0.2276E+03 0.2330E+03 -0.2986E-09
35 -0.2153E+03 -0.2243E+03 -0.8802E-08
36 -0.2357E+03 -0.2450E+03 -0.8542E-08
37 -0.3076E+02 -0.3172E+02 -0.4562E-09
38 -0.5613E+02 -0.5761E+02 -0.1311E-09
39 -0.8153E+02 -0.8350E+02 0.1936E-09
40 -0.1069E+03 -0.1094E+03 0.5184E-09
41 -0.1664E+04 -0.1702E+04 0.9392E-08
42 -0.1657E+04 -0.1695E+04 0.9659E-08

```

HS25 14 ftx14 ft LOADING RESULTS after 672.000 HOURS = 28.0000 DAYS

```

TIME= 672.0 HOURS
NODE NUMBER= 218
PLY NO., SIG11, SIG22, SIG12
STRESSES ARE IN PSI UNITS; LAYER COORDINATES
 1 0.5684E+03 0.1716E+03 -0.5280E+01
 2 0.5753E+03 0.1813E+03 -0.5259E+01
 3 0.5818E+03 0.1907E+03 -0.5238E+01
 4 0.5878E+03 0.1994E+03 -0.5217E+01
 5 0.5928E+03 0.2073E+03 -0.5196E+01

```

6	0.6001E+03	0.2188E+03	-0.5164E+01
7	0.6095E+03	0.2353E+03	-0.5111E+01
8	0.6214E+03	0.2582E+03	-0.5027E+01
9	0.6307E+03	0.2812E+03	-0.4922E+01
10	0.6343E+03	0.2983E+03	-0.4816E+01
11	0.6330E+03	0.3104E+03	-0.4711E+01
12	0.6302E+03	0.3175E+03	-0.4633E+01
13	0.3286E+04	0.2202E+03	-0.3630E+02
14	0.6263E+03	0.3205E+03	-0.4578E+01
15	0.6234E+03	0.3240E+03	-0.4528E+01
16	0.1932E+03	0.3135E+04	0.3547E+02
17	0.6192E+03	0.3266E+03	-0.4472E+01
18	0.6119E+03	0.3306E+03	-0.4382E+01
19	0.5996E+03	0.3347E+03	-0.4251E+01
20	0.5851E+03	0.3365E+03	-0.4120E+01
21	0.5706E+03	0.3383E+03	-0.3990E+01
22	0.5532E+03	0.3371E+03	-0.3859E+01
23	0.5410E+03	0.3361E+03	-0.3769E+01
24	0.2040E+04	0.3597E+01	-0.2949E+02
25	0.5333E+03	0.3353E+03	-0.3713E+01
26	0.5277E+03	0.3358E+03	-0.3663E+01
27	-0.2121E+02	0.1885E+04	0.2866E+02
28	0.5208E+03	0.3357E+03	-0.3608E+01
29	0.5120E+03	0.3347E+03	-0.3546E+01
30	0.5024E+03	0.3343E+03	-0.3472E+01
31	0.4928E+03	0.3338E+03	-0.3399E+01
32	0.4830E+03	0.3330E+03	-0.3325E+01
33	0.4405E+03	0.3210E+03	-0.3077E+01
34	0.2877E+03	0.2180E+03	-0.2655E+01
35	0.8773E+02	-0.3292E+03	-0.1888E+02
36	-0.6479E+02	-0.3553E+03	-0.1804E+02
37	-0.1056E+03	-0.4337E+02	-0.7759E+00
38	-0.2960E+03	-0.7596E+02	0.2646E+00
39	-0.4864E+03	-0.1085E+03	0.1305E+01
40	-0.6769E+03	-0.1411E+03	0.2345E+01
41	-0.1061E+05	-0.2182E+04	0.3939E+02
42	-0.1073E+05	-0.2180E+04	0.4023E+02